



Fakultät für Medizin

Institut für Medizinische Mikrobiologie, Immunologie und Hygiene

T cell receptor binding avidity of antigen-specific CD8⁺ cytotoxic T cells in chronic infection

Bianca Weißbrich

Vollständiger Abdruck der von der Fakultät für Medizin der Technischen Universität München zur Erlangung des akademischen Grades eines

Doktors der Naturwissenschaften

genehmigten Dissertation.

Vorsitzende: Univ.-Prof. Dr. U. Protzer

Prüfer der Dissertation:

1. Univ.-Prof. Dr. D. Busch
2. Univ.-Prof. Dr. Th. Hugel

Die Dissertation wurde am 28.05.2015 bei der Technischen Universität München eingereicht und durch die Fakultät für Medizin am 18.11.2015 angenommen.

Parts of this thesis have already been published:

M. Nauerth*, B. Weissbrich*, R. Knall*, T. Franz, G. Dossinger, J. Bet, P. J. Paszkiewicz, L. Pfeifer, M. Bunse, W. Uckert, R. Holtappels, D. Gillert-Marien, M. Neuenhahn, A. Krackhardt, M. J. Reddehase, S. R. Riddell, D. H. Busch: TCR-ligand k_{off} -Rate Correlates with the Protective Capacity of Antigen-Specific CD8⁺ T Cells for Adoptive Transfer. *Sci Transl Med* 5(192). 192ra187 (2013). (* contributed equally)

G. Dössinger, M. Bunse, J. Bet, J. Albrecht, P. J. Paszkiewicz, B. Weissbrich, I. Schiedewitz, L. Henkel, M. Schiemann, M. Neuenhahn, W. Uckert, D. H. Busch: MHC multimer-guided and cell culture-independent isolation of functional T cell receptors from single cells facilitates TCR identification for immunotherapy. *PLoS One* 8 (4). e61384 (2013).

P. Hombrink, Y. Raz, M. G. Kester, R. de Boer, B. Weissbrich, P. A. von dem Borne, D. H. Busch, T. N. Schumacher, J. H. Falkenburg, M. H. Heemskerk: Mixed functional characteristics correlating with TCR-ligand k_{off} -rate of MHC-tetramer reactive T-cells within the naive T-cell repertoire. *Eur J Immunol* 43 (11). 3038-3050 (2013).

B. Weissbrich, M. Nauerth, D. H. Busch: Adoptive immunotherapy: New assay for the identification of T cells with optimal avidity. *Oncoimmunology* 2(1). e26199 (2013).

M. Nauerth, B. Weissbrich, D. H. Busch: The clinical potential for k_{off} -rate measurement in adoptive immunotherapy. *Expert Rev Clin Immunol* 9(12). 1151-1153 (2013).

Content

1	Introduction.....	1
1.1	T cell mediated immunity.....	1
1.1.1	The T cell receptor (TCR)	2
1.1.1.1	Structure of the TCR complex	3
1.1.1.2	TCR repertoire diversity	4
1.1.2	Molecular interaction between the TCR and its ligand	5
1.1.2.1	MHC structure	5
1.1.2.2	TCR – pMHC interaction.....	6
1.2	TCR - pMHC binding strength	8
1.2.1	TCR affinity.....	8
1.2.2	TCR avidity	10
1.2.3	Structural TCR avidity	12
1.2.4	T cell activation upon ligand binding	14
1.2.4.1	T cell signaling.....	14
1.2.4.2	T cell activation	16
1.3	TCR avidity in infection.....	17
1.3.1	Cytomegalovirus (CMV)	18
1.3.1.1	CMV life cycle.....	19
1.3.1.2	CMV distribution and latent persistence.....	20
1.3.2	Cytotoxic CD8 ⁺ T cell responses towards CMV infection.....	23
1.3.2.1	T cell responses in the acute phase of CMV infection	23
1.3.2.2	T cell responses in the chronic phase of CMV infection	24
1.3.2.3	CMV, T cell dysfunction and immune senescence	25
2	Aim of this PhD thesis.....	27
3	Material and Methods.....	28
3.1	Material.....	28
3.1.1	Chemicals and reagents	28
3.1.2	Buffers and Media	29
3.1.3	Peptides	31
3.1.4	Antibodies.....	32
3.1.5	MHC <i>Streptamers</i>	33
3.1.6	Gels	33
3.1.7	Microscope and equipment for TCR-ligand k_{off} -rate measurements	34
3.1.8	Equipment.....	34
3.1.9	Software	35

3.2	Methods	35
3.2.1	Specific T cell populations	35
3.2.1.1	Human blood samples	35
3.2.1.2	Human T cell clones	35
3.2.1.3	Murine blood samples	36
3.2.1.4	TCR sequencing and TCR Transduction	37
3.2.2	Generation of murine MHC heavy chains with mutation III for fluorescence conjugation	37
3.2.2.1	Primer design	37
3.2.2.2	Mutagenesis-PCR	38
3.2.2.3	Transformation and plasmid preparation	38
3.2.2.4	Protein expression	39
3.2.3	Generation of <i>Streptamers</i>	40
3.2.3.1	Purification and refolding of MHC molecules	40
3.2.3.2	Dye-conjugation and purification	41
3.2.3.3	pMHC exchange	41
3.2.3.4	Multimerization of pMHCs	41
3.2.4	Functional analysis, T cell staining and FACS analysis	42
3.2.4.1	Secretion of IFN γ in an intracellular cytokine staining (ICCS)	42
3.2.4.2	Secretion of IFN γ in an ELISA	42
3.2.4.3	⁵¹ Chromium release assay	42
3.2.4.4	Antibody and Streptamer staining	43
3.2.4.5	FACS acquisition and analysis	43
3.2.4.6	Conventional pMHC multimer dissociation experiments	43
3.2.5	TCR-ligand k_{off} -rate assay	44
3.2.5.1	<i>Streptamer</i> staining and sorting	44
3.2.5.2	Performance of the k_{off} -rate assay	44
3.2.5.3	Data analysis	45
3.2.5.4	Bleaching measurements with beads	46
4	Results	47
4.1	Validation of the TCR-ligand k_{off} -rate assay	47
4.1.1	Conventional pMHC multimer dissociation experiments are difficult to standardize	47
4.1.2	Principle of the microscopic <i>Streptamer</i> -based TCR-ligand k_{off} -rate assay	50
4.1.3	TCR-ligand k_{off} -rate assay allows reproducible and standardized measurements of fast and slow dissociation kinetics	56
4.1.4	TCR-ligand $t_{1/2}$ values predict the functionality of antigen-specific T cells independently of multimer staining intensity	59

4.1.5	TCR-ligand $t_{1/2}$ values depend on the structure of the TCR rather than the cellular background	62
4.1.6	Complete TCR-ligand dissociation can be monitored at room temperature with accelerated $t_{1/2}$ values	67
4.1.7	Generation of fluorescence-conjugated murine pMHC monomers for TCR-ligand k_{off} -rate analysis.....	70
4.1.8	Optimization of the purification and analysis of purified <i>Streptamer</i> + T cells under the microscope.....	73
4.2	Human Cytomegalovirus-specific T cell populations	78
4.2.1	Strong differences in TCR-ligand $t_{1/2}$ of human CMV-specific T cells correlate to differential functionality	78
4.2.2	MHC-restriction and epitope recognition of CMV-specific T cell populations do not predict the TCR-ligand $t_{1/2}$	80
4.2.3	CMV IE1-specific T cell populations expand to large numbers	83
4.2.4	IE1-specific T cell populations vary in frequency and TCR-ligand $t_{1/2}$	83
4.2.5	HLA-B8/IE1 ₈₈ -specific T cell populations with long mean TCR-ligand $t_{1/2}$	85
4.2.6	HLA-IE1 ₁₉₉₋₂₀₇ -specific T cell populations can be cross-reactive for altered peptide ligands derived from different CMV strains.....	88
4.2.7	<i>Streptamer</i> frequency of CMV IE1-specific T cell populations of healthy human blood donors correlates to TCR-ligand $t_{1/2}$ values.....	93
4.3	Murine Cytomegalovirus-specific T cell populations	96
4.3.1	Reversible <i>Streptamer</i> staining on fresh or cryo-preserved whole blood allows the purification of MCMV-specific T cell populations for the TCR-ligand k_{off} -rate measurement	97
4.3.2	MCMV IE1- and m164-specific T cell populations expand during chronic infection in blood samples from 129/Sv x BALB/c mice	101
4.3.3	Mean TCR-ligand $t_{1/2}$ values of MCMV IE1- and m164-specific T cell populations do not change substantially during 12 month of infection	103
4.3.4	<i>Streptamer</i> frequency and mean TCR-ligand $t_{1/2}$ values of MCMV IE1- and m164-specific T cell populations are not related during 12 month of CMV infection ..	106
5	Discussion	108
5.1	Reproducible measurement of TCR-ligand $t_{1/2}$	108
5.2	TCR-ligand $t_{1/2}$ of human CMV-specific T cell populations	114
5.2.1	Disparate TCR avidities of human CMV-specific T cells.....	114
5.2.2	Expansion of T cell populations responding to latency-associated genes	115
5.2.3	Population size matters?	118
5.2.4	Clonal focusing during chronic CMV infection.....	118
5.3	TCR-ligand $t_{1/2}$ of murine CMV-specific T cell populations	121
5.3.1	Differences in TCR-ligand $t_{1/2}$ of murine and human CMV-specific T cell populations	122

5.4	Influences on the inverse repertoire focusing during chronic infection	125
5.4.1	CMV contribution to immune senescence.....	127
5.4.2	Therapeutic strategies to treat CMV-associated diseases.....	128
5.4.3	TCR avidity in malignancies	130
6	Summary	132
7	References	134
8	Acknowledgments	149

List of Figures

Figure 1-1: Effector mechanisms of CD8 ⁺ cytotoxic T cells.	2
Figure 1-2: Structure of the $\alpha\beta$ T cell receptor (TCR).	4
Figure 1-3: Structure of the major histocompatibility complexes I and II.	6
Figure 1-4: T cell receptor (TCR) binding mode to peptide MHC (pMHC).	7
Figure 1-5: Three dimensional TCR affinity measurements.	9
Figure 1-6: Functional TCR avidity describes the effector functions of antigen-specific T cells after peptide stimulation.	11
Figure 1-7: MHC multimers are used to detect and analyse antigen-specific T cells.	12
Figure 1-8: Force measurements to assess TCR binding strength.	13
Figure 1-9: Kinetic measurements of monomeric MHC II binding and unbinding on living T cells.	14
Figure 1-10: TCR-CD3 complex and initial signaling process.	16
Figure 1-11: Structure of the Cytomegalovirus virion.	19
Figure 1-12: CMV primary infection and life cycle.	20
Figure 1-13: CMV infection, distribution and persistence in different cell types.	21
Figure 1-14: Productive and latent CMV infection.	22
Figure 1-15: Different kinetic patterns of IE1 and pp65-specific T cell populations during CMV infection.	24
Figure 4-1: Basic principle of conventional pMHC multimer dissociation experiments.	48
Figure 4-2: Conventional pMHC multimer dissociation experiments discriminate high and low avidity T cell clones.	49
Figure 4-3: Conventional pMHC multimer dissociation experiments are difficult to reproduce.	50
Figure 4-4: Basic principle of the TCR-ligand k_{off} -rate assay.	51
Figure 4-5: Setup for the real-time analysis of fluorescence decay caused by MHC dissociation from antigen-specific T cells by flow cytometry or real-time microscopy.	52
Figure 4-6: TCR-ligand dissociation is monitored by real time microscopy on living antigen-specific T cells.	53
Figure 4-7: Bleaching rate on small beads is reproducible and comparable to bleaching rate on cells.	55
Figure 4-8: Reproducible dissociation half-life values ($t_{1/2}$) of MHC monomers in the TCR-ligand k_{off} -rate assay.	56
Figure 4-9: TCR-ligand k_{off} -rate assay in the presence or absence of MHC rebinding blocking antibody.	57
Figure 4-10: Dissociation of pMHC monomers in the TCR-ligand k_{off} -rate assay can be monitored without blockade of MHC rebinding.	58
Figure 4-11: Dissociation of pMHC monomers in the TCR-ligand k_{off} -rate assay is comparable with and without APC fluorochrome on the <i>Strep</i> -Tactin backbone.	59
Figure 4-12: pMHC multimer staining intensity to measure structural TCR binding strength.	60
Figure 4-13: T cell clones from the naïve T cell repertoire can be labeled with MHC multimers.	61
Figure 4-14: MHC multimer staining intensity of <i>in vitro</i> expanded T cell clones from the naïve T cell repertoire does not correlate with functional avidity.	61
Figure 4-15: Fast TCR-ligand k_{off} -rate of <i>in vitro</i> expanded T cell clones from naïve T cell repertoire correlates to low functional avidity.	62
Figure 4-16: Dissociation half-life times in the TCR-ligand k_{off} -rate assay are comparable during different activation states of analyzed cells.	63

Figure 4-17: Dissociation half-life times in the TCR-ligand k_{off} -rate assay correlate with functional avidity.	65
Figure 4-18: TCR-ligand dissociation half-life time and functional avidity of two human CMV-specific TCRs is maintained after transgenic re-expression.....	66
Figure 4-19: pMHC monomers dissociate completely from antigen-specific T cells at room temperature.	68
Figure 4-20: Dissociation of monomeric pMHC molecules is accelerated at higher temperatures.	69
Figure 4-21: Modification of conventional MHC I <i>Strep</i> -tagIII monomers for TCR-ligand k_{off} -rate analysis.	70
Figure 4-22: Phosphorylated primers allow efficient insertion of the linker sequence and the cysteine into the conventional pMHC I expression vectors for dye conjugation.	72
Figure 4-23: Combinatorial <i>Streptamer</i> staining allows simultaneous FACS sorting of two different antigen-specific T cell populations.	74
Figure 4-24: FACS sorting of CD8 ⁺ <i>Streptamer</i> ⁺ and CD8 ⁺ <i>Streptamer</i> ⁻ with subsequent second <i>Streptamer</i> staining allows serial purification of different antigen-specific T cell populations from one sample.	75
Figure 4-25: Serial FACS purification of T cell populations with different specificity from one sample is pure and allows microscopic analysis.	76
Figure 4-26: Sorting into a 96-well-V-bottom plate on ice increases cell recovery and minimized membrane reduces distribution of antigen-specific T cells on glass bottom during microscopic k_{off} -rate analysis.	77
Figure 4-27: Human CMV-specific T cells differ in their TCR-ligand $t_{1/2}$ values.	78
Figure 4-28: TCR-ligand $t_{1/2}$ correlates to functionality of human CMV-specific T cell populations.	79
Figure 4-29: TCR-ligand $t_{1/2}$ values from individual T cells are diverse for different HLA-types.	80
Figure 4-30: CMV gene expression is limited during latent infection.	81
Figure 4-31: TCR-ligand $t_{1/2}$ values are diverse for different antigen specificities.....	82
Figure 4-32: Fast TCR-ligand dissociation $t_{1/2}$ values and higher number of IE1-specific T cells.	82
Figure 4-33: CMV IE1-specific T cell populations can comprise large fractions of all CD3 ⁺ T lymphocytes in healthy human blood donors.	83
Figure 4-34: CMV HLA-B8/IE1 ₁₉₉₋₂₀₇ ^{KM} -specific T cell populations from healthy blood donors differ in their TCR-ligand dissociation kinetics.	84
Figure 4-35: CMV HLA-B8/IE1 ₁₉₉₋₂₀₇ ^{KM} -specific T cell populations from healthy blood donors differ in their functional avidity.....	85
Figure 4-36: T cell populations specific for the same CMV target antigen and the same MHC in the same donor have disparate characteristics.	86
Figure 4-37: T cell populations specific for different epitopes with disparate TCR-ligand $t_{1/2}$ and functionality.....	87
Figure 4-38: HLA-B8/IE1 ₈₈₋₉₆ -specific T cell populations with long TCR-ligand dissociation $t_{1/2}$ values.	88
Figure 4-39: Large CMV IE1 ₁₉₉₋₂₀₇ -specific T cell population of donor #1 can produce IFN γ in response to four epitope variants from different CMV strains.	90
Figure 4-40: Principle of the UV-peptide exchange.	91
Figure 4-41: Maleimide dye conjugation interferes with peptide exchange for the generation of fluorescently labeled MHC monomers.	92
Figure 4-42: Large CMV-specific T cell populations comprise predominantly T cells with fast TCR-ligand $t_{1/2}$	93

Figure 4-43: Mean TCR-ligand $t_{1/2}$ values of human CMV-specific T cell populations decrease with increasing size of the T cell population.	94
Figure 4-44: The frequency of CMV-specific T cell population is increasing with age.	95
Figure 4-45: Staining and purification of reversibly labeled <i>Streptamer</i> ⁺ T cells from murine blood samples for TCR-ligand k_{off} -rate analysis.	98
Figure 4-46: <i>Streptamer</i> staining on thawed murine blood samples does not require erythrocyte lysis before freezing.	99
Figure 4-47: <i>Streptamer</i> staining on thawed murine blood samples does not require erythrocyte lysis after freezing.	100
Figure 4-48: Scheme of mouse model for acute and chronic phase of CMV infection.	101
Figure 4-49: CMV IE- and m164-specific T cell populations increase in their frequency after infection with MCMV in 129/Sv x BALB/c mice.	102
Figure 4-50: Intermediate TCR-ligand $t_{1/2}$ values of MCMV-specific T cell population during acute phase of virus infection.	103
Figure 4-51: Mean TCR-ligand $t_{1/2}$ values of MCMV-specific T cell populations during acute and chronic phase of virus infection.	104
Figure 4-52: TCR-ligand $t_{1/2}$ values of T cell populations with identical specificity differ between individual syngeneic mice.	105
Figure 4-53: Mean TCR-ligand $t_{1/2}$ values of MCMV IE1- and MCMV m164-specific T cell populations do not decrease with increasing population size.	106
Figure 4-54: The variation of data from individual cells from MCMV-specific T cell populations is relatively broad as compared to TCR identical T cell lines.	107
Figure 5-1: Multiple parameters affecting inverse clonal focusing during chronic latent infection.	126

Abbreviations

2D	two dimensional
3D	three dimensional
ACT	ammoniumchloride/tris
AFM	atomic force microscopy
Ag	antigen
APC	allophycocyanin
APC	antigen presenting cell
APL	altered peptide ligand
APS	ammoniumpersulfate
β_2m	beta-2-microglobuline
BFP	biomembrane force probe
BSA	bovine serum albumin
CD	cluster of differentiation
CDR	complementarity determining region
CFU	colony forming unit
CMV	cytomegalovirus
^{51}Cr	chromium-51
C-region	constant region of the TCR
CTL	cytotoxic T lymphocyte
cv	coefficient of variation
d	day
dH ₂ O	distilled, deionized water
DC	dendritic cell
DNA	deoxyribonucleic acid
DTT	dithiothreitol
EBV	Epstein-Barr virus
EC ₅₀	peptide concentration mediating half-maximal effector function
EDTA	ethylenediaminetetraacetate
ELISPOT	enzyme linked immunospot technique
EMA	ethidium monazide bromide
FACS	fluorescence activated cell sorting
FCS	fetal calf serum
FITC	fluoresceinisothiocyanate
FPLC	fast protein liquid chromatography
FRET	fluorescence resonance energy transfer
h	hour
h	human
HIV	human immunodeficiency virus
HLA	human leukocyte antigen
HSCT	hematopoetic stem cell transplantation
ICCS	intracellular cytokine staining
IFN	interferon
Ig	immunoglobulin
IL	interleukin
IPTG	isopropyl- β -D-thiogalactopyranoside
IRP	immune risk phenotype
ITAM	immunoreceptor tyrosine-based activation motif
K _D	dissociation constant
kDa	kilo Dalton

$k_{\text{off-rate}}$	dissociation rate
$k_{\text{on-rate}}$	association rate
LAT	linker for activation of T cells
LB	Luria Bertoni medium
Lck	leukocyte-specific protein tyrosine kinase
LFA	leukocyte function-associated antigen
LSM	laser scanning microscop
m	murine
M	molar
MACS	magnetic-activated cell sorting
MFI	mean fluorescence intensity
MHC	major histocompatibility complex
min	minute
OD	optical density
PBMC	peripheral blood mononuclear cell
PCR	polymerase chain reaction
PBS	phosphate-buffered saline
PE	phycoerythrin
PFA	paraformaldehyde
PFU	plaque forming units
pMHC	peptide loaded major histocomaptibility complex
RBC	red blood cell
RNA	ribonucleic acid
rpm	rounds per minute
RT	room temperature
rxn	reaction
s	second
SD	standard deviation
SDS	sodium dodecyl sulfate
SPR	surface plasmon resonance
SA	Streptavidin
$t_{1/2}$	half-life
TAA	tumor-associated antigen
TBE	tris/borate/EDTA buffer
TCR	T cell receptor
TdT	terminal deoxynucleotide transferase
T_{FH}	follicular helper T cell
TEMED	N,N,N,N-Tetramethylethylendiamine
T_{H}	T helper cell
TNF	tumor necrosis factor
T_{reg}	regulatory T cell
Tris	tris-(hydroxymethyl)-aminomethane
$V\alpha / V\beta$	V alpha/V beta region of the TCR
V region	variable region of the TCR
V/D/J	variable, diversity and joining gene segments of the TCR
ZAP70	ζ -associated protein of 70 kDa

1 Introduction

1.1 T cell mediated immunity

The mammalian immune system is divided into an innate and adaptive branch. The innate immune system allows immediate recognition of common pathogenic patterns. The specific recognition and clearance (or efficient surveillance) of diverse pathogens is mediated by the adaptive immune system. Antibodies produced by B cells (humoral immune response) bind three-dimensional targets and extracellular pathogens, whereas the cellular immune response is mediated by T cells. T cells target peptides derived from pathogens presented on major histocompatibility complexes (MHCs) on the surface of other cells. They are subdivided into two major subsets based on the expression of their co-receptor CD4 and CD8. CD4⁺ helper T cells bind to peptides on MHC class II molecules that are mainly expressed on antigen presenting cells (APCs). Based on their immune modulatory functions CD4⁺ T cells are further classified into diverse groups: T_{H1} cells secrete interferon γ (IFN γ) and activate macrophages, T_{H2} secrete interleukin 4 (IL-4) and activate B cells, while IL-17 producing T_{H17} cells are associated in peripheral tissue inflammation. Further, the subset of regulatory CD4⁺ T cells (T_{reg}) inhibit inflammation, while follicular helper T cells (T_{FH}) mediate help in the germinal center (Swain et al., 2012). In contrast to CD4⁺ T cells, cytotoxic CD8⁺ T cells directly recognize intracellular pathogens on the surface of infected as well as malignant cells. They bind via their T cell receptor (TCR) to peptides loaded on MHC class I molecules on target cells. Upon binding and T cell activation, cytotoxic effector molecules are released into the contact zone to the target cell. Here, perforin can form a pore in the membrane of the target cell by polymerization, thereby causing influx of water and salts to induce osmotic cell lysis and in addition allowing other effector molecules such as granzymes secreted by a T cell to enter the target cell and induce apoptosis (Fig. 1-1 A). Another mechanism to induce apoptosis is the interaction of Fas-ligand (CD95L) with its receptor Fas (CD95) on target cells (Fig. 1-1 B). Cytotoxic T cells release cytokines such as IFN γ to inhibit viral replication or Tumor Necrosis Factor (TNF) α and β that bind to the TNF receptor on target cells to induce killing and up-regulation of MHC and CD95 expression (Fig. 1-1 C). In addition, these cytokines recruit and activate other immune cells such as macrophages (Andersen et al., 2006).

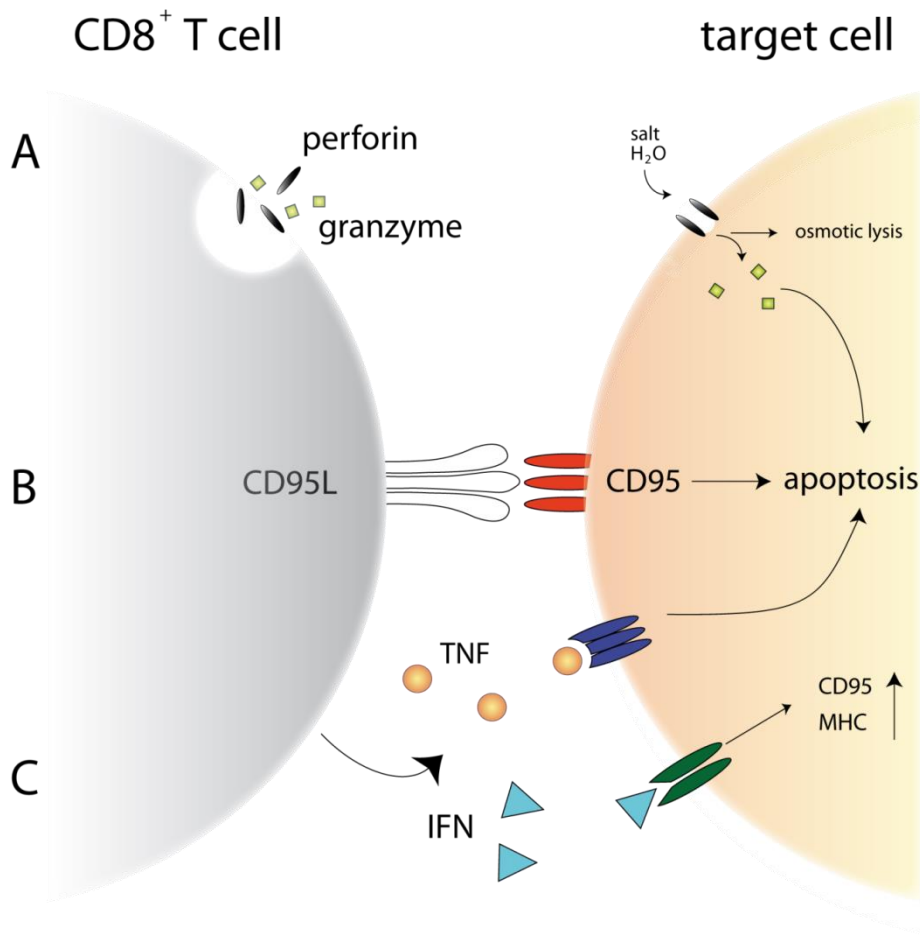


Figure 1-1: Effector mechanisms of CD8⁺ cytotoxic T cells.

(A) After binding of their T cell receptor (TCR) to specific peptide–MHC complexes on a target cell, cytotoxic T cells release lytic granules that contain perforin and granzyme B. Perforin polymerizes and forms pores in the target cell membrane, leading to an influx of water, salts and to osmotic cell lysis. The serine protease granzyme B activates effector caspases and apoptosis upon entry into the cell. (B) Cytotoxic T cells can induce apoptosis of targets cells by the binding of ligands to death receptors, such as CD95 on the target cell. (C) The release of cytokines can have direct and indirect effects on target cells. Tumor necrosis factor (TNF) binds to the receptor on the target cell to induce apoptosis. Interferon (IFN) binding to its receptor inhibits viral replication and up-regulates death receptor CD95, as well as expression of MHC on the cell surface which enhances the recognition of infected cells. The cytokines TNF and IFN recruit and activate other immune effector cells.

1.1.1 The T cell receptor (TCR)

The recognition of a broad range of different new pathogenic peptides by specific T cells is enabled by a high diversity of individual TCRs expressed on T cells. The TCR repertoire diversity is provided by TCR gene rearrangement, junctional modifications and the pairing of two different TCR chains ($\alpha\beta$ or $\gamma\delta$). During $\alpha\beta$ T cell development in the thymus, three TCR gene segments variable (V), diversity (D) and joining (J) are recombined to encode a unique

TCR β variable chain, followed by the somatic recombination of V and J segments for a unique TCR α variable chain (Davis and Bjorkman, 1988; Lieber, 1991).

1.1.1.1 Structure of the TCR complex

The overall TCR structure is related to the immunoglobulin structure of the B cell receptor or antibodies. Each of the polypeptide chain of the $\alpha\beta$ TCR consists of different parts. The largest part is the extracellular domain that includes a variable (V) and constant (C) region, followed by a hinge region. This hinge region contains a cysteine to link both TCR chains by a disulfide bond. The TCR chains are anchored on the cell with their transmembrane region and have a short intracellular region (Fig. 1-2). In the transmembrane region positively charged amino acids allow an interaction with the invariant chains of the CD3 complex that is always co-expressed on the cell surface with the TCR and mediates intracellular signaling upon T cell activation. Three hypervariable complementary determining regions (CDRs) on the relatively flat V region mediate the interaction to the pMHC ligand. While CDR1 and CDR2 are encoded by one of the variable genes in the germline (47 TRAV genes for the α and 57 TRBV genes for β), the CDR3 region results from junctional modifications (DNA nuclease activity and random N nucleotide addition) during V(D)J recombination. CDR3 is therefore characterized by the highest variability among individual TCRs (Davis and Bjorkman, 1988; Bridgeman et al., 2012).

Introduction

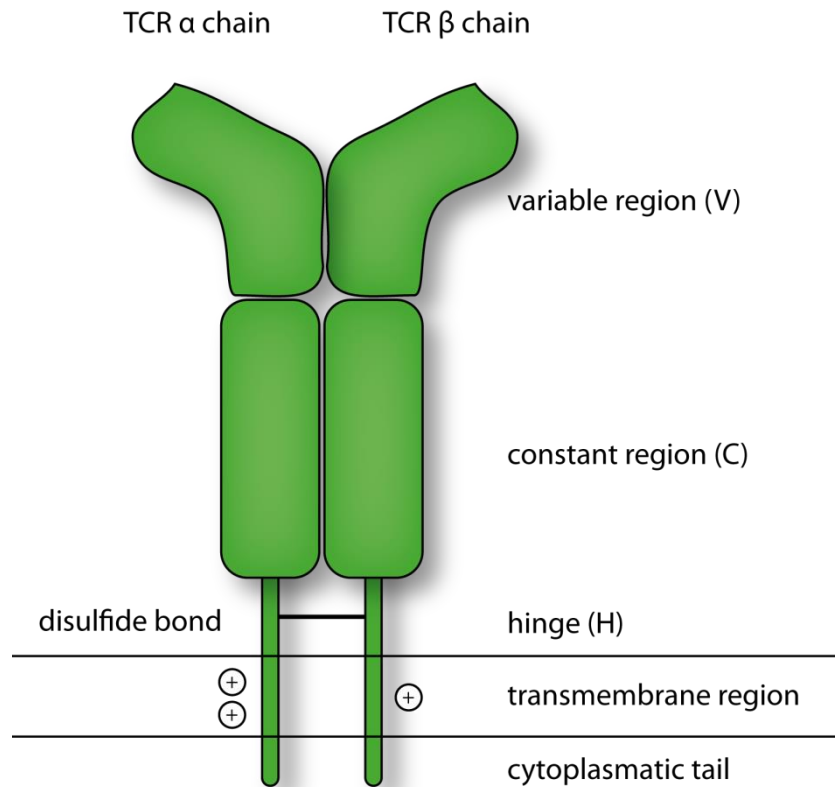


Figure 1-2: Structure of the $\alpha\beta$ T cell receptor (TCR).

Each TCR chain α and β consist of a variable region (V) that contains the complementary determining regions (CDRs) and mediates the interaction with the ligand; a constant region (C), a hinge region to associate both chains with a disulfide bond, as well as a transmembrane region and a short cytoplasmic tail. Positively charged (+) amino acids in the transmembrane region allow the association with the CD3 complex.

1.1.1.2 TCR repertoire diversity

The combinations of α and β TCR chain, junctional modifications and the somatic recombination of V(D)J in theory allow $10^{15} - 10^{20}$ combinations for unique $\alpha\beta$ TCRs (Davis and Bjorkman, 1988; Lieber, 1991). However, there is a huge gap of more than 10^8 -fold to the actual TCR diversity of 2.5×10^7 found in the periphery (Arstila et al., 1999). Only about 5% of the TCR combinations are selected during T cell development by binding self-MHC molecules sufficiently (positive selection), but binding weakly to self-peptides presented by MHCs (negative selection) in the thymus (Jameson et al., 1995). The frequency of naïve precursor T cells that bind a single specific pMHC is estimated around 6×10^{-7} and 5×10^{-6} (Alanio et al., 2010) which indicate a total T cell number of 15 000 – 125 000 per person. Peripheral TCR repertoire diversity is correlated to the efficiency of *de novo* immune responses (Nikolich-Zugich et al., 2004), while a high precursor frequency of an individual

Introduction

naïve T cell clone increases the magnitude of T cells recruited during an immune response (Moon et al., 2007; Obar et al., 2008). It is very intriguing how efficiently these low numbers of naïve T cells can generate robust immune responses. Naïve T cells migrate through lymph nodes throughout the whole body to eventually meet a dendritic cell (DC) presenting their cognate antigen. TCR binding to the pMHC, as well as the interaction of co-stimulatory molecules and signaling molecules are needed for the activation of the T cell and its clonal expansion. Thereby high numbers of antigen-specific T cells with different phenotypes are generated that migrate to the site of infection and can control the replication of the pathogen during the effector phase (7-10 days after infection). Afterwards, the number of specific T cells decrease about 90% (contraction phase) and only very low numbers of antigen-specific T cells are maintained as memory T cells, even in the absence of their antigen. These memory T cells allow a quick re-activation of effector function upon re-challenge with the respective pathogen (Stemberger et al., 2007b).

1.1.2 Molecular interaction between the TCR and its ligand

The interaction between the TCR and its ligand, the peptide loaded major histocompatibility complex (pMHC), is a major component to regulate activation and signaling in T cell development, naïve T cell priming, fate decision and function. Weak binding of individual TCRs to the MHC are necessary for the interaction; however, TCRs that bind too strongly to self-peptides might cause autoimmunity. The critical role of individual TCRs expressed on T cells is to distinguish between self and non-self and in addition to tightly regulate activation and effector functions upon TCR binding to the pMHC.

1.1.2.1 MHC structure

The MHC molecule is a polymorphic cell surface glycoprotein that has two major forms: MHC class II and MHC class I. MHC class II molecules are recognized by CD4⁺ helper T cells that are important to coordinate adaptive immunity. They usually present peptides derived from endocytosed proteins and are expressed mainly on antigen-presenting cells (APCs). In contrast, MHC class I complexes are expressed on nearly all body cells and present peptides from cytosolic proteins (e.g. viruses or over expressed malignant proteins) to mediate recognition by cytotoxic CD8⁺ T cells for direct target cell lysis (Bjorkman, 1997). In the MHC II complex, the α and β chain are anchored in the cellular membrane (Fig. 1-3 A), while MHC I is anchored with the $\alpha 3$ subdomain of a 44 kDa huge α chain (Bouvier, 2003).

Introduction

The subdomains $\alpha 1$ and $\alpha 2$ present the binding groove for the peptide (Bjorkman et al., 1987) and the soluble, much smaller 16 kDa β chain (β microglobulin) is associated with the α chain (Fig. 1-3 B). The MHC complex is only stable in the presence of a peptide (Ruppert et al., 1993; Bouvier and Wiley, 1994).

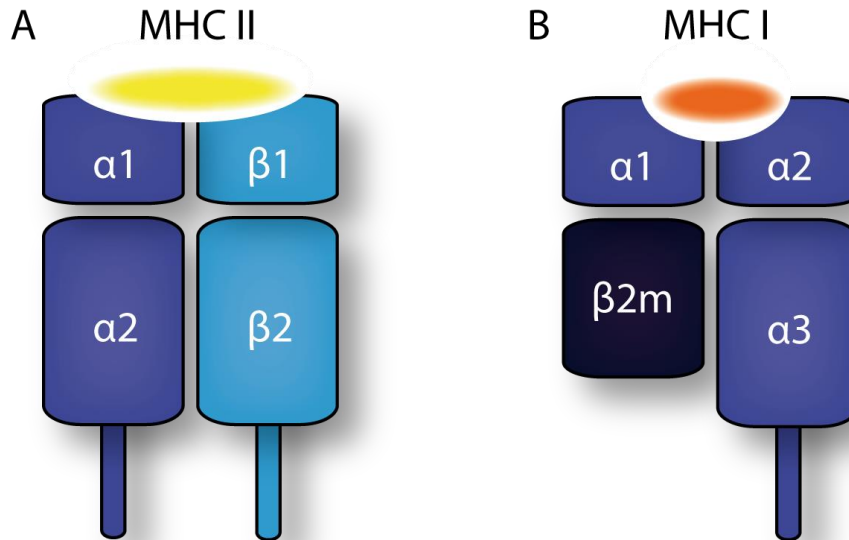


Figure 1-3: Structure of the major histocompatibility complexes I and II.

(A) MHC class II complex loaded with a specific peptide (yellow) is recognized by $CD4^+$ T helper cells and mainly presented on antigen presenting cells (APCs). (B) MHC class I loaded with a specific peptide (orange) is recognized by cytotoxic $CD8^+$ T cells and expressed on the surface of almost all body cells.

1.1.2.2 TCR – pMHC interaction

Insights into the TCR binding modes were derived from many studies on the crystal structure of a number of individual TCRs, pMHCs as well as TCR/pMHC complexes (Rudolph et al., 2006). The interaction between the TCR and the MHC is characterized by a common footprint. The TCR binds diagonally to the pMHC with the TCR α chain contacting the N-terminal end of the antigenic peptide and the TCR β chain directed towards the C-term of the peptide (Bjorkman, 1997) (Fig. 1-4).

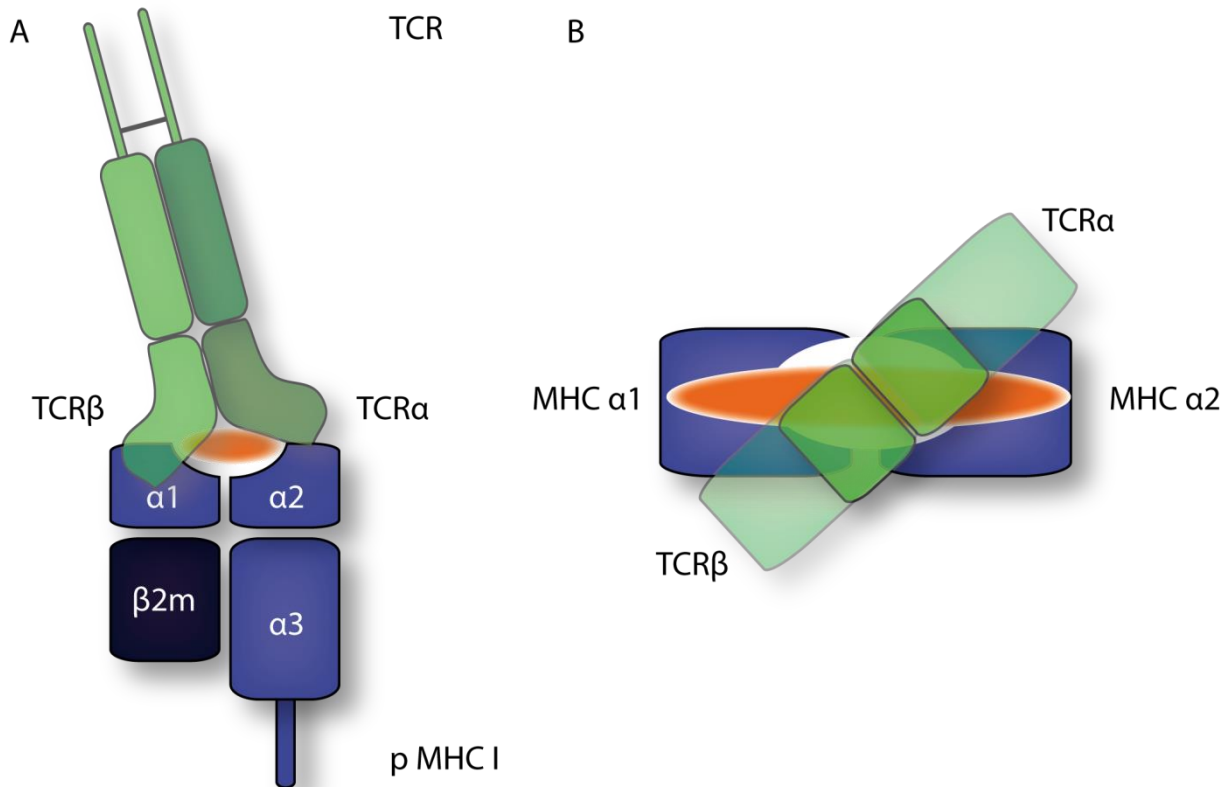


Figure 1-4: T cell receptor (TCR) binding mode to peptide MHC (pMHC).

(A) Diagonal orientation of the TCR to the surface of the pMHC. The TCRβ chain binds to the MHC I α1 (or MHC II α) and TCRα chain to MHC I α2 (or MHC II β) domain with its three CDR loops. (B) The pMHC molecule is shown from above. Adapted from (Bridgeman et al., 2012).

In the TCR – pMHC contact zone, the TCR CDR1 loops can bind to the MHC or the antigenic peptide. In contrast, CDR2 contacts the MHC, while CDR3 binds dominantly the peptide (Davis and Bjorkman, 1988; Jorgensen et al., 1992b; Jorgensen et al., 1992a). Despite common TCR binding modes (Reinherz et al., 1999; Hennecke et al., 2000), the interaction between an individual TCR and its cognate pMHC cannot be predicted by its sequence, but only by its crystal structure (Garboczi et al., 1996; Ding et al., 1998). Differences in TCR – pMHC binding modes further depend on the twist, tilt and shift of a TCR (Teng et al., 1998; Bridgeman et al., 2012). TCRs with identical CDR1 and CDR2 sequence have been shown to interact in different modes with pMHC (Teng et al., 1998) suggesting a plasticity in binding modes. Even the same TCR can change its binding mode between different ligands as shown in structural analysis of the murine 2C TCR in interaction with a self and foreign ligand (Colf et al., 2007; Bridgeman et al., 2012). Further, different TCRs can bind the same pMHC in

distinct ways (Ding et al., 1998; Macdonald et al., 2009). A number of conserved hotspot interaction between a TCR and a MHC have been suggested (Rudolph et al., 2006); however, some TCRs are able to bind a pMHC even independently from these described interactions (Tynan et al., 2005; Burrows et al., 2010). These effects might be partly explained by the additional conserved binding of the co-receptor CD8/CD4 to the MHC molecule. Taken together, although there is a general conserved binding mode of a TCR over the pMHC surface, the different molecular rules that determine TCR specificity may be distinct and still are not fully understood.

1.2 TCR - pMHC binding strength

The quantification of the binding strength between an individual TCR and its cognate ligand is of major interest in T cell immunology. Correlation of TCR binding strength to the functional outcome of the T cell in response to stimulation with its pMHC delivers important insight into how T cells are regulated to recognize and control invading or persisting pathogens, as well as malignancies, without causing any autoimmunity. Further, this would help to manipulate T cell responses, e.g. by optimizing vaccination strategies or passive immunization (adoptive T cell therapy).

1.2.1 TCR affinity

The major difference between T cell clones in the diverse TCR repertoire is their unique TCR. The structure of a TCR is genetically conserved in its sequence and determines the non-covalent intermolecular interaction to a pMHC ligand (hydrogen bonds, electrostatic interactions, Van der Waals forces). The strength of this interaction is the TCR affinity. A precise measurement of TCR affinity is the dissociation constant K_D , integrating pMHC association (k_{on} -rate) and dissociation (k_{off} -rate). For the widely used Biacore surface plasmon resonance (SPR) assay, the TCR and the pMHC are isolated from their cellular environment and analyzed in a fluid phase in three-dimensions (3D). Recombinant receptors (TCR) or ligands (pMHC) are immobilized on a sensor and the binding (k_{on} -rate in M^{-1}, s^{-1}) of increasing amounts of the interaction partner is detected by an increase in response units on the sensor. The dissociation (k_{off} -rate in s^{-1}) leads to a decrease in response units that can be monitored over the time (Fig. 1-5).

Introduction

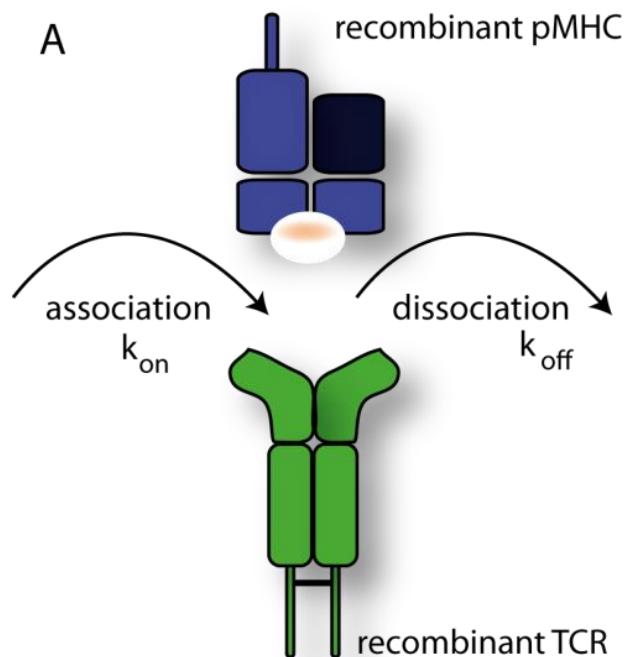


Figure 1-5: Three dimensional TCR affinity measurements.

The structure of an individual TCR defines the biochemical interactions with its pMHC ligand. Interaction between a TCR and a pMHC is defined by TCR binding affinity and can be determined by the dissociation constant defined by association- (k_{on}) and dissociation- (k_{off}) rate. pMHC and TCR are recombinantly expressed. TCR or pMHC are immobilized to a detector surface in biacore surface plasmon resonance experiments.

Due to their maturation in the thymus, TCRs bind their ligands in comparison to the closely related immunoglobulin receptors only weakly (antibody-ligand $K_D = \text{nM} - \text{pM}$ compared to TCR-ligand $K_D = 0.1$ to $> 500 \mu\text{M}$; with k_{on} and k_{off} -rates in the range of seconds; $K_D = k_{on}/k_{off}$) (van der Merwe, PA. and Davis, 2003; Bridgeman et al., 2012). Accumulating SPR data from a variety of different TCRs to their pMHC ligands and also altered peptide ligands delivered insight into the contribution of TCR affinity to T cell activation. Bridgeman *et al.* clustered a broad dataset of characterized TCRs based on their mean K_D values: TCR affinity to foreign or allogenic pMHC is strikingly high (mean $K_D = 8 \mu\text{M}$); pMHC I-specific TCRs have a higher affinity (mean $K_D = 32 \mu\text{M}$) as compared to pMHC II TCRs (mean $K_D = 92 \mu\text{M}$), and TCRs recognizing self-pMHC are at the lower range of affinities (mean $K_D = 90 \mu\text{M}$) (Bridgeman et al., 2012). The low affinity of self-reactive T cells can be explained by the thymic selection of T cells, preventing autoimmunity; however, representing a huge hurdle in tumor immunology where malignant cells often overexpress self-ligands (Davis et al., 2003; Huseby et al., 2006). Based on the majority of SPR measurements, the k_{off} -rate is suggested as the best correlative to T cell activation. There are nevertheless exceptions; a fast k_{on} -rate can compensate for a

Introduction

short k_{off} -rate (or dwell time) in high avidity CD8 and CD4 T cells upon stimulation with altered peptide ligands (APLs) (Boulter et al., 2007; Govern et al., 2010). Therefore, a high avidity TCR is characterized by either a slow k_{off} -rate or a fast k_{on} -rate (Bridgeman et al., 2012).

There is accumulating evidence that affinity values based on 3D SPR measurements do not reflect the *in situ* TCR – pMHC interaction of anchored molecules on opposing cells and do not correlate to T cell functionality (Adams et al., 2011). In addition, the challenging expression of TCRs does not allow for direct *ex vivo* analysis of antigen-specific T cell populations (Reiser et al., 2009). Another component directly involved in the biochemical TCR/pMHC interaction is the co-receptor CD8 binding to the $\alpha 3$ domain of the MHC heavy chain (Gao et al., 1997; Kern et al., 1998). This binding has been shown to stabilize the TCR/pMHC interaction 10-fold (Luescher et al., 1995; Garcia et al., 1996; Wooldridge et al., 2005). Both forms of the CD8 dimer ($\alpha\alpha$ or $\alpha\beta$) on its own bind with similar affinity to the MHC; however, there are disparate binding affinities for different MHC alleles ($K_D= 50\text{-}200\mu\text{M}$, summarized in (van der Merwe, PA. and Davis, 2003).

1.2.2 TCR avidity

In contrast to TCR affinity, the TCR avidity is not only influenced by the TCR structure, but additional parameters are taken into account. Here, TCRs are analyzed in their physiological context, meaning restricted in two dimensions in the membrane on the surface of a T cell. Most people define TCR avidity as the functional outcome of antigen-specific T cells upon stimulation with specific peptide. T cells are co-cultured with APCs loaded with increasing amounts of the respective target peptide and subsequently, the secreted cytokines or target cell lysis are analyzed as a readout for the T cells peptide sensitivity (Fig. 1-6). Often the peptide concentration that induces half-maximal effector function (EC_{50}) is used to compare the functional avidity of different T cells. Functional avidity is not only dependent on the hardwired TCR structure, but further influenced by cellular components defined by different T cell phenotypes and states of cell activation. The densities, as well as the distribution of TCRs, co-receptors and co-stimulatory molecules on the surface of a T cell, their motility in the cell membrane and further the efficiency of intracellular signaling are all components influencing the functional avidity of T cells (Viganò et al., 2012). Nevertheless, the TCR sequence and its structure have been shown to be a major determinant of functional avidity.

TCRs isolated from high versus low avidity T cells reconstitute their functional avidity upon transgenic re-expression on other cells (Morgan et al., 2003).

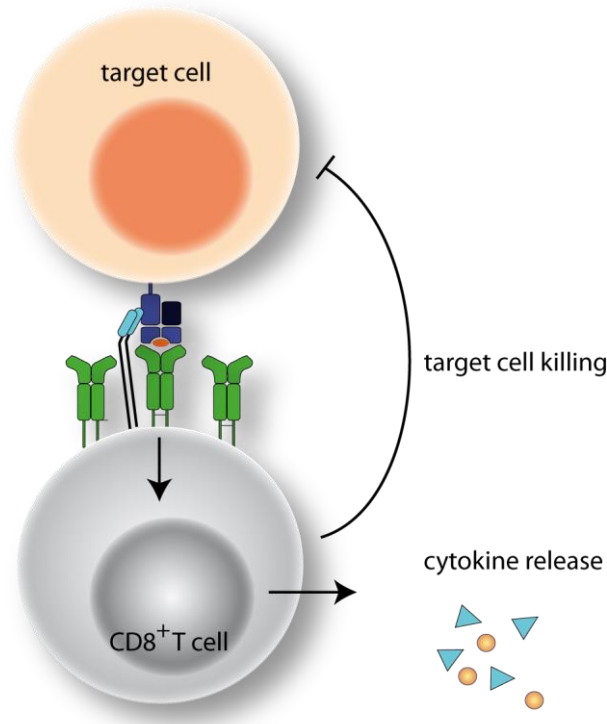


Figure 1-6: Functional TCR avidity describes the effector functions of antigen-specific T cells after peptide stimulation.

After binding of a specific pMHC ligand and T cell activation, the cytotoxic $CD8^+$ T cell produces cytokines and mediates target cell lysis. A dominant determinant of effector functions is the TCR binding affinity; however, cell intrinsic factors such as phenotype, TCR and co-receptor expression, as well as the composition of the cell membrane influence functional readouts.

Other methods to measure TCR avidity on cells are based on MHC multimer staining. Recombinant pMHC I molecules are multimerized on a fluorescence-conjugated Streptavidin to allow stable staining of the otherwise weak pMHC monomeric ligands. This interaction is even stronger and more stable for high avidity T cells, while MHC multimers can partly dissociate from low avidity T cells (Fig. 1-7). Based on this hypothesis, the MHC multimer staining intensity is often used to compare the TCR avidity among different cells. In addition, the dissociation of MHC multimer over the time from *ex vivo* T cells is analyzed to estimate TCR k_{off} -rate and half-life (Wang and Altman, 2003; Stone et al., 2011). Although these assays allow for direct *ex vivo* measurement on the T cell surface, they are unfortunately

prone to a high degree of variability and do not allow to compare different experiments (Wang and Altman, 2003).

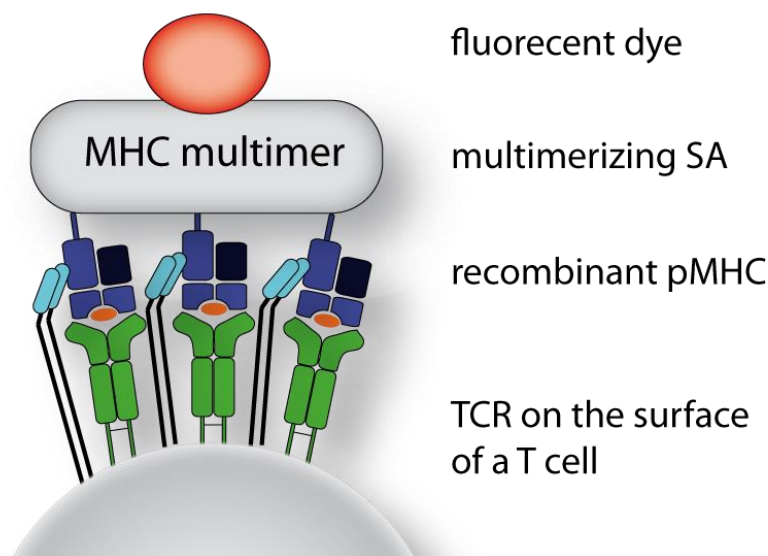


Figure 1-7: MHC multimers are used to detect and analyse antigen-specific T cells.

(A) Recombinant biotinylated pMHCs are multimerized on a Streptavidin (SA) coupled to a fluorescent dye. MHC multimers can stably bind to TCRs expressed in the surface antigen-specific T cells for *ex vivo* analyses. They are used for detection, purification of specific T cells and also to assess TCR binding avidity. TCR avidity is assessed as multimer binding by analysing multimer staining intensity, the concentration needed for maximal staining intensity or by multimer dissociation detected in the decrease of multimer fluorescence intensity over the time.

1.2.3 Structural TCR avidity

During the last years additional methods that assess TCR binding on the T cell surface have been developed. Biophysical methods were adapted to analyze the force of the interaction between immobilized recombinant expressed pMHC and TCRs expressed on T cells by atomic force microscopy (AFM) or a biomembrane force probe (BFP) (Huang et al., 2010; Puech et al., 2011). In AFM a cantilever tip coated with pMHC is approached to the T cell to initiate binding and is then separated with controlled force (Fig. 1-8 A). The bending of the cantilever differs if a binding of pMHC and TCR on the cell surface occurred (Puech et al., 2011). In the BFP assay, a red blood cell with a pMHC coated bead is approached to and separated from a T cell, both aspirated by micropipettes (Fig. 1-8 B) (Huang et al., 2010). The assays allow determining the adhesion frequency upon contact of cell and pMHC. In the BFP assay the RBC with pMHC and the T cell can also be clamped at a close position to estimate

Introduction

the binding and unbinding events during thermal fluctuation (Huang et al., 2010). Recently, in this assay, a constant force was applied in the clamped position and the life-time of TCR-pMHC interaction was determined. The authors suggest stabilized TCR – pMHC binding via catch bonds when slight forces are applied (forces that naturally occur in a synapse during T cell - APC interaction) (Pryshchep et al., 2014). The life-times were very short (0-60 seconds for the identical OT-1 TCR), complicating the comparison of different TCR-ligand binding- and dissociation kinetics.

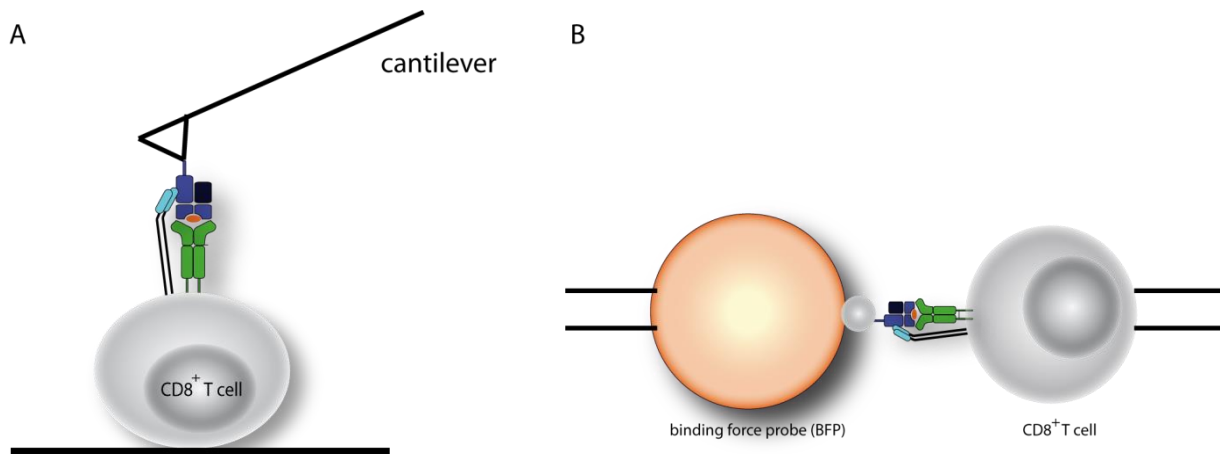


Figure 1-8: Force measurements to assess TCR binding strength.

(A) In atomic force microscopy (AFM) the tip of a cantilever is coated with a recombinant pMHC (dark blue). It is approached to the surface of a specific T cell to allow binding of the pMHC to the TCR (green) on the surface of the T cell and separated with constant force. After successful TCR-pMHC binding the bending of the cantilever is changed. (B) Similarly, a binding force probe (BFP) such as a red blood cell (RBC) carrying a pMHC coated bead is approached to and separated from a specific T cell. RBC and T cell are held and moved by micropipettes. In both assays, binding or adhesion frequency is used as a measure for TCR binding strength. Adapted from (Huang et al., 2010; Puech et al., 2011).

To allow kinetic analysis of pMHC association and dissociation on cells, fluorescence resonance energy transfer (FRET) between an antibody fragment (Fab) on the TCR and a MHC II monomer loaded with a fluorescently labeled peptide were used in single molecule microscopy (Fig. 1-9) (Huppa et al., 2010). The single molecule assay and the BFP assay measuring structural TCR avidity (trimolecular TCR/CD4 or CD8/pMHC interaction) on the two-dimensional surface of a T cell suggested accelerated binding kinetics as compared to recombinant expressed TCRs in SPR, especially in regards to the k_{on} -rate (Huang 2012, 2013), as well as a more relevant correlation to T cell activation (Adams et al., 2011).

Introduction

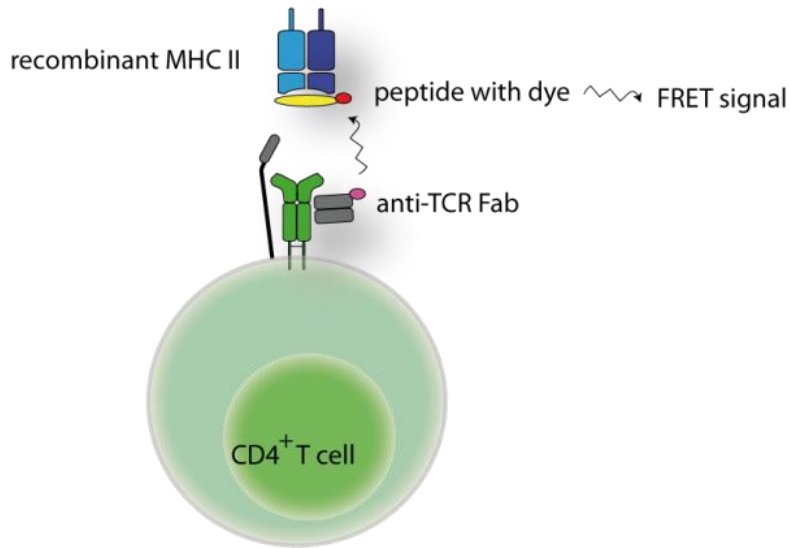


Figure 1-9: Kinetic measurements of monomeric MHC II binding and unbinding on living T cells.

Fluorescence resonance energy transfer (FRET) between a fluorochrome (magenta) on an antibody fragment (Fab) bound to the surface expressed TCR and a fluorochrome (red) on the peptide presented on a recombinant MHC II can be detected with single molecule microscopy. Adapted from (Huppa et al., 2010).

1.2.4 T cell activation upon ligand binding

The activation of a T cell is dependent on a variety of parameters: the duration of T cell – APC contact, the persistence of antigen, as well as the density of peptide on the MHC. Most importantly, the biochemical interaction between the TCR and its cognate pMHC (TCR affinity) regulates the activation (Corse et al., 2011). In this section, the molecules involved and the different hypotheses on the activation of a T cell are introduced.

1.2.4.1 T cell signaling

Since the TCR $\alpha\beta$ chains cannot mediate intracellular signaling, they are always associated with the CD3 complex. The CD3 complex consists of different transmembrane proteins (δ , ζ , γ , ϵ) that interact via negatively charged amino acids with the TCR transmembrane domains. To initiate T cell signaling, each δ , γ , ϵ chain carries one, each ζ chain two immunoreceptor tyrosine-based activation motifs (ITAMs) on their intracellular domain that can be phosphorylated upon TCR activation (Fig. 1-10). In addition to the TCR-pMHC interaction, the co-receptor CD4 or CD8 binds to the MHC and stabilizes the interaction. It is controversially discussed whether co-receptor binding initiates the contact to the MHC and

Introduction

allows the TCR to screen the peptide, or whether the TCR first binds to certain hotspots on the MHC and recruits CD8 to get involved in the tri-molecular binding (Jiang et al., 2011; Puech et al., 2011; Bridgeman et al., 2012). In addition to the prolonged TCR-pMHC I dwell time, the CD8 co-receptor recruits the src family kinase Lck to the CD3 complex where it can initiate cell signaling by phosphorylation of the ITAMs (Veillette et al., 1988; Purbhoo et al., 2001; Stepanek et al., 2014). It has been suggested that upon agonist pMHC binding, the TCR changes its conformation opening the ITAMs for Lck phosphorylation (conformational change model). In the kinetic segregation model, the TCR/co-receptor/pMHC interaction initiates enrichment of Lck and exclusion of other molecules from the immunological synapse by either molecule size or huge TCR-pMHC binding energy. The exclusion of molecules such as the transmembrane phosphatase CD45 triggers T cell signaling. The first step in the T cell signaling is the phosphorylation of tyrosine residues of the ITAMs on the CD3 chains by Lck, resulting in the recruitment of the kinase ZAP70 to the CD3 ζ chain that becomes also phosphorylated by Lck. Activated ZAP70 phosphorylates the linker for activation of T cells (LAT) and downstream adapter and signaling molecules are recruited, initiating a variety of downstream effects such as the enhanced affinity of integrins to stabilize cell-cell interaction and the transcriptional activation of genes associated with growth, differentiation, actin reorganization and proliferation (Fig. 1-10) (Brownlie and Zamoyska, 2013).

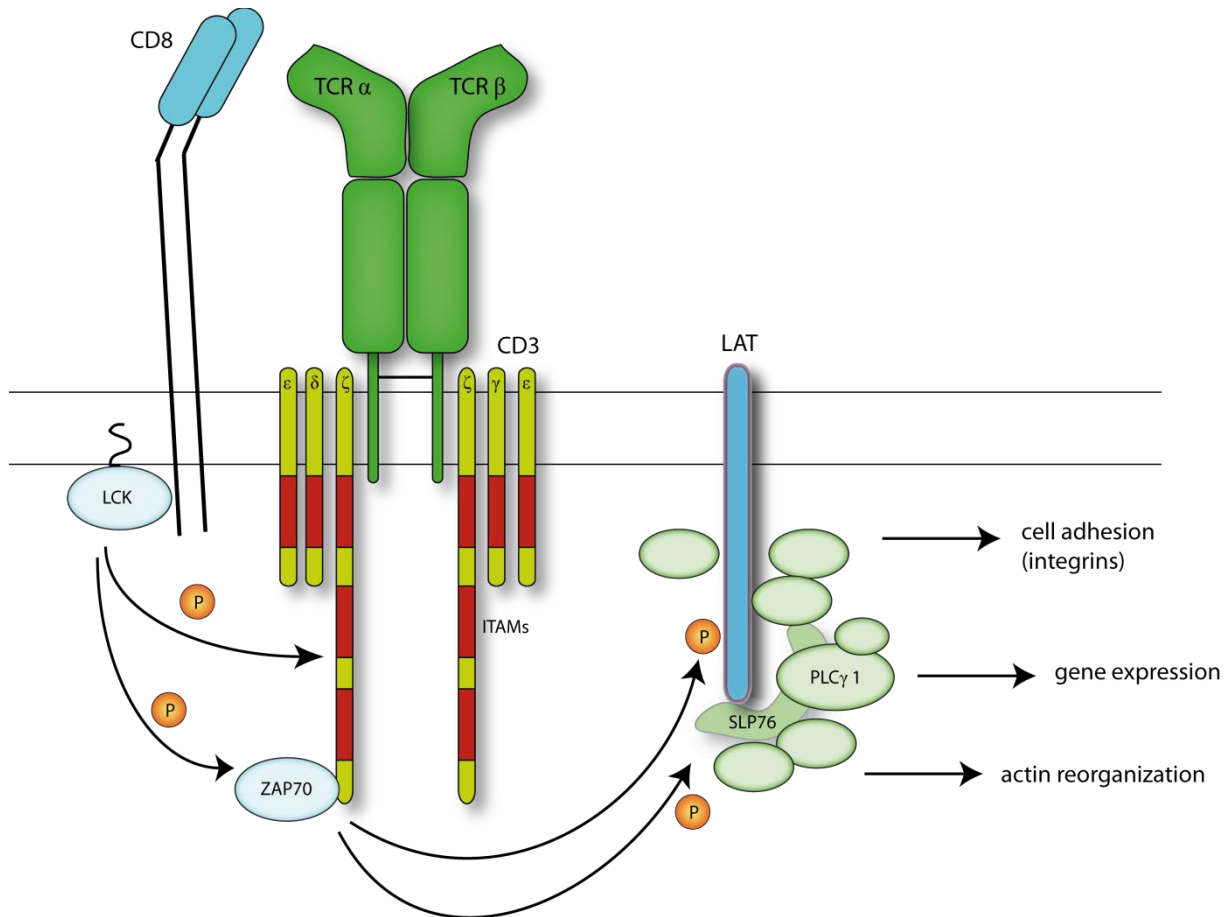


Figure 1-10: TCR-CD3 complex and initial signaling process.

After specific pMHC binding and T cell activation, Lck recruited by the co-receptor CD8 initiates phosphorylation of the ITAMs on the CD3 chains. Kinase ZAP70 is recruited and phosphorylated by Lck. Activated ZAP70 phosphorylates linker for activation of T cells (LAT) and adapter molecules. Downstream effects mediate cell adhesion by integrins, gene expression and actin reorganization. Adapted from (Brownlie and Zamoyska, 2013).

1.2.4.2 T cell activation

How the binding of a TCR activates intracellular signaling is very challenging to address. Two major models can be discussed: The occupancy model requires a sufficient number of TCRs engaged with its ligand (Lever et al., 2014), while the kinetic proofreading depends on the time, the TCR is engaged with a cognate pMHC (McKeithan, 1995).

The TCR affinity is the major determinant for the activation in the occupancy model and a low affinity TCR can only be activated by a high density of pMHC on the APC. In the kinetic proofreading model, a TCR can distinguish between agonist and antagonist because the T cell only becomes activated, if the complete intracellular activation cascade can be fulfilled. As

Introduction

soon as the pMHC dissociates from the TCR, the activating signals are reversed. Based on this model, further ideas have developed: The kinetic proofreading model with sustained activation allows a serial triggering to accumulate activating signaling steps during the re-binding of pMHC ligands. In this model, T cells with fast k_{off} -rates and relatively low TCR affinity (K_D) can become activated if the pMHC antigen density on the APC is high or if they have a high k_{on} -rate. Serial triggering models are in general more dependent on the number of contacts between the TCR and pMHC than the concentration of pMHC on the APC. The kinetic proofreading model with limited activation depends mostly on the number of contacts where each TCR engagement is essential for the signal activation pathway; however, it is less dependent on the density of pMHCs. In this model, the T cell returns to the basal activation status upon pMHC unbinding. This is a mechanism to prevent the activation of a T cell with antagonist ligands of low affinity. A further refining is the kinetic proofreading model with a negative feedback loop. Here, intermediate activation signaling events can be reversed by e.g. SHP1, a SH2 domain containing tyrosine phosphatase. This phosphatase can be recruited by Lck to associate with and dephosphorylate the TCR/CD3 complex. A recent review suggests the kinetic proofreading model with limited signaling as the best model to describe most of the published data on 3D and 2D TCR binding measurement and their correlation to T cell sensitivity or activation (Lever et al., 2014). The different models of T cell activation highlight the TCR affinity as a major determinant. Understanding the contribution of TCR affinity to activation during T cell priming or during an immune response in infection can influence the development of therapeutic strategies. Knowledge on TCR affinity could help guiding the selection of the antigen-specific T cells or TCRs for gene therapy with optimal avidity for adoptive T cell therapy or in immune monitoring as a diagnostic marker.

1.3 TCR avidity in infection

Besides the precursor frequency of naïve T cells, the antigen density and stability on the APC, the TCR avidity has a dominant role in the activation of naïve T cells during a *de novo* infection (Smith et al., 2000; Lanzavecchia, 2002). Upon primary infection, a variety of antigen-specific T cell clones with disparate affinities is clonally expanded building up a highly diverse immune response (Malherbe et al., 2004). Although low avidity T cells expand during this very early activation, they rapidly contract and high avidity are preferentially maintained during the memory phase (Zehn et al., 2009). Consequently, T cells that respond during a re-infection with the same pathogen are characterized by a higher TCR avidity

Introduction

indicating an affinity maturation or clonal focusing (Busch and Pamer, 1999; Peter A. Savage, Jay Boniface and Mark M. Davis, 1999; van Heijst, Jeroen W J et al., 2009). High avidity T cells can become activated by lower densities of pMHC on infected cells and initiate T cell effector function more rapidly in comparison to low avidity T cells (Derby et al., 2001). In addition, they are often cross-reactive to altered peptide ligands (APLs) (Chervin et al., 2009), in contrast to low avidity T cells not responding to APLs (Manning and Kranz, 1999). The transfer of antigen-specific high avidity T cells has been shown to mediate a better protection and pathogen clearance as compared to low avidity T cells. Taken together, these data illustrate that high avidity T cells are preferentially selected during acute infection and that they have a beneficial effect on the clearance of infection.

In these models of acute infection, the pathogen is eradicated and antigen-specific T cells are maintained in the absence of antigen. Some pathogens establish a chronic persistent infection such as the cytomegalovirus (CMV). CMV can be reduced to very low levels; however, it needs constitutive surveillance by T cells. CMV strongly interacts with the immune system and induces remarkable changes in the T cell responses that will be discussed in the following chapters.

1.3.1 Cytomegalovirus (CMV)

Human Cytomegalovirus (HCMV) is a highly prevalent beta herpes virus type 5. It infects 50 – 90 % of the population through the contact of mucosal epithelial cells with contaminated body fluids such as saliva. In comparison to its family member herpes simplex virus 1 and 2, Epstein-Barr virus, varicella-zoster virus and human herpes virus 6-8, HCMV has the largest genome of 235 kb encoding more than 200 genes. In a mature HCMV virion (200 – 300 nm) this genome is packaged in a double stranded linear DNA enclosed by an icosahedral capsid and enveloped by the tegument and a lipid bilayer containing viral glycoproteins (Fig. 1-11). The tegument mainly consists of the phosphoprotein 65 (pp65) or unique long 83 (UL83) and other viral proteins such as the virion transactivator pp71, the herpes core virion maturation protein pp150 and pp28, as well as small amounts of cellular and viral RNA. Tegument proteins are either involved in the assembly of virions and disassembly during virus entry or they modulate the host response upon infection. The glycoproteins gB, gH, gL, gM, gN, gO integrated in the host derived lipid bilayer mediate attachment and entry into target cells (Harari et al., 2004; Crough and Khanna, 2009).

Introduction

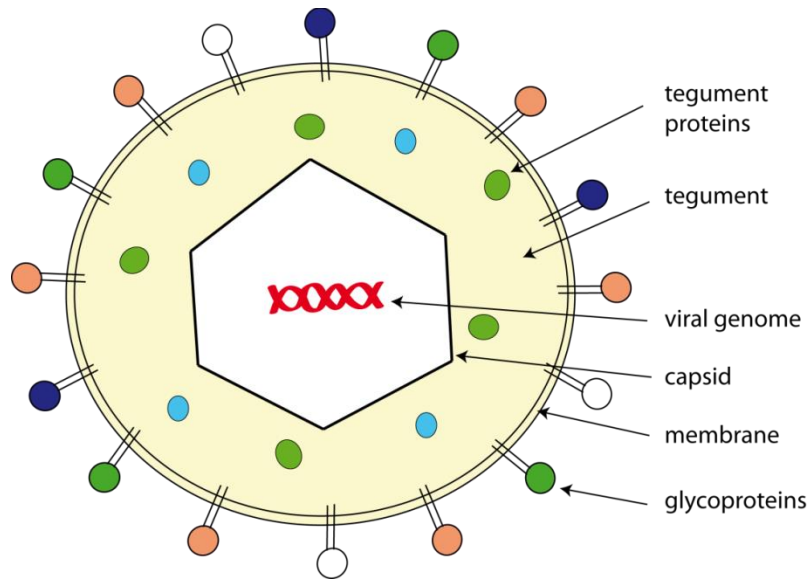


Figure 1-11: Structure of the Cytomegalovirus virion.

The double stranded viral DNA genome is encapsulated in an icosahedral capsid and enveloped by the tegument containing different tegument proteins and a membrane lipid bilayer. Different glycoproteins are integrated in this viral outer membrane.

1.3.1.1 CMV life cycle

The life cycle of HCMV is illustrated in Fig. 1-12. HCMV can enter target cells either directly through fusion or it can be taken up by endocytosis. To attach to a target cell, viral glycoproteins can interact with cellular receptors such as the platelet-derived growth factor α and mediate fusion of virus envelope with the cell membrane. The virus nucleocapsid is subsequently released into the cytoplasm and translocated into the nucleus. Here, the viral DNA is released and the transcription of genes in three overlapping phases is initiated. With the DNA release in the nucleus, the transcription of immediate early (IE) genes starts during the first 2 hours of infection. IE genes initiate the transcription of delayed early (E) genes during the first day and late (L) genes are transcribed as a third step after one day of infection. Different viral proteins are synthesized, accumulate and virus DNA is replicated to allow the encapsulation of the replicated DNA as capsids. The capsid is translocated to the cytoplasm where it is enveloped at the endoplasmic reticulum-Golgi intermediate compartment. The final envelopment is mediated at the cell membrane where the mature HCMV virion is released by exocytosis (Crough and Khanna, 2009).

Introduction

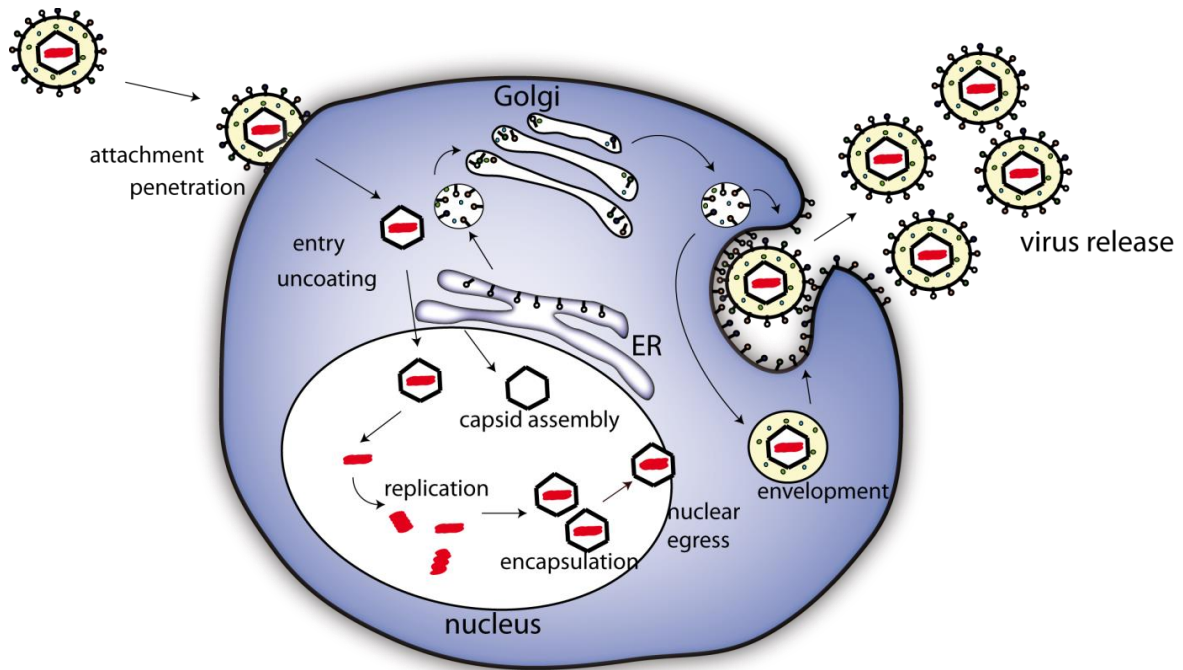


Figure 1-12: CMV primary infection and life cycle.

The CMV virion attaches to the cell surface where its nucleocapsid and tegument proteins immediately enter the cytosol. The nucleocapsid is translocated to the cellular nucleus. Here, the viral DNA is released, the transcription of viral genes and DNA replication starts. Capsid proteins are assembled in the nucleus to encapsulate the viral DNA. Encapsulated CMV DNA is released from nucleus to the cytosol where it is enveloped in a membrane containing viral tegument proteins. The virus particle is released from the cytosol and thereby coated with glycoproteins located at the cellular membrane. Adapted from (Crough and Khanna, 2009).

1.3.1.2 CMV distribution and latent persistence

During primary infection, CMV virions in body fluids such as salivary, urine or semen infect mucosal epithelia cells. The virus replicates and distributes infectious virions. Mainly myeloid cells including CD34⁺ hematopoietic cells and monocytes become infected. Monocytes circulate in the blood throughout the body and migrate to peripheral tissues. They differentiate into macrophages or dendritic cells, which initiates productive CMV infection and dissemination of infectious virions in surrounding tissues. Bone marrow CD34⁺ hematopoietic precursor cells (HPC) are an ideal reservoir for viral latency. They however can reactivate virus upon differentiation (e.g. into monocytes) and facilitate systemic distribution. Efficient proliferation of the virus is enabled by the productive infection of ubiquitous cell types, such as fibroblasts and smooth muscle cells. Transmission of HCMV to new hosts is mediated by shedding of virions from infected mucosa epithelia cells (Fig. 1-13) (Landais and Nelson, 2013).

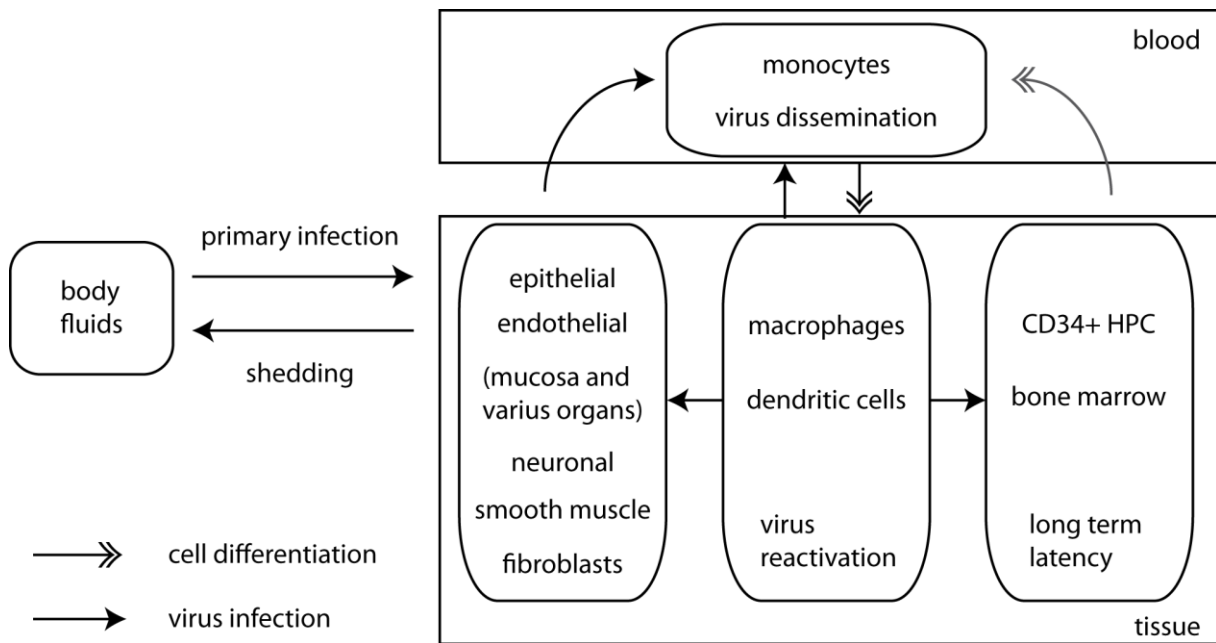


Figure 1-13: CMV infection, distribution and persistence in different cell types.

CMV virions in body fluids cause primary infection of mucosal epithelial and endothelial cells. In these cells, CMV replicates and sheds infectious virions into the body fluids. Circulating monocytes become infected and disseminate virus throughout the body. They migrate to peripheral tissues and differentiate into macrophages. From here, virus replicates, sheds and infects other body cells (e.g. neuronal, smooth muscle, fibroblasts) or CD34⁺ hematopoietic cells (HPC) in the bone marrow. Infected CD34⁺ HPCs are suggested to maintain long term latency and infection with CMV. Differentiation of CD34⁺ HPCs into monocytes allows repetitive dissemination of virus. Adapted from (Landais and Nelson, 2013).

HCMV establishes a life-long latent infection in cells such as monocytes, leukocytes, epithelial cells of salivary glands and cervix (Harari et al., 2004) with recurrent episodes of virus shedding and distribution. The mechanisms of how HCMV establishes viral latency and persistence are poorly understood. Viral latency in infected cells could be established through different mechanisms: 1. The virus enters the cell and directly goes into a latent state without reproduction. 2. After productive replication, additional viral gene products induce a switch into a latency phase or 3. During virus reproduction, the IE – E – L path is interrupted as soon as one of the CMV gene products is absent and the virus DNA genome is silenced (Crough and Khanna, 2009).

Notably, the transcription of viral genes is very distinct from productive infection. Transcription is limited to very few “latency-associated transcripts” (LAT). The most prominent are the major IE genes (Fig. 1-14). However, latency establishment and

Introduction

maintenance is not dependent on these genes (Crough and Khanna, 2009). One gene found to be required for initiation of viral latency is the UL138. Gene expression during latency might be initiated by stochastic desilencing of viral DNA, as well as strong enhancing promoters of certain genes and/or stability of the transcripts (Seckert et al., 2012). Reactivation from latency phase into the productive phase can be induced by immunosuppression, inflammation, infection or stress. One explanation is the binding of TNF α to its receptor on latent infected cells that induces activation of protein kinase C, NF- κ B and AP-1. They enhance the transcription of viral IE genes and thereby initiate the IE – E – L path of productive infection (Fig. 1-14). Additionally, inflammation results in increased cAMP level. Catecholamines, nor- and epinephrine and increased cAMP concentrations lead to IE1 promoter stimulation and virus reactivation (Crough and Khanna, 2009; Seckert et al., 2012).

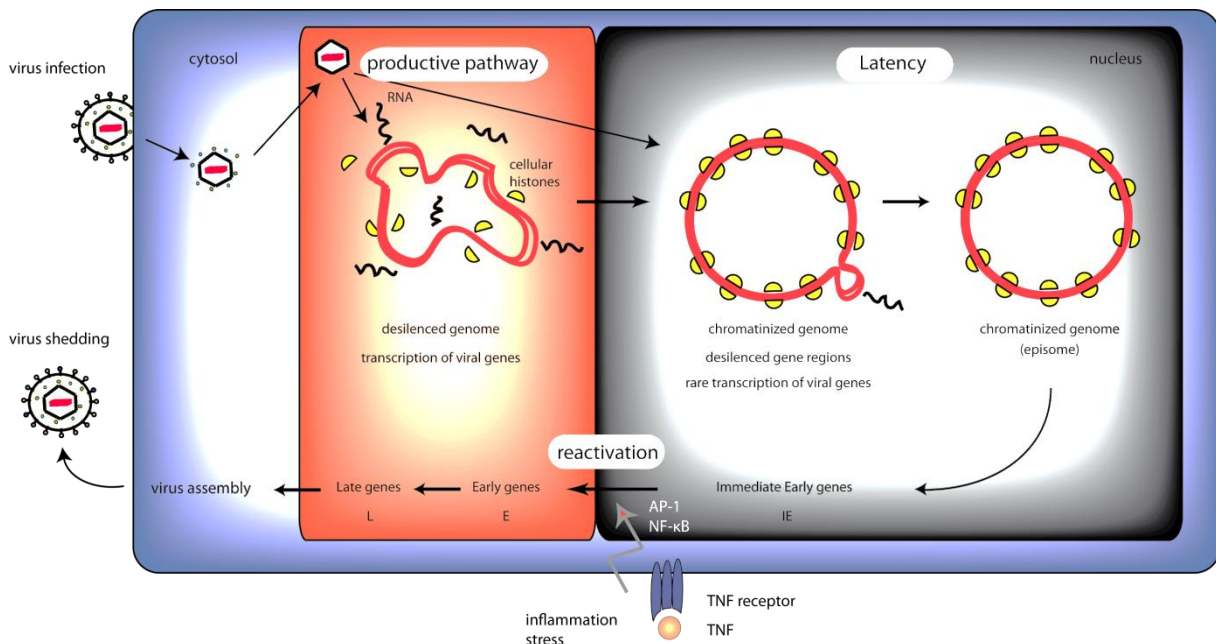


Figure 1-14: Productive and latent CMV infection.

After infection, viral DNA enters the cellular nucleus. During productive infection the genome is desilenced and viral genes are transcribed to assemble and release infectious virions. For viral latent infection, the transcription of genes stops and the viral genome is chromatinized. During latency some immediate early (IE) genes are transcribed stochastically. Successful CMV reactivation requires the progressive transcription of early (E) and late (L) genes that can be induced by inflammation, infection and stress via the induction of certain transcription factors. For example, binding of TNF to the TNF receptor activates cellular AP-1 and NF- κ B transcription factors that induce transcription of viral genes (Seckert et al., 2012).

1.3.2 Cytotoxic CD8⁺ T cell responses towards CMV infection

Primary infection with CMV is mostly asymptomatic in healthy individual, because the virus is targeted efficiently by different components of the immune system. Innate immune receptors recognize virus infection immediately, produce cytokines and recruit Natural Killer (NK) cells to limit virus dissemination. Virus particles are engulfed by dendritic cells that migrate to lymph nodes to present processed viral peptides to naïve T cells. Antigen-specific naïve T cells become activated, migrate to the site of infection and control viral replication and dissemination. In contrast to other infections, the virus persists and limits its immune recognition by entering the latency phase. A constitutive immune surveillance is needed to prevent viral re-activation. It is still discussed which cells are most important for immune surveillance. Most data indicates a major contribution of CD4⁺, NK and CD8⁺ T cells. CD4⁺ T cells are less protective than NK cells and the most important cells that prevent virus reactivation are the cytotoxic CD8⁺ T cells (Riddell and Greenberg, 1995). In the absence of NK and T cells, the CMV is a major cause of morbidity and mortality (La Rosa and Diamond, 2012).

The CMV targets recognized by antigen-specific T cells are very diverse and differ between individual hosts. Large screenings with peptide pools derived from different CMV genes used for stimulation of T cells from different donors revealed two CMV antigens as major T cell targets: The major tegument protein pp65 (UL83) that can be presented by a variety of different MHC alleles, and the abundantly recognized transcription factor IE1 (UL123). Other CMV genes such as pp150, gB, gH, pp50 and pp28 are recognized less frequently (Elkington et al., 2003; Sylwester et al., 2005). CMV-specific T cell populations change dramatically during the lifetime of the host in the chronic latent phase of the infection. The next sections will explain the current knowledge about T cell responses to CMV during acute and chronic infection.

1.3.2.1 T cell responses in the acute phase of CMV infection

Since primary infection with CMV causes only mild illness and is rarely detected in otherwise healthy individuals, the studies on T cell responses early after infection are limited (Waller et al., 2008). Most studies on primary CMV infection were done in patients after transplantation, after congenital infection or HIV infection. CMV-specific T cells expand in high numbers 10 days after initial infection, while the peak of CD8 T cell expansion occurs 14 days later (Gamadia et al., 2003; Harari et al., 2004). Although the initial T cell repertoire recruited

early during primary infection is diverse, it rapidly focused to one or two distinct TCR V β chains, each with a disparate V α and individual T cell clones are extensively expanded (Weekes et al., 1999; Harari et al., 2004). These dominant V β chains can differ among the individual donors as shown for the HLA-A2/pp65 (Wills et al., 1996; Peggs et al., 2002). The rapid repertoire focusing is caused by the selection of T cell clones with optimal TCR avidity. It could be shown that high avidity T cell clones are preferentially selected during acute infection (Lydie Trautmann, 2005; Price, 2005; Day et al., 2007). Interestingly, pp65-specific T cell responses are found in higher frequency as compared to IE1-specific T cells early after infection. T cells specific for pp65 contract after their peak expansion similar to T cells in other acute infections, while IE1-specific T cells can accumulate continuously (Fig. 1-15) (Khan et al., 2007).

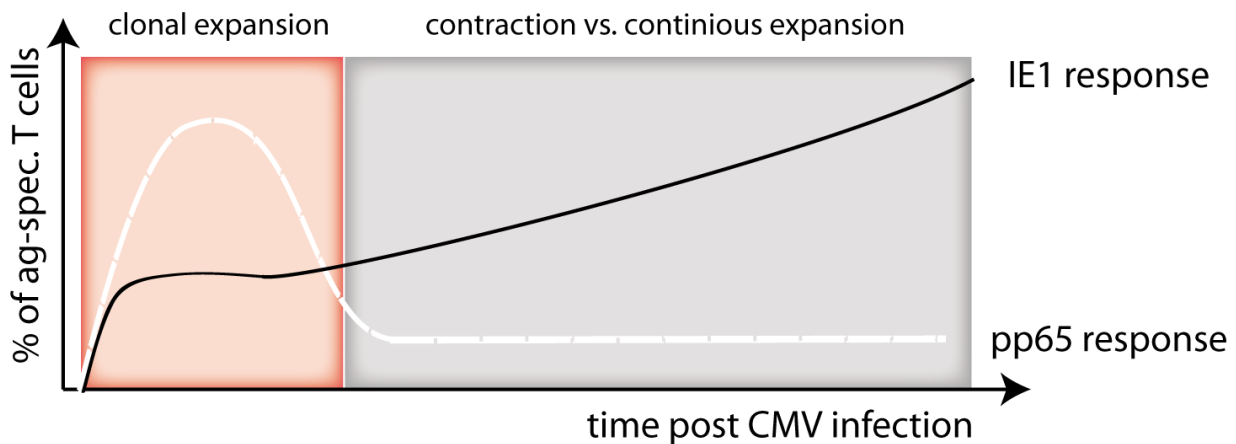


Figure 1-15: Different kinetic patterns of IE1 and pp65-specific T cell populations during CMV infection.

Similar to T cell responses during acute infection, pp65 expands during primary infection, followed by enormous contraction with low frequency antigen-specific (ag-spec.) T cells persisting. In contrast, IE1-specific T cells accumulate continuously after primary infection.

1.3.2.2 T cell responses in the chronic phase of CMV infection

In contrast to memory T cells that are maintained after clearance of the pathogen in the absence of antigen, CMV-specific T cells progressively shift towards a terminally differentiated phenotype (CD28⁻, CD27⁻, CCR7⁻, CD57⁺, CD45RA⁺, CD56⁺, CD244⁺, KLRG1⁺) with a limited proliferation capacity and short telomeres (Waller et al., 2008). In elderly hosts CMV-specific T cells with very low expression of activating co-receptor CD28 and re-expression of CD45RA accumulate (Khan et al., 2002b). Notably, antigen-specific

Introduction

CD45RA⁺ T cells during chronic infection were shown to be resistant to apoptosis and therefore very slowly disappear from the peripheral blood (Dunne et al., 2002; Wallace et al., 2004).

During the chronic phase of CMV infection certain T cell clones from the focused CMV-specific T cell repertoire expand further (Weekes et al., 1999; Khan et al., 2002a). CMV-specific CD4⁺ and CD8⁺ T cell populations become more and more oligoclonal (Trautmann et al., 2005; Gras et al., 2009). While the number of CD4⁺ T cells remain relatively constant, the CD8⁺ T cell clones expand extensively, especially in elderly hosts (Harari et al., 2004; Khan et al., 2004). The preferential accumulation of the CMV-specific T cells in the blood results from CMV infected cells in peripheral organs such as lung, cervix, salivary glands and retina (Ellefsen et al., 2002). Most people believe that continuous antigen stimulation during subclinical CMV reactivation results in the progressive clonal focusing towards T cell clones with high TCR avidity. Notably, the same antigen restriction in different unrelated donors often selects the same TCR α or β chains with high similarity or even identity in the CDR3 sequences (Khan et al., 2002b; Trautmann et al., 2005). Conserved TCRs were found to be dominant in the T cell population and characterized by high avidity, in contrast to other subdominant T cell clones (Price, 2005; Trautmann et al., 2005). In addition, Schwanninger *et al* found a distinct conserved T cell clone of high avidity only in aged hosts as compared to young and middle aged donors (Schwanninger et al., 2008).

1.3.2.3 CMV, T cell dysfunction and immune senescence

Controversially to the progressive TCR repertoire focusing towards dominant high avidity T cell clones, other studies revealed that largely expanded CMV-specific T cell populations in elderly are often characterized by T cell dysfunction (Ouyang et al., 2003; Ouyang et al., 2004). Longitudinal studies in healthy individuals correlated CMV infection with accelerated immune senescence and mortality in the elderly. They describe a relation between CMV infection and an immune risk phenotype (IRP) that is characterized by reduced survival rates, a low CD4/CD8 ratio, clonal expansions of highly differentiated CD8⁺ T cells, inflammatory cytokines in the blood and CMV related diseases (Olsson et al., 2000; Wikby et al., 2002). Best predictor of the IRP were clonal expansions of CMV-specific CD8⁺ T cells in the elderly infected donors (Hadrup et al., 2006). Furthermore, high levels of CMV reactive antibodies predicted mortality in another study (Strandberg et al., 2009). It was hypothesized that the

Introduction

enormous accumulation of certain CMV-specific T cell clones after many rounds of re-stimulation during subclinical CMV re-activation disrupts normal T cell homeostasis. Consequently the repertoire diversity in the naïve T cell compartment diminishes resulting in less efficient responses to *de novo* infections or vaccination (Akbar and Fletcher, 2005; Koch et al., 2006; Koch et al., 2007). Indeed, CMV seropositivity was correlated to impaired cellular response to EBV infection and poor responsiveness to influenza vaccination (Goronzy et al., 2001; Saurwein-Teissl et al., 2002; Trzonkowski et al., 2003; Khan et al., 2004). However, it remains unclear whether this dysfunction of CMV-specific T cells is a result of progressive loss of T cell function of the high affinity T cell clones selected early after primary infection or whether subdominant low affinity T cell clones are expanded during late phases of chronic CMV infection in elderly hosts.

2 Aim of this PhD thesis

Cytotoxic CD8⁺ T cells play a crucial role in clearance and control of intracellular pathogens. Upon clearance, antigen-specific T cells are maintained in low numbers in the absence of antigen. In contrast, antigen-specific CD8⁺ T cells in chronic persistent infection such as Cytomegalovirus (CMV) are frequently re-stimulated during subclinical virus reactivation to allow continuous immune surveillance. Similar to other infections, the T cell response after primary CMV infection is diverse and dominated by high avidity T cells. Notably, individual CMV-specific CD8⁺ T cell clones accumulate during latent infection to a remarkable size. Most people suggest that the dominance of individual CMV-specific T cell clones is a result of progressive focusing and expansion of a T cell clone with high TCR avidity. However, in elderly hosts these clonal expansions have been characterized by dysfunction and associated with a decrease in immunity towards new infections and vaccinations, as well as CMV-related diseases and increased mortality. It remains unknown if this dysfunction of expanded CMV-specific T cells is caused by a progressive loss of function during progression to terminally differentiated cells or whether at late time points during chronic CMV infection T cell clones with low structural TCR avidity are expanded. Most data on TCR avidity during CMV infection are based on functional analysis because methods to analyze structural TCR avidity of *ex vivo* isolated T cell populations are limited. Based on reversible MHC *Streptamer* staining a novel assay was recently developed to measure the dissociation (k_{off} -rate) of monomeric pMHC I ligands from the surface of living T cells as a crucial parameter determining structural TCR avidity.

The aim of this thesis was to analyze the TCR-ligand k_{off} -rate of *ex vivo* isolated CMV-specific T cell populations from different healthy donors in order to distinguish between structural TCR avidity and T cell functionality. To this end, first, the reproducibility of the *Streptamer*-based TCR-ligand k_{off} -rate assay was validated and the assay was compared to previous MHC multimer-based methods. The independence of the measurement from the cellular context was further analyzed by transgenic re-expression of analyzed TCRs on other cells. Second, a number of CMV-specific T cell populations of different healthy donors with the identical pMHC recognition but different size was analyzed with the novel assay and for cytokine production after specific peptide stimulation. Next, other MHCs as well as other CMV target epitopes from further CMV seropositive donors were analyzed and compared. Third, in order to control for the age, the time of infection and the genetic background, T cell populations from CMV infected mice were analyzed at different time points after infection.

3 Material and Methods

3.1 Material

3.1.1 Chemicals and reagents

Reagent	Supplier
Alexa-488-maleimide	Molecular Probes, Leiden, The Netherlands
Ammoniumchloride (NH ₄ Cl)	Sigma, Taufkirchen, Germany
Ampicillin	Sigma, Taufkirchen, Germany
Atto-565-maleimide	ATTO-TEC GmbH, Siegen, Germany
BCA assay reagents	Interchim, Montlucon, France
β-Mercaptoethanol	Sigma, Taufkirchen, Germany
Biocoll Ficoll solution	Biochrom, Berlin, Germany
Bovine serum albumin (BSA)	Sigma, Taufkirchen, Germany
Carbenicillin	Roth, Karlsruhe, Germany
Cytofix/Cytoperm	BD Biosciences, Heidelberg, Germany
D-biotin	Sigma, Taufkirchen, Germany
Dimethyl sulfoxid (DMSO)	Sigma, Taufkirchen, Germany
Ethanol	Klinikum rechts der Isar, Munich, Germany
Ethidium-monazide-bromide (EMA)	Molecular Probes, Leiden, The Netherlands
Fetal calf serum (FCS)	Biochrom, Berlin, Germany
Gentamycin	GibcoBRL, Karlsruhe, Germany
Gluthathione (oxidized)	Sigma, Taufkirchen, Germany
Gluthathione (reduced)	Sigma, Taufkirchen, Germany
Golgi-Plug	BD Biosciences, Heidelberg, Germany
Guanidine-HCl	Sigma, Taufkirchen, Germany
HCl	Roth, Karlsruhe, Germany
HEPES	GibcoBRL, Karlsruhe, Germany
Human serum	in-house production, Institut für Medizinische Mikrobiologie, Immunologie und Hygiene
IPTG	Sigma, Taufkirchen, Germany
L-Arginine	Roth, Karlsruhe, Germany
L-Glutamine	GibcoBRL, Karlsruhe, Germany
Leupeptin	Sigma, Taufkirchen, Germany

Material and Methods

Reagent	Supplier
Lysozym	Sigma, Taufkirchen, Germany
NaOH	Roth, Karlsruhe, Germany
Penicillin	Roth, Karlsruhe, Germany
Pepstatin	Sigma, Taufkirchen, Germany
PermWash	BD Biosciences, Heidelberg, Germany
pET3a expression vectors	Novagen, Darmstadt, Germany
Phosphate buffered saline (PBS)	Biochrom, Berlin, Germany
Propidium iodide (PI)	Molecular Probes, Invitrogen, UK
Roti Safe	Roth, Karlsruhe, Germany
RPMI 1640	GibcoBRL, Karlsruhe, Germany
Sodiumacetate	Sigma, Taufkirchen, Germany
Sodiumazide (NaN ₃)	Sigma, Taufkirchen, Germany
Sodiumchloride (NaCl)	Roth, Karlsruhe, Germany
Sodium-EDTA (Na-EDTA)	Sigma, Taufkirchen, Germany
Streptomycin	Sigma, Taufkirchen, Germany
<i>Strep</i> -Tactin-Allophycocyanin (APC)	IBA, Göttingen, Germany
<i>Strep</i> -Tactin-Phycoerythrin (PE)	IBA, Göttingen, Germany
<i>Strep</i> -Tactin Superflow 50% suspension	IBA, Göttingen, Germany
Tris-hydrochloride (Tris-HCl)	Roth, Karlsruhe, Germany
Trypan Blue solution	Sigma, Taufkirchen, Germany
Fluoresbrite YG Carboxylate	
Microspheres 10µm	Polysciences Europe, Eppelheim, Germany

3.1.2 Buffers and Media

Buffer	Composition
FACS buffer	1x PBS 0.5% (w/v) BSA pH 7.45

Material and Methods

Buffer	Composition
RP10 ⁺ cell culture medium	1x RPMI 1640 10% (w/v) FCS 0.025% (w/v) L-Glutamine 0.1% (w/v) HEPES 0.001% (w/v) Gentamycin 0.002% (w/v) Streptomycin 0.002% (w/v) Penicillin
Ammoniumchloride-Tris	0.17 M NH ₄ Cl 0.17 M Tris-HCl mix NH ₄ Cl and Tris-HCl at a ratio of 9:1
Refolding buffer	100 mM Tris-HCl 400 mM L-Arginin HCl 2 mM NaEDTA 0.5 mM ox. Gluthathione 5 mM red. Gluthathion ad 1 L H ₂ O, pH 8.0
Guanidine solution	3M Guanidine-HCl 10 mM NaAcetate 10 mM NaEDTA ad 100 ml H ₂ O, pH4.2
FPLC buffer	20 mM Tris-HCl 50 mM NaCl ad 1 L H ₂ O, pH 8.0
D-biotin 10 M stock solution	244.31 g D-biotin ad 100 ml H ₂ O, pH was brought to pH 11 to facilitate solution of D-biotin, then back down to pH 7

Material and Methods

Buffer	Composition
complete freezing medium (CFM)	FCS
	10% DMSO

3.1.3 Peptides

The following peptides were purchased from IBA, Göttingen, Germany

HCMV IE1 _{199-207KM}	(ELKRKMMYK)
HCMV IE1 ₈₈₋₉₆	(QIKVRVDMV)
HCMV IE1 ₃₁₆₋₃₂₄	(VLEETSVML)
HCMV pp65 ₄₁₇₋₄₂₆	(TPRVTGGGAM)
HCMV pp65 ₄₉₅₋₅₀₃	(NLVPMVATV)
HCMV pp65 ₃₆₃₋₃₇₃	(YSEHPTFTSQY)
HCMV pp50 ₂₄₅₋₂₅₃	(VTEHDTLLY)
SIY	(SIYRYYGL)
OVA ₂₅₇₋₂₆₄	(SIINFEKL)
MCMV IE1 ₁₆₈₋₁₇₆	(YPHFMPNTL)
MCMV m164 ₂₅₇₋₂₆₅	(AGPPRYSRI)

The following peptides were obtained from Andreas Mossmann, Helmholtz Zentrum Munich, Germany

HCMV IE1 _{199-207RM}	(ELRRKMMYM)
HCMV IE1 _{199-207KI}	(ELKRKMIYM)
HCMV IE1 _{199-207RI}	(ELRRKMIYM)

The following UV-cleavable peptides were obtained from Henk Hilkmann/Ton Schumacher, NKI, Amsterdam, Netherlands

HLA-A2 cleavable peptide	(KILGFV FJ V)
HLA-B8 cleavable peptide	(FLR G RA J LEY)

Material and Methods

3.1.4 Antibodies

Antibody	clone	supplier
Fc block (rat anti-mouse CD16/CD32)	2.4 G2	BD Bioscience, Heidelberg, Germany
Rat anti-mouse CD3 APC	145-2C11	BD Bioscience, Heidelberg, Germany
Rat anti-mouse CD8 α eFluor 450	53-6.7	eBioscience, San Diego, CA, USA
Rat anti-mouse CD19 PE-CF594	1D3	BD Bioscience, Heidelberg, Germany
Rat anti-mouse CD45 PE Cy7	30-F11	eBioscience, San Diego, CA, USA
Rat anti-mouse CD44 FITC	IM7	BD Bioscience, Heidelberg, Germany
mouse anti-human CD3 APC	UCHT1	Beckman Coulter, Marseille, France
mouse anti-human CD3 PE	UCHT1	Beckman Coulter, Marseille, France
mouse anti-human CD8 PB	B 9.11	Beckman Coulter, Marseille, France
mouse anti-human CD8 eFluor 450	OKT8	eBioscience, San Diego, CA, USA
mouse anti-human CD8 FITC	DK25	Dako, Glostrup, Denmark
mouse anti-human CD8 PE	DK25	Dako, Glostrup, Denmark
mouse anti-human HLA-ABC	W6/32	eBioscience, San Diego, CA, USA
mouse anti human CD19 ECD	J3-119	Beckman Coulter, Marseille, France
mouse anti human IFN γ FITC	B27	BD Bioscience, San Jose, CA, USA

Material and Methods

3.1.5 MHC *Streptamers*

HLA-B8 *Strep*-tagIII mutIII Atto565/h β ₂m /IE1₈₈₋₉₆ *Strep*-Tactin-APC/PE
HLA-B8 *Strep*-tagIII mutIII Atto565/h β ₂m /IE1_{199-207KM} *Strep*-Tactin-APC/PE
HLA-B8 *Strep*-tagIII mutIII Atto565/h β ₂m /UV peptide *Strep*-Tactin-APC
HLA-A2 *Strep*-tagIII mutIII Atto565/h β ₂m /IE1₃₁₆₋₃₂₄ *Strep*-Tactin-APC
HLA-A2 *Strep*-tagIII mutIII Atto565/h β ₂m /pp65₄₉₅₋₅₀₃ *Strep*-Tactin-APC/PE
HLA-B7 *Strep*-tagIII mutIII Atto565/h β ₂m /pp65₄₁₇₋₄₂₆ *Strep*-Tactin-APC
HLA-B7 *Strep*-tagIII mutIII Atto565/h β ₂m /pp65₄₁₇₋₄₂₆ *Strep*-Tactin-APC
HLA-A1 *Strep*-tagIII mutIII Atto565/h β ₂m / pp65₃₆₃₋₃₇₃ *Strep*-Tactin-APC
HLA-A1 *Strep*-tagIII mutIII Atto565/h β ₂m / pp50₂₄₅₋₂₅₃ *Strep*-Tactin-APC
HLA-A2 *Strep*-tagIII mutIII Atto565/h β ₂m /UV peptide *Strep*-Tactin-APC

H2-K^b *Strep*-tagIII mutIII Alexa488/m β ₂m /SIY *Strep*-Tactin-APC
H2-K^b *Strep*-tagIII/m β ₂m cys67 Alexa488/ OVA₂₅₇₋₂₆₄ *Strep*-Tactin-APC
H2-L^d *Strep*-tagIII mutIII Atto565/m β ₂m / IE1₁₆₈₋₁₇₆ *Strep*-Tactin-APC
H2-D^d *Strep*-tagIII mutIII Atto565/m β ₂m / m164₂₅₇₋₂₆₅ *Strep*-Tactin-APC

3.1.6 Gels

SDS-PAGE running gel	7 ml dH ₂ O
	4.38 ml 1.5 M Tris-HCl pH 8.8
	5.8 ml 30% Acrylamide 1% Bisacrylamide
	170 μ l 10% SDS
	8.8 μ l TEMED
	170 μ l 10% APS
SDS-PAGE stocking gel	6.2 ml dH ₂ O
	2.5 ml 0.5 M Tris-HCl pH 6.8
	1.2 ml 30% Acrylamide 1% Bisacrylamide
	100 μ l 10% SDS
	5 μ l TEMED
	100 μ l 10% APS

Material and Methods

Agarose gel	0.45 g Agarose
	40 ml TBE buffer
	1 μ l Ethidium bromide / Roti Safe

3.1.7 Microscope and equipment for TCR-ligand k_{off} -rate measurements

Leica SP5 confocal microscope (Leica, Bensheim, Germany)
Zeiss temperable insert P cooling device (Zeiss, Jena, Germany)
Huber Minichiller peltier cooler (Huber Kältemaschinenbau, Offenburg, Germany)
Metal inserts for cooling device (Locksmithery, Klinikum rechts der Isar, Munich, Germany)
Polycarbonate membrane, pore size 5 μ m (Millipore, Bergisch-Gladbach, Germany)
Metal shims (Schneider + Klein, Landscheid, Germany)

3.1.8 Equipment

Leica SP 5 confocal microscope Leica, Bensheim, Germany
Cyan ADP analyzer, Beckman Coulter, Fullerton, USA
MoFlo Cell Sorter, Beckman Coulter, Fullerton, USA
FPLC System Amersham, Munich, Germany
Varifuge 3.0RS centrifuge Thermo, Schwerte, Germany
Multifuge 3S-R centrifuge Thermo, Schwerte, Germany
Biofuge fresco table top centrifuge Thermo, Schwerte, Germany
Biofuge 15 table top centrifuge Thermo, Schwerte, Germany
RC26 Plus ultra-centrifuge Sorvall, Langenselbold, Germany
HE33 agarose gel casting system Hoefer, San Francisco, USA
Mighty Small SE245 gel casting system Hoefer, San Francisco, USA
NanoDrop spectrophotometer NanoDrop, Baltimore, USA
Gel Imaging System BioRad, Munich, Germany
Incubator Cytoperm 2, Heraeus, Hanau, Germany
Laminar flow hood HERA safe, Heraeus, Hanau, Germany
Waterbath LAUDA ecoline 019, Lauda-Königshofen, Germany
Photometer BioPhotometer, Eppendorf, Hamburg, Germany
Shaker Multitron Version 2, INFORS AG, Bottmingen, Switzerland

3.1.9 Software

FlowJo Treestar, Ashland, USA

Microsoft Office Microsoft, Redmond, USA

MetaMorph Online Molecular Devices, Downingtown, USA

Analyzer.nt Sebastian Nauerth, Department of Physics, LMU München

GraphPad Prism 5 GraphPad Software, La Jolla, USA

3.2 Methods

3.2.1 Specific T cell populations

3.2.1.1 Human blood samples

Peripheral blood was obtained from healthy adult donors of both sexes, diluted in PBS and peripheral blood mononuclear cells (PBMCs) were purified over a Ficoll gradient. PBMCs were used directly or frozen in CFM, stored in liquid nitrogen and thawed before analysis.

3.2.1.2 Human T cell clones

Human T cell clones were isolated by Jeannette Bet and Paulina Paszkiewicz as described in (Nauerth et al., 2013b): “Sort-purified *Streptamer*⁺ cells (HLA-B8/IE1₁₉₉₋₂₀₇KM, HLA-B8/IE1₈₈₋₉₆, HLA-A2/pp65₄₉₅₋₅₀₃ or HLA-B7/pp65₄₁₇₋₄₂₆) from CMV⁺ healthy donors were plated by limiting dilution (0.6 cells/well) and cocultured with 1*10⁴ γ -irradiated allogeneic LCLs (50 Gray) and 7.5*10⁴ PBMCs (35 Gray) in h-RP10⁺ (RPMI 1640, 10 % human serum, 0.025 % L-Glutamine, 0.1 % HEPES, 0.001 % Gentamycin, 0.002 % Streptomycin, 0.002 % Penicillin) supplemented with anti-CD3 monoclonal antibody (OKT-3, 30 ng/ml) and IL-2 (50 U/ml). 5*10⁴ cells were restimulated every 14 days with 1*10⁶ γ -irradiated allogeneic LCLs and 5*10⁶ PBMCs in h-RP⁺ supplemented with anti-CD3 monoclonal antibody. IL-2 (50 U/ml) was added one day later. Cells were analyzed from day 10 - 21 after restimulation.” On day 14 after restimulation, next round of restimulation was performed as described before or cells were rested in IL-15 for up to 7 days. T cell clones from the naïve repertoire were obtained from Pleun Hombrink and Mirjam Heemskerk as described in (Hombrink et al., 2013). Briefly, T cells were isolated from PBMCs by magnetic-activated cell sorting (MACS) using HLA-A1/pp65-PE multimers in combination with anti-PE antibody coated magnetic beads (Miltenyi Biotec, Bergisch Gladbach, Germany) and polyclonal expanded *in vitro* in the

Material and Methods

presence of irradiated autologous feeder cells, IL-2 (100 U/mL), IL-15 (5 ng/mL) and anti-CD3/CD28 Dynabeads (Invitrogen) for 2 weeks before second MHC multimer enrichment by MACS or fluorescence activated cell sorting (FACS) and expansion in the presence of irradiated feeder cells and PHA (0.5 µg/mL).

3.2.1.3 *Murine blood samples*

Murine blood samples were obtained from Thomas Marandu and Luka Cicin-Sain. Briefly, 129/Sv x BALB/c F1 mice were infected intraperitoneally (i.p.) with 10^5 Plaque forming Units (PFU) of MCMV at the age of 3, 6, 9 or 14 months (Cicin-Sain et al., 2012). At the age of 14 month (7 days post infection for the last cohort of mice) whole blood was taken, heparinized (2 U/ml) and transferred to cryotubes. 10% of DMSO was added to the whole blood and immediately put in a -80°C freezer as described previously for human blood (Alam et al., 2012). To obtain the maximal number of *Streptamer*⁺ T cells from the peripheral blood of mice, different purification protocols were tested. The protocol based on red blood cell lysis was performed first in 10 ml ACT buffer for 10 min, centrifugation at 460 x g, followed by 5 ml ACT for 5 min before stopping lysis with 5 ml RP⁺⁺ and centrifugation at 460 x g. For the Mini-Ficoll, peripheral blood was diluted 1:2 in PBS and 500 µl were overlaid on 750 µl Ficoll solution in a 1.5 ml Eppendorf tube, centrifuged 7 min 6000 rpm at RT in a table centrifuge without brake. Cells were aspirated from intermediate layer and collected in a precooled 96-V-bottom plate on ice and washed in FACS buffer twice by centrifugation at 460 x g for 2 min and discarding the supernatant. Red blood cell lysis with water was performed in 15 ml Falcon tubes by mixing blood 1:3 in PBS, spinning down 6 min at 460 x g and resuspending quickly in water by adding 9 ml water during vortexing and subsequent slow addition of 3 ml 4X PBS. Cells were pelleted 6 min at 460 x g, transferred to a 96-V-bottom-plate, resuspended quickly in 150 µl water by vortexing. 50 µl 4X PBS were added before centrifugation and resuspension in FACS buffer. Purified cells were cooled to 4°C and *Streptamer* staining was performed as described in 3.2.2.4. Staining whole blood was performed by adding 40µl Fc block (pre-diluted 1/100) to 80µl whole blood for 10 min before addition of different amounts of *Streptamer* solution (titrated from 100 µl to 5 µl) for 45 min and surface antibodies CD45 PE-Cy7 (1/50) and CD8 PB (1/100) for the last 20 min. Before FACS analysis, sample was diluted by adding 580 µl FACS buffer with PI (1/500). To decrease fluorescence background in the whole blood sample, cells were washed 3 times by

spinning down 2 min at 460 x g and resuspending in 200 µl cold FACS buffer. During FACS analysis, the threshold was set on CD45 PeCy7 to exclude the acquisition of erythrocytes.

3.2.1.4 TCR sequencing and TCR Transduction

TCRs of the CMV-specific T cell population of donor #1 or of T cell clones were amplified by RACE-PCR and subsequently sequenced by Georg Dössinger (Dössinger et al., 2013). The TCR transduction was performed by Georg Dössinger or Mario Bunse as described in (Nauerth et al., 2013b): “Briefly, TCR α - and β -chain were separately cloned in the retroviral vector MP71. Packaging was performed by triplasmid CaCl₂ transfection with the retroviral vector plasmid and the expression plasmids encoding the Moloney MLV *gag/pol* genes (pcDNA3.1MLVg/p) and the MLV-10A1 *env* gene (pALF-10A1) in Hek293T cells. Viral supernatant was spun down (800g) in Retronectin-coated 24 well plates together with Jurkat76 cells” or PBMCs “for 90 min at 32°C.”

3.2.2 Generation of murine MHC heavy chains with mutation III for fluorescence conjugation

Analog to the human pMHC I monomers used for TCR-ligand k_{off} -rate measurements (Nauerth, 2012), mutation III (mutIII) was inserted into the MHC heavy chain as a conjugation site for the fluorescent dye. This mutation carries a cysteine residue “to allow for a maleimide reaction of the dye with the free -SH group of the cysteine” (Nauerth, 2012). Correctly mutated pMHC I vectors were used for protein expression, purified and refolded before fluorescence conjugation as described in (Nauerth, 2012).

3.2.2.1 Primer design

To optimize mutagenesis of the MHC heavy chains, a primer pair with phosphorylated ends was designed. One primer carried the linker and cysteine at its end. The linear mutagenesis PCR product was ligated to obtain a circular vector with the mutated MHC heavy chain. PCR products were subsequently sequenced and used for protein expression. MHC molecules were mutated in a mutagenesis PCR using the following primers:

Forward	TAATAAGCTGATCCGGCTGCAACAAGCCG
Reverse	GCAGGAACCGCCTTTTTCGAACTGCGGGTGGCTCCAC

3.2.2.2 *Mutagenesis-PCR*

For mutagenesis 30ng template DNA, 0.02 rxn/ μ l Herculase polymerase, 1mM dNTPs and 0.2 μ M of each primer were used in a final volume of 50 μ l Herculase II buffer. The following conditions were chosen in the thermal PCR cycling steps for denaturation, annealing and extension:

	Temperature	Time	#	
1	95°C	2 min		
2	95°C	1 min		
3	58°C	45 sec		
4	72°C	5 min	2	30
5	72°C	6 min		
6	4°C	pause		

“After the PCR, template DNA was digested by incubation with DpnI endonuclease, which is specific for methylated and hemi methylated DNA. 10 μ l of the PCR samples were loaded on an agarose gel to check for the existence and the size of PCR products. The agarose gel was made with 50 ml TAE buffer, 0.4 g agarose and 2.5 μ l Roti Safe or 5 μ l EtBr. A 1 kB DNA ladder was used as marker, and 2 μ l 6x DNA loading dye was added to the samples for staining” as described in (Nauerth, 2012).

3.2.2.3 *Transformation and plasmid preparation*

“10 μ l of the reaction mixture were used to transform DH5 α bacteria with the mutated plasmids. Therefore, 100 μ l competent cells were cautiously thawed on ice and then 10 μ l PCR product was added. The mixture was incubated on ice for 30 min, and then heat shocked in a 42 °C water bath for 30 s. After 2 min incubation on ice, 150 μ l SOC-medium was added to each reaction mixture and incubated for 1 h at 37 °C. The mixtures were plated on ampicillin-containing agar plates to select only colonies containing the vector in 10, 50 and 2x100 μ l doses and incubated over night at 37 °C. One colony was picked from every transformation plate and inoculated into reaction tubes containing 6 ml LB-medium and 6 μ l ampicillin. The cultures were incubated over night at 37 °C and subsequently 1 ml bacteria sample was mixed 1:1 with glycerol for glycerol stocks and frozen at -20 C. For the plasmid preparation the Qiagen Plasmid Miniprep Kit was used. The preparation was performed according to protocol, and the isolated DNA was eluted with 50 μ l ddH₂O. DNA

concentrations were measured with NanoDrop. Following plasmid preparation all samples were sent to GATC Biotechnologies Ltd. for sequencing to confirm successful mutations” as described in (Nauerth, 2012).

3.2.2.4 Protein expression

“10 μ l heat competent BL21 (DE3) cells were mixed with 1 μ l DNA and transformed using the same protocol as the first transformation. The transformation products were plated on amp-containing agar plates and incubated over night at 37 °C. To test the expression of the protein in a small scaled preparation, cell culture bottles containing 20 ml LB-medium, 200 μ l 40% glucose and 20 μ l ampicillin were inoculated with 4-5 colonies from each agar culture plate. The cultures were shaken at 37 °C until OD₆₀₀ reached 0.3 and 1 ml glycerol stocks were taken. At OD₆₀₀ 0.7 a 0h sample was taken before induction and the cultures were induced using 1 μ l IPTG per ml culture. The cultures were shaken for further 3 h and a 3 h sample was taken after induction. The 0 h and 3 h samples were centrifuged at 9000 rpm for 3 min, the pellets washed with PBS and frozen at -20 °C or directly loaded on a SDS gel to check the expression and the size of the proteins. 15% SDS-PAGE gel was produced according to the common protocol. The sample pellets were dissolved in 100 μ l water, 13 μ l mixed with 2x SB and boiled at 96 °C for 5 min 10 μ l was run on the gel. If the small scaled approach revealed a sufficient expression of the protein, a large scale protein expression was started. 2 l culture flasks containing 1 l LB-medium, 10 ml 40% glucose and 1 ml carbenicillin were inoculated with 1 ml of bacterial solution consisting of 20 μ l bacteria in 7 ml LB-medium. The flasks were shaken at 180 rpm, 37 °C for approximately 8 hours until OD₆₀₀ reached 0.7 and protein expression was induced with 1 ml IPTG. After 3 h the mixtures there transferred to 500 ml centrifugation tubes and centrifuged for 10 min at 5 000 rpm (SLA 1500 rotor). The pellets were then frozen at -80 °C. For the purification of inclusion bodies the bacterial pellets were thawed on ice. The pellets were resuspended in 13 ml solution buffer and transferred to 50 ml centrifuge tubes. The pellets were homogenized using a sonicator. 100 μ l lysosome (50 mg/ml solution), 250 μ l DNase I (2 mg/ml) and 50 μ l MgCl₂ (0.5 M) was added and gently mixed. 12.5 ml lysis buffer was then added and mixed. The tubes were incubated at room temperature for 1 h. Then the tubes were frozen at -80 °C for 25 min and subsequently transferred to a 37 °C water bath for 30 min. 50 μ l MgCl₂ was added and incubated another 30 min at room temperature until viscosity decreased. Then 350 μ l NaEDTA (0.5 M) was added and the tubes centrifuged at 11 000 rpm, 4 °C for 20 min (Rotor SA 300, Sorvall). The supernatant was discarded and the pellets resuspended in 10 ml

washing buffer with Triton X on ice. The suspension was homogenized using the sonicator. Again the tubes were centrifuged, resuspended in 10 ml washing buffer without Triton X, and homogenized. The tubes were once more centrifuged and the supernatants discarded. The pellets were resuspended in 200 μ l urea and shaken over night at 4 °C. The next day the urea solution was transferred to ultracentrifugation tubes and centrifuged at 45 000 rpm for 20 min at 20 °C (Rotor Ti 70.1). The supernatants were pooled into a 15 ml falcon tube. The 0 h and 3 h samples were centrifuged at 9000 rpm for 3 min, washed with PBS, centrifuged again and the pellets frozen at -20 °C or directly loaded on a SDS gel to check the expression and the size of the proteins” as described in (Nauerth, 2012).

3.2.3 Generation of *Streptamers*

“To generate *Streptamers* for the TCR-ligand k_{off} -rate assay, first the MHC heavy chain was refolded with β_2m in the presence of the peptide of interest to build the complete and stable MHC complex. Subsequently, the purified complex has to be conjugated with a fluorescent dye and finally, the dye conjugated MHC molecules were multimerized on a *Strep*-Tactin backbone” as described in (Nauerth, 2012).

3.2.3.1 Purification and refolding of MHC molecules

“Heavy chain and β_2m proteins in 8 M Urea were diluted into refolding buffer containing high concentrations of the respective synthetic peptide (60 μ M/ml). Aliquots of the proteins were first diluted in 3 M guanidine buffer, injected directly into 200 ml refolding buffer three times every 3 h while vortexing heavily and incubated under constant agitation for 24 h at 10 °C. The refolding buffer contained a glutathion redox system to facilitate optimal formation of disulfide-bridges. After 24 h, the protein solution was concentrated to a volume of 10-20 ml over a 10 kDa membrane (Millipore, Eschborn, Germany), then further reduced to 1 ml using 10 kDa concentrator columns (Millipore, Eschborn, Germany). The flowthrough of the first concentration step still contained large amounts of peptide and could be used for a second refolding. Correctly folded MHC I molecules were purified by gel filtration (Superdex 200HR, Amersham, Munich, Germany) over a FPLC system (FPLC basic, Amersham, Munich, Germany), pooled and incubated overnight in a buffer containing NaN_3 , protease inhibitors (1 mM NaEDTA, Leupeptin, Pepstatin) and 0.1 mM DTT to keep the free cysteine in a reduced state. The next day, the buffer was exchanged against PBS pH 7.4 and the protein concentration determined by a standard BCA-assay” as described in (Nauerth, 2012).

3.2.3.2 Dye-conjugation and purification

After the refolding, pMHC complexes “were incubated with the respective fluorescent dye containing a maleimide group in a molar ratio of 1:10 for 2h at room temperature and in the dark. To separate unbound dye from dye-conjugated MHC molecules, illustra NAP-25 gravity flow columns (GE Healthcare, Buckinghamshire, UK) were used, pre-packed with Sephadex G-25 DNA grade resin. After columns were equilibrated with PBS pH 8.0, the protein dye reaction mix was pipetted on top of the column and waited until the mixture had entered the gel bed completely. 500µl of PBS pH 8.0 were added until it entered the gel bed completely. Subsequently, 3 ml PBS pH 8.0 were added to elute the protein. During elution, the separation of the dye conjugated MHC molecules (first, lighter colored band) from the unbound dye (second, deeper colored band) becomes visible. The first band was collected in a 10 kDa concentrator column (Millipore, Eschborn, Germany) and PBS pH 8.0 added to 4 ml volume. After concentration to 250 µl, 3750 µl PBS pH 8.0 containing NaN₃ and protease inhibitors (1 mM NaEDTA, Leupeptin, Pepstatin) were added, concentrated again to 500 µl and the protein stored in liquid nitrogen after measuring its concentration” as described in (Nauerth, 2012).

3.2.3.3 pMHC exchange

MHC I monomers were generated as described in 3.2.3 using UV cleavable peptides obtained from Ton Schumacher and Henk Hilkmann (Rodenko et al., 2006). 12 µg of dye conjugated or conventional UV peptide MHC I were exposed to 366nm UV light in the presence of 200 µM peptide in 120 µl PBS pH 8.0 in a 96-V-bottom well polypropylene plate for 20, 40 or 60 minutes at room temperature or on ice. To separate MHC aggregates, plate was spin down at 3300 x g for 5 min at room temperature and supernatant was transferred to a fresh polypropylene microplate. 45µl were incubated with 5µl of *Strep*-Tactin-APC and used for *Streptamer* staining as described below in 3.2.3.4.

3.2.3.4 Multimerization of pMHCs

For MHC *Streptamer* staining with up to 5 x 10⁶ cells, 1 µg of dye-conjugated MHC I and 0.75 µg (5 µl) *Strep*-Tactin-PE or *Strep*-Tactin-APC (IBA) were incubated for 45 minutes at 4°C in the dark in a final volume of 50 µl FACS buffer according to the manufacturer’s instructions.

3.2.4 Functional analysis, T cell staining and FACS analysis

3.2.4.1 *Secretion of IFN γ in an intracellular cytokine staining (ICCS)*

“T cells were incubated in the presence of the indicated amount of the respective peptides for 5 h in RP10⁺ supplemented with anti-CD28 and anti-CD49d (BD Biosciences). 2 μ g/well Brefeldin-A (Sigma) was added after 1 h. After stimulation cells were kept at 4°C and stained with EMA (0.1 μ g in 50 μ l FACS buffer) for 20 min under light. For surface staining, cells were incubated 20 min in the dark with anti-CD8 α monoclonal antibody before lysis in Cytotfix/Cytoperm (BD Biosciences) for 20 min and intracellular staining against IFN- γ (30 min, in the dark, on ice in BD Bioscience Perm/Wash buffer). The maximal percentage of IFN γ ⁺ CD8⁺ was normalized to 100% and a nonlinear curve was fitted into the normalized data in response to each peptide concentration. For CMV-specific T cell populations from different donors, 2*10⁶ PBMCs were incubated per sample” as described in (Nauerth et al., 2013b). To test the functionality of T cell clones, HLA-matching LCLs were loaded with the indicated amount of peptide and cocultured with the T cell clones at an effector to target ratio of 10:1

3.2.4.2 *Secretion of IFN γ in an ELISA*

T cell clones from the naïve repertoire were analyzed for IFN γ secretion after specific stimulation in an ELISA by Pleun Hombrink. Briefly, target cells were loaded with titrated amounts of the peptide for 1 h in 96-well plates at 37°C, washed and incubated for 24h with the T cell in an effector to target ratio of 1:5 or with TCR A/B transduced cells in a 1:1 effector to target ratio as described in (Hombrink et al., 2011). Subsequently, the supernatant was harvested and the concentration of IFN- γ measured by a standard ELISA.

3.2.4.3 *⁵¹Chromium release assay*

Specific killing was tested in a chromium release assay by incubation of effector T cells with ⁵¹Cr labeled and peptide loaded HLA/B8-expressing LCLs. “1*10⁶ HLA/B8-expressing LCLs were loaded with the indicated amounts of IE1₈₈₋₉₆ or IE1_{199-207KM} peptide (10⁻¹¹ to 10⁻⁵ M) and 1.85 MBq ⁵¹Cr for 1 h at 37°C. 10⁴ peptide loaded LCLs were incubated with 10⁵ cells of the respective T cell clone (10:1 effector to target ratio). To determine the spontaneous and maximal lysis, RP10⁺ or 5 % Triton X-100 was used, respectively, instead of effector cells. The cells were incubated for 4-5 h at 37°C, spun down and the supernatants were transferred to counting tubes. The amount of radioactivity in the supernatants was measured in a γ -

counter and the specific lysis for each sample was calculated” as described in (Nauerth et al., 2013b).

3.2.4.4 Antibody and Streptamer staining

For *Streptamer* and antibody staining, up to 5×10^6 cells were used per staining. Staining was performed in 96-well plates. Cells were rested for 30 min on ice, pelleted for 2 min at $460 \times g$, resuspended in *Streptamer* staining solution and incubated on ice in the dark for 45 min according to manufacturer’s instructions and as described in (Nauerth et al., 2013b). For *Streptamer* double staining, the first specificity was stained with *Streptamer*-PE for 45 min before washing three times and subsequent *Streptamer*-APC staining for the second specificity. Antibodies were added at the appropriate dilution for the last 20 min and propidium iodide (PI) for the last 5 minutes of the staining. The samples were washed three times in 200 μ l FACS buffer, resuspended in FACS and analyzed by flow cytometry.

3.2.4.5 FACS acquisition and analysis

“For FACS analysis, at least 10^5 cells of the populations of interest were acquired on a Cyan flow cytometer (Beckman Coulter, California, USA). Data analysis was performed using FlowJo software (Treestar, Ashland, USA)” as described in (Nauerth, 2012).

3.2.4.6 Conventional pMHC multimer dissociation experiments

“T cell clones were analyzed according to (Wang and Altman, 2003). Briefly, T cell clones were rested 30 minutes on ice before staining with conventional biotinylated HLA-B8/IE1₈₈₋₉₆ multimer-PE for 45 minutes. After washing, cells were resuspended in 200 μ L FACS in the presence or absence of 10 μ M W6/32 blocking antibody (anti-HLA-A, anti-HLA-B, and anti-HLA-C). Cells were kept at 4°C for 10h and aliquots were taken at the indicated time points. The maximal mean fluorescence intensity of living multimer PE⁺ was normalized to 100%, and the normalized data were plotted over the time. An exponential decay was fitted into the data and used to calculate the $t_{1/2}$ ” as described in (Nauerth et al., 2013b).

3.2.5 TCR-ligand k_{off} -rate assay

3.2.5.1 *Streptamer staining and sorting*

PBMCs or mouse blood cells were either freshly purified or thawed at 37°C in RP⁺ medium, “washed twice with FACS buffer and subsequently rested on ice for at least 30 minutes before staining, to minimize side effects of MHC multimer staining like internalization of the reagents. After that, the cells were spun down, resuspended in *Streptamer* solution and stained for 45 min on ice as described in” 3.2.4.4. “The cells were washed three times in ice-cold FACS buffer, resuspended in FACS buffer” and transferred to pre-cooled tubes.”The whole staining procedure was performed on ice and in a cooled centrifuge at all times. Cells were sorted on a MoFlo II Cell Sorter (DakoCytomation, Glostrup, Denmark) for living, CD8⁺, *Streptamer*⁺ cells. Specific cells were sorted into a cooled tube containing FCS, to avoid physical damage” as described in (Nauerth, 2012). Small samples and rare *Streptamer*⁺ T cell populations were collected in V-bottom wells filled with 200 µl FCS of a 96-well-plate on ice. Sorted cells had to be washed two times in FACS buffer. Upon *Streptamer* double staining, *Streptamer*-PE-specific T cell populations were sorted into 200 µl FCS containing 0.1 mM D-biotin to allow dissociation of *Strep*-Tactin-PE and restaining with respective *Streptamer*-APC after washing three times in FACS buffer. This allowed removing *Strep*-Tactin-PE in combination with pMHC-Atto565 with highly similar emission spectra before the k_{off} -rate analysis. For serial FACS sorting, CD8⁺ *Streptamer*⁺ cells were sorted in parallel to CD8⁺ *Streptamer*⁻ cells. CD8⁺ *Streptamer*⁺ cells were sorted as described above, while CD8⁺ *Streptamer*⁻ were washed and stained with *Streptamer*-APC of the next specificity and subsequently sorted again. Finally, after sorting and washing, cells were resuspended in a final concentration of 10⁴ cells in 1 µl FACS buffer for the microscopic TCR-ligand k_{off} -rate assay.

3.2.5.2 *Performance of the k_{off} -rate assay*

“All microscopic TCR-ligand k_{off} -rate measurements were performed on a Leica SP5 confocal laser scanning microscope” as described in (Nauerth, 2012). To allow constant temperature (4°C if not indicated otherwise) under the microscope, “a water cooling device was used, connected to a peltier cooler. A customized metal insert, which fits exactly into the cooling device, was sealed with a cover slip at the bottom to build a reservoir. 1 µl cell suspension was pipetted to the glass slide and immediately covered with a polycarbonate membrane” as described in (Nauerth, 2012). For low cell numbers, a smaller piece was cut out of the

membrane to minimize the spreading of the cells over the whole membrane. The membrane was “weighed down with a small metal shim, and subsequently, cold buffer was added. Cells were efficiently arrested in a thin layer between the membrane and the cover slip while the 5 μm pores in the membrane still allowed for rapid diffusion of D-biotin to the cells. A time series was started on the microscope, taking one picture every 10 seconds. After the first picture D-biotin was added and the time series was run until the complete dissociation of the MHCs. [...] To detect the fluorescence of a complete cell, the pinhole was opened until the thickness of the detected plane corresponded to the layer of the cells” (Nauerth, 2012). “To test the influence of a MHC blocking antibody in the TCR-ligand k_{off} -rate setup, the measurements were performed in the presence of 10 μM W6/32 antibody added in combination with D-biotin” as described in (Nauerth et al., 2013b).

For the analysis of the TCR-ligand k_{off} -rate on the population level by flow cytometry, D-biotin was injected into a customized tube with the *Streptamer*-stained antigen-specific T cells 30 s after starting the FACS acquisition and cells were constantly cooled to 4°C. Subsequent fluorescence decrease of *Strep*-Tactin-APC backbone and MHC-Alexa488 was monitored over a time frame of 15 min.

3.2.5.3 Data analysis

Microscopic images were analyzed as described in (Nauerth, 2012) using MetaMorph Online image analysis software (Molecular Devices, Downingtown, USA). “For each individual cell, integrated fluorescence intensity inside a gate containing the cell was measured over the whole time series that was acquired. The same gate was then put in close proximity to the cell, but not containing the cell, for measurement of background fluorescence intensity. Data were logged into Microsoft Excel (Microsoft, Redmond, USA). Further data analysis was done automatically by the Analyzer nt software (Sebastian Nauerth, LMU)” as described in detail in (Nauerth, 2012; Nauerth et al., 2013b). Briefly, background gate was subtracted from fluorescence intensity of each individual cell at every time point during acquisition. Background corrected fluorescence intensities were plotted over the time and starting as well as end point of exponential decay curve was selected manually. For optimal curve fitting, the starting point was set to approximately 80 % of the MHC dye intensity (when *Strep*-Tactin-APC backbone intensity was low and constant) and the end point was set to the last point of the plateau of the curve. By fitting the exponential model $y(t) = y_0 * e^{-k_{\text{off}} * t} - a * t$ into the selected data, the analyser.nt software calculated the k_{off} -rate, as well as the $t_{1/2}$ of every individual gated cell. The values were subsequently corrected for photo bleaching by

Material and Methods

subtracting the photo bleaching rate (k_{bleach}) of Atto565 beads acquired during each experiment.

Data acquired by flow cytometry was analyzed in FlowJo (Treestar, Ashland, USA). Cells were gated on the population of interest (living CD8⁺ *Streptamer*⁺ lymphocytes) and time intervals were set every 4.5 s over the 15 min acquisition. Mean intensity of the MHC as well as *Strep*-Tactin-APC backbone fluorescence of the antigen-specific T cells in every gate were exported into Microsoft Excel (Microsoft, Redmond, USA) and plotted versus the time to fit an exponential decay curve in GraphPad Prism 5 (GraphPad Software, La Jolla, USA) and calculate $k_{\text{off-rate}}$ and the $t_{1/2}$.

3.2.5.4 Bleaching measurements with beads

“To obtain a cell free testing system for the fluorescence intensity and the photo stability of fluorescent dyes under the microscope”, either *Strep*-Tactin beads were incubated with dye conjugated MHC molecule for multimerization on the bead surface or beads covalently coupled with fluorescent dye were used. Analogous to cells, beads were mounted under the microscope and exposed to the same laser intensities as used in the $k_{\text{off-rate}}$ assay. “Fluorescence intensities of the beads were monitored by taking pictures every 10s. The bleaching constant k_{bleach} was obtained from the exponent of the curve fitted into the data points” and subtracted from measured $k_{\text{off-rate}}$ values as described in (Nauerth, 2012; Nauerth et al., 2013b).

4 Results

4.1 Validation of the TCR-ligand k_{off} -rate assay

Antigen-specific T cells that expand to high frequency during chronic CMV infection are often characterized by very low functionality (Ouyang et al., 2003; Ouyang et al., 2004). It is not clear if these cells are expanded from the T cells recruited during the early, acute phase of infection. During acute phase of CMV infection, antigen-specific T cells are polyclonal and T cells with high effector functions towards their target epitopes are preferentially expanded (Day et al., 2007). Antigen-specific T cells during chronic latent CMV infection are repetitively stimulated by CMV infected cells and subsequently proliferate and secrete cytokines. Reoccurring stimulation might cause exhaustion and a loss of functionality of these CMV-specific T cell clones. On the other hand, T cell clones with TCRs of low structural binding avidity might be selected during late phase of chronic CMV infection. To investigate whether the low functionality of monoclonal, expanded CMV-specific T cell populations during late phase of CMV infection is caused by exhaustion of high avidity T cell clones or by the expansion of other T cell clones with a low structural binding avidity, the structural avidity hardwired in the TCR had to be discriminated from functional avidity. The TCR-ligand k_{off} -rate assay for murine and human antigen-specific T cells was recently established to measure the dissociation of pMHC monomers from cell surface expressed TCRs (Knall, 2007; Nauwerth, 2012). To allow robust and reproducible measurements of TCR avidity of antigen-specific CD8⁺ T cells in chronic CMV infection, a variety of different validation experiments were performed.

4.1.1 Conventional pMHC multimer dissociation experiments are difficult to standardize

One simple method often used to assess structural binding avidity of antigen-specific T cells are multimeric pMHC dissociation experiments (Wang and Altman, 2003). In this assay, biotinylated specific pMHC monomers multimerized on fluorescence conjugated Streptavidin are used to label antigen-specific T cells. In the multimeric complex, monomeric pMHC can spontaneously dissociate from individual TCRs. However, the pMHC remains in close proximity to the specific TCRs allowing rebinding and stable MHC multimer binding to the T cell (Fig. 4-1 A). Rebinding of the pMHC monomers to the TCRs can be prevented by the addition of blocking reagents, such as a monoclonal antibody against the pMHC interfering

Results

with the interaction between pMHC and TCR (Fig. 4-1 B). This allows the complete dissociation of the whole pMHC multimer complex that can be observed as a loss in fluorescence intensity (Fig. 4-1 C).

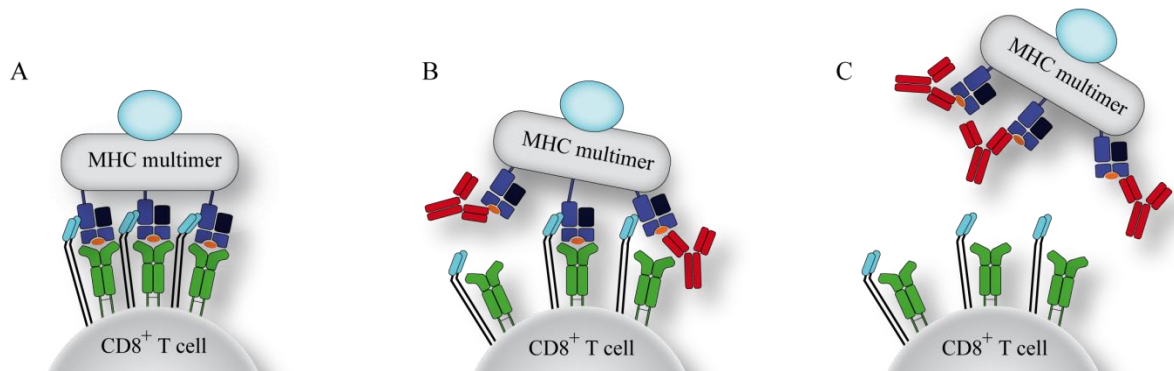


Figure 4-1: Basic principle of conventional pMHC multimer dissociation experiments.

(A) Biotinylated MHC multimers stably bind to antigen-specific CD8⁺ T cells because single MHC monomers remain in close proximity to the cell surface facilitating rebinding of TCRs. (B) MHC rebinding is prevented by a blocking antibody (red) resulting in the dissociation of the fluorescence conjugated pMHC multimer. (C) pMHC multimer dissociation can be monitored by the loss of fluorescence intensity. Adapted from (Nauerth et al., 2013b).

Two human CMV Immediate Early (IE) 1-specific T cell clones in conventional pMHC dissociation experiments were analyzed. When working at a low temperature (4°C), which is a prerequisite to prevent internalization of pMHC molecules bound to the TCR, the dissociation kinetics ($t_{1/2}$ values) were enormously long in the range of hours. T cell clone #1 (Fig. 4-2 A) had a 5600-fold longer dissociation $t_{1/2}$ of 6907 h as compared to T cell clone #2 ($t_{1/2} = 74$ min). In the presence of the anti-MHC blocking antibody (W6/32), the difference between T cell clone #1 and T cell clone #2 was 6666-fold and the dissociation $t_{1/2}$ values for both T cell clones were decreased, indicating the dependency of the assay on the blocking reagent (Fig. 4-2 A and B) (Nauerth et al., 2013b).

Results

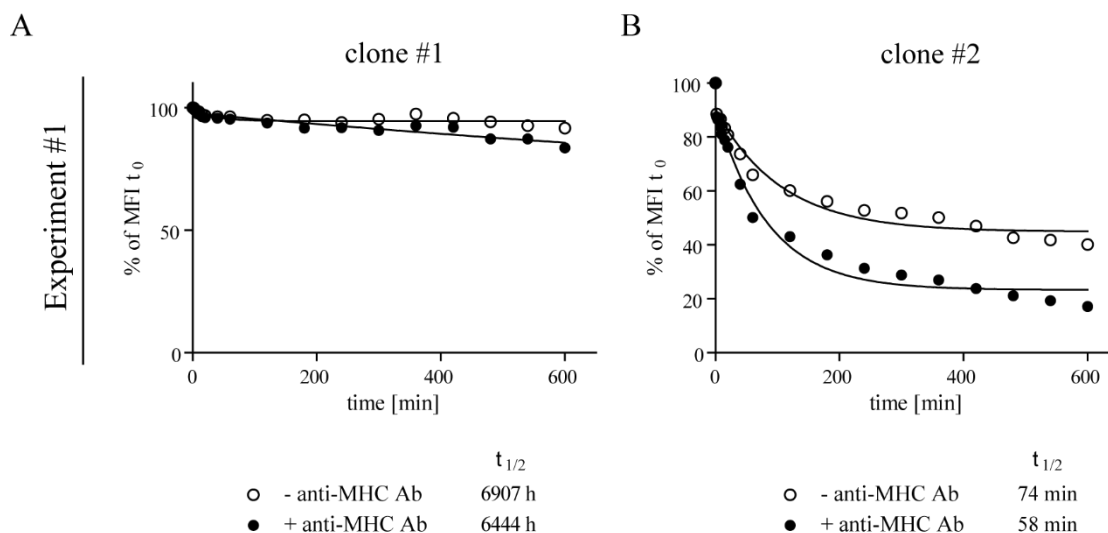


Figure 4-2: Conventional pMHC multimer dissociation experiments discriminate high and low avidity T cell clones.

HLA-B8/IE1₈₈₋₉₆-specific T cell clones #1 (A) and #2 (B) were analyzed in a conventional pMHC dissociation experiment. T cell clones stained with the specific pMHC multimer were incubated for 10h at 4°C in the presence (filled dots) or absence of 10µM of the anti-MHC antibody W6/32 (empty dots). Aliquots were taken at the indicated time points and analyzed by FACS. Half-life ($t_{1/2}$) values were calculated from the exponential decay curve fitted into the percent of initial mean fluorescence intensities (% of MFI t_0). Adapted from (Nauerth et al., 2013b).

Consequently, a high- and low-avidity T cell clone could be distinguished (T cell clone #1 and #2, respectively) within the pMHC multimer dissociation experiment. However, when repeating the experiment with the same T cells and reagents under the same conditions, the $t_{1/2}$ values were much longer with 223667h for T cell clone #1 and 411 min for T cell clone #2 (32652-fold difference) in the absence of a blocking antibody (Fig. 4-3 empty dots). Here, dissociation kinetics in the presence of a blocking antibody were again accelerated for both T cell clones (22470-fold difference between the T cell clones shown in Fig. 4-3 filled dots) (Nauerth et al., 2013b). The standardization of pMHC multimer dissociation experiments is difficult resulting in a high interassay variability. The dissociation rate of the multimeric complex may be influenced by the number of MHC molecules bound to a T cell, as well as the number of MHC molecules per multimer that is difficult to determine (Nauerth et al., 2013b). In addition, the nature and the concentration of the blocking reagents used to prevent rebinding of dissociated MHCs to TCRs has an influence on the dissociation rate (Wang and Altman, 2003; Nauerth et al., 2013b).

Results

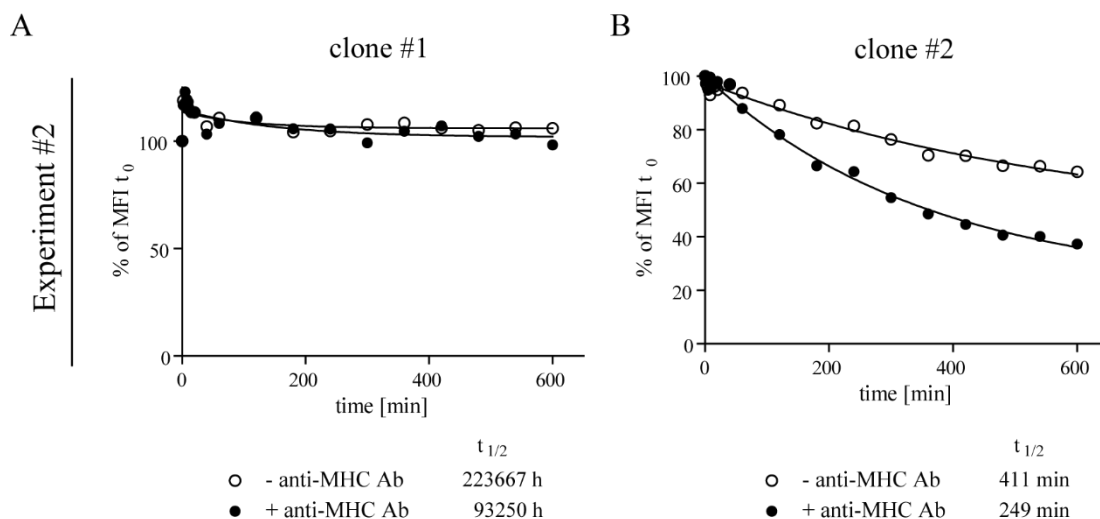


Figure 4-3: Conventional pMHC multimer dissociation experiments are difficult to reproduce.

HLA-B8/IE1₈₈₋₉₆-specific T cell clones #1 (A) and #2 (B) were analyzed in another conventional pMHC dissociation experiment under the same conditions as in Figure 4-2. T cell clones stained with the specific pMHC multimer were incubated for 10h at 4°C in the presence (filled dots) or absence of 10 μ M of the anti-MHC antibody W6/32 (empty dots). Aliquots were taken at the indicated time points and analyzed by FACS. Half-life ($t_{1/2}$) values were calculated from the exponential decay curve fitted into the percent of initial mean fluorescence intensities (% of MFI t_0). Adapted from (Nauerth et al., 2013b).

4.1.2 Principle of the microscopic *Streptamer*-based TCR-ligand k_{off} -rate assay

To improve conventional pMHC multimer-based dissociation measurements, the TCR-ligand k_{off} -rate assay was recently designed and established for murine and human antigen-specific CD8⁺ T cells (Knall, 2007; Nauerth, 2012). This assay is based on reversible *Streptamer* stainings (Knabel et al., 2002) and measures the dissociation kinetics of monomeric pMHC molecules from surface-expressed TCRs. The pMHC multimerization is based on the interaction between a *Strep*-tag sequence fused to the pMHC and *Strep*-Tactin (Voss and Skerra, 1997) allowing to stably label antigen-specific T cells (Fig. 4-4 A). The *Streptamer* complex is disrupted by D-biotin, which binds to the *Strep*-tag binding sites on *Strep*-Tactin with higher affinity, leaving monomeric pMHC bound to surface-expressed TCRs (Fig. 4-4 B) (Knabel et al., 2002). By conjugating the pMHC molecules to a fluorescent dye, the dissociation kinetics of monomerized pMHCs can be observed as the decay in fluorescence intensity (Fig. 4-4 C) (Nauerth et al., 2013b).

Results

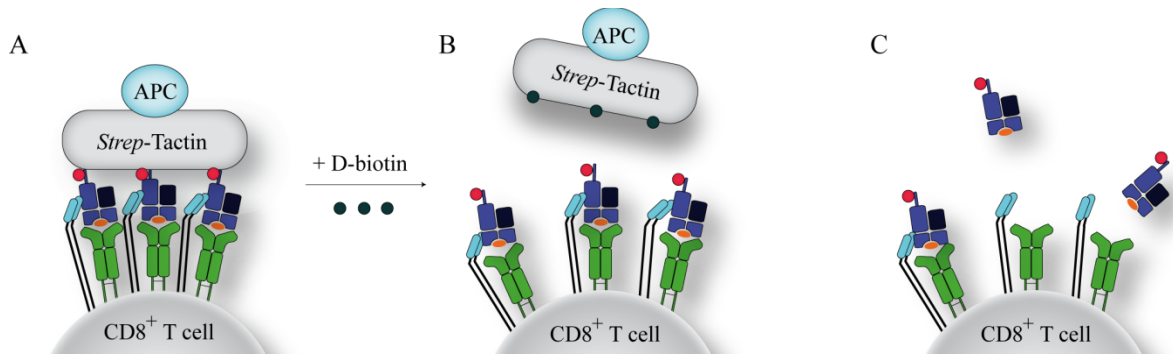


Figure 4-4: Basic principle of the TCR-ligand k_{off} -rate assay.

(A) MHC *Streptamers* stably bind to antigen-specific CD8⁺ T cells. In addition to the multimerizing *Strep-Tactin*-APC (blue), the pMHC monomers are conjugated to a fluorescent dye (red). (B) The *Streptamer* complex is disrupted upon addition of D-biotin that competes with the pMHC binding sites on *Strep-Tactin*. (C) Fluorescence conjugated pMHC monomers bound to surface expressed TCRs dissociate depending on the TCR/CD8 binding avidity. pMHC monomer dissociation can be monitored by the loss of fluorescence intensity. Adapted from (Nauerth et al., 2013b).

The decay of fluorescence intensity can be measured by flow cytometry on the population level or by real-time microscopy on single cell level. For the analysis by flow cytometry, D-biotin is injected into a customized, constantly cooled tube with the *Streptamer* stained antigen-specific T cells 30 s after starting the FACS acquisition (Fig. 4-5 A). Subsequent fluorescence decrease of *Strep-Tactin*-APC backbone and MHC-Alexa488 is monitored over a time frame of 15 min. Mean fluorescence intensity (MFI) of the bulk of antigen-specific T cells is plotted every 4.5 s and an exponential decay curve is fitted into the data to calculate k_{off} -rate. For real-time microscopic analysis of fluorescence loss, the *Streptamer* stained antigen-specific T cells are purified and mounted on to a microscopic setup that is constantly cooled to 4°C (Fig. 4-5 B).

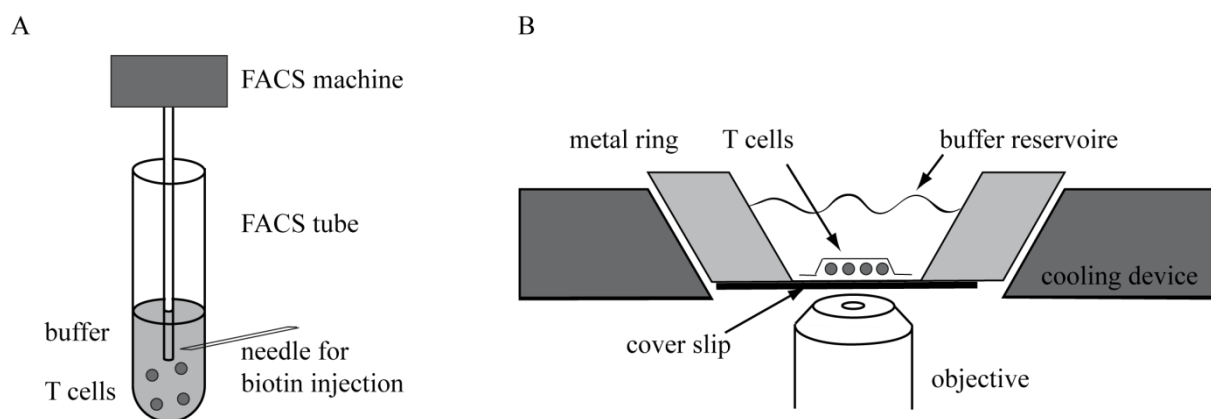


Figure 4-5: Setup for the real-time analysis of fluorescence decay caused by MHC dissociation from antigen-specific T cells by flow cytometry or real-time microscopy.

(A) *Streptamer* labeled antigen-specific T cells are analyzed in customized tubes that are supplied with a needle for injection of D-biotin during the acquisition by flow cytometry. (B) Purified *Streptamer* labeled antigen-specific T cells are mounted onto a buffer reservoir on the inverse microscope. Buffer reservoir consists of a metal ring sealed with a glass cover slip. To arrest T cells efficiently, a membrane is put on top of the cells and weighted down with a metal shim. Adapted from (Nauerth et al., 2013b).

The *Streptamer* staining for APC-backbone and Atto565-MHC fluorescence of individual T cells on the microscopic setup are shown in Fig. 4-6 A before the addition of biotin (0 s) and at the indicated time points after the addition of D-biotin. For the determination of TCR-ligand k_{off} -rate and $t_{1/2}$ of one individual T cell, the cell is selected as a region of interest (ROI, red). The integrated fluorescence intensity of that region is acquired and subtracted by the integrated background intensity of a ROI of identical size from the background. The fluorescence intensities are subtracted by the background fluorescence for each time point and the dissociation $t_{1/2}$ is calculated after fitting an exponential decay curve (Fig. 4-6 B) (Nauerth et al., 2013b).

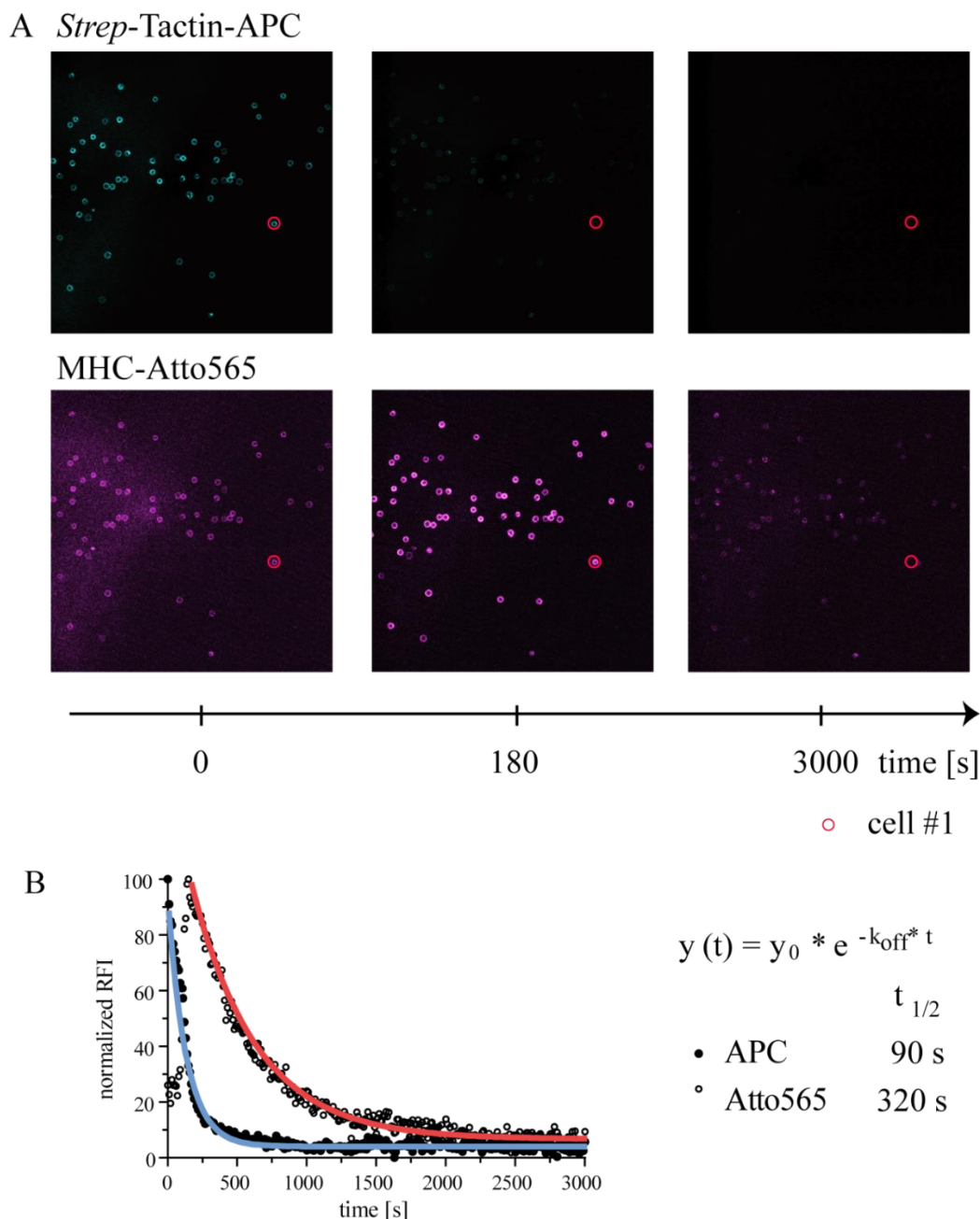


Figure 4-6: TCR-ligand dissociation is monitored by real time microscopy on living antigen-specific T cells.

(A) A bulk of FACS purified, living *Streptamer*⁺ CD8⁺ T cells was mounted to the microscopic TCR-ligand k_{off} -rate assay setup and analyzed for *Strep*-Tactin-APC and MHC I-Atto565 fluorescence every 10 s before and after the addition of 1mM D-biotin. The dissociation of *Strep*-Tactin-APC backbone (top, blue) and pMHC-Atto565 monomers (bottom, magenta) was monitored as the decrease of fluorescence intensity. Individual T cells are selected as a region of interest (ROI, red) to acquire the integrated fluorescence intensity of the region and the integrated intensity of a ROI of identical size in the background is subtracted. (B) The background corrected relative fluorescence intensities (RFI) for *Strep*-Tactin-APC and pMHC-Atto565 for cell #1 illustrated in the red ROI in A were plotted for each time point and the half-life time of TCR-pMHC interaction ($t_{1/2}$) was calculated after fitting an exponential decay curve into the data.

Results

Fluorescently labeled individual single cells in the microscopic TCR-ligand $k_{\text{off-rate}}$ setup are repetitively exposed to laser emission. The repetitive exposure to laser emission causes irreversible damage of the fluorochrome resulting in the loss of fluorescence intensity called photo bleaching. Therefore the observed decrease of fluorescence intensity of pMHC monomer dissociation in the TCR-ligand $k_{\text{off-rate}}$ assay had to be corrected for photo bleaching. To determine the photo bleaching rate depending on the power and frequency of laser emission, fluorochrome labeled cells and beads were analyzed in the TCR-ligand $k_{\text{off-rate}}$ setup. *Streptamer*-stained antigen-specific T cells were not exposed to D-biotin to allow a stable staining throughout the bleaching measurement. Here, the mean bleaching rate (k_{bleach}) of 0.0004 s^{-1} was very low (Fig. 4-7 A). However, for many *Streptamer*-stained T cells the initial staining intensity of the pMHC-Atto565 in the complex was only very weak, as the dye is quenched by the *Strep*-Tactin molecule. Bleaching could only be determined, if the cells had a very bright initial staining intensity. Further, the k_{bleach} values determined on T cells were variable (coefficient of variation/cv = 81%). For this reason, different *Strep*-Tactin coated beads multimerized with the Atto565-conjugated *Strep*-tagged pMHC monomers were tested. *Strep*-Tactin bead #1 was mainly coated on the surface (Fig. 4-7 B). However, the mean bleaching rate of 0.003 s^{-1} was 10-fold higher in comparison to *Streptamer*-stained T cells, probably due to their huge size and over 10-fold higher staining initial relative fluorescence intensity/RFI t_0 (Fig. 4-7 B). Despite their size and high initial RFI, the mean k_{bleach} of *Strep*-Tactin bead #2 with a broader distribution of *Strep*-Tactin was comparable to the bleaching on cells (0.0002 s^{-1} in Fig. 4-7 C). Optimal determination of the bleaching constant was obtained using small beads covalently coupled to Atto565 dye (Fig. 4-7 D). The beads were similar in size ($10\mu\text{m}$), similar in initial relative fluorescence intensity (RFI of about 10^4) and a similar mean k_{bleach} of 0.0005 s^{-1} was determined compared to *Streptamer* stained T cells with a minimal degree of variation (cv = 16%). These beads allowed a reproducible measurement of the bleaching rate that reflects the bleaching of pMHC-Atto565 dye on the T cells during the TCR-ligand $k_{\text{off-rate}}$ measurement.

Results

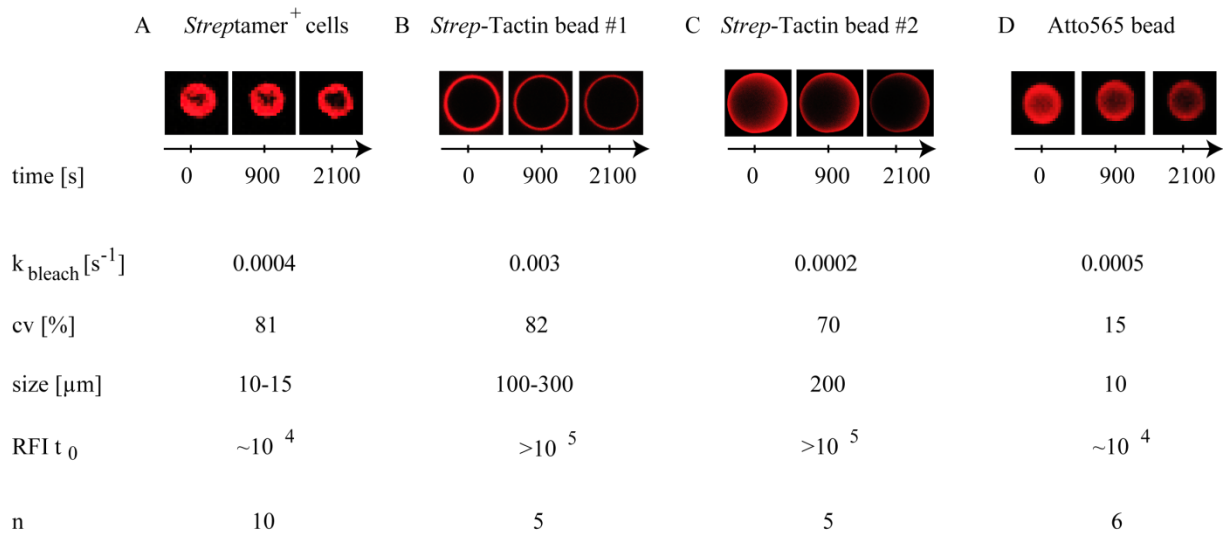


Figure 4-7: Bleaching rate on small beads is reproducible and comparable to bleaching rate on cells.

Representative image of (A) a pMHC-Atto565 stained T cell clone, (B and C) a *Strep*-Tactin bead multimerized with *Strep*-tagIII pMHC-Atto565 monomers and (D) a bead covalently coupled to Atto565 dye before/0 s, 900 s and 2100 s after exposure to 561nm laser emission every 10 s in the microscopic TCR-ligand k_{off} -rate setup in the absence of D-biotin. Indicated are the mean bleaching rate (k_{bleach}), the coefficient of variation (cv), the size, the relative fluorescence intensity before acquisition (RFI t_0) and the number of cells/beads analyzed (n).

Results

4.1.3 TCR-ligand k_{off} -rate assay allows reproducible and standardized measurements of fast and slow dissociation kinetics

To compare the *Streptamer* k_{off} -rate assay with conventional multimer dissociation experiments, the T cell clones shown in Fig. 4-2 and 4-3 were analyzed. In contrast to conventional multimer dissociation experiments, *Streptamer* k_{off} -rate assay measurements of the T cell clones were much more reproducible, as shown in Fig. 4-8 A and C, in different dissociations of two or three independent experiments. The mean $t_{1/2}$ values for T cell clone #1 and #2 are summarized on the right in Fig. 4-8 B and D. T cell clone #1 had an about fourfold longer $t_{1/2}$ of 200 s in comparison to clone #2 with a mean $t_{1/2}$ of 55 s (Nauerth et al., 2013b).

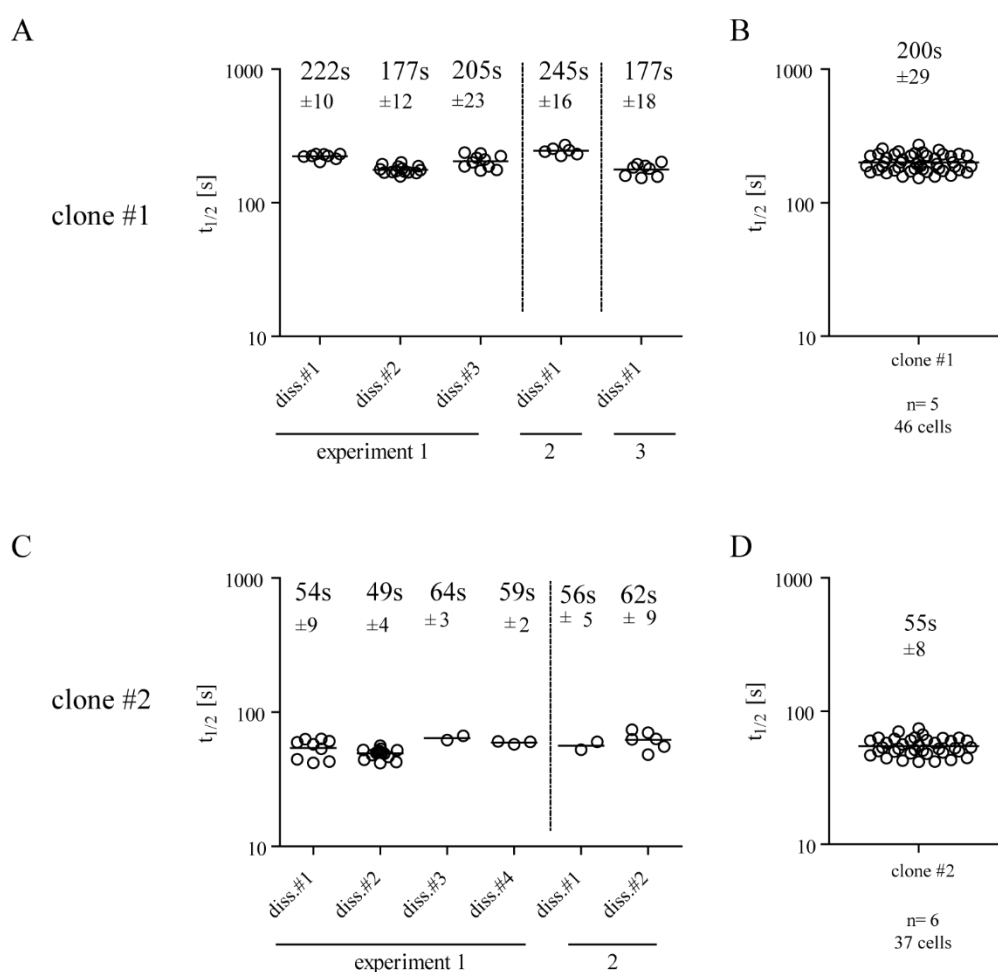


Figure 4-8: Reproducible dissociation half-life values ($t_{1/2}$) of MHC monomers in the TCR-ligand k_{off} -rate assay.

Repetitive analysis of T cell clones in the *Streptamer*-based TCR-ligand k_{off} -rate assay. (A) Independent dissociations (diss) and experiments for CMV-specific T cell clone #1 and (B) T cell clone #2 from Fig. 4-2 and 4-3. Each dot represents the $t_{1/2}$ of one cell analyzed. Numbers indicate the mean $t_{1/2} \pm \text{SD}$ of each dissociation. (B) Summary of $t_{1/2}$ values of individual cells from T cell clone #1 and (D) T cell clone #2 with the mean $t_{1/2} \pm \text{SD}$. Adapted from (Nauerth et al., 2013b).

Results

In theory, once the *Streptamer* complex is disrupted by D-biotin, rebinding of monomerized pMHC to TCRs on the T cell surface is unlikely. In contrast to pMHC multimer dissociation experiments, the dissociation of monomeric pMHCs is supposed to be independent from the addition of a blocking reagent. The influence of the addition of a blocking reagent in the TCR-ligand k_{off} -rate setup was tested as illustrated in Fig. 4-9.

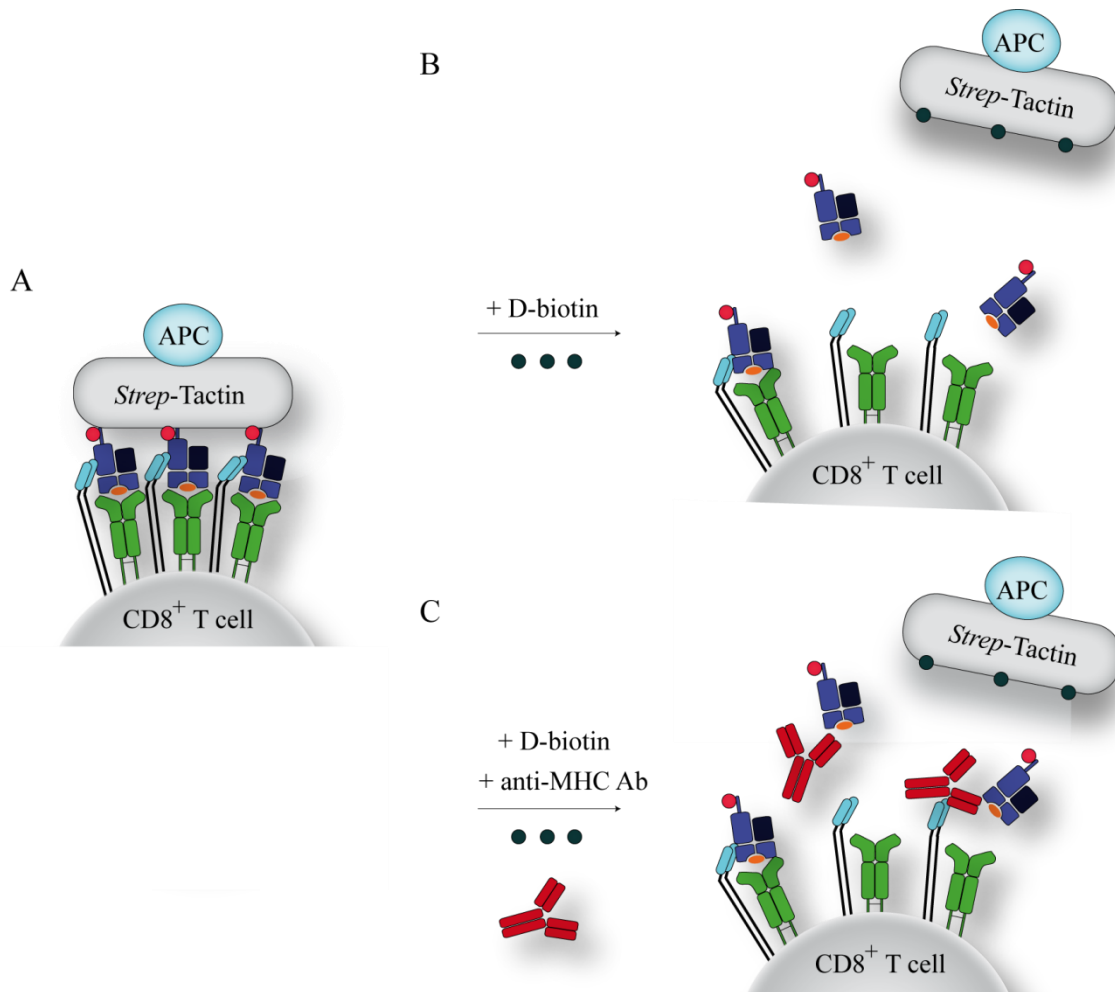


Figure 4-9: TCR-ligand k_{off} -rate assay in the presence or absence of MHC rebinding blocking antibody.

D-biotin in combination with (C) or without anti-MHC antibody (Ab) (B) was added to the *Streptamer* stained T cells (A) in the cooled buffer reservoir to a final concentration of 1mM D-biotin and 10 μ M antibody. Subsequent dissociation of *Strep-Tactin*-APC and monomeric MHC molecules was observed as a decay of the fluorescence by real-time microscopy. Adapted from (Nauerth et al., 2013b).

Results

Dissociation $t_{1/2}$ values of a high avidity T cell clone was minimally increased from 200 s to 168 s in the presence of the blocking antibody (Fig. 4-10 A). For a low avidity T cell clone there was no difference in the dissociation values without or with the addition of the blocking antibody (Fig. 4-10 B; 28 and 29 s, respectively). Therefore, the *Streptamer* k_{off} -rate assay is not substantially affected by pMHC rebinding, strongly improving the reproducibility of the measurements in comparison to conventional dissociation experiments (Nauerth et al., 2013b).

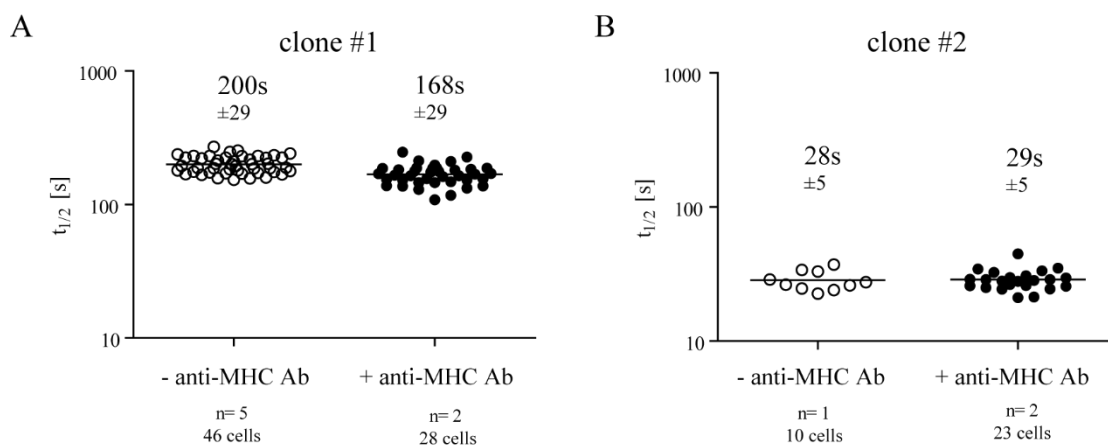


Figure 4-10: Dissociation of pMHC monomers in the TCR-ligand k_{off} -rate assay can be monitored without blockade of MHC rebinding.

TCR-ligand $t_{1/2}$ values of CMV-specific T cell clones with high (A) or low avidity (B) in the absence (-Ab) or presence of anti-MHC blocking antibody (+Ab). The $t_{1/2}$ values of individual cells are plotted with the mean $t_{1/2} \pm$ SD. Adapted from (Nauerth et al., 2013b).

Furthermore, the influence of the fluorescent dye APC conjugated to the *Strep*-Tactin backbone molecule on the TCR-ligand k_{off} -rate measurement was tested. Using *Strep*-Tactin without fluorochrome conjugation, the $t_{1/2}$ values of two T cell clones with distinct avidities were reproducible, indicating no influence of the APC on the Atto565 fluorescence decrease (Fig. 4-11) (Nauerth et al., 2013b).

Results

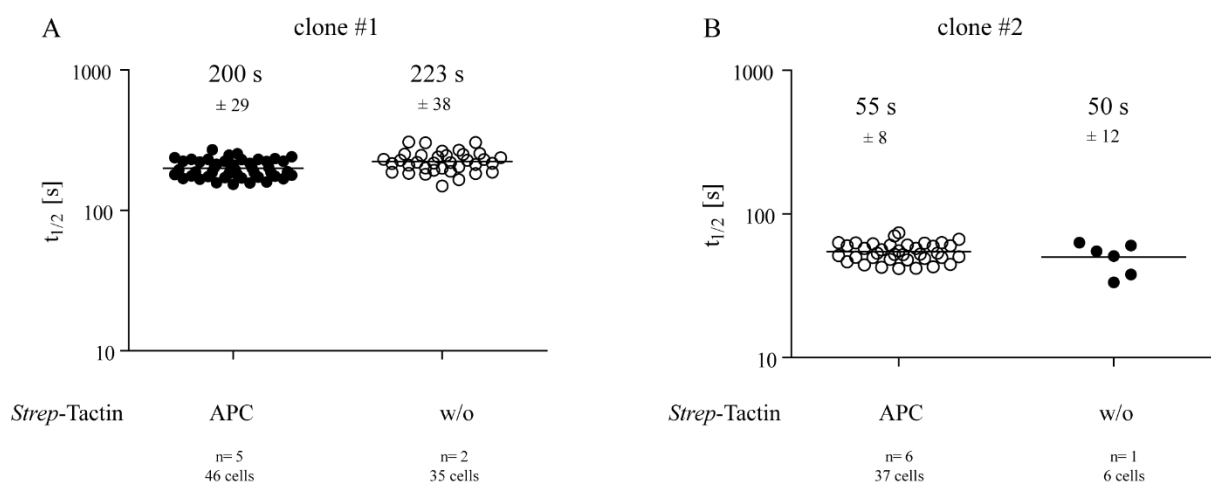


Figure 4-11: Dissociation of pMHC monomers in the TCR-ligand k_{off} -rate assay is comparable with and without APC fluorochrome on the *Strep-Tactin* backbone.

TCR-ligand $t_{1/2}$ values of CMV-specific T cell clones with high (A) or low avidity (B) stained with *Streptamers* consisting of Atto565-labeled MHC monomers multimerized either on *Strep-Tactin*-APC or *Strep-Tactin* devoid of a fluorochrome label (w/o). The $t_{1/2}$ values of individual cells are plotted with the mean $t_{1/2} \pm \text{SD}$. Adapted from (Nauerth et al., 2013b).

4.1.4 TCR-ligand $t_{1/2}$ values predict the functionality of antigen-specific T cells independently of multimer staining intensity

Another simple multimer-based method to assess the structural TCR-ligand binding strength is the analysis of the multimer staining intensity (MFI). This parameter is believed to be a predictor for T cell functionality directed against the respective epitope. Here, T cells are labeled with specific, fluorescence conjugated MHC multimers (Fig. 4-12 A). The fluorescence intensity of the multimer should reflect the number of multimers bound to the T cell surface. High avidity TCRs are characterized by a slow dissociation (k_{off} -rate) and/or rapid association (k_{on} -rate) of MHC multimers. This combination results in the binding of a high amount of multimers and consequently result in a high multimer MFI (Fig. 4-12 B). Low avidity T cells, in contrast, are characterized by a fast dissociation and/or slow association of MHC multimers. Consequently, they are supposed to be only weakly stained with low MFI due to a lower amount of MHC multimers on the T cell surface (Fig. 4-12 C).

Results

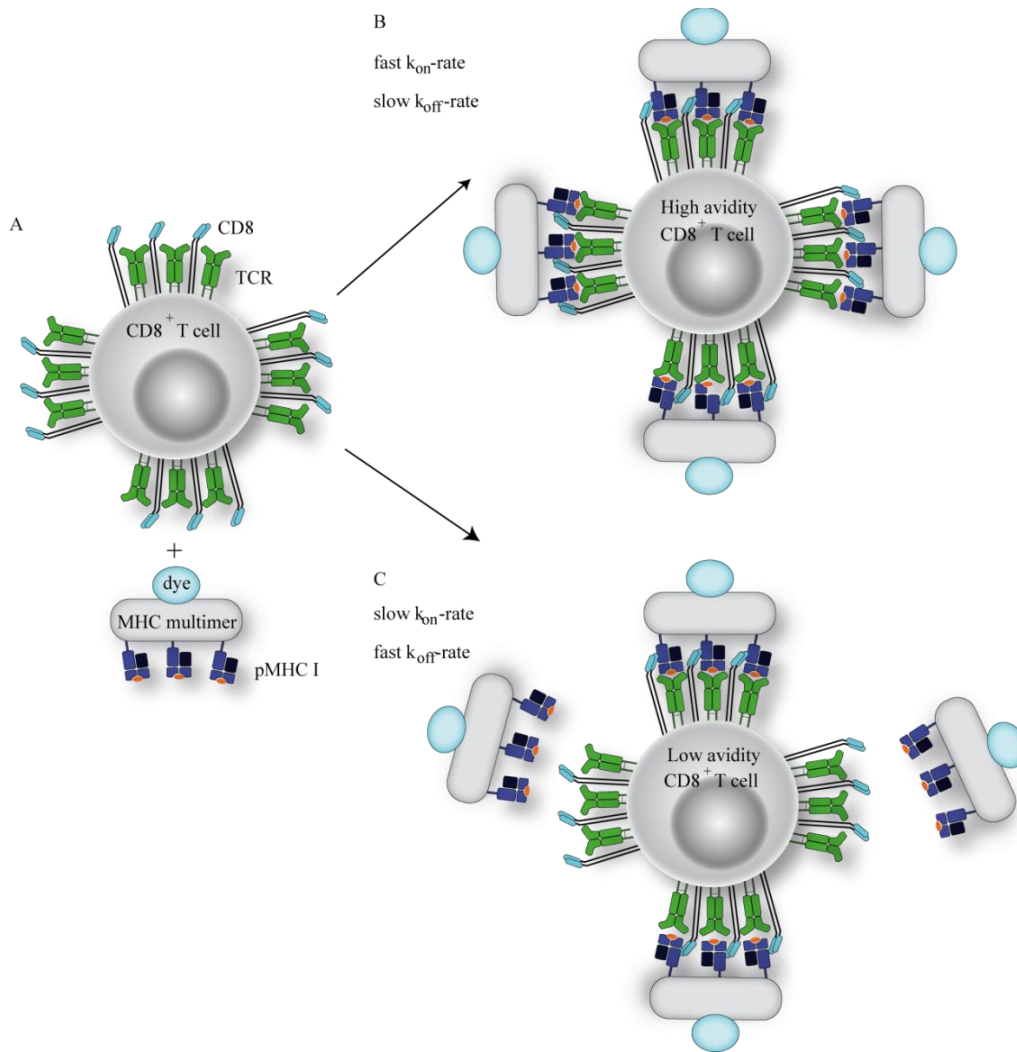


Figure 4-12: pMHC multimer staining intensity to measure structural TCR binding strength.

(A) Antigen-specific CD8⁺ T cells are labeled with fluorescence conjugated MHC multimers. (B) High avidity T cells with fast k_{on} -rates and slow k_{off} -rates can bind greater amounts of MHC multimer and are therefore stained brighter. (C) Low avidity T cells with slow k_{on} -rates and fast k_{off} -rates bind less amounts of MHC multimer resulting in weaker staining MHC staining intensity.

A number of different CMV-specific T cell clones that were isolated based on MHC binding from the naïve T cell repertoire and expanded *in vitro* were analyzed for their MHC multimer staining intensity and peptide sensitivity by Pleun Hombrink and Mirjam Heemskerck (Hombrink et al., 2013). Five representative T cell clones were stained equally well with the HLA-A1/pp65 multimer as shown in Fig. 4-13.

Results

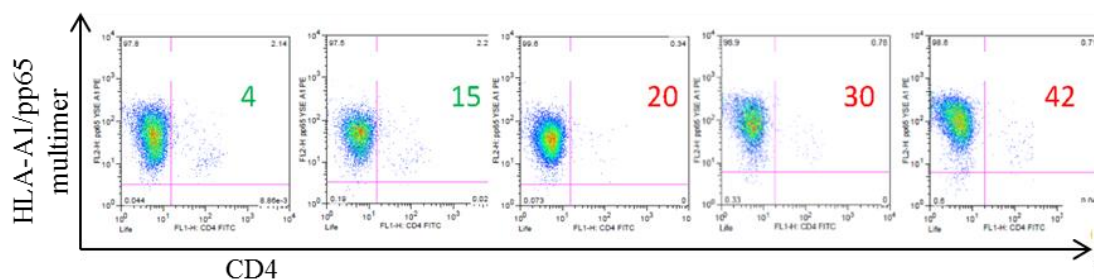


Figure 4-13: T cell clones from the naïve T cell repertoire can be labeled with MHC multimers.

T cell clones isolated based on MHC multimer binding were stained with HLA-A1/pp65-specific multimers after *in vitro* expansion.

T cell clones 30 and 42 had a higher mean fluorescence intensity in comparison to T cell clones 4, 15 and 20 (Fig. 4-14 A). However, when analyzing the T cell clones for their functional capacity by stimulation with the respective peptide at different concentrations, only clones 4 and 15 were able to produce IFN γ (Fig. 4-14 B). There was no correlation between multimer staining intensity and functionality of these T cell clones.

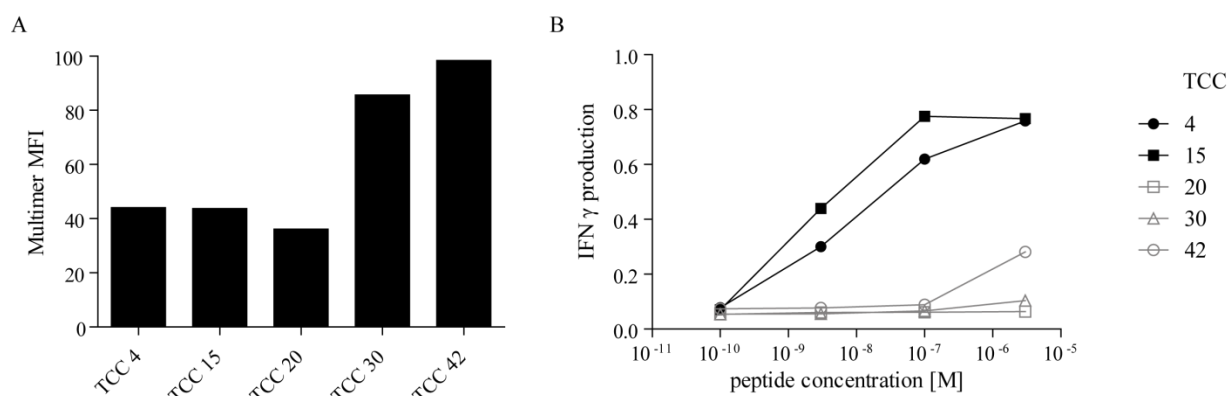


Figure 4-14: MHC multimer staining intensity of *in vitro* expanded T cell clones from the naïve T cell repertoire does not correlate with functional avidity.

(A) Mean fluorescence intensities (MFI) of the MHC multimer staining for T cell clone 4, 15, 20, 30 and 42 are plotted. (B) HLA-A1/pp65-specific T cell clones and lymphoblastoid cell line (LCL) target cells loaded with the indicated concentration of the pp65 YSE were incubated overnight. IFN- γ production in the supernatant was measured by ELISA.

Subsequently, the T cell clones were analyzed in the *Streptamer*-based TCR-ligand k_{off} -rate assay. T cell clones 4 and 15 had long mean $t_{1/2}$ (109 s and 127 s, respectively), whereas T cell clones 20, 30 and 42 were characterized by very fast mean $t_{1/2}$ (28 s, 35 s and 23 s, respectively) (Fig. 4-15). In contrast to the multimer staining intensity, these mean $t_{1/2}$ values

Results

for the T cell clones were correlating with the ability to produce IFN γ in response to the target epitope (Hombrink et al., 2013). The TCR-ligand k_{off} -rate assay can therefore predict the functionality of antigen-specific T cells independently of MHC multimer staining intensity.

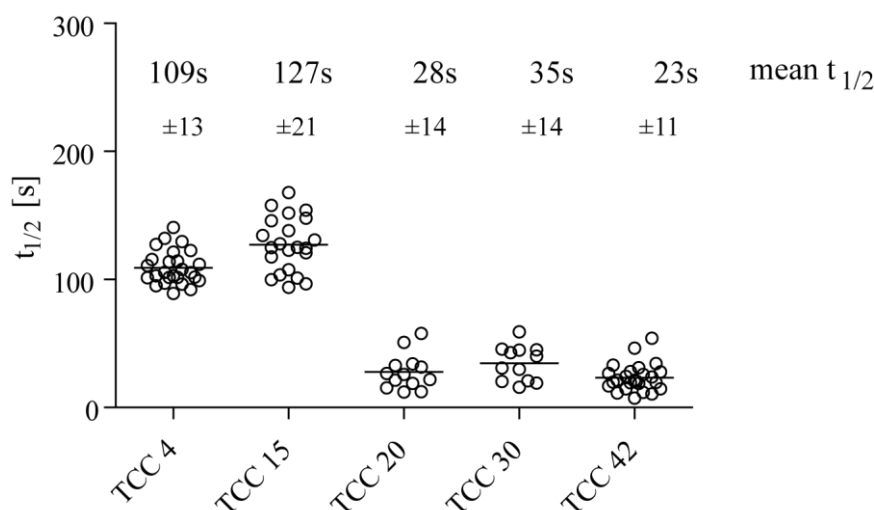


Figure 4-15: Fast TCR-ligand k_{off} -rate of *in vitro* expanded T cell clones from naïve T cell repertoire correlates to low functional avidity.

TCR-ligand $t_{1/2}$ values of HLA-A1/pp65-specific T cell clones 4, 15, 20, 30 and 42 derived from the naïve T cell repertoire. Numbers in the graph indicate the mean $t_{1/2}$ with standard deviation (\pm SD) for each measurement. Adapted from (Hombrink et al., 2013).

4.1.5 TCR-ligand $t_{1/2}$ values depend on the structure of the TCR rather than the cellular background

In order to analyze if the *Streptamer* TCR-ligand k_{off} -rate measurement is influenced not only by the structure of the TCR, but further by the cellular background such as the activation status, a number of different CMV-specific T cell clones was tested under different conditions. Different T cell clones of low and high avidity with an identical TCR (TCR sequencing data generated by Georg Dössinger; not shown) had comparable dissociation curves and kinetics calculated. Figure 4-16 A and B illustrate the dissociation curve of individual cells and Figure 4-16 C and D summarize the $t_{1/2}$ values of all cells analyzed. The dissociation kinetics for low and high avidity T cell clones at early as well as at late time points after *in vitro* stimulation during a resting phase in IL-15 were comparable (Fig. 4-16 C and D, respectively). Summarizing, neither the activation status of the cell, nor the expression of the TCR on a different T cell clone influences TCR-ligand k_{off} -rate measurement as shown for low and high avidity T cell clones. These similar mean $t_{1/2}$ values demonstrate that the

Results

TCR-ligand k_{off} -rate measurement is mainly dependent on the structure of the TCR and relatively independent from the cellular background of T cells analyzed (Nauerth et al., 2013b).

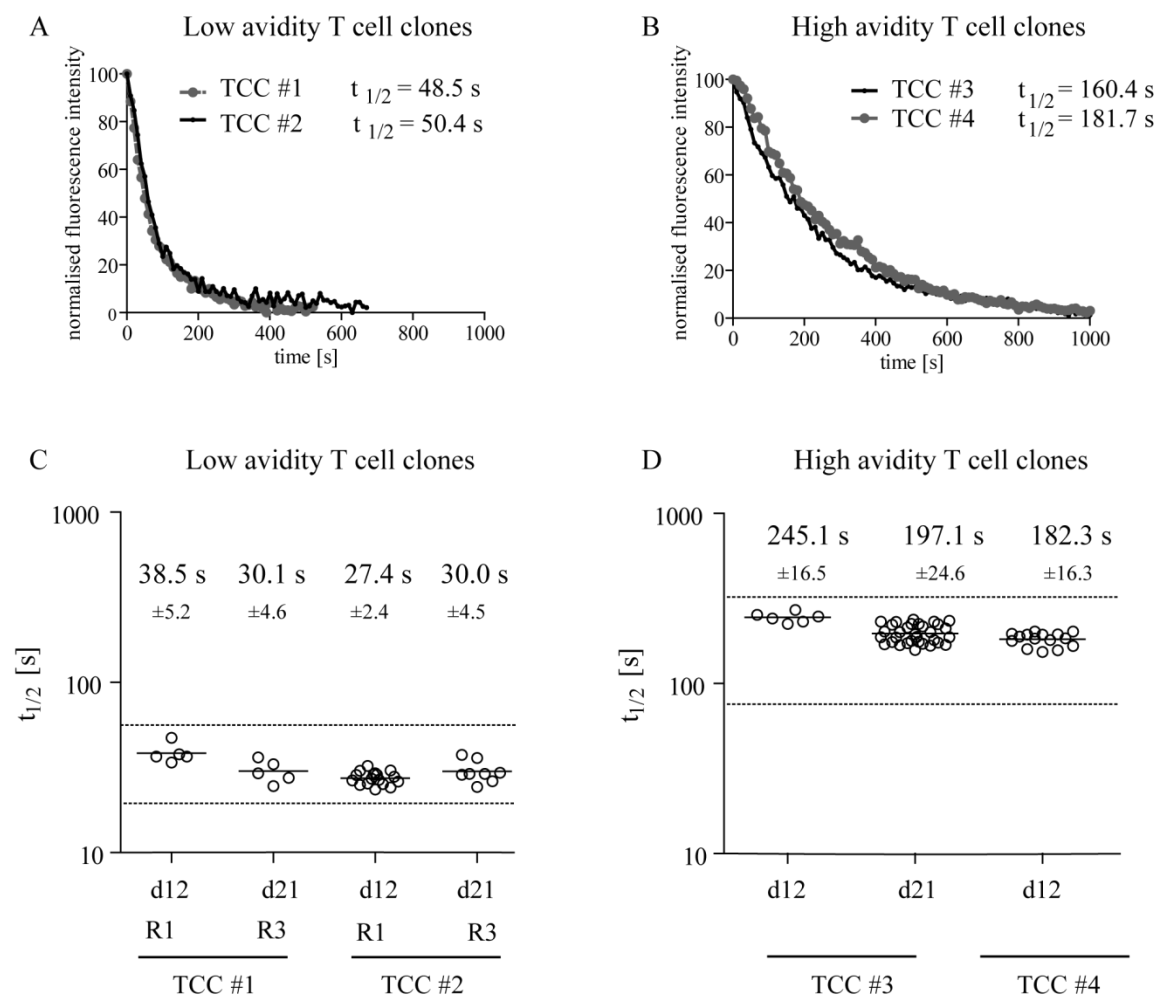


Figure 4-16: Dissociation half-life times in the TCR-ligand k_{off} -rate assay are comparable during different activation states of analyzed cells.

(A) Representative dissociation curves and $t_{1/2}$ values calculated of single cells of different T cell clones expressing identical TCRs with fast (TCC #1 and TCC #2) and (B) slow dissociation $t_{1/2}$ times (TCC #3 and TCC #4). Indicated is the normalized fluorescence intensity of pMHC monomers over the time monitored by real-time microscopy. (C) Summarized $t_{1/2}$ values of the T cell clones TCC #1 and TCC #2 with fast and (D) TCC #3 and TCC #4 with slow dissociation kinetics analyzed early after T cell restimulation (“d12”) or in a resting phase after restimulation (“d21”). The $t_{1/2}$ of individual cells are plotted with the mean $t_{1/2} \pm \text{SD}$ for each condition. Adapted from (Nauerth et al., 2013b).

Results

To investigate the correlation between k_{off} -rate values and functional avidity of T cells, two human T cell clones specific for different epitopes derived from human CMV immediate-early 1 antigen (IE1) were analyzed (Fig. 4-17 A). HLA-B8/IE1₈₈₋₉₆-specific T cell clone B had a longer mean $t_{1/2}$ (178 s) compared to HLA-B8/IE1_{199-207KM}-specific T cell clone A (41 s) (Fig. 4-17 B). In a chromium release assay and intracellular cytokine staining (ICCS), clone B reached half-maximal lysis of peptide-pulsed target cells and half-maximal IFN- γ production (EC_{50}) at lower peptide concentrations in comparison to clone A (Fig. 4-17 C and D). Functional avidity of the clones correlated with the different $t_{1/2}$ determined in the k_{off} -rate assay (Nauerth et al., 2013b).

Results

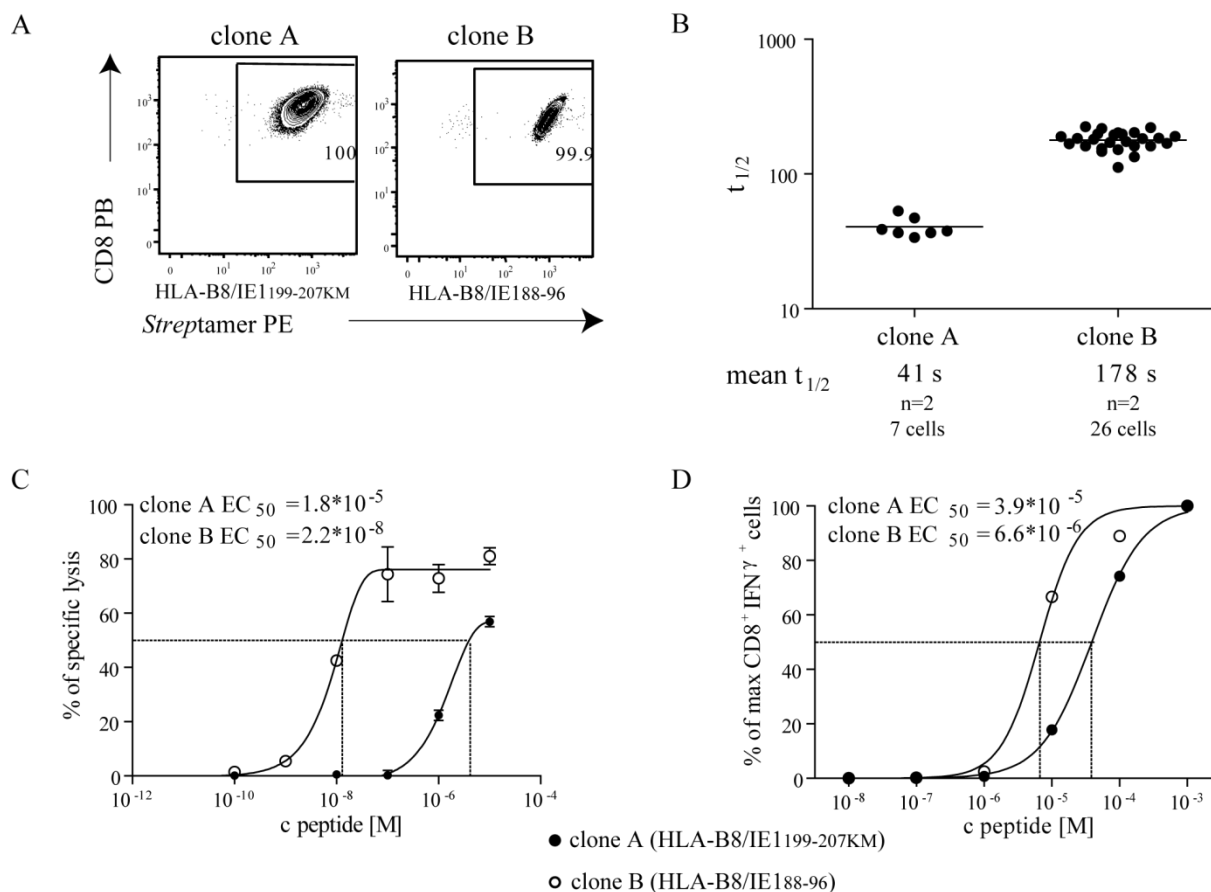


Figure 4-17: Dissociation half-life times in the TCR-ligand k_{off} -rate assay correlate with functional avidity.

(A) Streptamer stainings of HLA-B8/IE1_{199-207KM}-specific T cell clone A and HLA-B8/IE1₈₈₋₉₆-specific T cell clone B (gated on living lymphocytes). (B) TCR-ligand $t_{1/2}$ values of T cells of clone A and clone B with the mean $t_{1/2}$ and standard deviation (\pm SD). (C) Target cell killing of T cell clones A and B. T cell clones were incubated at an effector to target ratio of 10:1 with HLA/B8-expressing LCLs, which were labeled with ⁵¹Cr and loaded with the indicated amount of IE1_{199-207KM} or IE1₈₈₋₉₆ peptide. Specific target cell lysis was measured in a γ -counter from the supernatant. A non-linear regression curve was fitted into the data to calculate the peptide concentration for the half maximal lysis (EC_{50}). (D) IFN γ production was measured after incubation of T cell clones and HLA/B8-expressing LCLs loaded with the indicated amounts of IE1_{199-207KM} or IE1₈₈₋₉₆ peptide in an effector to target ratio of 10:1. A non-linear regression curve was fitted into the normalized data to calculate the peptide concentration for the half maximal lysis (EC_{50}). Adapted from (Nauerth et al., 2013b).

TCRs from both clones A and B were isolated and expressed on CD8 α^+ Jurkat cells by Georg Dössinger, purified by FACS (Fig. 4-18 A) and analyzed in the TCR-ligand k_{off} -rate assay in cooperation with Magdalena Nauerth. Highly comparable $t_{1/2}$ values of T cell clones and transduced Jurkat cells demonstrate that the TCR is the main determinant of measured k_{off} -rates (Fig. 4-18 B) (Nauerth, 2012; Nauerth et al., 2013b). Further, to test the functionality upon TCR re-expression, healthy donor PBMCs were transduced with the respective TCRs by

Results

Mario Bunse and stimulated with peptide loaded target cells. TCR A needed higher effector: target ratios for specific killing and higher amounts of the peptide on target cells for production of IFN γ (Fig. 4-18 C and D). The maintenance of the functional avidity after re-expression of TCRs on other cells emphasizes the structural TCR binding strength as a major determinant of T cell functionality.

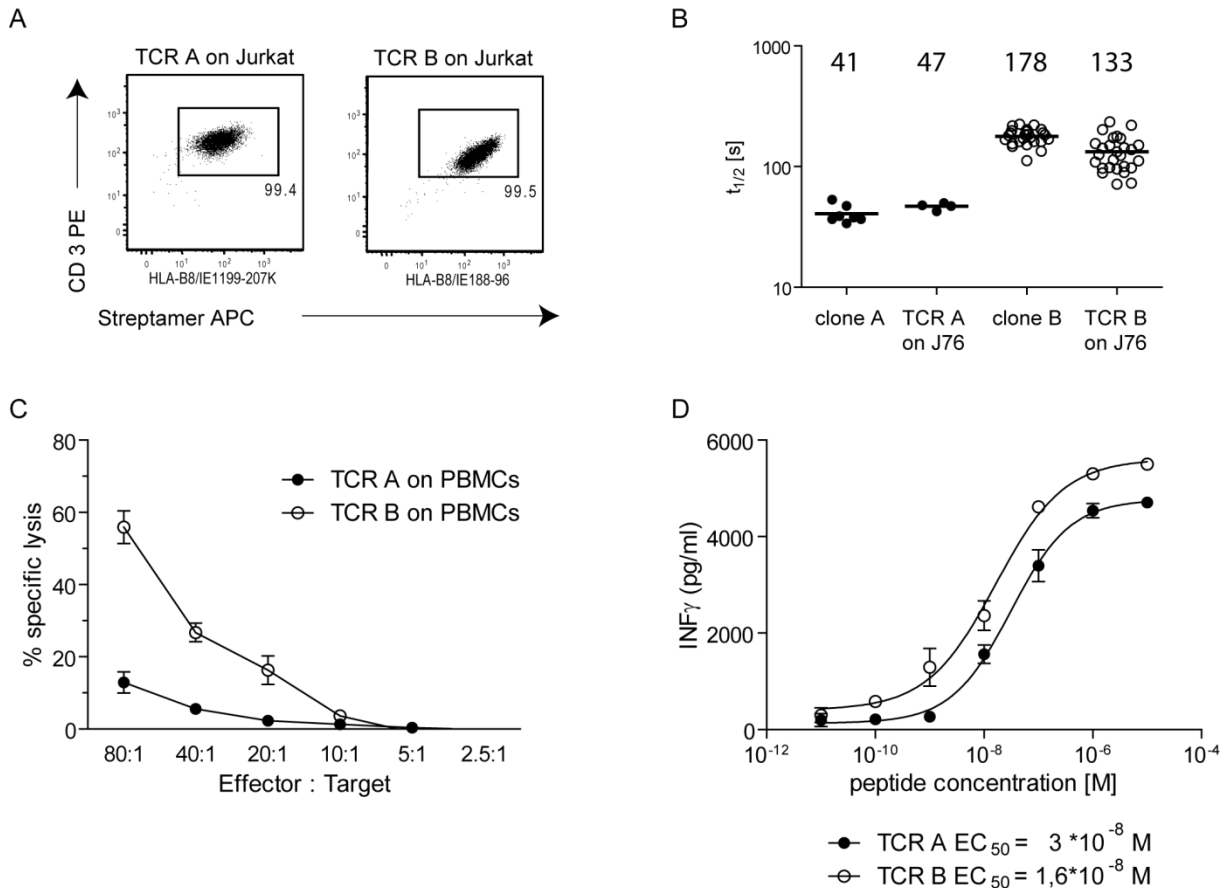


Figure 4-18: TCR-ligand dissociation half-life time and functional avidity of two human CMV-specific TCRs is maintained after transgenic re-expression.

(A) FACS dot plots displaying *Streptamer*- and CD3-stainings of HLA-B8/IE1₁₉₉₋₂₀₇KM-specific TCR A and HLA-B8/IE1₈₈₋₉₆-specific TCR B on Jurkat76 cells (gated on living lymphocytes). (B) TCR-ligand $t_{1/2}$ values of TCR A and TCR B re-expressed on Jurkat76 T cells in comparison the $t_{1/2}$ values of their respective originating T cell clones A and B. Numbers in the graph indicate the mean $t_{1/2}$ with standard deviation (\pm SD) for each measurement. (C) Target cell killing of PBMCs transduced with TCR A (black) or TCR B (white). T cells were incubated for 4h at the indicated effector to target ratios (E:T) with 51 Cr labeled and peptide loaded HLA/B8-expressing LCLs (10 μ M of IE1₁₉₉₋₂₀₇K or IE1₈₈₋₉₆). Specific target cell lysis was measured in a γ -counter from the supernatant. (D) IFN γ secretion was measured in the supernatant by ELISA after 24h co-incubation of TCR A (black) or TCR B (white) expressing PBMCs either with HLA/B8-expressing LCLs loaded with 10^{-5} – 10^{-11} M of specific peptide at an effector to target ratio of 1:1. A non-linear regression curve was fitted into the data to calculate the peptide concentration for the half maximal lysis (EC_{50}). Adapted from (Nauerth et al., 2013b).

4.1.6 Complete TCR-ligand dissociation can be monitored at room temperature with accelerated $t_{1/2}$ values

TCR-ligand dissociation kinetics depend on the temperature during the measurement. To prevent internalization of pMHCs upon binding to the surface expressed TCRs, all measurements were performed at 4°C under constant cooling (Knabel et al., 2002). To investigate how much changes in temperature influence the dissociation kinetics in the setup, the murine 2C TCR was analyzed in combination with its high avidity ligand H2-K^b/SIY or with the low avidity ligand H2-K^b/dEV8 at higher temperatures. D-biotin was injected into a customized FACS tube with the H2-K^b/SIY *Streptamer*-stained 2C cells 30 s after starting the FACS acquisition at room temperature (22°C) (Fig. 4-19 A). Subsequent fluorescence decrease of *Strep*-Tactin-APC backbone and pMHC-Alexa488 was monitored for 15 min (Fig. 4-19 B). The MFI of all cells in a time gate of every 4.5 s (200 gates for 15 min) were plotted and exponential decay curves fitted into the data to calculate k_{off} -rate of *Strep*-Tactin APC-backbone (blue) and pMHC-Alexa488 (green) (Fig. 4-19 C). Despite the increased risk of TCR internalization at temperature above 4°C, a complete dissociation of the monomeric pMHC from the T cells could be observed at room temperature.

Results

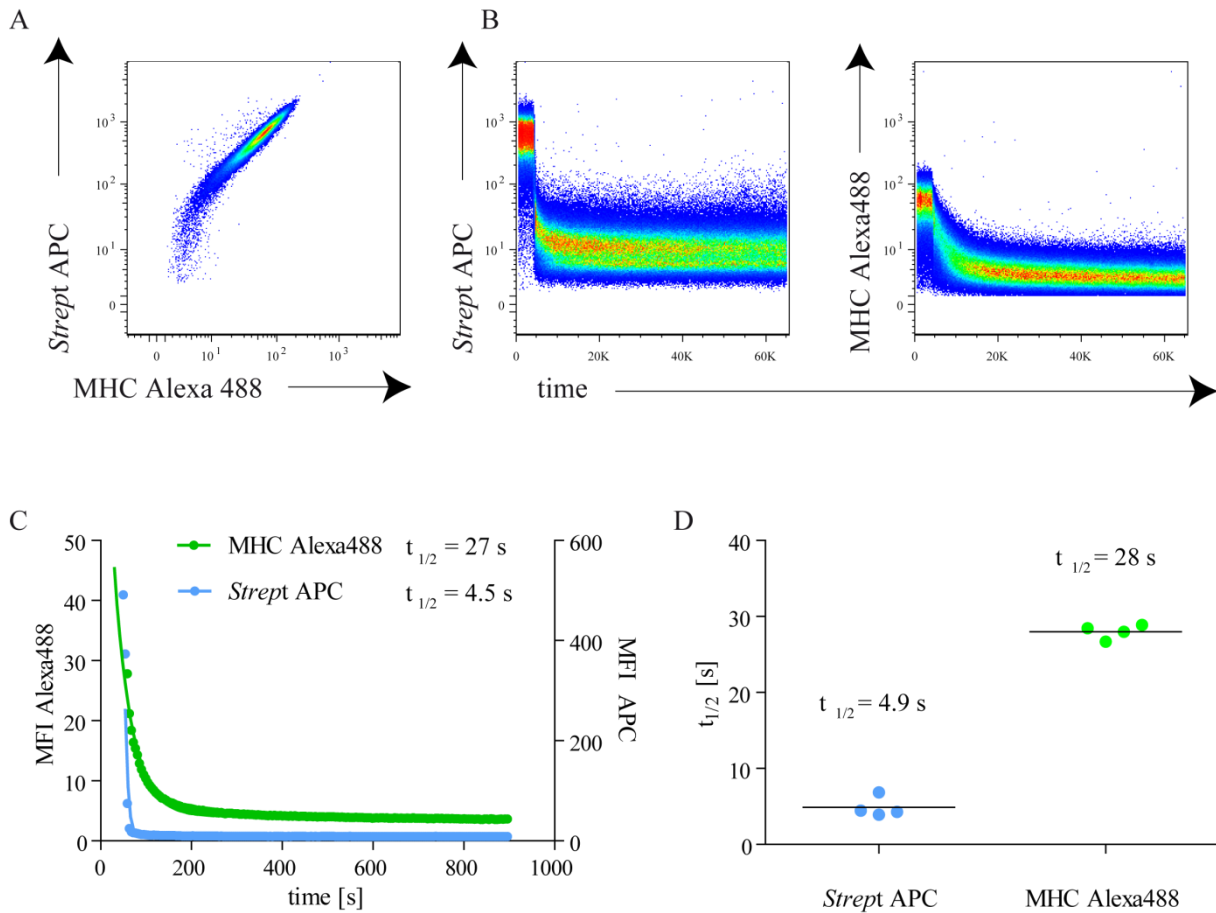


Figure 4-19: pMHC monomers dissociate completely from antigen-specific T cells at room temperature.

(A) FACS dot plots displaying H2-K^b/SIY *Streptamer*-APC and pMHC-Alexa488-stainings of murine T cell line 2C (gated on living lymphocytes). (B) Dissociation of *Streptactin*-APC and pMHC-Alexa488 was monitored over 15 min after addition of D-biotin in a final concentration of 1mM at room temperature. (C) Geometric mean values of *Streptactin*-APC and pMHC-Alexa488 were plotted in a series of 200 gates and a one-phase decay curve was fitted into the data to calculate $t_{1/2}$. (D) The $t_{1/2}$ values for the measurement at room temperature of four independent dissociation experiments of a bulk of 2C cells analyzed by time-lapse flow cytometry are plotted with their mean $t_{1/2}$.

Results

Further, high avidity ligand H2-K^b/SIY and weak avidity ligand H2-K^b/dEV8 were analyzed on 2C transgenic T cells in the microscopic k_{off} -rate setup at 22°C and compared the $t_{1/2}$ values to the $t_{1/2}$ values at 4°C (Fig. 4-20). Mean $t_{1/2}$ for H2-K^b/SIY dissociation from 2C cells at room temperature was comparable for the flow cytometric and the standard real-time microscopic analysis (Fig. 4-19 mean $t_{1/2}$ = 32 s and Fig. 4-20 and mean $t_{1/2}$ = 28 s). The mean $t_{1/2}$ for the high avidity and the low avidity ligand were accelerated two-fold with increasing temperatures from 4°C to 22°C.

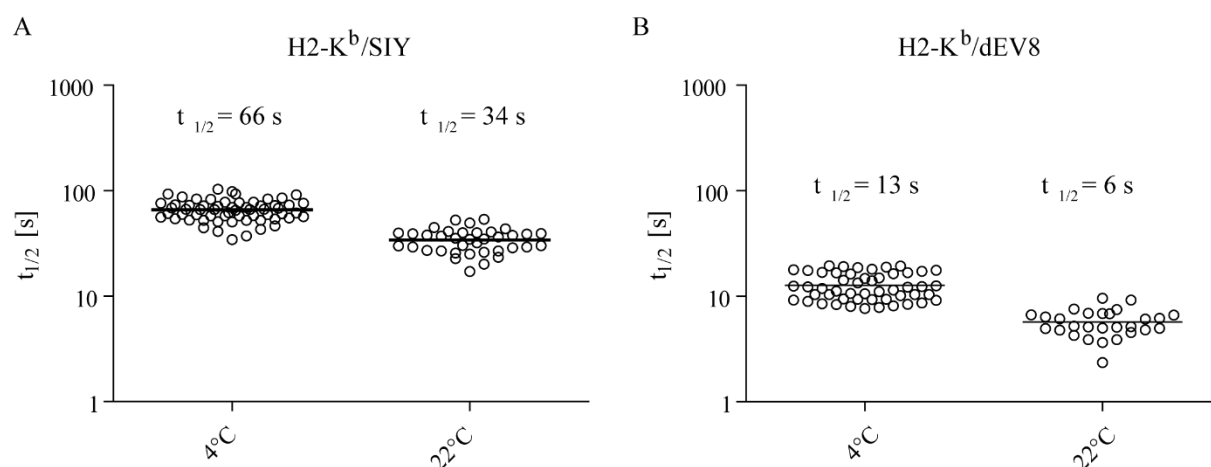


Figure 4-20: Dissociation of monomeric pMHC molecules is accelerated at higher temperatures.

The $t_{1/2}$ values of individual 2C cells analyzed at 4 and 22°C (room temperature) by real-time microscopy in the conventional k_{off} -rate setup are plotted with their mean $t_{1/2}$ for a high affinity ligand H2-K^b/SIY (A) and low affinity ligand H2-K^b/dEV8 (B).

Taken together, testing the TCR-ligand k_{off} -rate assay on a number of T cell clones under different conditions demonstrated that it is a highly reproducible measurement of the structural TCR binding strength relatively independent from cellular background of the antigen-specific T cells. Consequently, this assay allows distinguishing between the quality of the TCR and the quality and functionality of a T cell and offers a great tool to analyze the clonally expanded and functional exhausted antigen-specific CD8⁺ T cells in response to CMV epitopes during chronic infection.

4.1.7 Generation of fluorescence-conjugated murine pMHC monomers for TCR-ligand k_{off} -rate analysis

In order to analyze different MCMV-specific T cell responses in the TCR-ligand k_{off} -rate assay, fluorescence-conjugated murine pMHC monomers had to be generated by insertion of a linker and a cysteine at the end of the respective MHC heavy chain and *Strep*-tag sequence in a pET3a vector (Fig. 4-21).

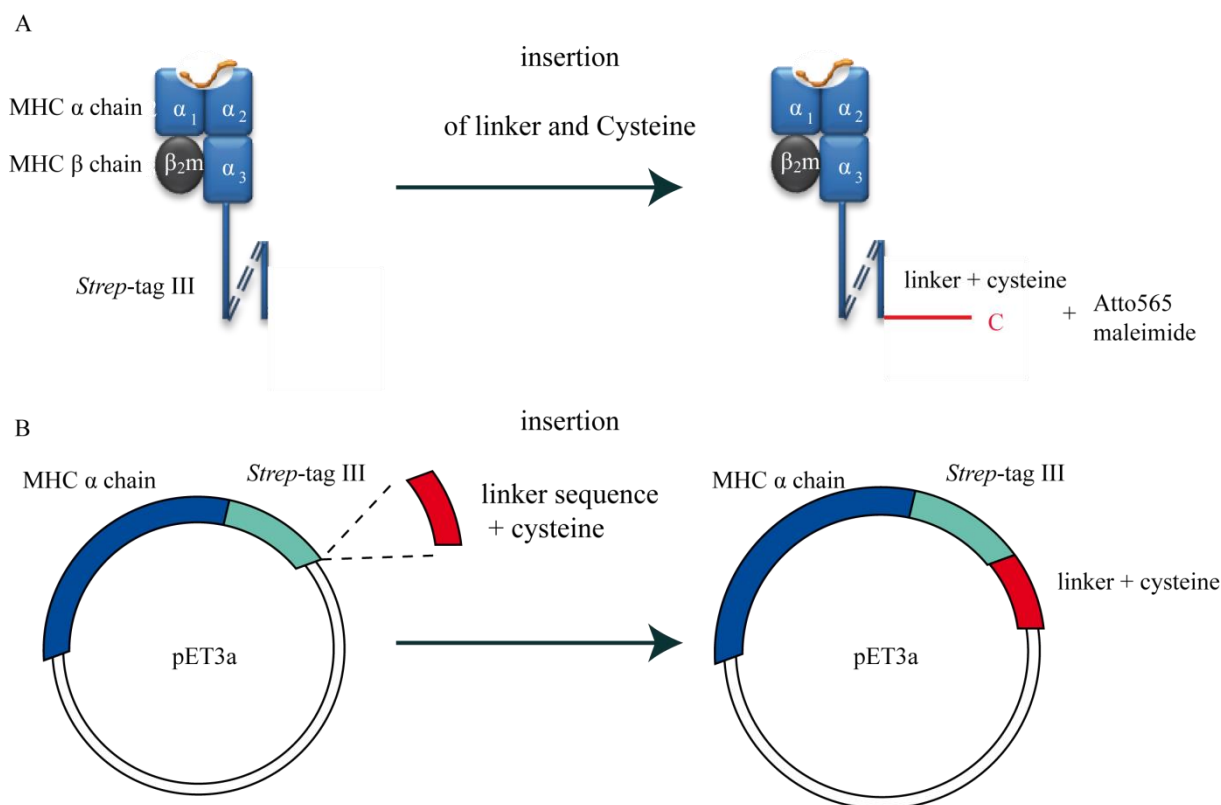


Figure 4-21: Modification of conventional MHC I *Strep*-tagIII monomers for TCR-ligand k_{off} -rate analysis.

(A) Scheme of the pMHC I monomers used for conventional *Streptamer* staining and the modified pMHC I monomers that can be conjugated to the Atto565 dye and used for k_{off} -rate analysis. (B) Scheme of DNA expression (pET3a) vectors for conventional pMHC I *Strep*-tagIII monomers and insertion of modification used for the generation of fluorescently labeled pMHC I *Strep*-tagIII mutant monomers.

Results

Several approaches of site directed mutagenesis PCRs with different conditions failed as the linker and cysteine was too long for insertion (Fig. 4-22 A). The following mutagenesis approach allowed efficient mutation of MHC expression vectors: A primer pair with phosphorylated ends was designed with primer #1 binding at the first position after the *Strep*-tag in the vector region and primer #2 binding to the *Strep*-tag sequence and carrying the insert as an overlapping end. After PCR amplification, the phosphorylated ends of the primers were ligated and a circular vector with the MHC–*Strep*-tag and the insert at the end of the *Strep*-tag was generated (Fig. 4-22 B). The respective MHC heavy chain was expressed in *E.coli*, purified and used for refolding of the MCMV specific immune dominant pMHC monomers H2-D^b/M45, H2-K^b/M38, H2-K^b/m139, H2-K^b/IE3, H2-L^d/IE1 and H2-D^d/m164. After refolding, Atto565 dye was conjugated over a maleimide reaction to the cysteine of the respective pMHC I monomers. Unfortunately, the H2-K^b/m139 did not stain specific T cells. The cysteine in the m139 peptide (TVYGFCLL) was presumably also conjugated to an Atto565 dye during the maleimide reaction abolishing the interaction between the pMHC I and the specific TCRs.

Results

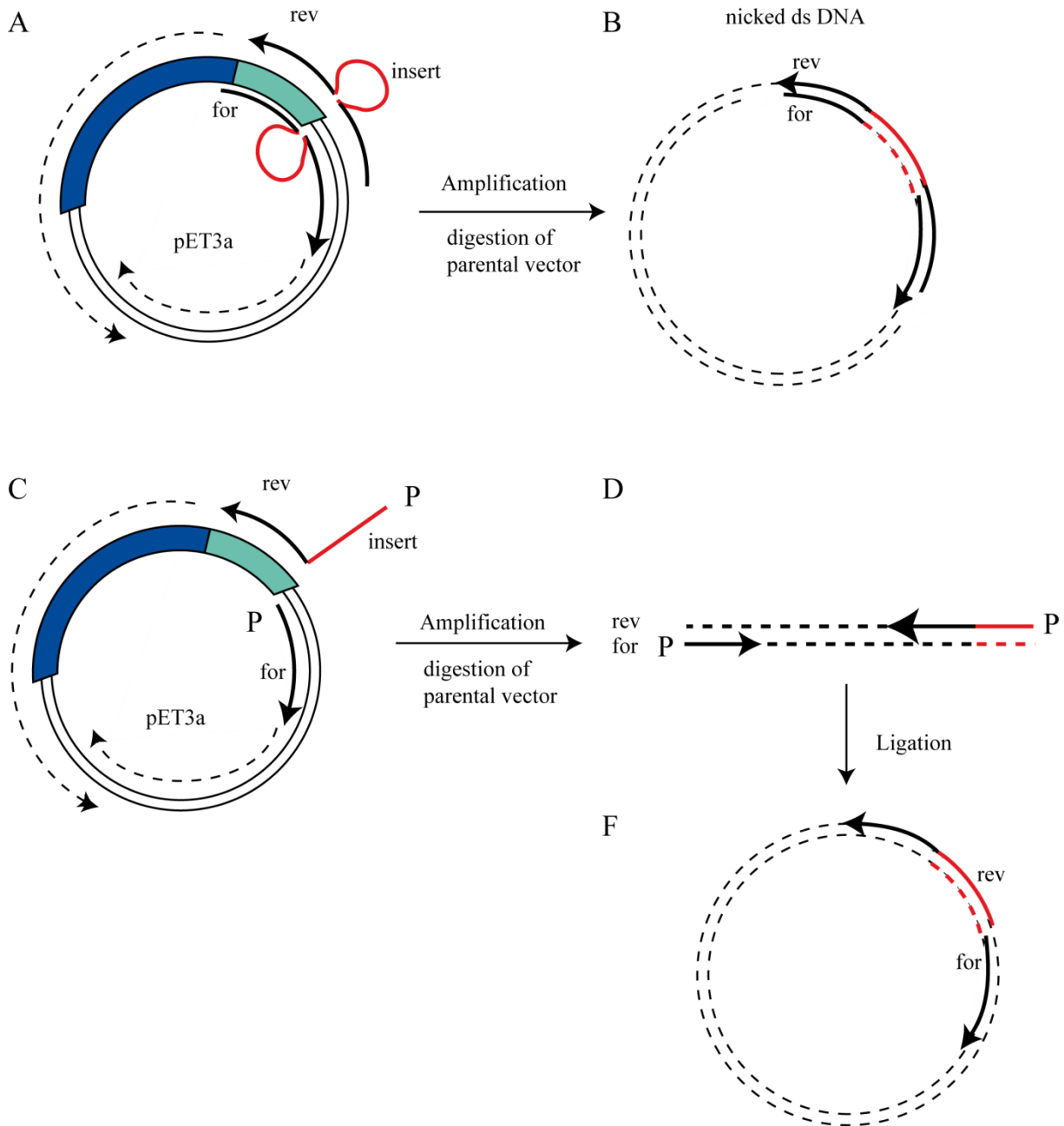


Figure 4-22: Phosphorylated primers allow efficient insertion of the linker sequence and the cysteine into the conventional pMHC I expression vectors for dye conjugation.

Schemes illustrating the mutagenesis approaches for the insertion of the linker and cysteine into the conventional expression vector carrying the MHC heavy chain (dark blue) and the *Strep-tagIII* (light blue). (A) Site directed mutagenesis PCR using long mutagenesis primers to insert the linker and cysteine (red). (B) Newly synthesized circular vector with insert. (C) Site directed mutagenesis PCR using phosphorylated (P) primers that result in a linearized PCR product (D). (E) Linearized PCR product is ligated to a circular vector. for – forward primer, rev – reverse primer, ds – double stranded, pET3a – DNA vector

4.1.8 Optimization of the purification and analysis of purified *Streptamer*⁺ T cells under the microscope

CD8⁺ T cell responses to CMV antigens are often very diverse with more than one CMV-*Streptamer*-specific T cell population in the same sample. To enable the analysis of multiple *Streptamer*-specific T cell populations from one sample in the TCR-ligand k_{off} -rate assay, the purification of *Streptamer*⁺ antigen-specific T cells was optimized. *Streptamer* staining is currently limited to two available reversible *Strep*-Tactin backbone fluorescences: *Strep*-Tactin conjugated to APC or PE (IBA) (Fig. 4-23 A). Staining of MHC *Streptamer*-APC in combination with *Streptamer*-PE enables the parallel FACS purification of at least two different CMV-specific T cell populations from the same sample. The interaction between *Strep*-tags on MHC monomers and *Strep*-Tactin binding sites of reversible MHC *Streptamers* is weaker in comparison to the biotin –Streptavidin interaction of conventional MHC multimers (Knabel et al., 2002). Therefore, the fluorescence conjugated *Strep*-Tactin backbones of two different MHC *Streptamers* can exchange causing a shift in fluorescence of the respective other fluorochrome. Optimal conditions to prevent the exchange of *Strep*-Tactin backbone molecules between different MHC specificities are the following. *Streptamer*-APC and -PE were not stained simultaneously but after one another. The first specificity was stained with MHC *Streptamer*-PE, washed regularly and MHC *Streptamer*-APC staining followed for the second specificity. Further, staining a smaller CMV-specific T cell population first (2% of CD8⁺ lymphocytes), reduced the *Strep*-Tactin backbone exchange during the second MHC *Streptamer*-APC staining of a larger CMV-specific T cell population (Fig. 4-23 B). When the large CMV-specific T cell population (10.8% of CD8⁺ lymphocytes) was stained at first with the MHC *Streptamer*-PE, the APC fluorescence of the *Streptamer*-PE⁺ T cell population increased after the second MHC *Streptamer*-APC staining (Fig. 4-23 C). Although both *Streptamer* staining combinations allowed a clear separation of the two CMV-specific T cell populations (Fig. 4-23), for purification of two CMV-specific T cell populations from one sample, the larger CMV-specific T cell population was always stained first with *Streptamer*-PE before the second staining of the smaller CMV-specific T cell population in APC (Fig. 4-23 C).

Results

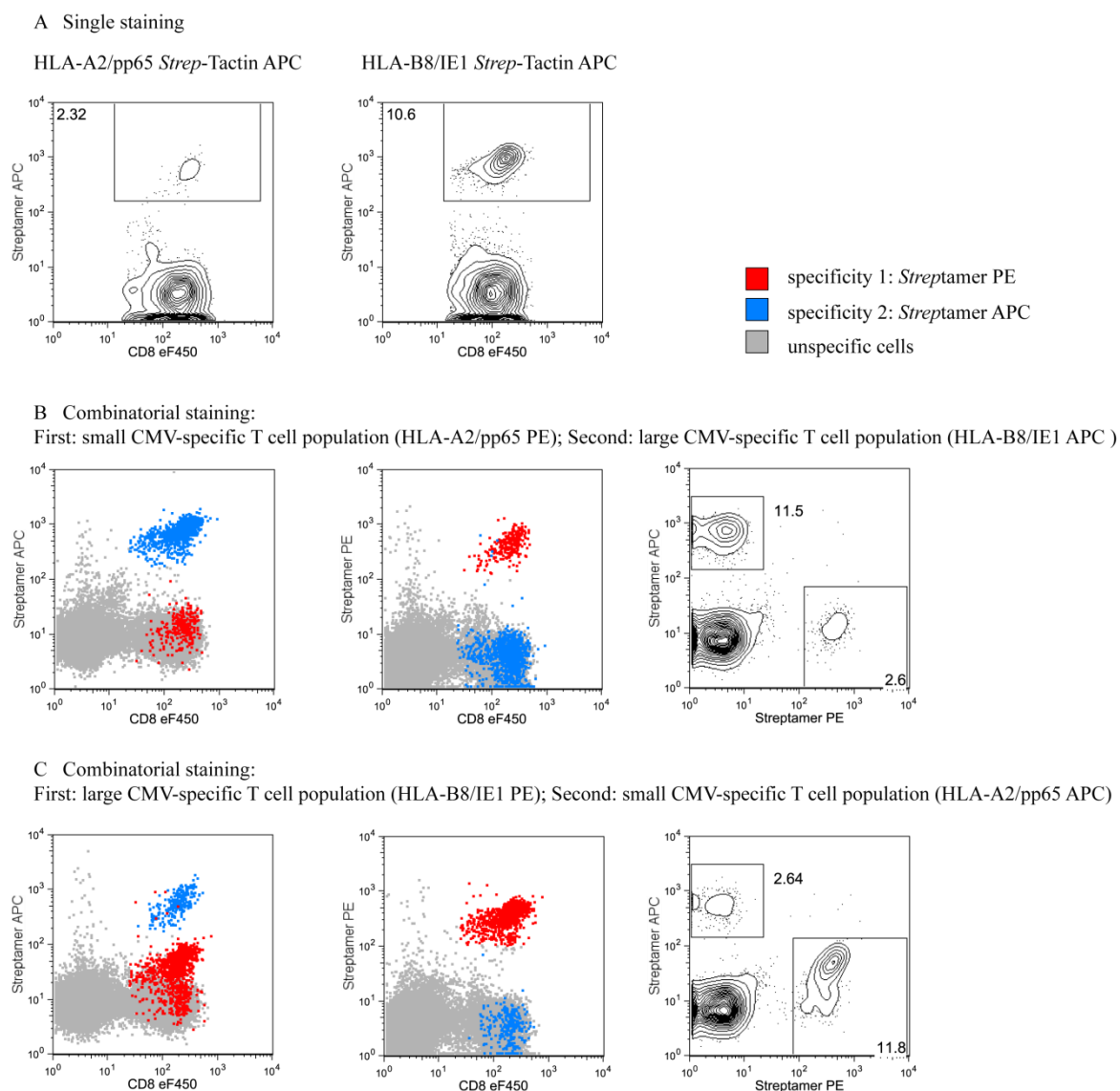


Figure 4-23: Combinatorial *Streptamer* staining allows simultaneous FACS sorting of two different antigen-specific T cell populations.

(A) *Streptamer*-APC stainings for HLA-A2/pp65 and HLA-B8/IE1₈₈ in two separate single stainings. (B and C) Combinatorial *Streptamer* staining with HLA-A2/pp65 *Streptamer* PE first, second staining HLA-B8/IE1₈₈ (B) and reversed (C). All FACS Plots are pregated on living CD19⁻ CD8⁺ lymphocytes from the same CMV seropositive donor. Numbers indicate the Streptamer⁺ frequency of CD8⁺ T cells.

Results

In addition to the combinatorial *Streptamer*-PE and -APC staining, human CMV-specific *Streptamer*⁺ T cells were purified in combination with *Streptamer*⁻ CD8⁺ T cells during FACS sorting (Fig. 4-24 A). Thereby, CD8⁺ T cells that contained the CMV-specific T cells of other specificities were retained from the same sample. CD8⁺ *Streptamer*⁺ T cells were analyzed in the k_{off} -rate assay and CD8⁺ *Streptamer*⁻ T cells were stained with the *Streptamer* of a novel specificity and subsequently sorted for a second time by FACS before k_{off} -rate analysis (Fig. 4-24 B).

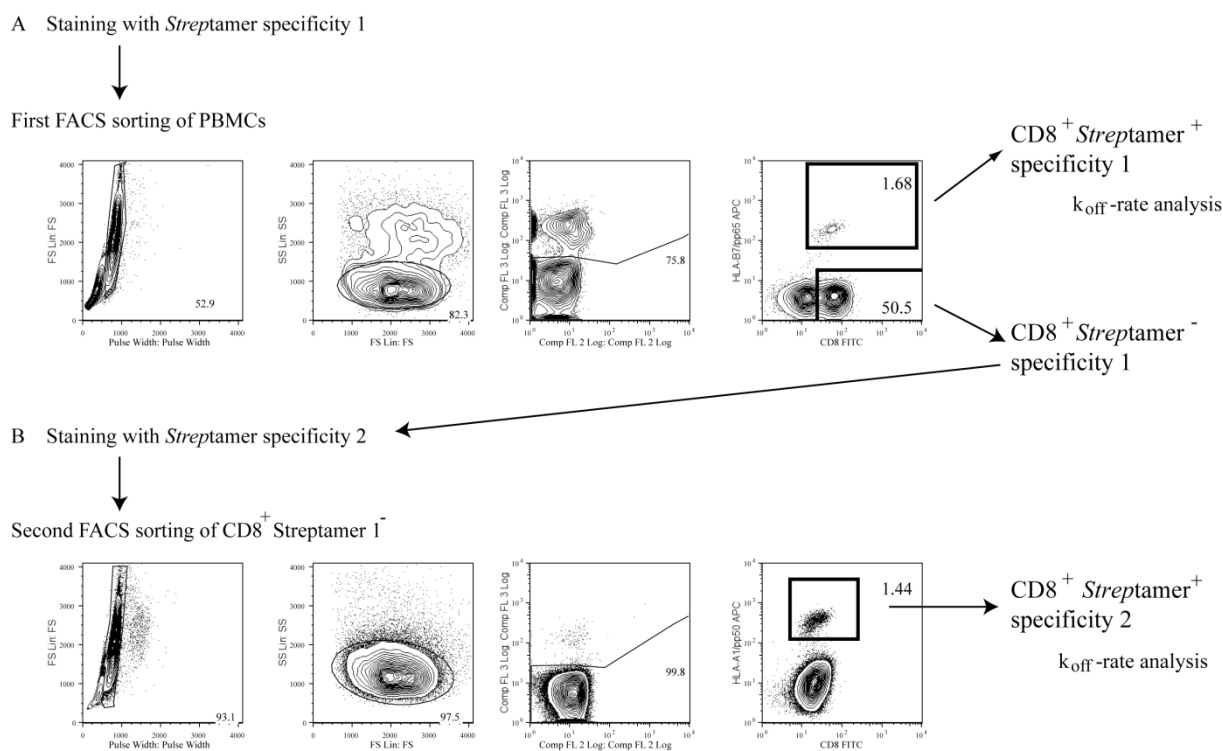


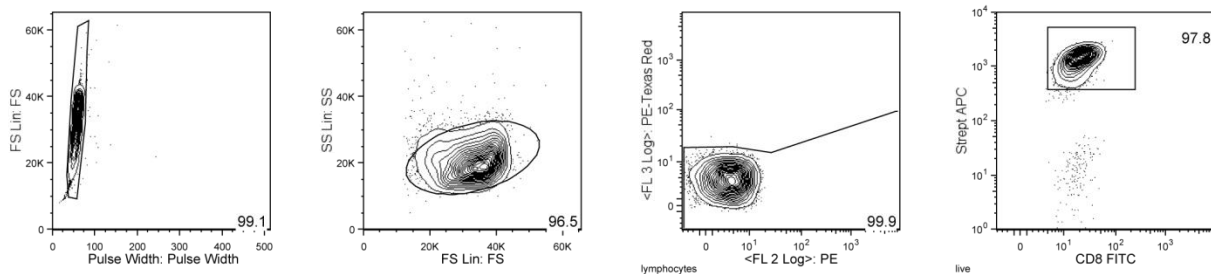
Figure 4-24: FACS sorting of CD8⁺ *Streptamer*⁺ and CD8⁺ *Streptamer*⁻ with subsequent second *Streptamer* staining allows serial purification of different antigen-specific T cell populations from one sample.

(A) The first *Streptamer* staining sample is sorted for living CD19⁻ CD8⁺ *Streptamer*-APC⁺ of specificity 1 and CD19⁻ CD8⁺ *Streptamer*-APC⁻. CD19⁻ CD8⁺ *Streptamer*-APC⁺ T cells can be directly analyzed in the TCR-ligand k_{off} -rate assay. (B) Unspecific CD19⁻ CD8⁺ *Streptamer*-APC⁻ are subsequently stained with *Streptamer*-APC of a second specificity and sorted for CD8⁺ *Streptamer*-APC⁺ before TCR-ligand k_{off} -rate analysis.

Results

The purified antigen-specific T cell populations for both specificities 1 and 2 were pure and could be analyzed directly in the TCR-ligand k_{off} -rate assay on the microscope (Fig. 4-25).

A CD8⁺ *Streptamer*⁺ specificity 1



B CD8⁺ *Streptamer*⁺ specificity 2

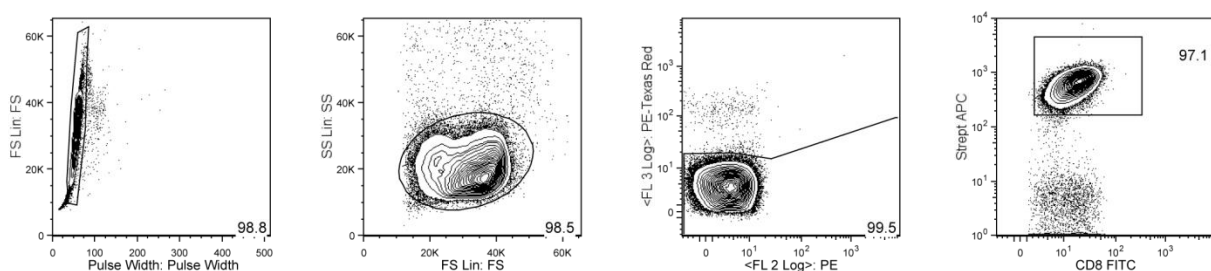


Figure 4-25: Serial FACS purification of T cell populations with different specificity from one sample is pure and allows microscopic analysis.

Purity controls of FACS sorted CD8⁺ *Streptamer* specificity 1⁺ (A) and CD8⁺ *Streptamer* specificity 1⁻ cells remained and sorted with *Streptamer* specificity 2 (B) from the same sample of Fig. 4-24.

The number of antigen-specific T cells decreased during the FACS sorting into cooled collection tubes and subsequent transfer of purified cells into a 96-well-plate after the first washing step. Sorting *Streptamer*⁺ T cells directly into one well of a 96-well-V-bottom plate filled with 200 μ l filtered FCS reduced the cell loss during sorting. For constant cooling, the plate was put on a bucket filled with ice (Fig. 4-26 A). During the real-time TCR-ligand k_{off} -rate measurement on the microscope, it was not possible to observe most of the purified *Streptamer*⁺ T cells distributed over the area of a circular membrane that is needed to efficiently arrest the cells during acquisition (compare to Fig. 4-5 B). The usage of a smaller fragment of the membrane reduced the distribution of the cells on the glass surface and thereby the number of cells needed for each dissociation experiment (Fig. 4-26 B and C).

Results

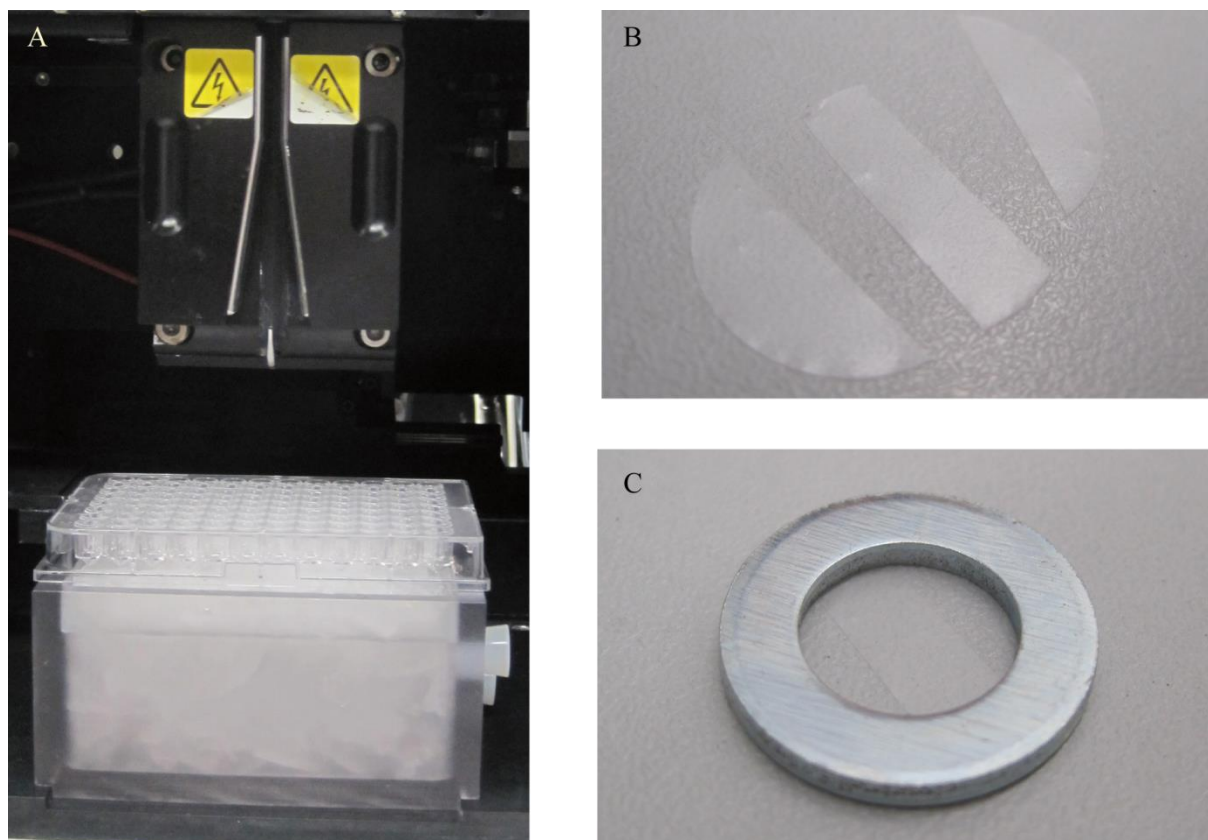


Figure 4-26: Sorting into a 96-well-V-bottom plate on ice increases cell recovery and minimized membrane reduces distribution of antigen-specific T cells on glass bottom during microscopic k_{off} -rate analysis.

(A) *Streptamer*-stained antigen-specific T cells are sorted and collected in a 96-well-V-bottom plate on ice filled with 200 μ l of ice-cold FCS. (B) Polycarbonate membrane is cut into smaller fragments and (C) put on top of purified *Streptamer*⁺ antigen-specific T cells weighted down with a metal ring to reduce movement of cells and distribution of purified T cell on the microscopic k_{off} -rate setup in the cooled buffer reservoir.

In summary, the simultaneous purification of different CMV-specific T cell populations from one sample by combinatorial *Streptamer* staining and serial FACS purification, as well as FACS sorting into a 96-well-plate and minimizing the size of the membrane used for the reduction of cell movement during the acquisition, reduced the minimal number of *Streptamer*⁺ antigen-specific T cells needed for a TCR-ligand k_{off} -rate experiment from about 30 000 to 5 000 cells.

4.2 Human Cytomegalovirus-specific T cell populations

The TCR-ligand k_{off} -rate assay allows a reproducible measurement of a major parameter of structural TCR avidity that can be compared to the functionality of antigen-specific T cell populations. During acute CMV infection, specific T cell populations are often characterized by small size, high clonal diversity and high functionality (Day et al., 2007). In the chronic phase of infection, CMV-specific T cell populations can comprise a large fraction of all T cells. These T cell populations mainly consist of only one or a few dominant T cell clones (T cell clonal expansions; TCE) and often have an exhausted phenotype with low functionality (Khan, 2002; Khan et al., 2010; Griffiths et al., 2013).

4.2.1 Strong differences in TCR-ligand $t_{1/2}$ of human CMV-specific T cells correlate to differential functionality

To find out whether antigen-specific T cell populations differ in their structural TCR binding avidity in a chronic infection, a number of human CMV-specific T cell populations with different epitope specificities and HLA-restrictions from healthy CMV seropositive blood donors were analyzed in the *Streptamer*-based TCR-ligand k_{off} -rate assay. Dissociation $t_{1/2}$ values of individual T cells from 17 CMV-specific T cell populations differed remarkably as summarized in Figure 4-27. Individual TCR-ligand $t_{1/2}$ values ranged from 17 to 500 seconds with a median of 95 seconds.

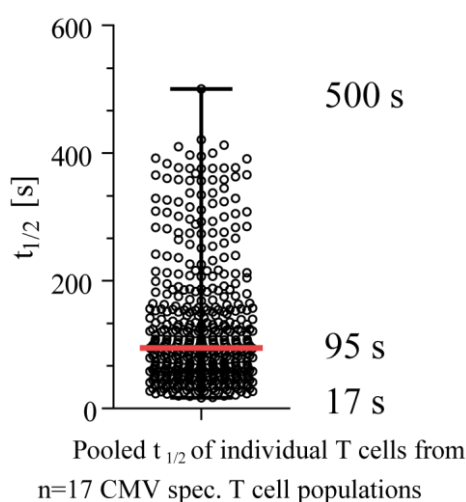


Figure 4-27: Human CMV-specific T cells differ in their TCR-ligand $t_{1/2}$ values.

17 human CMV-specific T cell populations were isolated by FACS from peripheral blood of CMV seropositive healthy donors. Pooled TCR-ligand $t_{1/2}$ of individual cells from all populations are illustrated with the median (95 s), minimum (17 s) and maximum (500 s) $t_{1/2}$ value.

Results

Because the TCR binding strength is believed to be a major determinant of T cell functionality (Zeh et al., 1999; Derby et al., 2001), the distinct TCR-ligand $t_{1/2}$ values of individual T cells indicate differences in the functionality of the CMV-specific T cells. The functionality of eight *ex vivo* isolated CMV-specific T cell populations was determined and compared (Fig. 4-28). PBMCs were isolated and stimulated with titrated amounts of the respective CMV peptide before intracellular cytokine staining for IFN γ . By fitting a non-linear regression curve into the data, the peptide concentration for half-maximal cytokine production (EC_{50}) for each CMV-specific T cell population was calculated. Here, low EC_{50} values indicate a high peptide sensitivity and high functionality. Some T cell populations were characterized by fast mean $t_{1/2}$ (38 – 53 seconds) as well as low functionality indicated by high EC_{50} concentrations (10^{-5} – 10^{-8} M). In this range of low TCR avidity an increase of mean $t_{1/2}$ was related to strong differences in EC_{50} . Intermediate or high avidity T cell populations with a mean $t_{1/2}$ of more than 60 seconds were characterized by higher peptide sensitivity of 10^{-9} – 10^{-10} M (Fig. 4-28).

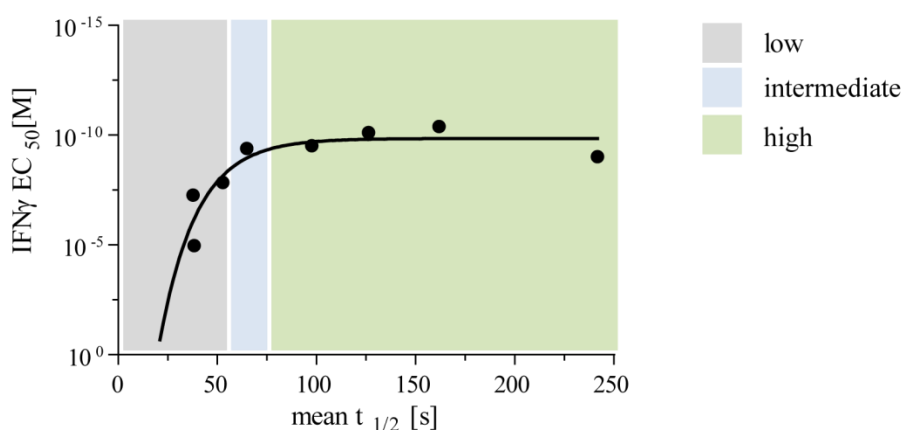


Figure 4-28: TCR-ligand $t_{1/2}$ correlates to functionality of human CMV-specific T cell populations.

Mean TCR-ligand $t_{1/2}$ of eight individual CMV-specific T cell populations from peripheral blood of healthy CMV seropositive donors are plotted against the peptide concentration for half-maximal IFN γ cytokine production (EC_{50}). The mean $t_{1/2}$ summarizes the $t_{1/2}$ values of individual cells from one CMV-specific T cell populations. PBMCs from the respective donor were isolated, stimulated with titrated amount of the respective CMV peptide, stained and analyzed by FACS for intracellular IFN γ secretion. Data was fitted with a non-linear curve to determine the EC_{50} .

Results

The broad spread of individual TCR-ligand $t_{1/2}$ and the correlation of mean $t_{1/2}$ to the ability to secrete IFN γ in response to peptide stimulation strongly suggest great differences in the functionality of human CMV-specific T cell populations isolated from healthy CMV seropositive blood donors. Therefore, the TCR-ligand k_{off} -rate assay can potentially guide the selection of donor cells for clinical application or be used to monitor the quality of an induced or existing immune response.

4.2.2 MHC-restriction and epitope recognition of CMV-specific T cell populations do not predict the TCR-ligand $t_{1/2}$

T cell populations specific for human CMV are very diverse depending on the CMV target antigen, different epitopes derived from the antigen and the MHC-restriction. TCR-ligand $t_{1/2}$ of CMV-specific T cell populations with identical MHC-restriction was compared to investigate whether certain MHC-alleles (human leukocyte antigen/HLA-types) correlate to a certain structural TCR avidity. TCR-ligand $t_{1/2}$ values were diverse and comparable among the different HLA-types, indicating that the HLA-type does not predict a certain TCR-ligand k_{off} -rate (Fig. 4-29).

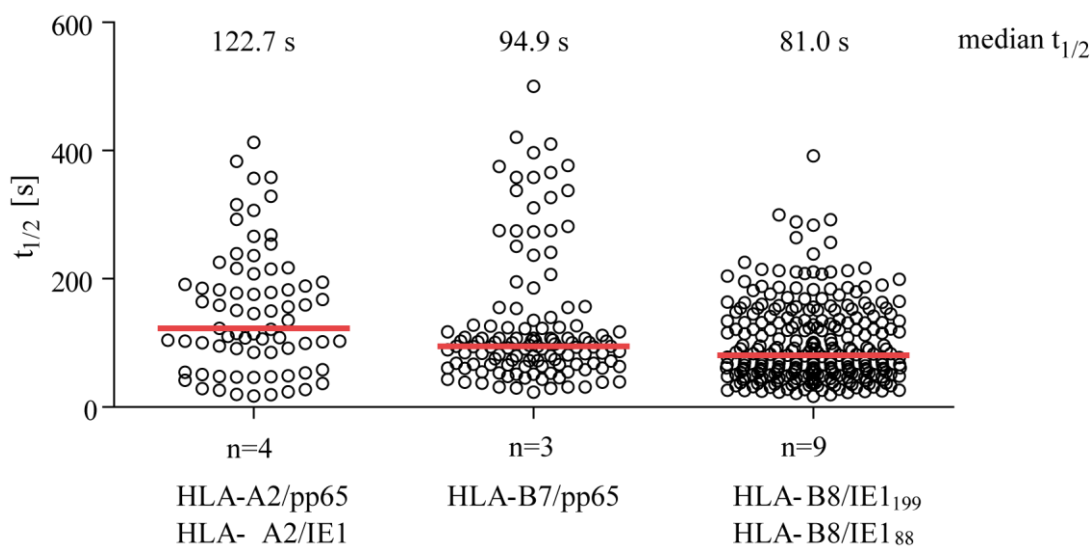


Figure 4-29: TCR-ligand $t_{1/2}$ values from individual T cells are diverse for different HLA-types.

Pooled TCR-ligand $t_{1/2}$ of individual T cells from CMV-specific T cell populations with the indicated HLA-type. n indicates the number of different T cell populations.

Results

Further, CMV target antigens were compared. During acute infection and CMV reactivation a variety of CMV gene products can be present in the infected cell. CMV genes are transcribed in the following order: 1. immediate early (IE); 2. early (E) and 3. late CMV genes (L). Epitopes from the different CMV genes can be processed and presented at the cell surface (Fig. 4-30 A). In contrast, during CMV latency, the double stranded circular CMV genome is silenced and only certain genes are rarely expressed (Fig. 4-30 B). Immediate early (IE) genes of virus replication have been shown to be transcribed sporadically during latency to initiate the transcription cascade (Seckert et al., 2012). Epitopes from IE genes might therefore be presented on the surface of infected cells during CMV latent infection.

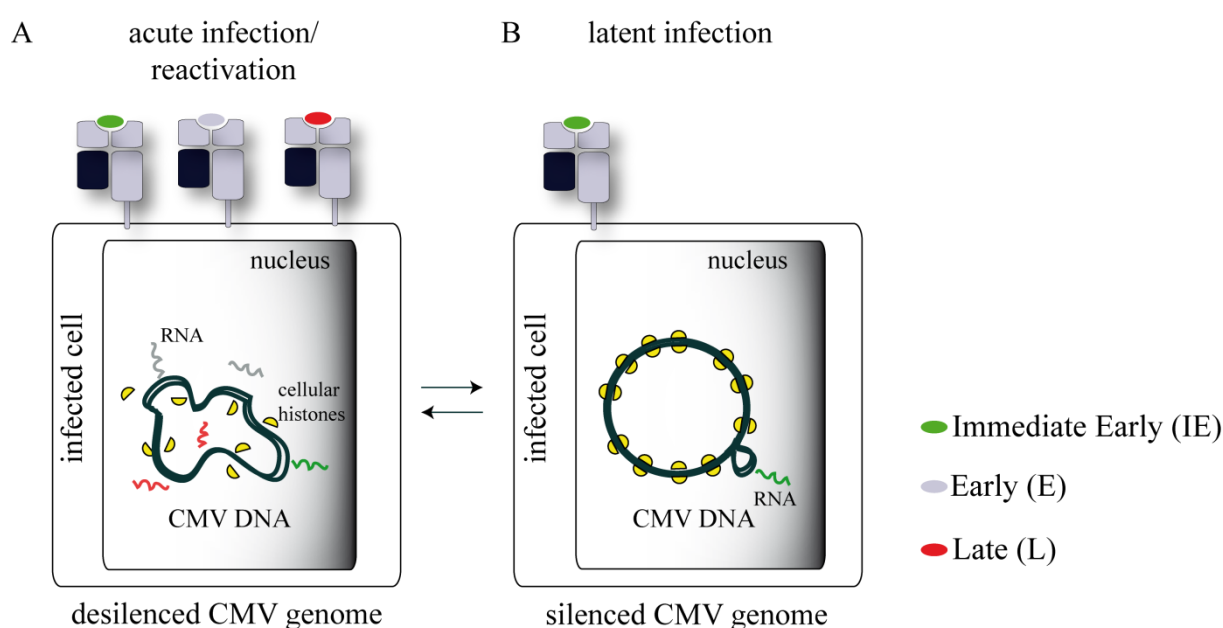


Figure 4-30: CMV gene expression is limited during latent infection.

(A) The CMV genome is transcriptionally active during acute infection and upon viral reactivation. CMV genes are transcribed in the following order: 1. immediate early (IE), 2. early (E), 3. late (L) viral genes. Epitopes from the different CMV gene products can be presented by MHCs on the surface of infected cells. (B) During CMV latent infection, the CMV DNA genome is inactive and silenced. Only very few genes, such as IE genes, are transcribed and can be presented on the cell surface.

The spread in TCR-ligand $t_{1/2}$ values of individual cells from T cell populations specific for a late gene product present during the acute infection or viral reactivation (the tegument protein pp65) was similar to the individual $t_{1/2}$ values of latency-associated immediate early 1 (IE1) epitopes (Fig. 4-31). Therefore, the CMV target antigen is not a major determinant of TCR avidity; however, IE1-specific T cell populations had a slightly faster median $t_{1/2}$ as compared to pp65-specific T cells.

Results

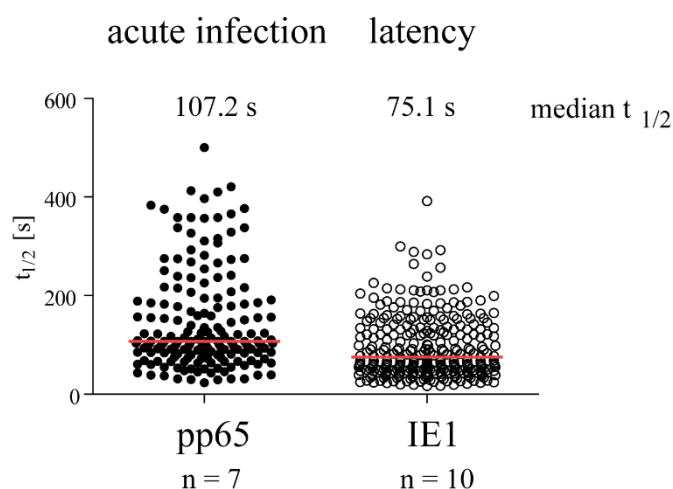


Figure 4-31: TCR-ligand $t_{1/2}$ values are diverse for different antigen specificities.

Pooled TCR-ligand $t_{1/2}$ of individual T cells from CMV-specific T cell populations targeting the indicated CMV antigen that is either expressed during acute (A) or acute as well as latent CMV infection (B). n indicates the number of different T cell populations in one group.

Notably, the comparison of two T cell populations specific for either IE1 or pp65 restricted by HLA-A2 in the same donor revealed different characteristics. The two T cell populations differed strongly in their size, with the HLA-A2/IE1-specific T cell population more than four-fold bigger than the HLA-A2/pp65 population (Fig. 4-32 A). In addition, the HLA-A2/pp65-specific T cells had long TCR-ligand $t_{1/2}$ values, while dissociation $t_{1/2}$ of T cells from the HLA-A2/IE1 specific T cell population were very fast (Fig. 4-32 B).

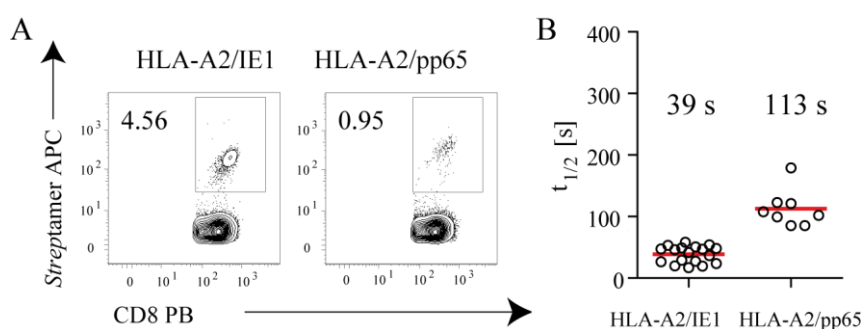


Figure 4-32: Fast TCR-ligand dissociation $t_{1/2}$ values and higher number of IE1-specific T cells.

(A) *Streptamer* stainings and frequency of the CMV seropositive healthy blood donor (gated on living $CD8^+$ lymphocytes). (B) Living $CD8^+$ *Streptamer* HLA-A2/IE1- or HLA-A2/pp65-specific T cells were purified by FACS and analyzed in the *Streptamer*-based k_{off} -rate assay. The $t_{1/2}$ values of individual cells from *ex vivo* isolated T cell populations are plotted with the mean $t_{1/2}$ indicated.

4.2.3 CMV IE1-specific T cell populations expand to large numbers

MHC multimer frequencies of living CD3⁺ in the blood of healthy CMV seropositive donors that were collected and analyzed by Julia Albrecht and Michael Neuenhahn were grouped by the CMV target antigens IE1, pp65 or pp50. The size of the population differed remarkably with some T cell populations expanding up to 55% of the CD3⁺ T lymphocytes. Notably, IE1-specific T cell populations included the populations with the highest frequencies and a high median frequency as compared to pp50- and pp65-specific T cell populations. T cell populations specific for pp65 were smaller as compared to others (Fig. 4-33).

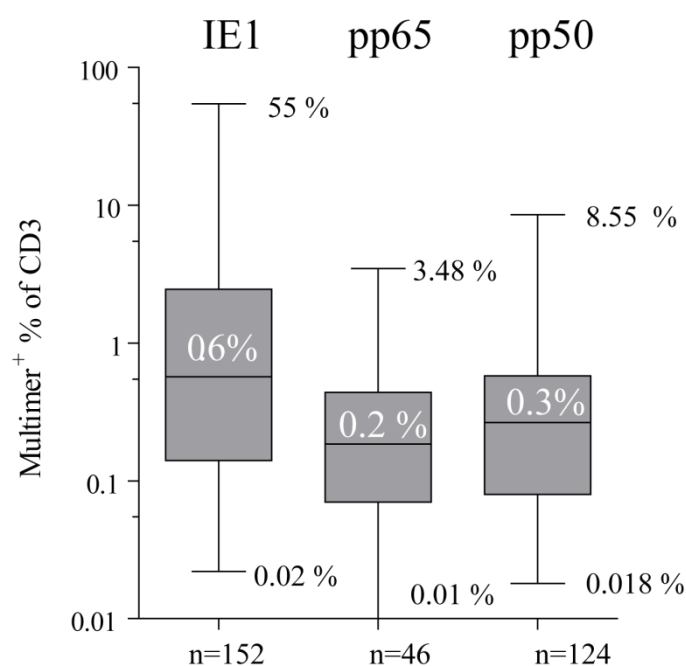


Figure 4-33: CMV IE1-specific T cell populations can comprise large fractions of all CD3⁺ T lymphocytes in healthy human blood donors.

Frequency of CMV antigen-specific T cell populations (gated on pMHC multimer⁺ and CD3⁺ living T cells) of different CMV seropositive healthy donors. Shown are individual populations recognizing CMV pp65, pp50 or IE1 epitopes restricted by different HLA-molecules (HLA-A2, HLA-B8, HLA-A1, HLA-B7, HLA-B35, HLA-A11, HLA-A24, HLA-C7). Numbers indicate the minimum, median and maximum frequency of all data summarized for each group.

4.2.4 IE1-specific T cell populations vary in frequency and TCR-ligand $t_{1/2}$

T cell populations of six further donors reactive against the same pMHC (HLA-B8/IE1₁₉₉₋₂₀₇) were analyzed. The frequencies of the *Streptamer*⁺ T cell population in the living CD8⁺ T cells (Fig. 4-34 A) as well as the mean $t_{1/2}$ were remarkably different in the respective donors

Results

(Fig. 4-34 B). These data indicate that neither the human leukocyte antigen (HLA) restriction nor the epitope recognition is a major determinant for a distinct k_{off} -rate of CMV-specific populations (Nauerth et al., 2013b). Interestingly, T cell populations with a high frequency of *Streptamer*-specific T cells ($> 5\%$ of living CD8^+ lymphocytes; donor #1 to #4) had very fast mean $t_{1/2}$ (< 100 s) and a narrow range of $t_{1/2}$ of individual T cells analyzed, whereas donor #5 and #6 with lower *Streptamer*⁺ frequency ($< 1\%$ of living CD8^+ lymphocytes) had longer mean $t_{1/2}$ (≥ 100 s) with a broader distribution of individual data points.

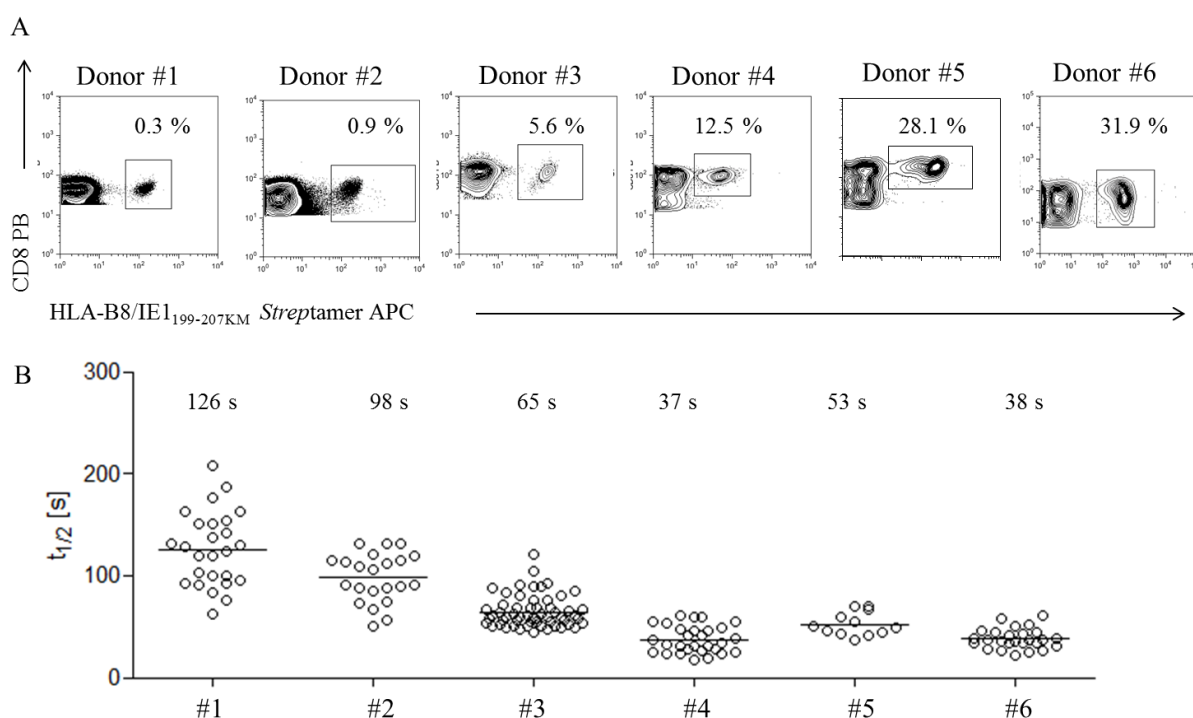


Figure 4-34: CMV HLA-B8/IE1_{199-207KM}-specific T cell populations from healthy blood donors differ in their TCR-ligand dissociation kinetics.

(A) HLA-B8/IE1_{199-207KM} *Streptamer* stainings of healthy blood donor#1 - #6 (gated on living CD8^+ lymphocytes). (B) HLA-B8/IE1_{199-207KM}-specific CD8^+ T cell populations isolated from the different donors were analyzed in the *Streptamer*-based k_{off} -rate assay. The $t_{1/2}$ values of individual cells from each *ex vivo* analyzed T cell population are plotted with the mean $t_{1/2}$ indicated. Adapted from (Nauerth et al., 2013b).

Fast dissociation rates of donor #1 – donor #4 were associated with low functional avidity, whereas donor #6 with long dissociation $t_{1/2}$ had high functional avidity in an intracellular staining for $\text{IFN}\gamma$ after stimulation with different concentrations of the peptide (Fig. 4-35) (Nauerth et al., 2013b). Because of limited cell material donor #5 was not tested in the cytokine secretion assay.

Results

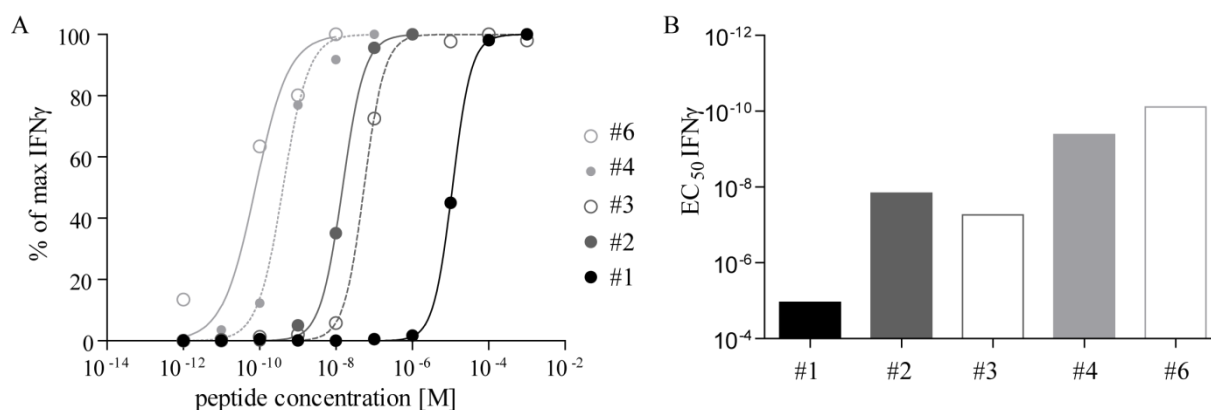


Figure 4-35: CMV HLA-B8/IE1₁₉₉₋₂₀₇KM-specific T cell populations from healthy blood donors differ in their functional avidity.

(A) PBMCs were isolated from healthy blood donors #1 - #6 and $1 \cdot 10^6$ cells were stimulated with the indicated concentrations of IE1₁₉₉₋₂₀₇KM peptide. IFN γ production was assessed by ICCS. All values were normalized to maximal IFN γ production and the peptide concentration for half maximal IFN γ production (EC_{50}) was calculated after fitting a non-linear regression curve. Adapted from (Nauerth et al., 2013b). (B) EC_{50} values are compared for every donor.

4.2.5 HLA-B8/IE1₈₈-specific T cell populations with long mean TCR-ligand $t_{1/2}$

Next, different epitopes derived from the IE1 antigen were compared. Donor #1 had a very large HLA-B8/IE1₁₉₉₋₂₀₇-specific T cell population as well as a small HLA-B8/IE1₈₈₋₉₆-specific T cell population. Comparing the populations allowed analyzing T cells recognizing the same CMV antigen restricted by the same HLA-molecule in the same donor. While HLA-B8/IE1₁₉₉₋₂₀₇ consisted of one dominant specific T cell clone (TCR sequences analyzed by Georg Dössinger) that was expanded to 32% of CD8⁺ T cells, the HLA-B8/IE1₈₈₋₉₆-specific T cell population was small and composed of a variety of individual T cell clones (Fig. 4-36) (Dössinger et al., 2013).

Results

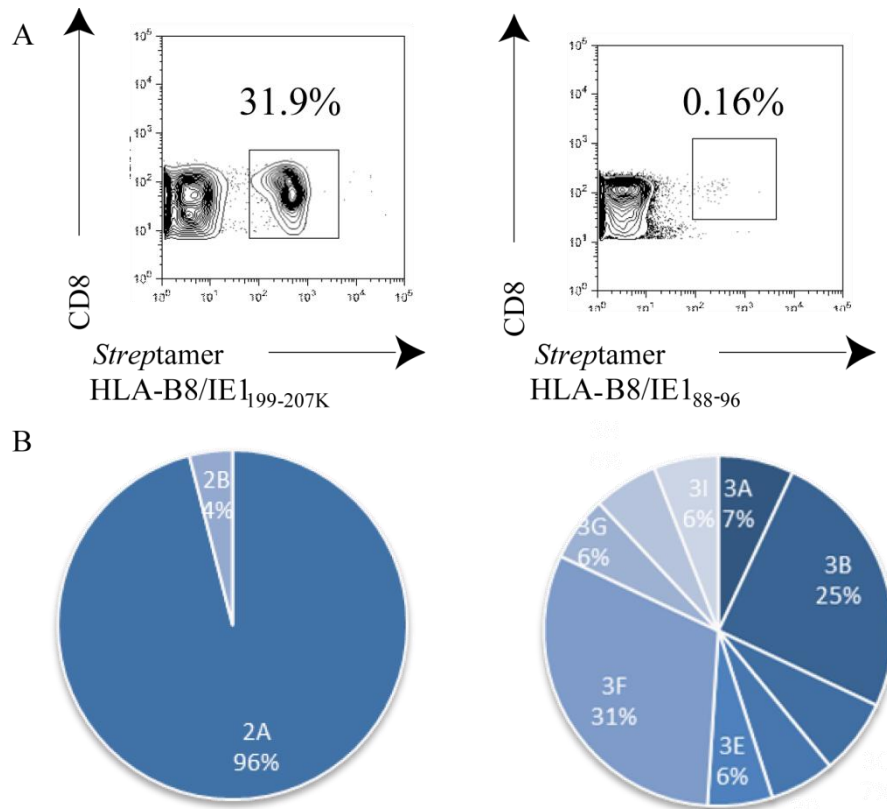


Figure 4-36: T cell populations specific for the same CMV target antigen and the same MHC in the same donor have disparate characteristics.

(A) Streptamer stainings of healthy blood donor #1 for the HLA-B8/IE1_{199-207K} and HLA-B8/IE1₈₈₋₉₆ epitope (gated on living CD8⁺ lymphocytes). (B) TCRs of single T cells from both specific T cell populations were sequenced (left HLA-B8/IE1_{199-207K}, n=25; right HLA-B8/IE1₈₈₋₉₆ n=16). The Pie charts illustrate the proportion of the individual TCRs sequenced in the population. Adapted from (Dössinger et al., 2013).

Both IE1-specific T cell populations were analyzed in the k_{off} -rate assay in cooperation with Magdalena Nauerth. In contrast to the large HLA-B8/IE1_{199-207KM}-specific T cell population with a fast mean pMHC dissociation $t_{1/2}$ of 38 s, the small HLA-B8/IE1₈₈₋₉₆-specific T cell population had different TCR-ligand $t_{1/2}$ values for individual T cell reflecting the clonal diversity of this population (Fig. 4-37 A) (Nauerth, 2012; Nauerth et al., 2013b). The long mean $t_{1/2}$ of 162 s indicated a high structural TCR avidity and correlating with high functional avidity determined in an IFN γ ICCS after stimulation with titrated amount of the specific epitope ($EC_{50}=4*10^{-11}$ M; Fig. 4-37 B).

Results

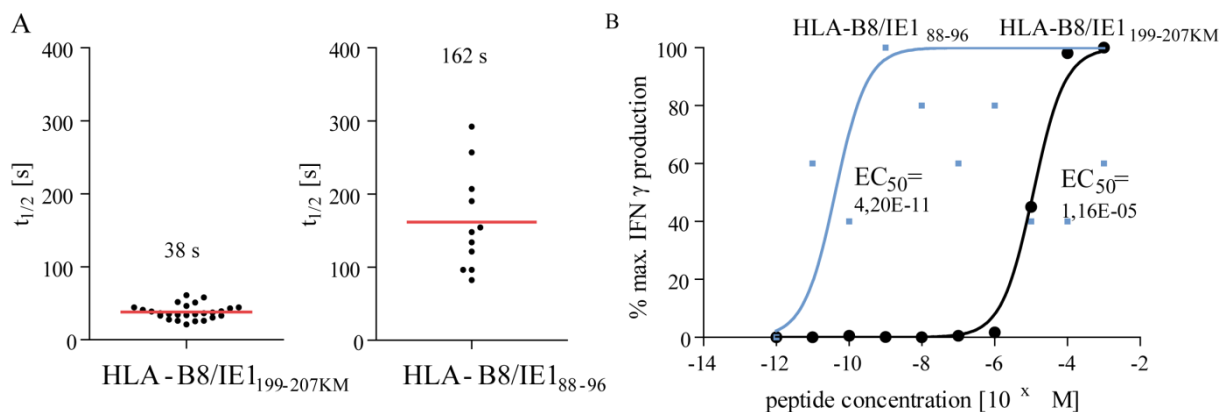


Figure 4-37: T cell populations specific for different epitopes with disparate TCR-ligand $t_{1/2}$ and functionality.

(A) Living $CD8^+$ *Streptamer*⁺ from donor#1 were purified by FACS and analyzed in the *Streptamer* k_{off} -rate assay. The $t_{1/2}$ of individual cells from *ex vivo* isolated T cells are plotted with the mean $t_{1/2}$ indicated. Adapted from (Nauerth et al., 2013b). (B) PBMCs were isolated and stimulated with the indicated concentrations of the respective peptide (IE1₁₉₉₋₂₀₇ or IE1₈₈₋₉₆). IFN γ production was assessed by ICCS. All values were normalized to maximal IFN γ production and the peptide concentration for half maximal IFN γ production (EC_{50}) was calculated after fitting a non-linear regression curve.

Further, additional HLA-B8/IE1₈₈₋₉₆-specific T cell populations from two other healthy donors were analyzed in the TCR-ligand k_{off} -rate assay. Both T cell populations were characterized by long TCR-ligand $t_{1/2}$ values (mean $t_{1/2} \geq 100$ s; Fig. 4-38 A). In contrast to the HLA-B8/IE1₈₈₋₉₆-specific T cell population of donor #1, the T cell population from donor #7 and #8 were largely expanded (6% and 9% *Streptamer*⁺ T cells of $CD8^+$ lymphocytes, respectively). Despite the high *Streptamer* frequency, the dissociation rates of individual T cells were slow and donor #8 had a very wide distribution of individual values (Fig. 4-38 B), as compared to the HLA-B8/IE1_{199-207KM}-specific T cell populations from the donors #1 to #6 in Figure 4-34. This data indicates that IE1₈₈₋₉₆ epitopes are recognized with higher avidity as compared to IE1₁₉₉₋₂₀₇ epitope although both epitopes from the same CMV antigen are restricted by the same HLA-molecule.

Results

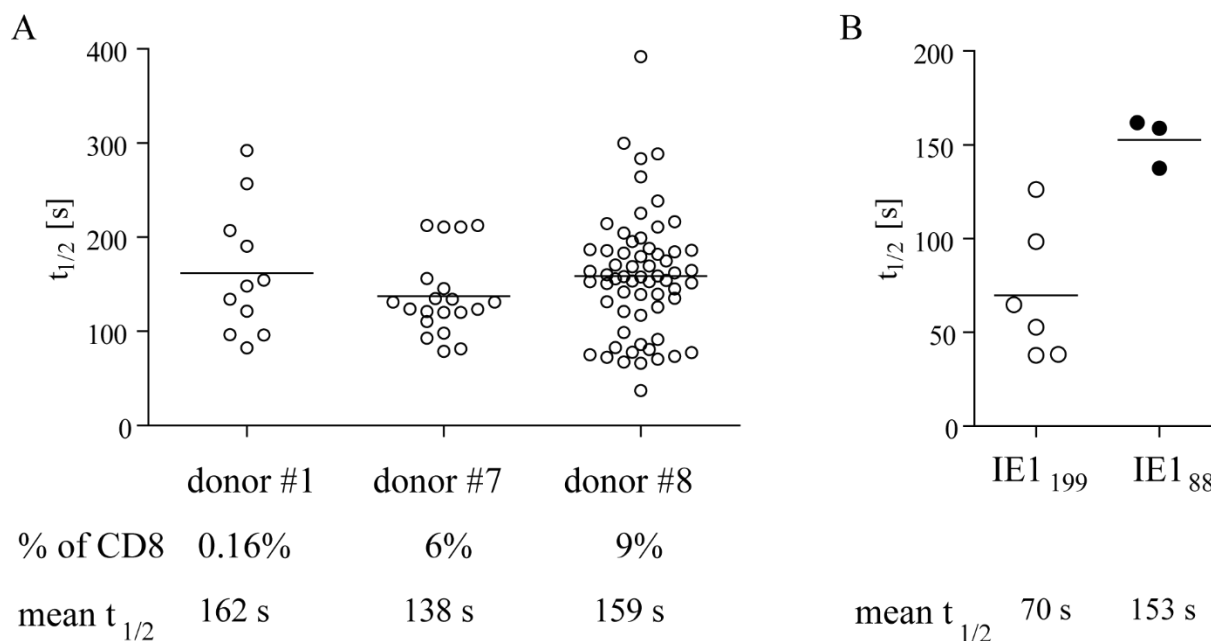


Figure 4-38: HLA-B8/IE1₈₈₋₉₆-specific T cell populations with long TCR-ligand dissociation $t_{1/2}$ values.

(A) Living CD8⁺ *Streptamer*⁺ T cells were purified by FACS and analyzed in the *Streptamer* k_{off} -rate assay. The $t_{1/2}$ of individual cells from *ex vivo* isolated T cells are plotted with the mean $t_{1/2}$ indicated. (B) Mean $t_{1/2}$ values of T cell populations from different donors are plotted for the respective specificity and the mean of this data for IE1₁₉₉₋₂₀₇ and IE1₈₈₋₉₆ is indicated.

4.2.6 HLA-IE1₁₉₉₋₂₀₇-specific T cell populations can be cross-reactive for altered peptide ligands derived from different CMV strains

The higher avidity of IE1₈₈₋₉₆-specific T cell populations in comparison to the IE1₁₉₉₋₂₀₇ epitope in one donor could imply differences in the selection of specific T cells with disparate TCR avidities. Despite CMV infection and protective immune CD8 T cell responses, healthy individuals can be infected with additional CMV strains. The different CMV strains can persist simultaneously in the same host. The large CMV genome is very stable; however, the strains differ in certain genes. Interestingly, some of these sequence differences were found in immunodominant epitopes targeted by CMV-specific T cell populations. One of the regions varying in its sequence between the different CMV strains is the position 199-207 in the IE1 gene. The altered peptide ligands that derive from different CMV strains are summarized in Table 1 (Elkington et al., 2003; Smith et al., 2014). HLA-B8/IE1₁₉₉₋₂₀₇-specific T cell populations from healthy CMV seropositive hosts either recognized only one specific peptide sequence in cytokine secretion assays after stimulation with the peptide, or the T cell population was cross-reactive towards more than one peptide ligand (Elkington et al., 2003).

Table 1: Differences in amino acid sequences of immunodominant epitope CMV IE1 position 199-207 (Elkington et al., 2003; Khan et al., 2004; Smith et al., 2014).

	sequence	abbreviation	CMV strain
1	ELKRKMMYM	KM	Toledo
2	ELRRKMMYM	RM	Towne, strain W, Merlin, AD169
3	ELKRKMIYM	KI	TB40E, Davis
4	ELNRKMIYM	NI	
5	ELRRKMIYM	RI	hypothetical peptide, not published

The cross-reactivity towards altered peptide ligands derived from different CMV strains could therefore be one explanation for the weak TCR avidity of HLA-B8/IE1₁₉₉₋₂₀₇-specific T cell populations that were analyzed in the TCR-ligand k_{off} -rate assay. In the analysis the ELKRKMMYM peptide (“KM”) that is found in the CMV Toledo strain was used. To investigate whether this sequence is found in virus of the donor, sequencing of CMV isolated from the peripheral blood of donor #1 was performed. Unfortunately, during the chronic phase of CMV infection, it is very difficult to detect any virus DNA in the blood and the sequencing was not successful. For this reason, the T cell population of donor #1 was tested for its cross-reactivity towards two common altered peptide ligands and another hypothetical peptide variant that carried both amino acid variants at position 201 and 205 obtained from Andreas Mossmann and listed in Table 1. PBMCs of donor #1 were analyzed in an intracellular cytokine staining after stimulation of titrated amounts of the respective peptide. The CMV-specific T cell population of donor #1 produced IFN γ in response to all four different IE1₁₉₉₋₂₀₇ variants (Fig. 4-39 A). The functional avidity towards “KM” and “RM” was highly similar ($EC_{50} = 3 \cdot 10^{-6}$ and $2 \cdot 10^{-6}$, respectively). The stimulation with the epitope ligands carrying isoleucine at position 205 “KI” and the hypothetical “RI” resulted in more efficient cytokine production at lower peptide concentrations (EC_{50} of $1.5 \cdot 10^{-8}$ and $1.3 \cdot 10^{-8}$, respectively (Fig. 4-39 B)).

Results

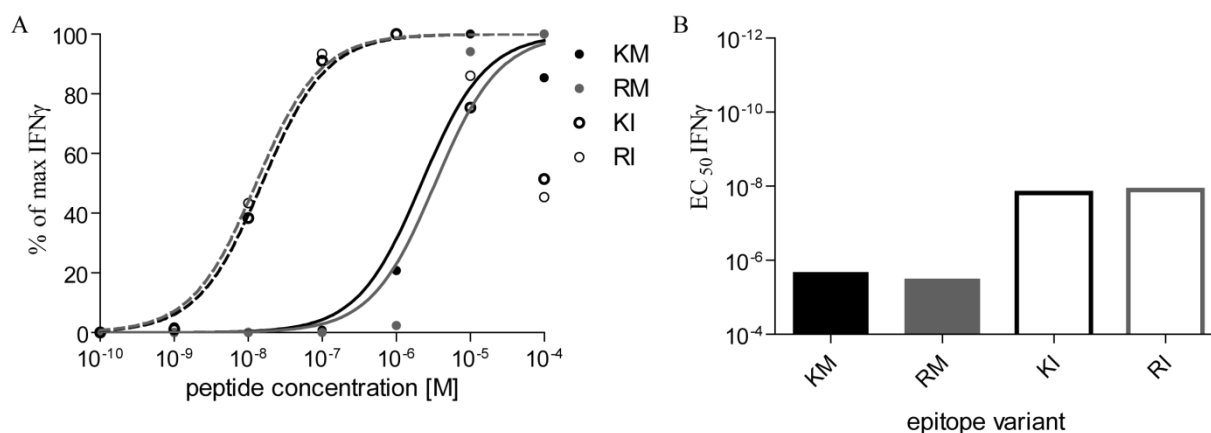


Figure 4-39: Large CMV IE1₁₉₉₋₂₀₇-specific T cell population of donor #1 can produce IFN γ in response to four epitope variants from different CMV strains.

(A) PBMCs were isolated from healthy blood donors #1 and stimulated with the indicated concentrations of respective IE1₁₉₉₋₂₀₇ peptide. IFN γ production was assessed by ICCS. All values were normalized to maximal IFN γ production and the peptide concentration for half maximal IFN γ production (EC₅₀) was calculated after fitting a non-linear regression curve. (B) EC₅₀ values are compared for every epitope variant.

To allow a TCR-ligand k_{off} -rate analysis of the altered peptide ligands indicated in Table 1, the peptide exchange technology (Rodenko et al., 2006) was adapted to the generation of fluorescently labeled pMHC monomers. Therefore, peptides carrying an UV cleavable amino acid were obtained from Henk Hilkmann and Ton Schumacher. The cleavable peptides were used for the refolding of MHC monomers. The pMHC monomer forms a stable complex, until it is exposed to UV light (> 350nm) and the peptide is cleaved. In the absence of a novel peptide of interest, the MHC I complex is degraded. In contrast, in the presence of a novel peptide, the MHC I complex is rescued and a MHC loaded with a novel peptide of interest is generated (Fig. 4-40).

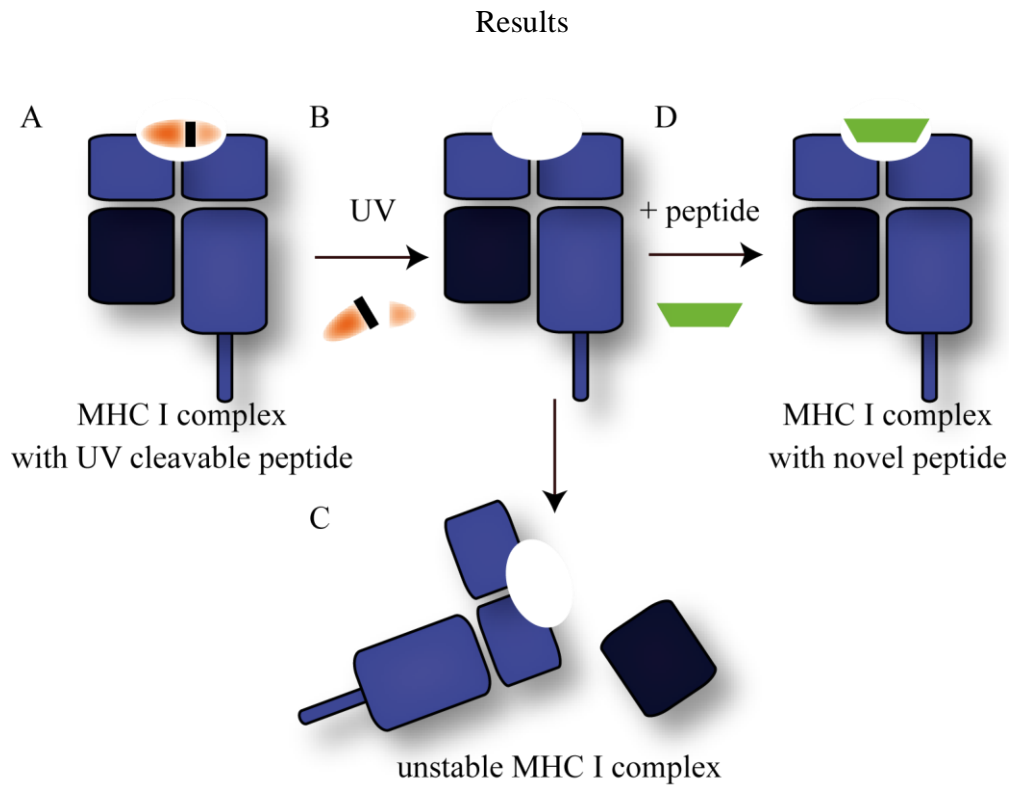


Figure 4-40: Principle of the UV-peptide exchange.

(A) MHC I complex loaded with a UV cleavable peptide are generated. (B) During exposure to UV light ($> 350\text{nm}$) the peptide is cleaved. (C) In the absence of peptide, the MHC I complex is degraded. (D) In the presence of peptide the MHC I complex is rescued and MHC I complex with a novel peptide is generated. Adapted from (Rodenko et al., 2006).

The UV exchange was tested for HLA-B8 and HLA-A2 complexes and used for several *Strep*tamer stainings on specific T cells. Unfortunately, the maleimide dye conjugation of *Strep*-tagged UV-peptide MHC monomers abolished the specific staining after peptide exchange. However, MHC *Strep*-tagged UV-peptide MHC monomers without the maleimide reaction stained specific T cells brightly after the peptide exchange reaction (Fig. 4-41). Consequently, the UV peptide exchange in combination with the generation of fluorescently labeled HLA-B8 and HLA-A2 molecules failed and needs to be further modified.

Results

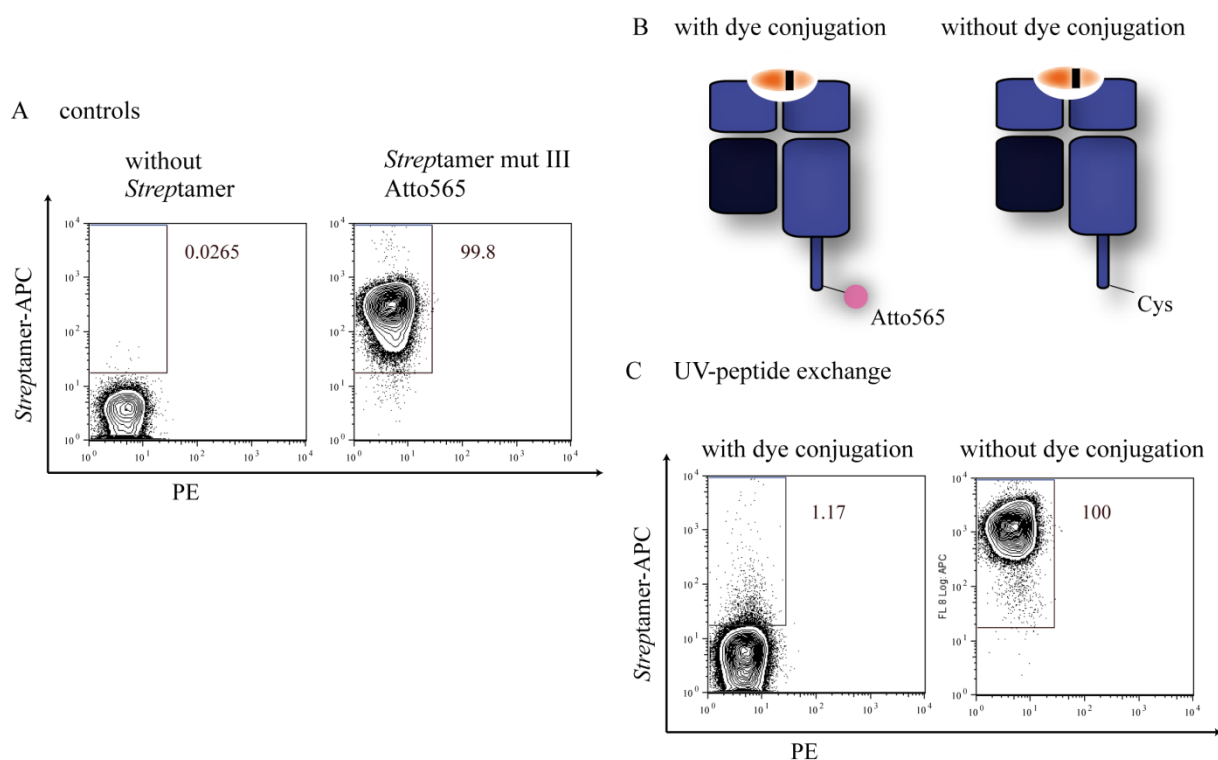


Figure 4-41: Maleimide dye conjugation interferes with peptide exchange for the generation of fluorescently labeled MHC monomers.

MHC monomers after UV-peptide exchange were tested for their staining on human CMV-specific T cell clones. (A) Staining without *Streptamer* or with *Streptamer* consisting of MHC monomers that were refolded conventionally with the respective peptide and *Strep*-Tactin APC were used as negative and positive controls, respectively (gated on living lymphocytes) (B) Scheme of the MHC monomers with the UV cleavable peptide, that were exchanged with the novel peptide, multimerized with *Strep*-Tactin APC and used for staining of the specific T cells. Left MHC monomer was incubated with the maleimide dye Atto565 before UV-peptide exchange and *Streptamer* staining, whereas the dye conjugation was not performed on the right MHC monomer. Both MHC monomers were refolded from the same batch. (C) *Streptamer* staining consisting of MHC monomers with previous dye conjugation and UV-peptide exchange (left) and *Streptamer* staining consisting of MHC monomers without previous dye conjugation after UV-peptide exchange (gated on living lymphocytes).

4.2.7 *Streptamer* frequency of CMV IE1-specific T cell populations of healthy human blood donors correlates to TCR-ligand $t_{1/2}$ values

TCR-ligand $t_{1/2}$ values of individual cells from T cell populations were grouped based on the size of the respective T cell population. The distribution and the mean $t_{1/2}$ values of T cell populations up to 10% of CD8⁺ T cells were similar (Fig. 4-43). In contrast, cells from T cell populations with a higher frequency up to 30% had $t_{1/2}$ values in a narrow range around a lower mean $t_{1/2}$ of 41 seconds.

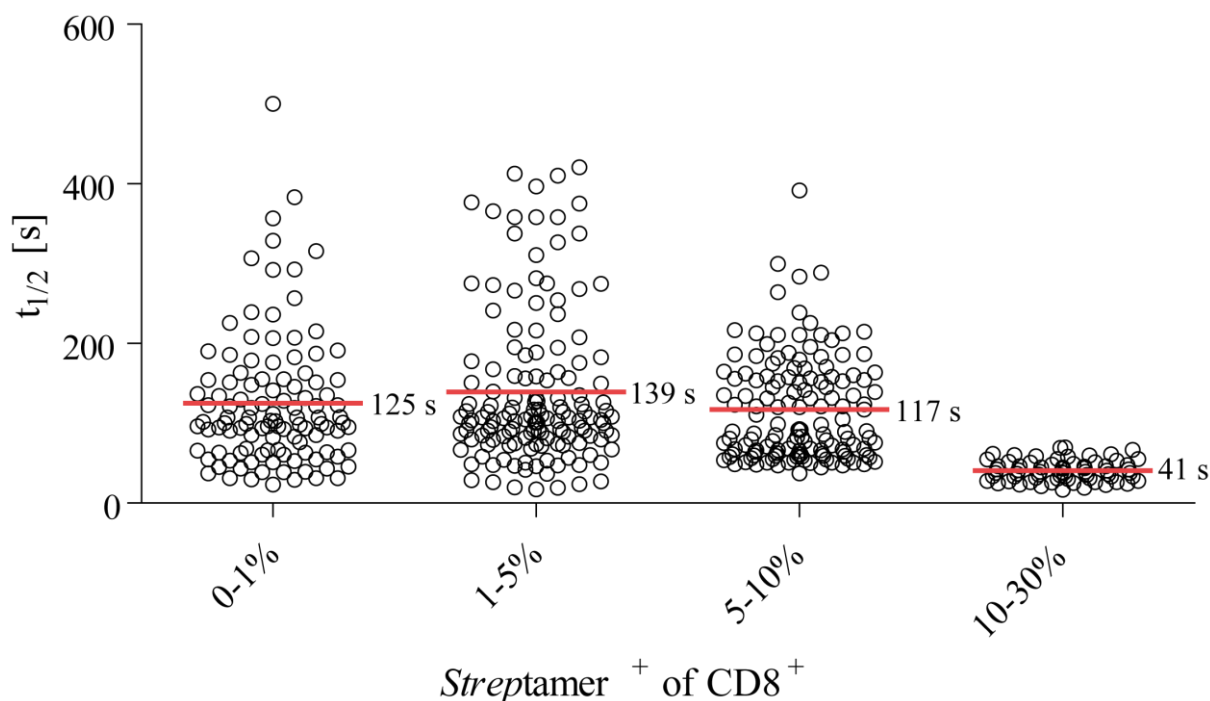


Figure 4-42: Large CMV-specific T cell populations comprise predominantly T cells with fast TCR-ligand $t_{1/2}$.

Pooled TCR-ligand $t_{1/2}$ of individual T cells from CMV-specific T cell populations of indicated size with mean $t_{1/2}$ values indicated (*Streptamer* % of CD8⁺ living lymphocytes). Per group n=5, n=6, n=3 and n=3 different CMV-specific T cell populations were pooled, respectively for group 0-1%, 1-5%, 5-10% and 10-30%.

Results

Finally, the mean TCR-ligand $t_{1/2}$ values of all analyzed CMV-specific T cell populations of healthy CMV seropositive blood donors that differed in specificity and restriction by HLA-molecules were compared. Mean $t_{1/2}$ values were plotted against the *Streptamer*⁺ frequency of living CD8⁺ T cells. Small IE1-specific T cell populations (low frequency) mainly had very long mean TCR-ligand k_{off} -rate values, whereas IE1-specific T cell populations of big size (high frequency) had very short mean TCR-ligand $t_{1/2}$ values. In contrast, there was no correlation between the size of the specific T cell population and the mean dissociation $t_{1/2}$ of pp65-specific T cell populations (Fig. 4-44 A). Further, pp65-specific T cell populations had generally longer mean $t_{1/2}$ values as compared to IE1-specific T cell populations (Fig. 4-44 B).

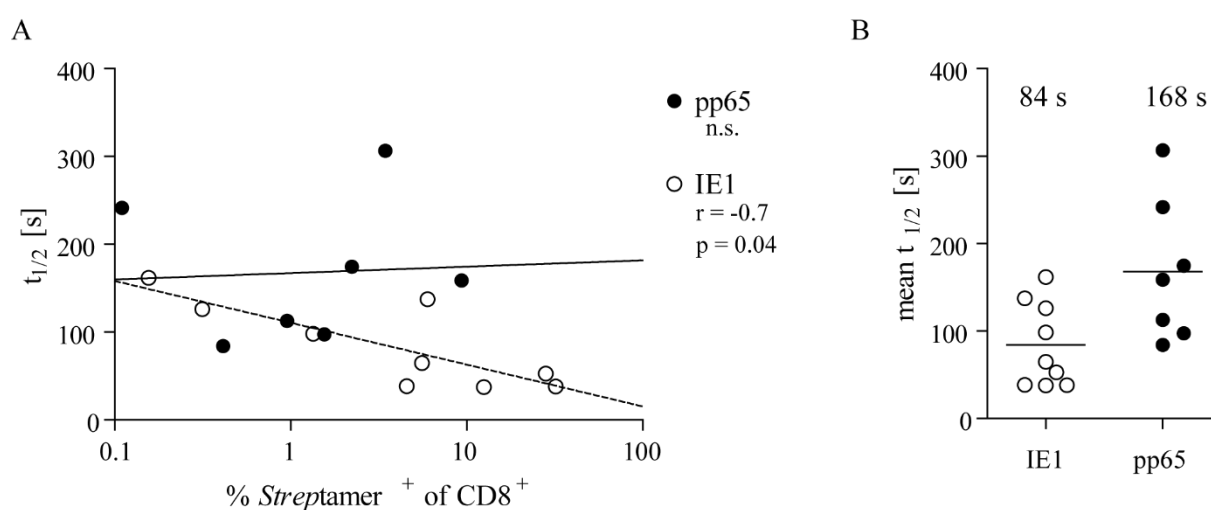


Figure 4-43: Mean TCR-ligand $t_{1/2}$ values of human CMV-specific T cell populations decrease with increasing size of the T cell population.

(A) Mean TCR-ligand $t_{1/2}$ values of CMV-specific T cell populations from different healthy CMV seropositive blood donors are plotted versus their frequency of *Streptamer*⁺ cells from CD8⁺ T cells (size). CMV IE1-specific T cell populations are illustrated by empty dots and CMV pp65-specific T cell populations by filled dots. Dependence between frequency and mean $t_{1/2}$ was tested by Spearman's rank correlation and r and p -value are indicated for IE1-specific T cell populations. n.s. not significant (B) Plotted are the mean TCR-ligand $t_{1/2}$ values comparing IE1-specific and pp65-specific T cell populations. Bar indicates mean $t_{1/2}$ value.

Results

Largely expanded CMV-specific T cell populations have been dominantly described in elderly donors (Ouyang et al., 2003; Ouyang et al., 2004). Consequently, the frequencies of CMV *Streptamer*⁺ T cell populations were compared to the age of the donors. Donors with increasing age had a tendency towards CMV-specific T cell populations of higher frequencies. However, there was no significant correlation between the age and the *Streptamer* frequency or the age and the mean TCR-ligand $t_{1/2}$ value (Fig. 4-45). The time of CMV infection might be a more relevant parameter influencing the size and TCR avidity of CMV-specific T cell populations. The time after infection in human donors is however difficult to determine and not known for the samples analyzed in the TCR-ligand k_{off} -rate assay.

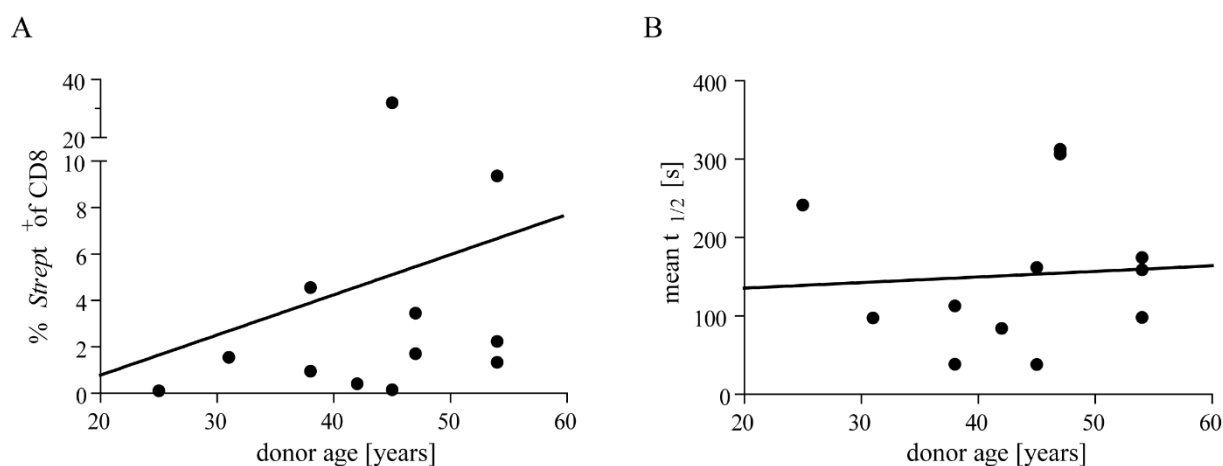


Figure 4-44: The frequency of CMV-specific T cell population is increasing with age.

The *Streptamer* frequency of CD8⁺ T cells of different specificities from different healthy blood donors is plotted versus the age of the respective donors. Indicated is the linear regression line (n.s. in Spearman's rank correlation).

Summarizing, CMV-specific T cell populations of healthy human CMV seropositive donors can expand to a large fraction of the CD8⁺ T cells. Here, largest T cell populations are detected for CMV IE1 epitopes expanding up to more than 50% of all T cells as compared to pp65 or pp50 epitopes. Mean TCR-ligand $t_{1/2}$ values as a measure for the quality of the TCR are decreased with an increasing size of the specific T cell population. As mainly IE1-specific T cell populations expand to large size, the TCR-ligand $t_{1/2}$ of IE1-specific T cell populations was lower when compared to pp65- and pp50-specific populations. This is meaningful as a low TCR-ligand $t_{1/2}$ was associated with low functionality towards the tested epitopes. CMV-specific T cell populations are currently tested for adoptive T cell therapy and differences in the functionality may influence the efficacy of these therapies.

4.3 Murine Cytomegalovirus-specific T cell populations

Low TCR-ligand $t_{1/2}$ values of largely expanded T cell populations from human blood samples of healthy CMV seropositive donors suggest a model of a selection of a few low avidity T cell clones due to frequent proliferation and exhaustion of preferentially high avidity T cell clones during reoccurring antigen stimulation in chronic infection (Buchholz et al., 2011). However, the human data cannot prove this concept. Increasing age of the donors may be correlated with the time after initial CMV infection, but the accurate time point after CMV infection is unknown. Further, different CMV strains can infect the same host that carry sequence variances in immunodominant regions of their genes. The infection with different CMV strains is very difficult to monitor, as the sequencing of viral DNA from the peripheral blood of latent infected donors is very challenging. In addition to the diversity of the target epitope ligands, the immune responses in individual donors are very diverse and difficult to compare with each other. The immune monitoring of healthy human infected with CMV over many years is often not feasible. The murine CMV is very similar in terms of gene functions, course of the infection and the CMV-specific immune responses. MCMV-specific memory T cells in mice also target a variety of different CMV antigens. The T cell populations differ in their expansion kinetics: Some T cell population expand to a large fraction of all T cells, as observed for human CMV-specific T cell populations, whereas other specificities contract after acute infection and are maintained in a small frequency. The murine CMV infection is therefore used as a model for the human infection. TCR-ligand k_{off} -rates of CMV IE1- and CMV m164-specific T cell populations were determined at different time points after infection in order to detect differences in structural TCR avidity.

4.3.1 Reversible *Streptamer* staining on fresh or cryo-preserved whole blood allows the purification of MCMV-specific T cell populations for the TCR-ligand k_{off} -rate measurement

As for human samples, blood samples from the infected mice were analyzed. To be able to isolate as many CMV-specific T cells as possible from the blood, different cell purification protocols were compared (Fig. 4-45 A). Separation of lymphocytes by density centrifugation (Mini-Ficoll) or osmotic red cell lysis in water (H₂O lysis) decreased the fraction of CD8⁺ T cells in the sample and therefore resulted in a decreased recovery of *Streptamer*⁺ CMV-specific T cells. Best results were obtained when purifying *Streptamer*-specific T cells from samples lysed with tris-buffered ammonium chloride (ACT) or from whole blood samples (Fig. 4-45 A). However, *Streptamer* staining in whole blood samples caused a high APC fluorescence background. The APC background fluorescence in *Streptamer* negative cells could be decreased by titrating the *Streptamer* solution from 100µl staining mix (left) to only 5µl per 20µl whole blood (right, Fig. 4-45 B). For 150µl whole blood 37.5 µl of *Streptamer* solution diluted in 62.5 µl FACS buffer was used for staining before FACS sorting of *Streptamer*⁺ T cells. This protocol allowed the isolation of *Streptamer*⁺ T cells from murine whole blood samples by FACS sorting and subsequent analysis in the TCR-ligand k_{off} -rate setup. Remaining erythrocytes increased the number of total events in each sample for FACS sorting and therefore the sample had to be further diluted and the time for the purification was increased. To accelerate the FACS sorting of whole blood we added the CD45 PeCy7 antibody and sorted only CD45 PeCy7⁺ leukocytes by selecting the fluorescence as a detection trigger. Erythrocytes were therefore not detected and analyzed to accelerate the sorting (Fig. 4-45 C).

Results

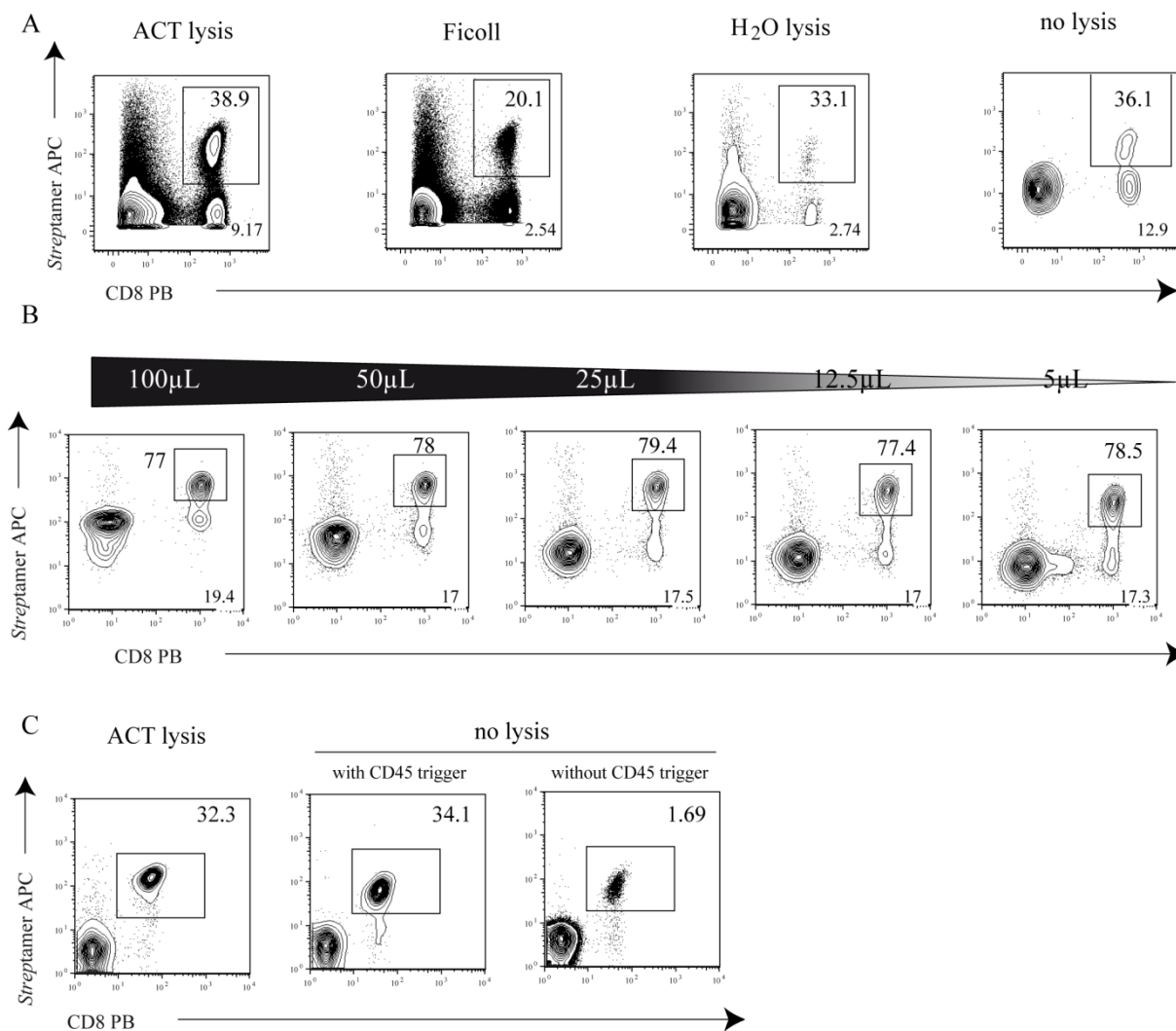


Figure 4-45: Staining and purification of reversibly labeled *Streptamer*⁺ T cells from murine blood samples for TCR-ligand k_{off} -rate analysis.

(A) H2-K^b/OVA-specific *Streptamer* staining on cells from murine blood samples purified by different approaches: 1. Leukocytes were purified by erythrocyte lysis based on Tris-Buffered ammonium chloride (1st left, ACT), 2. by water (H₂O), 3. by density centrifugation (Mini-Ficoll), or 4. Staining was performed on a whole blood sample (right). (B) Titration of specific *Streptamer* APC staining solution on whole blood samples of OT-1 mice. Indicated volume of *Streptamer* solution (100µl – 5µl) was added to 20µl whole blood, incubated for 45 min and analyzed by FACS. (C) FACS sorting of OT-1 blood samples, either lysed by ACT (left) or not lysed and stained with *Streptamer*. Gating is shown for sorting with or without detection trigger on CD45 PeCy7 as a marker for leukocytes (middle and right, respectively). All samples are pre-gated on living lymphocytes. Upper numbers indicate the *Streptamer*⁺ frequency of all CD8⁺ T cells. Lower numbers indicate the CD8⁺ T cell frequency of living lymphocytes.

Results

Further, a protocol for the cryo-conservation of whole blood samples for subsequent *Streptamer* staining, FACS sorting and TCR-ligand k_{off} -rate analysis was established and validated. As TCR-ligand k_{off} -rate analysis can reproducibly be performed on frozen and thawed antigen-specific T cells (Nauerth, 2012), this approach allowed an independently performance of the TCR-ligand k_{off} -rate on samples collected at identical time points. ACT lysis before freezing allowed the FACS sorting of a clear lymphocyte population with a bright *Streptamer* staining (Fig. 4-46 A). Conventional cryopreservation of the lysed sample was compared to a protocol described for the freezing of non-lysed human whole blood by the addition of 10% DMSO before freezing in (Alam et al., 2012). After thawing the non lysed whole blood sample from the same mouse, remaining erythrocytes were detectable (FSC low, SSC high) and a shift in APC fluorescence of *Streptamer*⁺ cells (Fig. 4-46 B). However, in the whole blood sample a higher number of *Streptamer*⁺ T cells could be detected (3080 *Streptamer*⁺ T cells compared to 1575 *Streptamer*⁺ T cells from 150 μ l blood).

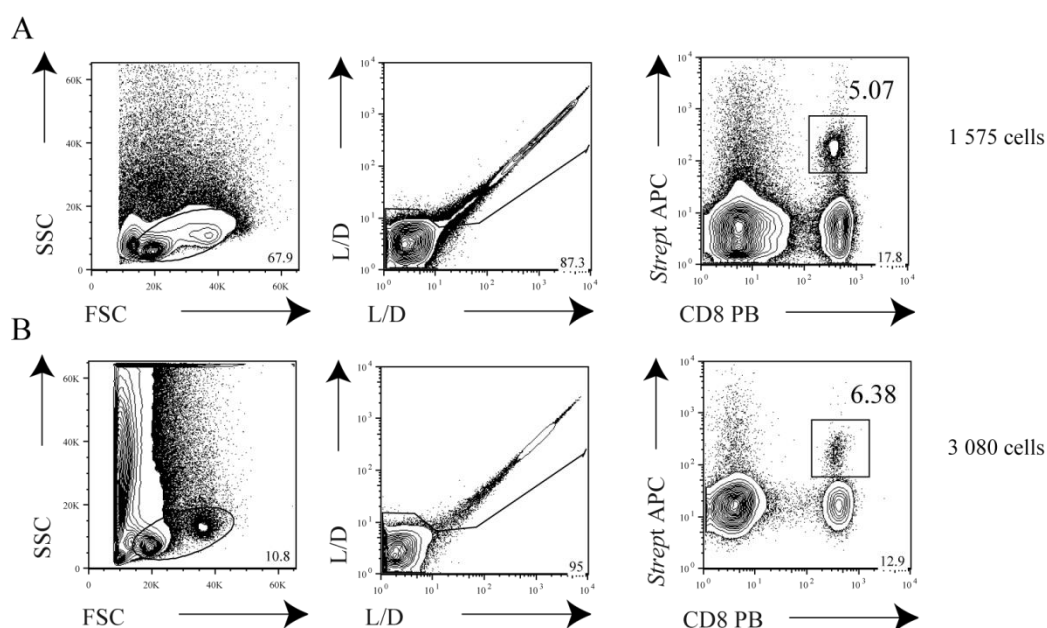


Figure 4-46: *Streptamer* staining on thawed murine blood samples does not require erythrocyte lysis before freezing.

FACS plots and *Streptamer* stainings of thawed murine blood samples. (A) Blood sample with erythrocytes lysis by ACT before freezing. (B) Blood sample without any previous erythrocyte lysis. Freezing, storage in -80°C and liquid nitrogen and thawing procedure were identical for both samples. Numbers in the gate indicate the *Streptamer*⁺ frequency of living CD8 T cells. Numbers next to FACS plots indicate the cell number of *Streptamer*⁺ CD8⁺ T cells recovered from each sample.

Results

To optimize staining and cell purification, an ACT lysis was tested versus non-lysed cells after the freezing and thawing of a whole blood sample that was obtained from Thomas Marandu and Luka Cicin-Sain (Fig. 4-47 before cryopreservation). Again, no lysis allowed the recovery of a higher number of *Streptamer*⁺ cells from the same blood volume of the sample as compared to ACT lysed cells. Background in APC fluorescence of *Streptamer* negative cells could further be reduced by one washing step after the staining (Fig. 4-47 after cryopreservation).

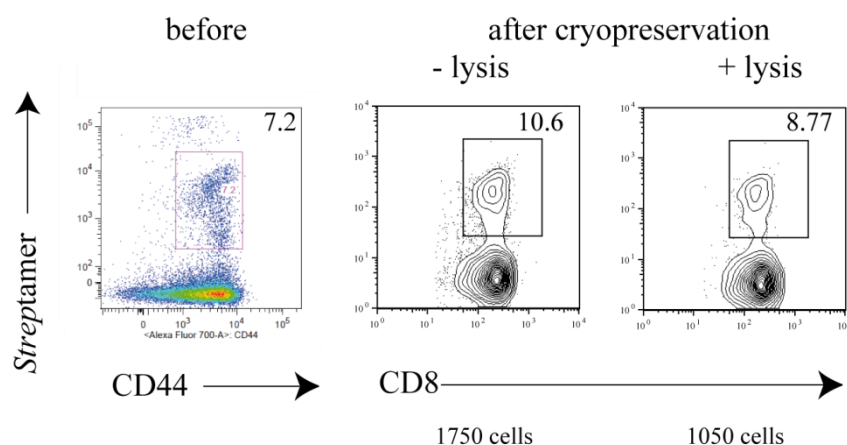


Figure 4-47: *Streptamer* staining on thawed murine blood samples does not require erythrocyte lysis after freezing.

Streptamer staining of blood from MCMV infected BALB/c mouse. Before freezing (left), after freezing of whole blood, thawing and staining (middle) and after freezing of whole blood, thawing and staining after ACT lysis (right). All samples are pre-gated on living lymphocytes. Upper numbers indicate the *Streptamer*⁺ frequency of all CD8⁺ T cells. Numbers below indicate cell number of *Streptamer*⁺ CD8⁺ T cells analyzed from each sample.

These protocols allowed a simple cryopreservation, *Streptamer* staining and FACS purification for the TCR-ligand k_{off} -rate analysis of whole blood samples from MCMV infected mice with a recovery of high cell numbers.

4.3.2 MCMV IE1- and m164-specific T cell populations expand during chronic infection in blood samples from 129/Sv x BALB/c mice

To mix different MHC alleles and thereby generate a broad diversity of different CMV-specific T cell responses, 129/Sv mice (H2-K^b) were crossed to BALB/c mice (H2-K^d, H2-D^d, H2-L^d) and their offspring was analyzed. Thomas Marandu and Luka Cicin-Sain kindly provided the blood samples of 14 month old 129/Sv x BALB/c F1 mice infected for 12, 9, 6 month or one week as indicated in Fig. 4-48.

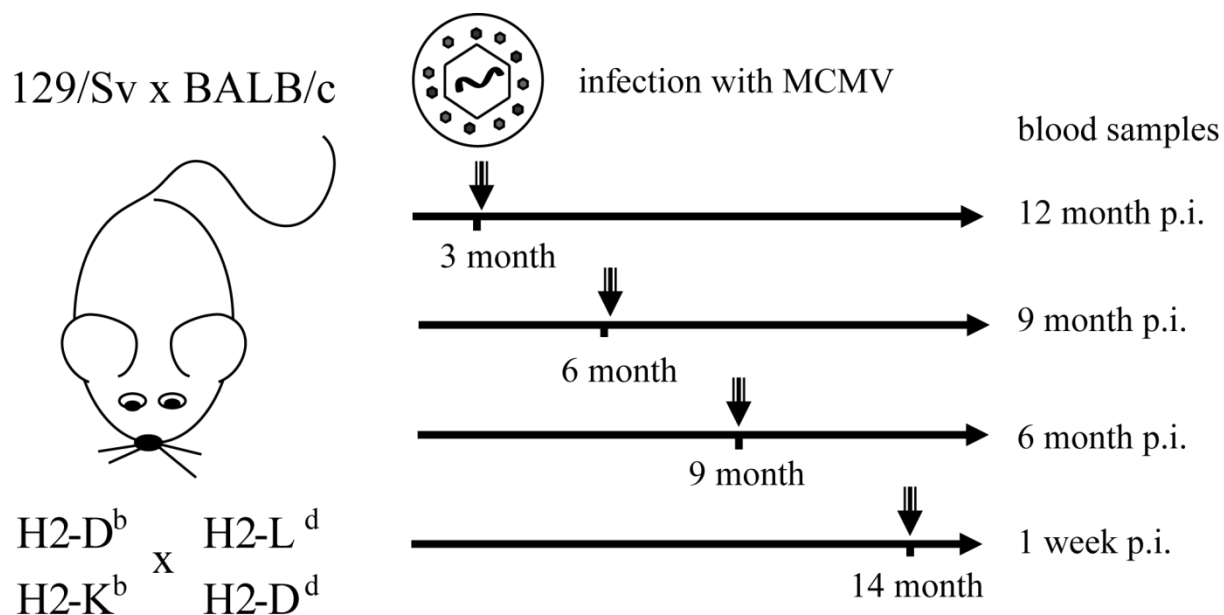


Figure 4-48: Scheme of mouse model for acute and chronic phase of CMV infection.

129/Sv mice were crossed to BALB/c to generate F1 offspring with different MHC alleles as indicated. Mice were infected with one dose of MCMV at different time points as indicated. Blood from mice was collected at the age of 14 month from mice either during an acute phase of CMV infection (1 week post infection) or during the chronic latent CMV infection (6, 9 or 12 month post infection).

The frozen whole blood samples were thawed without lysis for subsequent *Streptamer* staining, sorting and TCR-ligand k_{off} -rate analysis. The frequency of *Streptamer*⁺ of living CD8⁺ T cells one week after infection was 2% H2-L^d/IE1- and 5 % H2-D^d/m164-specific T cells, respectively (Fig. 4-49 A). H2-L^d/IE1-specific T cells expanded to 8 -13 % of living CD8⁺ T cells 24 weeks after MCMV infection and did not expand further at later time points. In contrast, H2-D^d/m164-specific T cells already had a higher frequency of 15 - 22 % of living CD8⁺ T cells 24 week after infection and expanded even further up to 25 % *Streptamer*⁺ T cells of living CD8⁺ T cells. Representative FACS plots of *Streptamer*-specific T cells for

Results

each time point analyzed are shown in Fig. 4-49 A. A summary of the *Streptamer* frequency of individual mice analyzed in the TCR-ligand k_{off} -rate assay is illustrated in Fig. 4-49 B.

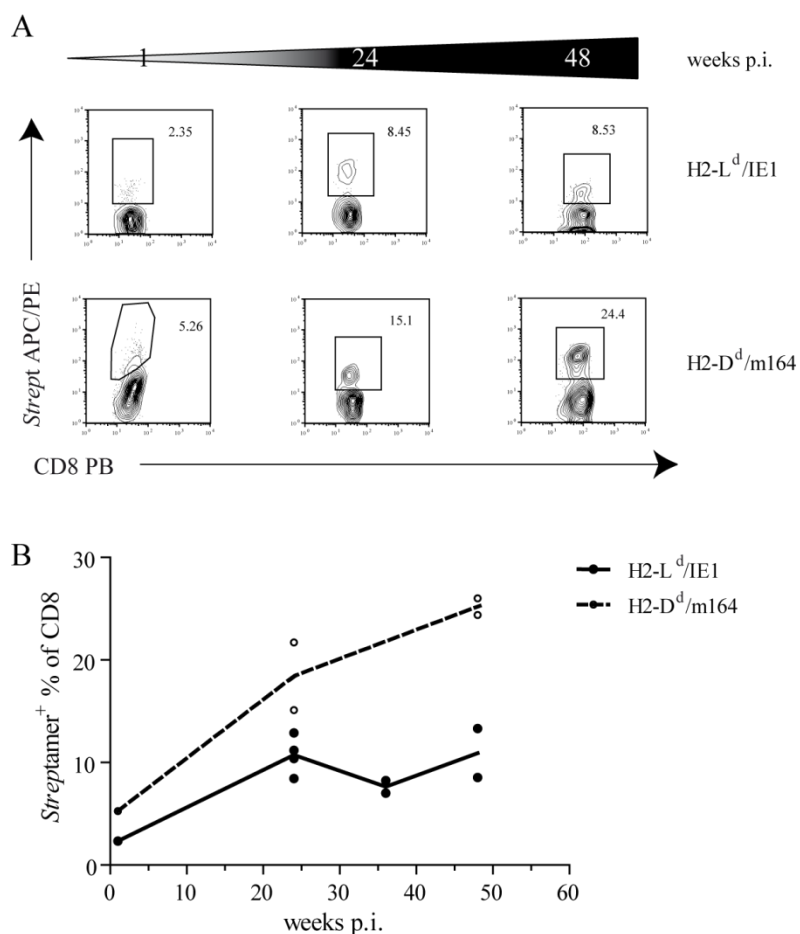


Figure 4-49: CMV IE- and m164-specific T cell populations increase in their frequency after infection with MCMV in 129/Sv x BALB/c mice.

(A) FACS plots of H2-L^d/IE1- and H2-D^d/m164-specific *Streptamer*-APC or -PE stainings in mice infected at the indicated time points. Samples are representative and pre-gated on living CD8⁺ T cells. Numbers in the gates indicate the *Streptamer*⁺ frequency of all CD8⁺ T cells (B) Frequency of H2-L^d/IE1- or H2-D^d/m164-specific *Streptamer*⁺ T cells (black filled dots and empty dots, respectively) of mice infected with MCMV as indicated. Each dot represents one mouse analyzed.

4.3.3 Mean TCR-ligand $t_{1/2}$ values of MCMV IE1- and m164-specific T cell populations do not change substantially during 12 month of infection

TCR-ligand $t_{1/2}$ values were determined for CMV H2-L^d/IE1- and CMV H2-D^d/m164-specific T cell populations of the respective mice infected with MCMV. Both specificities had similar and intermediate $t_{1/2}$ values one week after infection (Fig. 4-50; 96 ±43 s for IE1 and 87±36 s for m164).

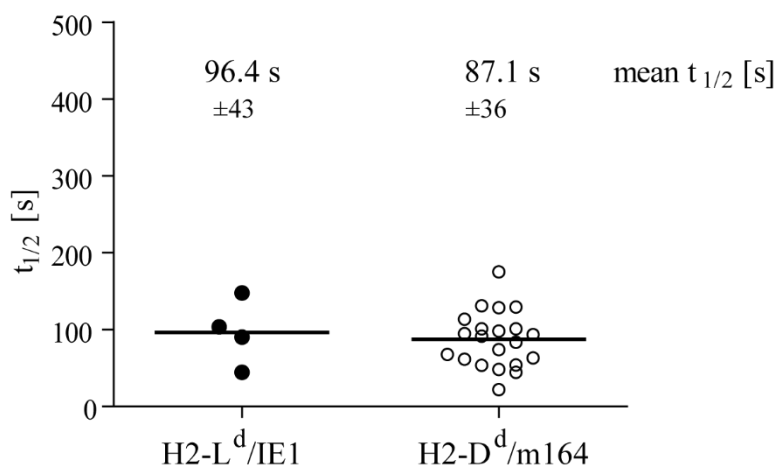


Figure 4-50: Intermediate TCR-ligand $t_{1/2}$ values of MCMV-specific T cell population during acute phase of virus infection.

TCR-ligand $t_{1/2}$ values of individual T cells derived from CMV IE1- or CMV m164-specific T cell populations of two different 129/Sv x BALB/c mice one week p.i.. *Streptamer*⁺ T cells were isolated from heart blood by FACS. Mean $t_{1/2}$ values ±SD are indicated.

Results

Surprisingly, despite an increase in the *Streptamer* frequency the mean $t_{1/2}$ values did not decrease for MCMV-specific T cell populations at later time points than one week post infection. The mean $t_{1/2}$ at 24 or 36 weeks after infection increased slightly (Fig. 4-51 A and B). 48 weeks after MCMV infection, however, the mean $t_{1/2}$ slightly decreased for both CMV IE1- and CMV m164-specific T cells (Fig. 4-51).

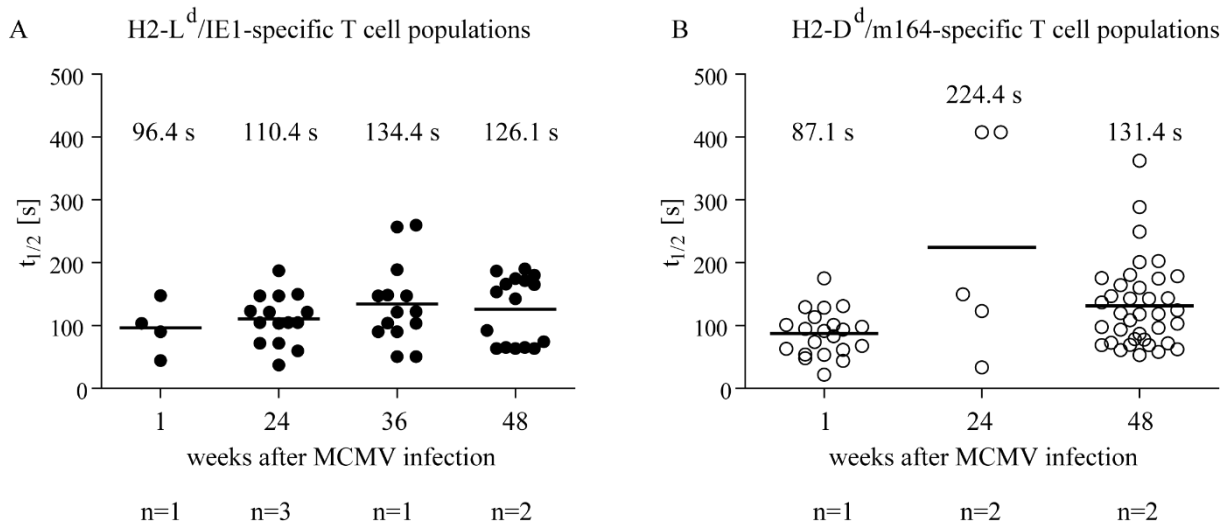


Figure 4-51: Mean TCR-ligand $t_{1/2}$ values of MCMV-specific T cell populations during acute and chronic phase of virus infection.

Summarized data of TCR-ligand $t_{1/2}$ values of T cell populations with the indicated specificity isolated from the blood of 129/Sv x BALB/c mice infected with MCMV 1 – 48 weeks before analysis as indicated below (week(s) after MCMV infection). (A) TCR-ligand $t_{1/2}$ values of H2-L^d/IE1-specific T cell populations or (B) H2-D^d/m164-specific T cell populations with the mean $t_{1/2}$ indicated for every time point. n indicates the number of mice analyzed.

Results

Interestingly, when comparing the MCMV IE1- and MCMV m164-specific T cell populations of different mice infected for 12 month, the mean $t_{1/2}$ was different between the two individual syngeneic mice (Fig. 4-52). While mouse #1 (left) had an IE1-specific T cell population with a long mean $t_{1/2}$ (171 s) and a m164-specific T cell populations with an intermediate mean $t_{1/2}$ (99 s), for IE1- and m164-specific T cell populations of mouse #2 (right) it was the other way around (IE1 = 99 s and m164 = 154 s).

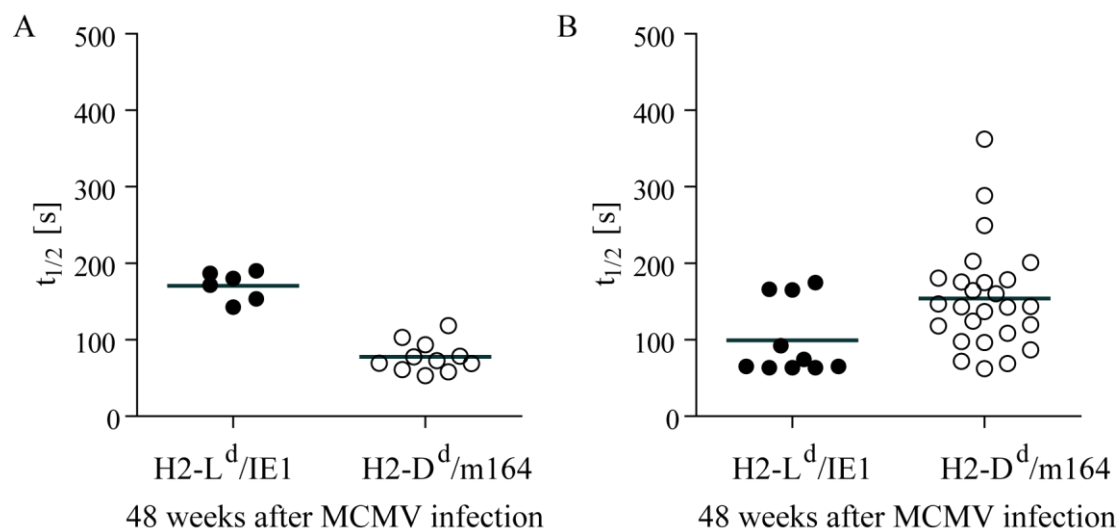


Figure 4-52: TCR-ligand $t_{1/2}$ values of T cell populations with identical specificity differ between individual syngeneic mice.

(A) $t_{1/2}$ values of IE1- and m164-specific T cells 12 month after infection with MCMV in the 129/Sv x BALB/c mouse #1 (A) and mouse #2 (B). Red lines indicate mean $t_{1/2}$ values (171±20; 78±20; 99±49 and 154±68 s, from left to right)

4.3.4 *Streptamer* frequency and mean TCR-ligand $t_{1/2}$ values of MCMV IE1- and m164-specific T cell populations are not related during 12 month of CMV infection

Interestingly, the mean $t_{1/2}$ values did not correlate to the frequency of *Streptamer*-specific T cells for both specificities IE1 (black dots) and m164 (empty dots, Fig. 4-53 A) indicating that there was no selection of low avidity T cell clones in largely expanded IE1- or m164-specific T cell populations up to 12 month after the primary MCMV infection. The mean $t_{1/2}$ values for IE1 were slightly faster in comparison to m164-specific T cell populations (Fig. 4-53 B).

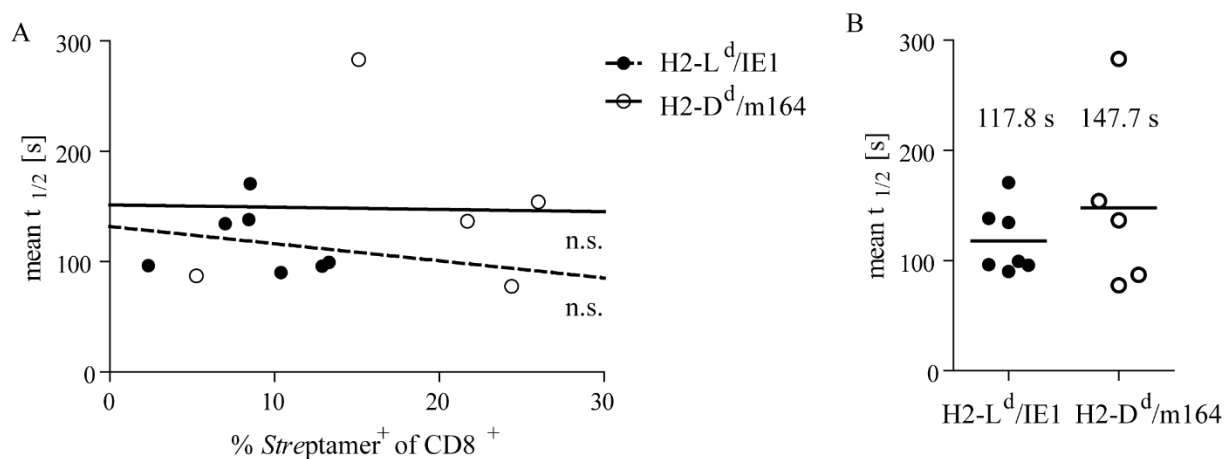


Figure 4-53: Mean TCR-ligand $t_{1/2}$ values of MCMV IE1- and MCMV m164-specific T cell populations do not decrease with increasing population size.

(A) Mean TCR-ligand $t_{1/2}$ values \pm SD of T cell populations with the indicated specificity isolated from the blood of MCMV infected 129/Sv x BALB/c mice plotted against the *Streptamer*⁺ frequency of CD8⁺ T cells. n.s. not significant. Dependence between frequency and mean $t_{1/2}$ was tested by Spearman's rank correlation. (B) Mean TCR-ligand $t_{1/2}$ values of the different mice comparing IE1 and m164 as target antigens.

Further, the distribution of individual data points of each MCMV-specific T cell population, here illustrated as the coefficient of variation (cv), was much broader as compared to the cv of T cell lines that carry only one identical TCR (Fig. 4-54). This diversity in individual $t_{1/2}$ values indicate that the clonal composition of the T cell population analyzed was still diverse.

Results

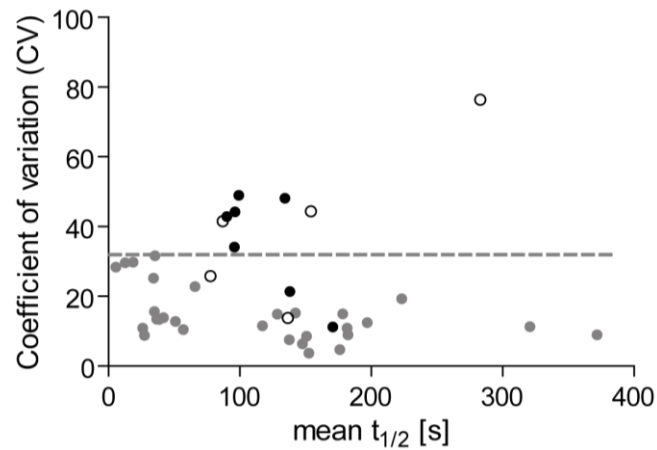


Figure 4-54: The variation of data from individual cells from MCMV-specific T cell populations is relatively broad as compared to TCR identical T cell lines.

Coefficient of variation (cv) of data for the TCR-ligand k_{off} -rate analysis of the IE1- (black filled dots) and m164-specific T cell populations (empty dots) plotted with cv values of TCR identical T cell lines (grey dots). Grey dotted line indicates a cv threshold indicating the variation measured on TCR identical T cells in the TCR-ligand k_{off} -rate assay.

In summary, although IE1- and m164-specific T cell populations expanded in MCMV infected mice during chronic phase of the infection, the TCR-ligand $t_{1/2}$ values did not correlate to their *Streptamer* frequency of living CD8 T cells in 129/Sv x BALB/c mice infected up to 12 month with MCMV. However, mean $t_{1/2}$ slightly increased 24 and 36 weeks after the infection as compared to the acute infection (1 week p.i.), followed by a slight decrease of mean $t_{1/2}$ for both epitopes at the latest time point after infection (12 month p.i.).

5 Discussion

Chronic persistent Cytomegalovirus (CMV) infection in healthy individuals is efficiently controlled by cytotoxic CD8⁺ T cells; however, in elderly hosts CMV-specific CD8⁺ T cells frequently expand to large numbers that are dysfunctional and CMV infection is associated with decreased immunity and increased mortality. In addition to common tests for antigen-specific *in vitro* functionality, the TCR-ligand dissociation $t_{1/2}$ values of CMV-specific T cell populations from CMV seropositive healthy blood donors were characterized with a novel assay assessing the intrinsic binding strength of individual TCRs. Contrary to other existing methods to analyze TCR affinity or avidity, the TCR-ligand k_{off} -rate assay allows a reproducible measurement and comparison of the TCR-ligand $t_{1/2}$ hardwired in the structure of individual TCRs from *ex vivo* isolated T cell populations. Individual TCR dissociation $t_{1/2}$ values from CMV-specific T cells were very diverse indicating differences in their functionality. In addition to the CMV pp65-specific T cell populations analyzed in most CMV studies, T cells specific for epitopes derived from the latency-associated IE1 gene were analyzed in this study. The size of an IE1-specific T cell population was inversely correlated to the mean TCR-ligand $t_{1/2}$. Large CMV IE1-specific T cell populations were not only low for their *in vitro* functionality, but also dominantly consisting of T cells with weak structural TCR avidity as indicated by rapid TCR-ligand dissociation $t_{1/2}$. Consequently, low functionality in these large CMV-specific T cell populations is not caused by the loss of effector functions during persistent antigen stimulation, but the selection of T cell clones with weak TCR binding avidity. By trying to model TCR affinity driven selection of CMV-specific T cells in the mouse, the high avidity T cells were maintained in murine CMV (MCMV)-specific T cell populations that expanded during 12 month of chronic infection. In addition to the TCR avidity/affinity and duration of antigen exposure, other parameters such as thymic output and precursor frequency of antigen-specific naïve T cells, as well as target antigen expression and processing may influence the selective expansion of certain T cell clones in a chronic infection.

5.1 Reproducible measurement of TCR-ligand $t_{1/2}$

The major parameter for T cell functionality is hardwired in the structure of the TCR and determines the biochemical interaction with a specific ligand. However, functionality is influenced by many parameters, such as the activation status of the cell, the expression of the TCR and co-receptors, the composition of the cell membrane and the efficiency of

Discussion

downstream signaling. Most studies analyzing TCR avidity in infection rely on functional readouts because the methods to analyze structural TCR avidity or TCR affinity are limited. To assess the structural binding strength hardwired in the TCR of antigen-specific T cells during an infection, the novel TCR-ligand k_{off} -rate assay based on reversible MHC *Streptamer* reagents was used. The multimeric structure of the *Streptamer* can be disrupted, leaving monomeric pMHC ligands on the surface of antigen-specific T cells that dissociate depending on the individual TCR binding strength. The pMHC ligands are conjugated to a fluorescent dye to monitor the dissociation as loss of fluorescence over the time (Fig. 4-4). The setup of the assay is simple and applicable to a variety of T cells with different specificities; the dissociation $t_{1/2}$ values are reproducible and minimally influenced by the cellular background.

Streptamer-stained T cells are either analyzed by flow cytometry on the population level or mounted to a reservoir on the microscope to allow single cell analysis (Fig. 4-5). Bleaching of the pMHC dye during the acquisition of the same T cell over the time under the microscope can be optimally corrected by the analysis of fluorescence loss during laser exposure of covalently fluorochrome labeled small beads (Fig. 4-7). The fluorochrome APC on the multimerizing *Strep*-Tactin backbone reagent is not interfering with the dissociation kinetics of the pMHC (Fig. 4-11), but it can be used to purify the *Streptamer*-specific T cells by FACS (Fig. 4-23 - 4-25) and to determine the starting point for monomeric pMHC dissociation upon vanishing of *Strep*-Tactin APC fluorescence (Fig. 4-6). Conventional MHC molecules that are used for reversible *Streptamer* stainings can be easily and efficiently modified for the TCR-ligand k_{off} -rate assay by mutagenesis of the DNA vectors with phosphorylated primers inserting a linker and a cysteine for fluorescence conjugation (Fig. 4-21 and 4-22). In the k_{off} -rate setup, the temperature needs to be constantly controlled. Optimal temperatures that prevent T cell activation and thereby internalization of the pMHC monomers bound to the TCR are low (4°C). However, complete dissociation of pMHC monomers can be observed even at 22°C with a two-fold decrease in $t_{1/2}$ (Fig. 4-19 and 4-20).

CMV-specific T cell populations can consist of a diversity of different T cell clones (Day et al., 2007) and become further limited in the TCR repertoire diversity (Ouyang et al., 2003; Ouyang et al., 2004). For information on the diversity of T cells in a population, the TCR-ligand single cell setup on the microscope was used. All validation experiments have been performed with this setup. Although the setup is simple, the image acquisition and analysis is time consuming and not applicable for high-throughput analysis. In contrast, the acquisition

Discussion

and data analysis in the flow cytometry setup is faster. It determines the mean $t_{1/2}$ of all T cells analyzed with one cell at one time point, but does not follow up a single cell over the whole time, and is therefore optimal for T cells expressing identical TCRs.

In contrast to the dissociation kinetics determined in conventional MHC multimer dissociation experiments (Fig. 4-1 - 4-3), the $t_{1/2}$ values of T cell clones analyzed repetitively in the same or in another experiment are reproducible for fast and slow dissociation kinetics in the TCR-ligand k_{off} -rate assay (Fig. 4-8). Conventional MHC multimer-based assays are complicated by multivalent binding and dissociation rates resulting in very long $t_{1/2}$ values in the range of minutes to hours (Wang and Altman, 2003), in contrast to dissociation of monomeric pMHC in the range of seconds determined in surface plasmon resonance (SPR) or the k_{off} -rate assay (Garcia et al., 1997). Additionally, the nature, affinity and the concentration of the blocking reagent that is needed to prevent rebinding of dissociated pMHC monomers has a great impact on the obtained dissociation $t_{1/2}$ (Wang and Altman, 2003). In the *Streptamer* k_{off} -rate assay, antigen-specific T cells can be analyzed in the absence of a blocking reagent (Fig. 4-11), allowing a reproducible measurement of the $t_{1/2}$. The TCR-ligand $t_{1/2}$ values of CMV-specific T cell clones were correlated to their *in vitro* functionality. Although many people use the MHC multimer staining intensity as a readout for TCR avidity (Maeda et al., 2014; Nelson et al., 2015), it did - for example - not correlate to functionality for a number of CMV-specific T cell clones isolated from the naïve T cell repertoire. Despite a bright staining of specific MHC multimer, the majority of T cell clones isolated from a naïve repertoire produced low amounts of IFN γ in response to the target epitope (Fig. 4-13 and 4-14). In the *Streptamer* k_{off} -rate assay the long TCR-ligand $t_{1/2}$ values of T cell clones 4 and 15 correlated to IFN γ production (Fig. 4-14 and 4-15). The assay can therefore predict functionality of T cells potentially used for adoptive cell transfer (Hombrink et al., 2013). Similar $t_{1/2}$ values of CMV-specific T cell clones analyzed at different days after or even different rounds of *in vitro* re-stimulation (Fig. 4-16), as well as the comparable $t_{1/2}$ maintained upon transgenic re-expression of individual TCRs on Jurkat cells (Fig. 4-18) emphasize the low contribution of cellular factors, such as TCR expression or activation status of the cell on the measurement. The $t_{1/2}$ is determined as a structural and not a functional readout of TCR binding strength depending mainly on the TCR. The gold standard to determine the biochemical interaction between TCR and its ligand is the measurement of association and dissociation of pMHC in surface plasmon resonance (SPR) in Biacore assays, where pMHCs and TCRs need to be provided as highly purified proteins. Because the expression of soluble TCRs is technically challenging, SPR is difficult to use for analysis of a broader spectrum of TCRs (Reiser et al.,

Discussion

2009). In addition, there is accumulating evidence that affinity values based on three-dimensional SPR measurements do not reflect the physiological TCR – pMHC interaction of anchored molecules on opposing cells. Recombinant expressed TCRs were shown to have altered binding kinetics as compared to TCRs expressed on the cell surface (Adams et al., 2011; Liu et al., 2014b). Novel approaches measure binding kinetics on the surface of antigen-specific T cells with increased dissociation rates as well as faster association rates as compared to SPR. The adhesion frequency assay from Huang and colleagues is based on external forces applied to approach and disrupt the analyzed T cell and the artificial red blood target cell with micropipettes which does not reflect the physiological situation of a T cell and its target cell. In this assay the contribution of a monomeric TCR-pMHC interaction is difficult to resolve, because the adhesion and disruption used for the calculation of k_{on} - and k_{off} -rate might be influenced by the number, distribution and the orientation of TCRs on the T cell, as well as the number and distribution of pMHCs loaded on the contact zone of the artificial red blood target cell (Huang et al., 2010; Adams et al., 2011). Similarly, the kinetics of individual TCR microclusters in the FRET-based single molecule assay are very diverse, allowing to measure k_{off} -rates in an artificial synapse, but not revealing insights on a monomeric TCR-ligand interaction that can be compared among a variety of different TCRs (Huppa et al., 2010). The *Streptamer*-based k_{off} -rate assay combines the resolution of a monomeric TCR-ligand dissociation and the application on the surface of living T cells. Analog to the adhesion frequency and the FRET single molecule assay, it enables analysis of membrane-anchored TCRs in their physiological context and the contribution of the co-receptor CD8 binding to the $\alpha 3$ domain of the MHC heavy chain (Gao et al., 1997; Kern et al., 1998). In contrast to the FRET single molecule assay, where one FRET partner is coupled to the specific peptide, it can be applied to a variety of T cells from different samples. The combined binding strength of a TCR and the CD8 to a pMHC monomer is described as structural TCR avidity, while TCR affinity is used for the binding strength of only the TCR to the pMHC. Although CD8 alone binds the MHC with weak affinity, it is estimated to stabilize the TCR - pMHC interaction 10-fold (Luescher et al., 1995; Garcia et al., 1996; Wooldridge et al., 2005). CD8 co-receptor binding in the *Streptamer* k_{off} -rate assay prolongs the TCR/CD8-ligand $t_{1/2}$ values for the two ligands H2-K^b/dEV8 and H2-K^b/SIY of the murine 2C TCR 1.6- and 3.7-fold as compared to SPR measurements, respectively (Garcia et al., 1997; Degano et al., 2000). In the current setup, the TCR-ligand k_{off} -rate assay cannot segregate TCR from CD8 co-receptor binding. Differences in the expression of CD8 may influence the dissociation kinetics in the assay. TCR-ligand k_{off} -rate values of a TCR expressed on the

Discussion

CD8 $\alpha\alpha$ homodimer expressing Jurkat cells were slightly accelerated as compared to the parental CD8 $\alpha\beta^+$ T cell clone (Fig. 4-18 B, TCR B). The binding affinity of both forms of the CD8 dimer ($\alpha\alpha$ or $\alpha\beta$) on its own have similar affinity to the MHC (van der Merwe, PA. and Davis, 2003); however, the data indicates that the combined TCR/CD8-pMHC structural avidity is decreased 1.3-fold in the absence of CD8 β expression. In addition, T cell clones can decrease functional TCR avidity in response to strong TCR stimulation by down-regulating their CD8 β expression (Sharma and Alexander-Miller, 2011) supporting a strong effect of CD8 expression. Dissociation kinetics of T cell clones were similar at different time points after *in vitro* re-stimulation, despite potential differences in the TCR as well as CD8 expression (Fig. 4-17). To which degree differences in the CD8 expression influence the TCR-ligand k_{off} -rate remains to be investigated. Mutated MHC molecules that abolish CD8 binding to the $\alpha 3$ domain (Purbhoo et al., 2001) or TCR transgenic T cells that lack the expression of CD8 can be utilized to analyze TCR-ligand k_{off} -rate in the absence of CD8 binding. Unfortunately, CD8 independent MHC multimer or MHC *Streptamer* staining is restricted to selected high affinity TCRs (Moore et al., 2009). *Streptamer* staining is a prerequisite for the TCR-ligand k_{off} -rate assay. T cell populations that produce cytokines but are not stained with the respective pMHC multimer were detected in rare cases for e.g. HCMV IE1 (Khan et al., 2010). However, here the failure of stable binding of the pMHC multimer may be a result of combing a peptide variant with an incorrect MHC molecule. For example, it has been shown that the HLA-B702 IE1 CRVLCCYVL peptide is actually only recognized by specific T cells upon presentation on the HLA-C702 (Ameres et al., 2013). In other cases, low TCR expression or density can cause a weak *Streptamer* staining, making the analysis of TCR-ligand k_{off} -rate inaccurate or even impossible. Similarly, low TCR-pMHC II binding affinities of CD4 $^+$ T cells hamper reversible MHC staining at low temperatures (Wooldridge et al., 2009). To increase sensitivity of the *Streptamer* k_{off} -rate assay, the monitoring of dissociation (as well as association) of dye conjugated pMHC can potentially be transferred/adapted to single molecule analysis by total internal reflection (TIRF) microscopy (Huppa et al., 2010; Ratzke et al., 2012).

Most data based on SPR suggest that TCRs with long $t_{1/2}$ correlate to high functionality (Krogsgaard and Davis, 2005). Some high affinity TCRs however can compensate short $t_{1/2}$ with a high k_{on} -rate (Boulter et al., 2007; Govern et al., 2010). The setup of the *Streptamer* k_{off} -rate assay does not allow analyzing the k_{on} -rate. Consequently, high avidity T cells with a fast k_{on} -rate, but short $t_{1/2}$ might not be detected. The correlation between the mean $t_{1/2}$ and the

Discussion

functionality determined as peptide concentration for half-maximal IFN γ production (EC_{50}) supports that these T cells are rare (Fig. 4-28). In addition, only T cells with long TCR-ligand $t_{1/2}$ contributed to low amounts of bacterial or viral load in mouse models. Small differences in the $t_{1/2}$ values mediated huge differences in protection upon adoptive transfer experiments (Knall, 2007; Nauerth et al., 2013b). Another explanation for the rare detection of T cells with fast $t_{1/2}$ but high functionality is that $t_{1/2}$ values of high avidity TCRs are slightly influenced by rebinding of monomeric pMHC. While the $t_{1/2}$ in the presence of MHC blocking antibody was nearly identical for a low avidity T cell clone, the $t_{1/2}$ in the presence of blocking antibody was slightly decreased from 200 seconds to 168 seconds for a high avidity T cell clone (Fig. 4-10). In the context of a TCR with high a k_{on} -rate, the “ k_{off} -rate” measured in the setup might be prolonged.

Although the structure of the TCR is believed to be the major determinant of T cell functionality or functional TCR avidity (Morgan et al., 2003), functional TCR avidity of a T cell may change irrespectively of the TCR structure (Moore et al., 2009). To analyze to which extend TCR structure determines T cell functionality on a single cell, the *Streptamer* k_{off} -rate assay can potentially be combined with the imaging of early signaling events of T cells such as a recombinant EGFP ZAP70 signaling molecule (O'Donoghue et al., 2013) or the analysis of calcium flux in the T cells (Liu et al., 2014a). Further, transfer of T cells with different, defined TCRs into mice challenged with an infection or a tumor will give more insights on the correlation of TCR-ligand $t_{1/2}$ and protection.

The validation measurements demonstrate that the TCR-ligand k_{off} -rate assay is suitable to analyze the $t_{1/2}$ as a component of structural TCR avidity of a variety of different CMV-specific T cell populations from different donors and distinguish it from the T cell functionality. The assay allows investigation of differences in the structural TCR avidity of antigen-specific T cells in the context of repetitive antigen stimulation during chronic infection. Understanding the changes in the T cell response during chronic infection does not only enable to monitor the quality of the existing immune response, e.g. during aging, but also to identify T cells with optimal avidity for adoptive T cell transfer. It can further be applied to antigen-specific T cells in other infections as well as malignancies to allow an *ex vivo* characterization of the $t_{1/2}$ to indicate the quality of a TCR.

5.2 TCR-ligand $t_{1/2}$ of human CMV-specific T cell populations

With the novel TCR-ligand k_{off} -rate assay we addressed the question whether repetitive antigen exposure during chronic infection causes changes in the TCR avidity of antigen-specific T cells. We analyzed CMV-specific T cell populations from infected healthy blood donors because CMV is a virus with a high incidence and has major implications during immune suppression after transplantation. Further, it is discussed to contribute to immune senescence during aging in healthy individuals. TCR-ligand $t_{1/2}$ values of individual human CMV-specific T cells differed to a large degree. While neither the antigen recognition, nor the HLA-restriction indicated a distinct $t_{1/2}$, an increasing frequency of antigen-specific T cells correlated with a fast TCR-ligand $t_{1/2}$ and low functionality. In contrast to the pp65 antigen expressed during active virus infection, the correlation was only detected for T cells specific for the immediate early 1 (IE1) antigen that is also expressed during latent virus infection. Taken together, continuous stimulation of IE1-specific T cells during acute and chronic CMV infection may result in proliferation induced senescence of high avidity T cell clones, resulting in the preferential expansion of low avidity T cell clones at late time points after infection.

5.2.1 Disparate TCR avidities of human CMV-specific T cells

Human CMV-specific T cells were remarkable different in their TCR-ligand $t_{1/2}$ values. The $t_{1/2}$ values of individual T cells ranged from very fast 17 up to long 500 seconds (Fig. 4-27). As the mean $t_{1/2}$ of *ex vivo* T cell populations correlated to the ability to secrete IFN γ (Fig. 4-28), these differences indicate distinct quality of the TCR of individual CMV-specific T cells. In contrast to a study that characterized HIV-, EBV- and CMV-specific T cells restricted to HLA-B8 with higher peptide sensitivity and elevated polyfunctionality as compared to HLA-A2-specific T cells (Harari et al., 2007), we did not observe a skewing towards an HLA-type with disparate TCR-ligand $t_{1/2}$ values (Fig. 4-29). Comparing groups recognizing the different CMV antigens IE1 and pp65 indicated no intrinsic TCR-ligand $t_{1/2}$ for certain specificity (Fig. 4-31). Although we observed a similar spread in TCR-ligand $t_{1/2}$ values for pp65- and IE1-specific T cells, the median $t_{1/2}$ was slightly lower for IE1 (Fig. 4-30). Analyzing one donor having a HLA-A2/pp65- as well as a HLA-A2/IE1-specific T cell population illustrated that IE1-specific T cell populations can have faster TCR-ligand $t_{1/2}$ values if they have a larger frequency (Fig. 4-32). To learn more about the distribution of TCR-ligand k_{off} -rates for distinct specificities, the number of antigen-specific T cell populations analyzed in the

Discussion

Streptamer-based k_{off} -rate has to be further increased. Comparison of CMV-specific T cells to antigen-specific T cells in other infections, as well as in malignancies or in the naïve repertoire will further resolve the range of functional TCR-ligand $t_{1/2}$ and detect differences for certain antigens. For example, high avidity T cells specific for self-antigens are negatively selected during thymic development. Structural TCR avidity needs to be balanced in order to prevent autoimmune reaction and on the other hand recognize tumor cell overexpressing self-antigens (Hurwitz et al., 2014). Therefore, T cells in malignancies are often characterized by lower avidity as compared to T cells in infections (Aleksic et al., 2012). Due to positive selection during thymic development, all TCRs bind the MHC to some degree. To activate a T cell it requires a minimum of TCR binding avidity. T cell populations in the range of fast dissociation $t_{1/2}$ less than 60 seconds need high amounts of peptide to become activated, in contrast to T cell populations with prolonged $t_{1/2}$ (≥ 60 seconds; Fig. 4-28). This data indicates the lower threshold for optimal TCR avidity. The plateau of the curve is reached at 100 seconds, pointing to minor differences in the T cell functionality of T cells with a $t_{1/2}$ of more than 100 seconds. However, most data suggests T cells with higher avidity are more effective and protective in infections and malignancies (Zeh et al., 1999; Derby et al., 2001). Accumulating data on the TCR-ligand $t_{1/2}$ in combination with functional *in vitro* and *in vivo* tests, especially with T cell clones or transgenic T cells, will increase the knowledge on optimal TCR avidity and help identifying T cells with optimal functionality. Importantly, there is accumulating evidence for an upper threshold of TCR avidity which might depend strongly on the nature of the infection or disease (Hebeisen et al., 2013b; Hebeisen et al., 2013a). Especially in malignancies the optimal TCR avidity may be lower as compared to infections in order to reduce the risk of autoimmunity and cross reactivity (Hurwitz et al., 2014).

5.2.2 Expansion of T cell populations responding to latency-associated genes

In a large number of different seropositive healthy blood donors, we detected strong differences in the frequency of CMV-specific T cells. Many T cell populations specific for IE1 expanded to large numbers of more than 50% of all CD3⁺ T cells. T cell populations for the other antigens analyzed (pp50 and pp65) also expanded, however to a smaller degree as compared to IE1 (Fig. 4-32). In one of the largest studies investigating immune responses to a variety of different CMV epitopes based on cytokine secretion, the tegument protein pp65 has been described as a major immunogenic CMV target, followed by IE1 and others such as

Discussion

pp50 (Sylwester et al., 2005). While pp65 responses were detected abundantly among many different donors in CD4 and CD8 T cells, the IE1 response in one individual donor was often larger in comparison to pp65 or pp50, supporting a preferential expansion of IE1-specific T cells in CMV infection. By comparing HLA-A2/IE1- and HLA-A2/pp65-specific T cell populations based on multimer staining, IE1-specific T cells were identified as a much bigger and terminally differentiated population as compared to pp65-specific T cells (Khan et al., 2002a). Further, Khan and colleagues observed a decreased ratio of cytokine producing cells to multimer stained cells in the elderly indicating a low functionality (Khan et al., 2004). In this study, he observed IE1- and pp50-specific T cell populations in individual elderly donors up to 32% and pp65-specific T cells with maximal 18 % of CD8⁺ T cells in one donor.

Expansion of pp65-specific T cells is observed only in rare cases of elderly individuals with frequencies up to 23% (Khan et al., 2002b; Lachmann et al., 2011) or 10% of CD8⁺ T cells (Lachmann et al., 2011). In our cohort, the maximal size of pp65-specific T cells was 3.5 % of CD3⁺ T cells (Fig. 4-32). During acute infection, pp65 is immediately recognized upon virus entry, while IE1 first needs to be transcribed early after infection (Landolfo et al., 2003). In contrast, during chronic CMV infection, pp65 is expressed infrequently in the lytic cycle of the virus resulting in low expansion of antigen-specific T cells, while IE1 expression during latency preferentially expands IE1-specific T cells (Khan et al., 2007). Consequently, latent expression of IE1 epitopes might cause expansion of specific T cells, while CMV reactivation or *de novo* infection with other CMV strains results in a temporary expansion or accumulation of pp65-specific T cells.

Comparing T cell populations with the same specificity from different donors (same MHC, same antigen and epitope) demonstrated that the TCR-ligand $t_{1/2}$ does not depend on the staining reagent, the peptide or the MHC, but on the frequency of specific T cells (Fig. 4-34, 4-35). Notably, we found two IE1-specific T cell populations with very opposed characteristics in the same donor: One large, oligoclonal population with fast TCR-ligand $t_{1/2}$ and low functionality and a small and polyclonal population with long $t_{1/2}$ and high functionality (Fig. 4-36 and 4-37). Interestingly, in three donors that we analyzed, T cell populations targeting the HLA-B8/IE1₈₈₋₉₆ epitope were characterized by higher TCR avidity, despite an exhausted T cell population targeting another epitope of the same antigen in donor #1, or despite relatively high frequency (6 and 9% of CD8⁺ T cells in Fig. 4-38). In the study of Khan and colleagues, they also found HLA-B8/IE1₁₉₉₋₂₀₇ with the highest frequency as compared to other IE1 epitopes (Khan et al., 2004). Antigen density is discussed as a major driver for immune senescence in chronic infection (Zuniga and Harker, 2012). Therefore,

Discussion

differences in the frequency and density of peptide presentation on the target cell might be an explanation why HLA-B8/IE1₁₉₉₋₂₀₇-specific T cells have different characteristics as compared to HLA-B8/IE1₈₈₋₉₆. For example, the binding affinity to the MHC or proteasomal processing of the IE1₈₈₋₉₆ epitope may be less efficient. Some epitopes are not processed by the regular proteasome but exclusively by specific proteasomes, such as the immunoproteasome only expressed in professional antigen-presenting cells (APCs). Antigen-specific T cells in CMV can be stimulated by infected normal body cells, such as epithelial cells expressing the normal proteasome, as well as by APCs expressing the immunoproteasome. In mice it has been shown, that CMV-specific T cells expand in response to stimulation by non-hematopoietic cells in the lymph node (Torti et al., 2011). Expansion of HLA-B8/IE1₁₉₉₋₂₀₇-specific T cells might be preferred because the epitope is preferentially processed on infected body cells. Analyzing additional samples of HLA-B8/IE1₈₈₋₉₆ with larger frequencies (>10%) will gain further insights whether the samples analyzed are rather an exception than a rule. Notably, the IE1₁₉₉₋₂₀₇ epitope varies in its amino acid sequence among different CMV strains as summarized in table 1 (Elkington et al., 2003; Khan et al., 2004). TCR-ligand k_{off} -rate measurements for all donors were performed based on the “KM” pMHC ligand; however, the specific T cell population of donor #1 also recognized the peptide variants “RM”, “KI” and the hypothetical epitope “RI”. The sensitivity for the isoleucine variants “KI” and “RI” was two log scales higher as compared to the epitope used for k_{off} -rate measurement (Fig. 4-39). With this EC_{50} the T cell population is however still in the range of lower avidities ($EC_{50} = 1.3 - 1.5 \cdot 10^{-8}$ M compare to Fig. 4-28). Consequently, we clearly defined the big IE1₁₉₉₋₂₀₇ T cell population of donor #1 for all four potential peptide targets as a low avidity T cell population. The generation of dye conjugated MHC monomers with exchange peptides for the screening of different epitope variants in the *Streptamer* k_{off} -rate assay failed with the conventional setup (Fig. 4-40 – 4-41), but modifications and alternative protocols can be tested to analyze the TCR-ligand $t_{1/2}$ for different variants of HLA-B8/IE1₁₉₉₋₂₀₇-specific T cell populations. Cross-reactivity of individual T cell clones is potentially another driving factor for clonal expansion and exhaustion in chronic infection. In HIV infection, expansion of crossreactive T cell clones was detected in response to a mutation in the immunodominant HIV epitope. These T cells had a high avidity and correlated to a good prognosis in HIV infected patients (Ladell et al., 2013). Loss of this T cell clone correlated to disease progression in the patients (Victor Appay, unpublished). Therefore, the simultaneous infection with CMV strains expressing different IE1₁₉₉₋₂₀₇ variants might increase a selective pressure on cross-reactive T cell clones and accelerate clonal focusing. On the other hand,

mutations in the IE1₁₉₉₋₂₀₇ epitope might be an immune evasion mechanism of CMV as a result of e.g. preferential processing of this epitope on infected cells and efficient recognition by specific T cells.

5.2.3 Population size matters?

For T cells derived from CMV-specific T cell populations with a frequency of more than 10% of CD8⁺ T cells, we found lower TCR-ligand $t_{1/2}$ values in a narrow range (Fig. 4-42). This is reflected in the negative correlation of population frequency and mean TCR-ligand $t_{1/2}$ of IE1-specific T cell populations (Fig 4-43). In contrast, this correlation was not true for pp65-specific T cell populations. For this antigen, we did not find and analyze donors with T cell populations with a frequency over 10%. To analyze whether big pp65 T cell populations are characterized by low structural and functional TCR avidity, more samples with a size of over 10% need to be analyzed. Further, pp50-specific T cell populations will be analyzed to detect the relation between population size and TCR-ligand $t_{1/2}$ for other CMV targets. The reasons for the massive expansion of CMV-specific T cells are still poorly understood. Antigen presence in a time dependent manner are discussed (Waller et al., 2008; Zuniga and Harker, 2012), so large CMV-specific T cell populations were mostly found in groups of old donors (Ouyang et al., 2003; Ouyang et al., 2004). In the samples analyzed in the TCR-ligand k_{off} -rate assay, we found expanded T cell populations with increasing age; however, there was no correlation between the age and the frequency or the mean TCR-ligand $t_{1/2}$ (Fig. 4-45). Because the time point of CMV infection is not known for the donors, we do not know for how long the donors of different age were infected. In summary, for human CMV-specific T cell populations of healthy CMV seropositive blood donors, we detected fast dissociation-rates (k_{off} -rates) of expanded IE1-specific T cells. In contrast, pp65-specific T cells were smaller in size and characterized by longer dissociation $t_{1/2}$. This data indicates a selective expansion of low avidity T cells specific for IE1 and maintenance of pp65-specific T cells in human CMV infection.

5.2.4 Clonal focusing during chronic CMV infection

Repetitive antigen encounter during acute infection is believed to preferentially expand antigen-specific T cells of high avidity by equilibrating differences in the precursor frequency (Busch and Pamer, 1999; Smith et al., 2000; Lawson et al., 2001; Lanzavecchia, 2002), the

Discussion

fast TCR-ligand $t_{1/2}$ values of largely expanded IE1-specific T cells can be explained by the hypothesis of the ‘clonal changing of the guard’ during chronic infection (Buchholz et al., 2011). Here, T cell responses are diverse during early time points after infection. T cell clones with high avidity are stimulated, proliferate and control the virus. Strong and repetitive stimulation results in telomere shortening and senescence or apoptosis of the high avidity T cell clones. Lower avidity T cells consequently become stimulated, expand and mediate antiviral immunity, until they become dysfunctional and proliferate massively. Contrary to this hypothesis, it is believed that CMV-specific T cell populations carry TCRs of high affinity. T cell clones of high avidity selected during acute CMV infection (Day et al., 2007) are suggested to be maintained over long periods in healthy individuals (Waller et al., 2008), because the TCR repertoire for CMV-specific T cell populations has been shown to be maintained at least for four to five years in different donors (Iancu et al., 2009; Klarenbeek et al., 2012). The selection of public TCRs with high similarity in different donors is believed to result from progressive clonal focusing of high avidity T cell clones based on their TCR-ligand interaction *in vivo* that is even accelerated during inflammation and CMV reactivation (Price et al., 2005; Trautmann et al., 2005). T cell clones with identical $V\alpha$ and similar $V\beta$ TCR derived from the populations analyzed by Trautmann and colleagues had very similar pMHC binding modes and high TCR affinity as determined by crystal structure and SPR (Gras et al., 2009; Reiser et al., 2009). Clonal focusing of high affinity T cell clones is suggested to further increase during aging and long-term CMV infection, as Schwanninger and colleagues detected T cell clones with very high TCR affinity exclusively in a group of elderly donors as compared to a younger cohort (Schwanninger et al., 2008). The functionality of CMV-specific T cells in elderly CMV seropositive hosts is controversially discussed. While some groups observe a maintenance of functionality (Lachmann et al., 2011; Lelic et al., 2012), others observed an accumulation of CMV-specific clonal expansions with very low functionality in the elderly (Ouyang et al., 2003; Ouyang et al., 2004). Theoretically, CMV-specific T cells with high TCR affinity recruited during acute CMV infection could lose their functionality in response to repetitive antigen stimulation in some donors. However, the dysfunctionality of the large and oligoclonal HLA-B8/IE1₁₉₉₋₂₀₇-specific T cell population of donor #1 correlated to a fast TCR-ligand $t_{1/2}$ indicating a low structural TCR avidity (Fig. 4-36 and 4-37). Supporting these findings, largely expanded CMV-specific T cell populations in elderly donors did not bind MHC multimer and secreted cytokines in response to their specific peptide highly dependent on the CD8 contribution (Khan et al., 2010) or they bound MHC multimer only with CD8 contribution (Griffiths et al., 2013). Importantly, most studies

Discussion

suggesting high avidity T cell responses in CMV infection in the elderly focus on pp65-specific T cell populations (Price et al., 2005; Trautmann et al., 2005; Schwanninger et al., 2008; Gras et al., 2009; Reiser et al., 2009). TCR avidity of pp65-specific T cell populations might be different as compared to IE1-specific T cell populations. In contrast to IE1-specific T cell populations, TCR-ligand $t_{1/2}$ values were longer and we could not correlate the population size to the mean TCR-ligand $t_{1/2}$ for pp65-specific T cell populations (Fig. 4-44). The exclusive expression of pp65 during lytic infection could have different effects on shaping the clonal repertoire of antigen-specific T cells as compared to IE1 that is expressed during virus latency. This is also reflected in the different expansion kinetics of IE1- and pp65-specific T cells (Khan et al., 2007). Notably, T cells specific for IE1 expand to a larger degree as compared to pp65 (Fig. 4-33).

The controversial discussion on the structural TCR avidity or TCR affinity of CMV-specific T cell populations is not only caused by complexity of the virus, differences in the genetic background of the host and environmental factors such as opportunistic infections, but further by the limitations and heterogeneity of methods to assess the TCR avidity. Measurements are either based on SPR (Trautmann et al., 2005; Gras et al., 2009; Reiser et al., 2009), MHC multimers with CD8 binding abrogation (Price et al., 2005; Griffiths et al., 2013), conventional pMHC multimer dissociation (Schwanninger et al., 2008) or functional readouts (Elkington et al., 2003; Sylwester et al., 2005; Khan et al., 2010; Lachmann et al., 2011). Our data on CMV-specific T cell populations allows comparing TCR avidity of the different CMV-specific T cell populations. In contrast to CMV populations that can compensate low affinity TCRs with the CD8 contribution found by Khan and colleagues (Khan et al., 2010), our measurement revealed very fast TCR-ligand $t_{1/2}$ despite CD8 contribution for certain populations (Fig. 4-34 and 4-43). The assay can only be used for *Streptamer*-stained T cells, however, in rare cases antigen-specific T cells are not stably labeled with the respective MHC multimer (Khan et al., 2010). In addition, some subdominant T cell clones might be difficult to detect and contribute less to the measurement. For example, in the big T cell population of donor #1 we found a subdominant T cell clone that should further be characterized for its TCR-ligand $t_{1/2}$. Other studies suggest that subdominant T cell clones in CMV-specific T cell population have lower TCR avidity (Khan et al., 2002b; Price et al., 2005). However, at later time points after infection, these low avidity T cell clones might expand and dominate the response, while senescent high avidity T cells are maintained but do not contribute to the immune response. Transferring or combining the approach to single cell analysis could improve the analysis of rare subdominant T cell clones.

Discussion

Taken together, the data on TCR avidity during chronic infection is controversially discussed. In contrast to the repertoire focusing and maintenance of high avidity T cell clones, our data suggests a reverse clonal focusing in chronic latent CMV infection. In response to persistent antigen stimulation of epitopes expressed during latent infection, specific T cell clones with high avidity are deleted and result in the expansion of low avidity T cell clones; however, further experiments and models are necessary to gain insight on the selection of antigen-specific T cell clones during chronic infection.

5.3 TCR-ligand $t_{1/2}$ of murine CMV-specific T cell populations

Although increasing age raises the chance to be infected with CMV for long periods of time, the time point after infection in humans remains unknown. In addition, differences in the genetic background, T cell responses, infection dose, CMV strains, as well as other infections and further environmental factors complicate the interpretation of results in human CMV infection. Importantly, the accessibility of human samples from different organs (peripheral blood, spleen, lymph nodes) and the long time periods limit the feasibility of longitudinal studies in human CMV seropositive healthy donors. For these reasons, many studies on CMV are performed in the mouse model. Murine CMV has a high similarity in the genes and their functions, the clinical symptoms and immune responses resemble human CMV infection. Importantly, CD8 T cell responses either show a pattern similar to acute infection with expansion of antigen-specific T cells after initial infection, subsequent contraction and maintenance of a low number of memory T cells or an inflational T cell response (Sierro et al., 2005; Munks et al., 2006a; Munks et al., 2006b). Similar to human studies, the inflation of CMV-specific T cells has been suggested to cause an attrition of the TCR repertoire decreasing the immunity towards novel infection in aged mice (Messaoudi et al., 2004; Cicin-Sain et al., 2012; Smithey et al., 2012). To test the TCR-ligand $t_{1/2}$ of T cell clones selected during chronic CMV infection under conditions that are easier to control, we analyzed antigen-specific T cell populations in the mouse model. In mice with a diverse set of MHC alleles, we did not observe changes in the TCR-ligand $t_{1/2}$ of T cell populations in response to two inflational endogeneous epitopes up to 12 month after CMV infection.

5.3.1 Differences in TCR-ligand $t_{1/2}$ of murine and human CMV-specific T cell populations

Blood samples from 129/Sv mice crossed to BALB/c mice infected with murine CMV were used as a model representing the human blood samples analyzed in the TCR-ligand k_{off} -rate assay (Fig. 4-48). H2-L^d/IE1- and H2-D^d/m164-specific T cell populations expanded in response to long infection, while T cell recognizing peptides in the context of 129/Sv- or C57BL/6-associated MHC alleles such as H2-K^b/m139, H2-K^b/IE3 were maintained in small frequency. TCR-ligand $t_{1/2}$ early after infection was similar for H2-L^d/IE1- and H2-D^d/m164-specific T cells, indicating a recruitment of T cell clones with comparable TCR avidity (Fig. 4-50). Although H2-L^d/IE1-specific T cell populations expanded to a larger degree as compared to H2-D^d/m164 (20% and 10% of living CD8 lymphocytes 50 weeks after infection, respectively; Fig. 4-49), the TCR-ligand $t_{1/2}$ values were similar (≥ 100 seconds; Fig. 4-51 – 4-53).

In contrast to human CMV-specific T cell populations, differences in the TCR-ligand $t_{1/2}$ of H2-L^d/IE1- and H2-D^d/m164-specific T cell populations at the varying time points after infection were small, indicating few changes in the structural TCR avidity. We did not observe a correlation between size of antigen-specific T cell populations and the TCR-ligand $t_{1/2}$ (Fig. 4-53). T cell responses 12 month after infection might still be very diverse as indicated by the high coefficient of variation of $t_{1/2}$ values from individual T cells (Fig. 4-54). Clonal composition can be investigated further by TCR V β staining or TCR sequencing of the populations. The diversity of IE1- and m164-specific T cell populations could be an explanation for the little differences in TCR-ligand $t_{1/2}$ at different time points after infection. It can result from different aspects: a high number of different CMV target epitopes that are recognized by CMV-specific T cells, a constant output of naïve T cells from the thymus and short time periods of persistent antigen stimulation on specific T cell clones.

First, the contribution of two dominant protective T cell populations (IE1 and m164) to the immune response may slow down the clonal exhaustion of high avidity T cell clones. Although they recognize different antigens, IE1- and m164-specific T cell populations compete for the antigen on the target cell. While IE1- and m164-specific T cell populations on their own have a similar protective capacity upon transfer into irradiated BALB/c mice, there is no beneficial effect of the simultaneous transfer of both specificities (Ebert et al., 2012). Most likely, the target cell is recognized by either one IE1- or one m164-specific T cell, which in consequence prevents the activation of the other specific T cell. In the 129/Sv x BALB/c model the number of different CMV target antigens is very high and diverse, which

Discussion

might drag the effects of chronic antigen exposure on the selection of specific T cell clones in one specific T cell population.

Second, the output of naïve T cells from the thymus of 12-14 month old mice might be higher as compared to aged humans. Similar to humans, the TCR repertoire diversity progressively decreases with age (Rudd et al., 2011), which is associated with impaired immunity to *de novo* infection (Yager et al., 2008). In humans, the removal of the thymus from newborns accelerated immune aging by stopping the output and thus decreasing the frequency as well as repertoire diversity of naïve T cells (Sauce et al., 2009). In thymectomized children, as well as in elderly humans, the number of naïve T cells in the periphery is preserved by homeostatic proliferation in response to elevated IL-7 serum levels (Sauce et al., 2012). In contrast, in mice the output of naïve T cells from the thymus is maintained lifelong (den Braber et al., 2012). Consequently, naïve antigen-specific T cell clones of high avidity might be still recruited into the m164- and IE1-specific T cell populations in the mice 12 month after infection and dominate the immune response. Indeed, Snyder *et al* revealed that naïve T cells can be recruited into existing inflational CMV-specific T cell responses (IE3, M38 and m139) in >3month infected C57BL/6 mice (Snyder et al., 2008).

Third, murine and human T cells might have similar lifespans; however, in the human they can be exposed to persistent antigen for much longer periods of time. Most importantly, telomere length of murine T cells remains stable based on continuous high telomerase activity (Akbar et al., 2000). In contrast, human T cells lose telomerase activity *in vitro* upon the third stimulation (Valenzuela and Effros, 2002) and undergo progressive telomere shortening upon each following cell division until a critical telomere length induces the cell cycle arrest.

Currently, another mouse model with the SIINFEKL model epitope derived from chicken ovalbumin expressed on different CMV genes in the C57BL/6 mouse is tested. Interestingly, SIINFEKL-specific T cell populations can differ substantially in their phenotype depending on the gene expression of the epitope. Expression in the context of the late M45 gene that is processed during lytic CMV infection selects a robust but low number of specific T cells with minor changes in the TCR-ligand $t_{1/2}$ at different time point after infection. In contrast, IE2 expression during latency induces the accumulation of specific T cells with low avidity at late time points after infection. Similar to the human CMV IE1-specific T cell populations, the TCR-ligand $t_{1/2}$ of SIINFEKL-specific T cell populations decreased depending on the size of the T cell population (data generated by Florian Voit; not shown). Differences between the wild type CMV infected 129/Sv x BALB/c and the latent or lytic expression of SIINFEKL

Discussion

peptide in CMV infected C57BL/6 mice suggest additional parameters that accelerate negative repertoire focusing in response to persistent antigen stimulation. First, the latent persistent expression of the antigen as compared to expression during reactivation induces the expansion of low avidity T cells. Second, efficient peptide presentation on target cells might dictate dominance of one specific inflational T cell response. SIINFEKL-specific T cell population in response to latent IE2 expression suppresses the inflation of other endogenous T cell populations (Farrington et al., 2013). Contrarily, endogenous CMV-specific T cell populations, such as M38, m139 and IE3 in C57BL/6 or IE1 and m164 in BALB/c can expand simultaneously in wild type CMV infected mice (Munks et al., 2006a). Differences in proteasomal peptide-processing, peptide-loading on the MHC, the affinity of the peptide to the MHC, as well as interference of the virus with MHC expression result in differences of the expression on the target cell. High and stable expression of the epitope increases antigen driven proliferation and the selective pressure on a specific T cell population. The suppression of other inflational CMV-specific T cell populations by SIINFEKL-specific T cells as well as another introduced epitope derived from the herpes virus glycoprotein B (Dekhtiarenko et al., 2013) might result from the competition of the specific T cells on the level of the antigen expressed on the cell. T cells specific for epitopes with lower epitope expression are stimulated less frequently. Indeed, the SIINFEKL affinity to H2-K^b is high and the pMHC is abundantly expressed in MCMV IE-SIINFEKL infected C57BL/6 (Farrington et al., 2013) as well as in MCMV m164-SIINFEKL infected BALB/c mice (Lemmermann et al., 2010).

In addition, the precursor frequency of SIINFEKL-specific T cells in the naïve repertoire of C57BL/6 mice is supposedly low (Obar et al., 2008). A low precursor frequency and a low output of naïve antigen-specific T cells from the thymus limits the replacement of dysfunctional T cell clones and might accelerate the negative repertoire focusing during persistent antigen stimulation. In theory, m164- and IE1-specific T cell populations in the 129/Sv x BALB/c mice could have higher frequencies and TCR diversity in the naïve repertoire as compared to SIINFEKL-specific T cells, which remains to be tested.

In conclusion, the data on murine CMV-specific T cell populations hints to highly complex and interfering processes on the level of the T cells and on the level of the antigen expression shaping the clonal repertoire in chronic infection. Parameters on different levels seem to influence the expansion and clonal selection of specific T cells. The diverse T cell response with a number of different CMV antigen targets, a continuous output of naïve T cells from the thymus in combination with limited replicative senescence may allow to maintain high avidity

T cells in IE1- and m164-specific T cell populations in CMV infected 129/Sv x BALB/c mice as compared to human CMV-specific T cell populations.

5.4 Influences on the inverse repertoire focusing during chronic infection

In our model the repetitive antigen exposure in chronic infection drives the expansion of specific T cells and dominantly selects low avidity T cells (inverse repertoire focusing). Antigen-specific T cell clones compete based on their TCR avidity. High avidity T cells (H) respond preferentially to the target epitopes because they bind stably to the pMHC on infected or antigen presenting cells, suppressing the binding of lower avidity T cells. Strong TCR avidity allows T cells to respond to limited numbers of pMHC on infected target cells (Derby et al., 2001) and long TCR – pMHC interaction induces strong signaling and prolongs the exposure to effector molecules during contact to the target cell or antigen presenting cell (APC). After long time periods of persistent antigen stimulation, high avidity T cell clones are either lost by proliferation induced senescence or they become anerg and nearly undetectable in peripheral blood in response to missing or inhibitory signals. Subsequently, low avidity T cell clones (L) bind to their antigen, proliferate, mediate effector functions and expand, dominating the T cell response. Differences between human samples and mouse models suggest other parameters in addition to TCR affinity, time and antigen abundance influencing the repertoire focusing of antigen-specific T cell populations in chronic infection:

T cells specific for antigens expressed persistently during chronic infection are expanded (grey cells), while others remain in smaller size and maintain their clonal composition for long time periods (black cells, Fig. 5-1). On the level of the specific T cells a high precursor frequency, diverse TCR repertoire and a high output of naïve T cells from the thymus allow replacement of deleted or anerg T cell clones in response to continuous antigen stimulation. In addition, a high number of different T cell populations specific for epitopes expressed during latency may increase competition and further slowdown replicative senescence of individual T cells in one T cell population. Further, the antigen expression influences clonal focusing of specific T cells. Persistent antigen expression during latent infection (white epitope), high peptide loading and stability on target cells, a large number of infected target cells as well as the interaction with inhibitory or dysfunctional dendritic cells presenting peptides from apoptotic, latent infected cells contribute to an acceleration of inverse repertoire focusing (Fig. 5-1).

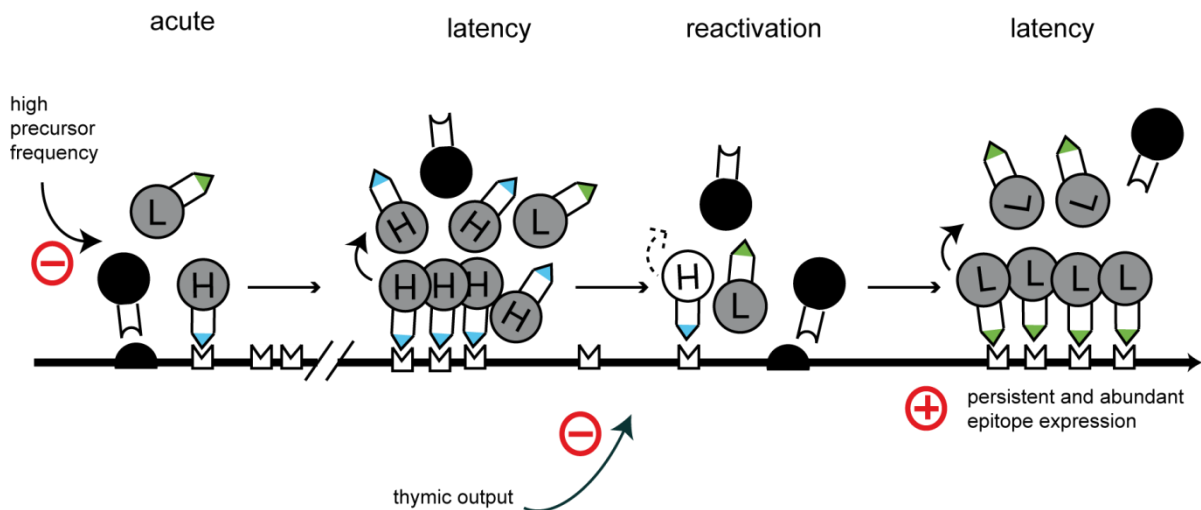


Figure 5-1: Multiple parameters affecting inverse clonal focusing during chronic latent infection.

T cells specific for epitopes expressed during acute infection and virus reactivation (black cells) are maintained in low numbers and proliferate sporadically after antigen stimulation (A - D). Persistent and abundant expression of target epitopes induces proliferation and expansion of specific high avidity T cell clones (B; grey cells H). After long time periods high avidity T cells disappear from the T cell population because they become senescent or unresponsive to antigen stimulation (C; white cell H). In the absence of high avidity T cells, low avidity T cells proliferate in response to antigen stimulation and dominate the T cell response (D). High precursor frequency, diverse TCR repertoire and a high output of naïve T cells from the thymus allow replacement of high avidity T cells decelerating inverse clonal repertoire focusing in chronic infection (-). Persistent and abundant epitope expression on the other hand accelerates the repertoire focusing (+). H – high avidity T cell, L – low avidity T cell.

A large frequency of specific T cells can therefore indicate a low TCR avidity (fast TCR-ligand $t_{1/2}$). Inefficient control of CMV infection caused by the absence of high avidity T cells at late time points after infection (such as in elderly hosts) might result in higher antigen load and subsequent clonal expansion of low avidity T cells. On the other hand, low levels of antigens on infected cells spread all over the body may result in expansion of antigen-specific T cells at any time during CMV infection. In this context, it is possible that during early time points of infection, large CMV-specific T cell populations consist of dominantly high avidity T cells until they undergo proliferation induced senescence (Fig. 5-1 B). Depending on a high precursor frequency and high thymic output, high avidity T cells may dominate the CMV-specific T cell response for sustained time periods. Further TCR-ligand k_{off} -rate measurements will allow monitoring the TCR avidity of specific T cell populations during

repertoire focusing in CMV infection and potentially predict the immune status and risk phenotype of elderly CMV seropositive hosts.

5.4.1 CMV contribution to immune senescence

High avidity T cells are believed to be superior in infection and malignancies (Zeh et al., 1999; Derby et al., 2001). In chronic infection, however, the optimal TCR avidity is not known. Lower avidity of specific T cells might even be beneficial to prevent immunopathology (Zuniga and Harker, 2012). In particular a limited response towards IE1 that is expressed on latent infected cells throughout the body might be essential to prevent immunopathology. In contrast, pp65 is expressed on acutely infected cells or upon virus reactivation. Similar to acute infection, T cells with higher TCR avidity might be necessary to prevent virus dissemination and reactivation.

Why CMV-specific T cell populations expand to these large numbers and how the large populations influence the immunity of the host is still not well understood. The differentiated phenotype of largely expanded CMV-specific T cell populations suggests a proliferation in response to antigen stimulation. In mice, peripheral CMV-specific T cells are constitutively replaced by memory T cells from the lymph node that become activated by CMV infected non-hematopoietic cells and migrate to the periphery, as well as newly recruited antigen-specific naïve T cells (Snyder et al., 2008; Torti et al., 2011). In humans, it is difficult to assess the primary lymphoid organs and data is mostly based on peripheral CMV-specific T cell populations. Remmerswaal *et al* revealed a lower frequency and polyfunctionality (increased IL-2 secretion) of CMV-specific T cell populations from human lymph nodes as compared to peripheral blood (Remmerswaal, Ester B M et al., 2012). However, this study does not analyze the TCR sequences and it remains elusive, whether the lymphoid T cells replace CMV-specific T cells continuously in the periphery in analogy to mice or whether peripheral CMV-specific T cells accumulate homeostatically as a result of resistance to apoptosis as suggested by others (Khan et al., 2002b; Griffiths et al., 2013). Griffith *et al* found long telomeres and anti-apoptotic molecules in expanded low avidity T cell populations of elderly healthy donors that can be identified by CD45RA expression. They conclude that these T cell populations are maintained in response to IL15 that is secreted by blood leukocytes induced by high levels of IFN α during CMV reactivation (Griffiths et al., 2013). Long telomeres of low avidity T cell populations can further be explained by the inverse clonal focusing described above. Low avidity T cells do not respond to the CMV antigen

Discussion

stimulation as long as high avidity T cells are functional, thereby maintaining long telomeres. Only after senescence or loss of high avidity T cells they start to proliferate and control virus infection.

In principle, the large number of antigen-specific T cells might ensure the surveillance of CMV in all infected cells distributed over the whole body. This hypothesis is supported by the need of higher numbers of T cells for comparable success upon adoptive transfer after CMV dissemination to end-stage organs as compared to prophylactic transfer before CMV dissemination in irradiated mice (Holtappels et al., 2008). In addition, specific T cell populations can expand to large size at early time points after CMV infection in humans and mice without clinical symptoms (Karrer et al., 2003; Munks et al., 2006a; Khan et al., 2007). An expansion of IE1-specific T cell populations was even correlated to a good prognosis after allogenic stem cell transplantation (Sacre et al., 2008). Young hosts might even benefit from CMV infection by constant levels of low immune activation (Sansoni et al., 2014). On the other hand, a replication deficient single-cycle MCMV is sufficient to induce inflation of CMV-specific T cells in mice (Snyder et al., 2011). The expanded, large CMV-specific T cell populations compete for space and resources with other T cells. Therefore, CMV is discussed to contribute to immune aging by limiting the repertoire and frequency of naïve T cells and the response to novel infection (Sauce et al., 2009). CMV infection is correlated to an immune risk phenotype and accelerated immune aging (Olsson et al., 2000; Wikby et al., 2002; Hadrup et al., 2006). At least in mice, Cicin-Sain *et al* proved that the CMV infection caused an increased number of CD8 effector T cells and decreased number of naïve T cells resulting in a decreased immunity to *de novo* infection (Cicin-Sain et al., 2012).

5.4.2 Therapeutic strategies to treat CMV-associated diseases

To prevent detrimental immunological changes associated with CMV infection in the aged host, strategies to either prevent CMV infection by boosting the immune system are needed. Boosting the immune system could be achieved with recruiting T cell clones by e.g. systemic vaccination (prophylactic or therapeutic), increasing the function of the thymus or the adoptive transfer of T cells (Buchholz et al., 2011). It is of interest to understand whether high avidity T cells in persistent CMV infection are clonally deleted or whether they are functionally inhibited (exhaustion or anergy) and rarely detectable. Analyzing the TCR-ligand $t_{1/2}$ as well as the TCR sequences of specific T cells from lymph nodes of IE2-SIINFEKL infected mice will allow us to detect potential remaining high avidity T cells. Dysfunctional

Discussion

CMV-specific T cells with high structural TCR avidity may be boosted by blocking immune checkpoints such as PD-1 (Sester et al., 2008, Dirks et al., 2013, 2013; Macaulay et al., 2013), may offer an attractive therapeutic strategy in elderly with a CMV related risk phenotype or transplanted patients. Notably, as compared to other chronic infections such as human immunodeficiency or hepatitis infection, not all CMV-specific T cell populations are exhausted and do express PD-1 (Hertoghs, Kirsten M L et al., 2010). More importantly, benefits of such therapies should be traded against the risk of adverse effects. In the absence of T cell clones with high structural TCR avidity the transfer of ‘fresh’ potent long-living T cell clones could allow to replace dysfunctional clonally expanded T cell clones and control viral replication (Buchholz et al., 2011). As a consequence, CMV reactivation, as well as the resulting re-stimulation of specific T cells might be less frequent. In a study by Hadrup *et al* the polyclonality of a CMV-specific T cell population in elderly hosts correlated with a low risk phenotype in CMV seropositive hosts (Hadrup et al., 2006). The TCR-ligand k_{off} -rate can facilitate the monitoring of the quality of the existing immune response in healthy individuals and indicate a risk phenotype, as well as induced immunity after vaccination or adoptive T cell transfer.

TCR-ligand k_{off} -rate may also help to guide the selection of T cells with optimal avidity for adoptive T cell therapy in malignancies, as well as in CMV reactivation of immunocompromised host. Transfer of CMV-specific T cell populations can prevent CMV dissemination in the absence of existing immunity after bone marrow transplantation and accelerate immune reconstitution (by preventing infection of the bone marrow). This approach is currently tested in humans (Cobbold et al., 2005; Einsele et al., 2008; Feuchtinger et al., 2010; Schmitt et al., 2011; Odendahl et al., 2014). Often large cell numbers of antigen-specific T cells are used for adoptive T cell transfer and generated by several rounds of *in vitro* expansion or isolated by multimer (Einsele et al., 2008) as well as reversible *Streptamer* staining of CMV-specific T cell populations (Schmitt et al., 2011; Odendahl et al., 2014). The data of this thesis indicates that the frequency of CMV-specific T cell populations negatively correlates with the TCR-ligand $t_{1/2}$. Although bigger populations might be easier to enrich for adoptive T cell therapy, they might be characterized by lower TCR avidity and therefore less functional upon adoptive transfer into the patient. Small T cell populations with long TCR-ligand $t_{1/2}$ and a diverse set of T cell clones may mediate optimal protection for CMV reactivation in immunocompromised patients that otherwise suffer from severe CMV-associated morbidity and mortality. At least in acute infection, very low numbers of specific T

cells can be sufficient to induce a diverse, robust and protective T cell response (Stemberger et al., 2007a; Buchholz et al., 2013; Gerlach et al., 2013; Graef et al., 2014; Stemberger et al., 2014). Preclinical transfer experiments of specific T cell lines with distinct TCR avidities revealed that T cells with long TCR-ligand $t_{1/2}$ indeed resulted in lower virus load during acute MCMV infection of immunocompromised mice as compared to a T cell line with shorter $t_{1/2}$ (Ebert et al., 2012; Nauerth et al., 2013b). The characterization of numerous antigen-specific T cells and the correlation of TCR-ligand k_{off} -rates to the therapeutic efficacy of adoptively transferred T cells will be important for the future (Weissbrich et al., 2013).

5.4.3 TCR avidity in malignancies

Similar to chronic infection, the persistent exposure to tumor-associated antigens could cause the deletion or dysfunction of high avidity T cell clones in a variety of malignancies (Pauken and Wherry, 2015). In addition to extrinsic parameters such as suppressive cells (T_{regs} , suppressive myeloid cells) and suppressive cytokines (IL-10) in the tumor microenvironment, clonal deletion of high avidity T cells, as well as T cell exhaustion or anergy may be induced by target epitopes expressed on tumor cells. Dysfunctional tumor-specific T cells could be re-activated by blocking the T cell intrinsic inhibitory pathways via cytotoxic T-lymphocyte-associated Protein 4 (CTLA-4) or PD-1. The treatment resulted in promising clinical responses in patients with melanoma, as well as other malignancies (Callahan et al., 2014). The combination of CTLA-4 and PD-1 blockade in advanced melanoma patients revealed rapid and strong clinical responses in 40 – 53 % of the patients with over 80% reduction in tumor burden for most patients and manageable adverse effects (Wolchok et al., 2013). However, patients that did not show any response to the anti-CTLA-4 and anti-PD-1 treatment may lack T cells with a sufficient structural TCR avidity for epitopes expressed on tumor cells. Clonal deletion of high avidity T cell clones may be accelerated as compared to chronic infection, because the accelerating parameters discussed in Fig. 5-1 appear in most malignancies: The naïve repertoire and thymic output of tumor-specific T cells is often limited due to negative selection in the thymus and the antigens may be expressed abundantly by cancer cells or (inhibitory) dendritic cells. Measuring TCR-ligand $t_{1/2}$ of tumor-infiltrating T cells could detect differences in the TCR avidity and potentially allow identifying patients that respond to checkpoint inhibitors such as anti-CTLA-4 or anti-PD-1. Patients that lack high avidity tumor-specific T cells may be in addition treated with adoptive transfer of tumor-specific T cells. Here, the TCR-ligand k_{off} -rate assay can guide the selection of specific T cell

Discussion

populations or identify TCRs for genetic engineering with optimal TCR affinity. Selecting TCRs with optimal structural TCR avidity for malignant diseases may be more challenging as compared to T cell populations specific for foreign antigens. Although high TCR avidity results in enhanced tumor cell recognition, high avidity T cells may be more susceptible to tolerance induction in the tumor microenvironment (Janicki et al., 2008; Zhu et al., 2013). Most importantly, high TCR avidity needs to be balanced versus adverse side effects caused by the recognition of the specific epitopes (on-target toxicity) or cross recognition of similar epitopes on healthy cells (off-target toxicity). Isolation of high affinity TCRs from patients responding to immunotherapy for genetic engineering of cells for adoptive transfer has been shown to be safe and induce strong clinical responses (Restifo et al., 2012). To increase TCR affinity, mutations in the TCR α or TCR β chain were introduced, thereby increasing tumor recognition in the patients (Robbins et al., 2011). However, enhancing TCR affinities increases the risk for autoimmunity or even mortality due to on- and off-target toxicity. Recently, T cell products engineered with affinity-enhanced melanoma antigen family A3 (MAGEA3)-specific TCRs induced mortality in different clinical trials: A protein expressed in pulsating cardiac tissue (Cameron et al., 2013) was recognized by the transferred MAGEA3-specific T cells resulting in cardiovascular toxicity and death in two patients (Linette et al., 2013). In another trial, transferred MAGEA3-specific T cells recognized epitopes in the normal brain and induced coma followed by death in two of nine patients (Morgan et al., 2013). While these trials demonstrate the potency of adoptively transferred T cells, they also highlight the need for refined methods for the identification of putative safety issues. The target epitopes for T cell therapies need to be chosen carefully and unmodified high affinity TCRs within the range of physiological affinities may reduce the risk for severe side effects. TCR-ligand k_{off} -rate measurements of naturally occurring tumor-specific T cells of patients with strong clinical responses but minor side effects may allow to identify optimal TCR avidities in malignancies (Nauerth et al., 2013a; Weissbrich et al., 2013).

6 Summary

Cytomegalovirus (CMV) is a common opportunistic infection and persists in infected individuals. Reactivation of the virus is mainly controlled by cytotoxic CD8⁺ T cells in immunocompetent hosts. However, CMV infection is associated with decreased immunity and even mortality in elderly hosts (Olsson et al., 2000; Wikby et al., 2002; Hadrup et al., 2006). It is frequently observed that only one or a few CMV-specific T-cell clones expand to large frequency with increasing age and these cells are characterized by low functionality (Ouyang et al., 2003; Ouyang et al., 2004). Functionality is supposed to be lost by repetitive antigen encounter during chronic CMV infection and subsequent exhaustion of T cell clones with T cell receptors (TCRs) that bind strongly to the CMV target epitopes.

To test the relation between functionality and the TCR binding strength of CMV-specific T cells, a novel MHC *Streptamer*-based TCR-ligand k_{off} -rate assay recently developed in our laboratory was used (Nauerth et al., 2013b). In this assay, the dissociation- (k_{off} -) rate of fluorescently labeled MHC monomers loaded with a specific peptide (TCR-ligand) from living antigen-specific CD8⁺ T cells is monitored. TCR-ligand k_{off} -rate values of CMV-specific T cell clones were highly reproducible and independent of the fluorescence staining intensity. Further, comparable k_{off} -rates of T cell clones with different activation status and maintenance of the k_{off} -rate after transgenic re-expression of high and low avidity TCRs on other cells indicate that the values mainly depend on the structure of the TCR rather than the cellular background.

Individual T cells from different CMV-specific T cell populations of human healthy CMV seropositive blood donors varied to a large degree in their k_{off} -rate values ($t_{1/2} = 17 - 500$ s), reflecting strong differences in their functionality. Indeed, the mean $t_{1/2}$ values of individual T cell populations correlated to their functionality measured by cytokine production after stimulation with the specific peptide. Neither the MHC restriction, nor the CMV target antigen correlated with certain $t_{1/2}$ values. However, a large frequency (size) of CMV-specific T cell populations was associated with fast $t_{1/2}$ values (low structural TCR avidity). Largely expanded T cell populations with fast $t_{1/2}$ were specific for immediate early 1 (IE1), which is expressed during CMV latency. These data suggest that high avidity T cell clones are lost in CMV-specific T cell populations accumulating during the chronic latent CMV infection resulting in an inverse repertoire focusing towards low avidity T cell clones (Akbar and Fletcher, 2005; Buchholz et al., 2011).

Summary

In a murine CMV infection model with a diverse MHC I background, IE1- and m164-specific T cell populations expanded to large size. In contrast to human CMV-specific T cell populations, $t_{1/2}$ values did not correlate to the population frequency and were similar after acute infection and time points up to 12 month after infection which might be a consequence of continuously replacement of CMV-specific T cell clones from the thymus (Snyder et al., 2008). The strong expansion in combination with a decrease in $t_{1/2}$ after ≥ 200 days infection of a T cell population with low precursor frequency (Obar et al., 2008) responding to a stable and abundant expressed epitope during latent MCMV infection (Farrington et al., 2013) in mice with a less diverse MHC I genetic background, reveals dominant parameters resulting in an inverse clonal focusing during chronic latent CMV infection.

While the mechanisms of deletion or inhibition of high avidity CMV-specific T cells remain unclear, the findings of this PhD thesis may be relevant for the immune monitoring during aging of CMV seropositive individuals to trace the immune risk profile and the differences in $t_{1/2}$ values highlight the TCR-ligand k_{off} -rate as a quality parameter guiding the selection of antigen-specific T cells for adoptive therapy in a number of diseases.

7 References

- Adams, J.J., Narayanan, S., Liu, B., Birnbaum, M.E., Kruse, A.C., Bowerman, N.A., Chen, W., Levin, A.M., Connolly, J.M., Zhu, C., Kranz, D.M., Garcia, K.C., 2011. T cell receptor signaling is limited by docking geometry to peptide-major histocompatibility complex. *Immunity* 35 (5), 681–693. 10.1016/j.immuni.2011.09.013.
- Akbar, A.N., Fletcher, J.M., 2005. Memory T cell homeostasis and senescence during aging. *Current opinion in immunology* 17 (5), 480–485. 10.1016/j.coi.2005.07.019.
- Akbar, A.N., Soares, M.V., Plunkett, F.J., Salmon, M., 2000. Differential regulation of CD8+ T cell senescence in mice and men. *Mechanisms of ageing and development* 121 (1-3), 69–76.
- Alam, I., Goldeck, D., Larbi, A., Pawelec, G., 2012. Flow cytometric lymphocyte subset analysis using material from frozen whole blood. *Journal of immunoassay & immunochemistry* 33 (2), 128–139. 10.1080/15321819.2011.604370.
- Alanio, C., Lemaitre, F., Law, Helen K W, Hasan, M., Albert, M.L., 2010. Enumeration of human antigen-specific naive CD8+ T cells reveals conserved precursor frequencies. *Blood* 115 (18), 3718–3725. 10.1182/blood-2009-10-251124.
- Aleksic, M., Liddy, N., Molloy, P.E., Pumphrey, N., Vuidepot, A., Chang, K.-M., Jakobsen, B.K., 2012. Different affinity windows for virus and cancer-specific T-cell receptors: Implications for therapeutic strategies. *European Journal of Immunology* 42 (12), 3174–3179. 10.1002/eji.201242606.
- Ameres, S., Mautner, J., Schlott, F., Neuenhahn, M., Busch, D.H., Plachter, B., Moosmann, A., Britt, W.J., 2013. Presentation of an Immunodominant Immediate-Early CD8+ T Cell Epitope Resists Human Cytomegalovirus Immunoavoidance. *PLoS Pathogens* 9 (5), e1003383. 10.1371/journal.ppat.1003383.
- Andersen, M.H., Schrama, D., thor Straten, P., Becker, J.C., 2006. Cytotoxic T cells. *The Journal of investigative dermatology* 126 (1), 32–41. 10.1038/sj.jid.5700001.
- Arstila, T.P., Casrouge, A., Baron, V., Even, J., Kanellopoulos, J., Kourilsky, P., 1999. A direct estimate of the human alphabeta T cell receptor diversity. *Science (New York, N.Y.)* 286 (5441), 958–961.
- Bjorkman, P.J., 1997. MHC restriction in three dimensions: a view of T cell receptor/ligand interactions. *Cell* 89 (2), 167–170.
- Bjorkman, P.J., Saper, M.A., Samraoui, B., Bennett, W.S., Strominger, J.L., Wiley, D.C., 1987. Structure of the human class I histocompatibility antigen, HLA-A2. *Nature* 329 (6139), 506–512. 10.1038/329506a0.
- Boulter, J.M., Schmitz, N., Sewell, A.K., Godkin, A.J., Bachmann, M.F., Gallimore, A.M., 2007. Potent T cell agonism mediated by a very rapid TCR/pMHC interaction. *European journal of immunology* 37 (3), 798–806. 10.1002/eji.200636743.
- Bouvier, M., 2003. Accessory proteins and the assembly of human class I MHC molecules: a molecular and structural perspective. *Molecular immunology* 39 (12), 697–706.
- Bouvier, M., Wiley, D.C., 1994. Importance of peptide amino and carboxyl termini to the stability of MHC class I molecules. *Science (New York, N.Y.)* 265 (5170), 398–402.
- Bridgeman, J.S., Sewell, A.K., Miles, J.J., Price, D.A., Cole, D.K., 2012. Structural and biophysical determinants of $\alpha\beta$ T-cell antigen recognition. *Immunology* 135 (1), 9–18. 10.1111/j.1365-2567.2011.03515.x.
- Brownlie, R.J., Zamoyska, R., 2013. T cell receptor signalling networks: branched, diversified and bounded. *Nature reviews. Immunology* 13 (4), 257–269. 10.1038/nri3403.
- Buchholz, V.R., Flossdorf, M., Hensel, I., Kretschmer, L., Weissbrich, B., Graf, P., Verschoor, A., Schiemann, M., Hofer, T., Busch, D.H., 2013. Disparate Individual Fates Compose Robust CD8+ T Cell Immunity. *Science* 340 (6132), 630–635. 10.1126/science.1235454.

References

- Buchholz, V.R., Neuenhahn, M., Busch, D.H., 2011. CD8+ T cell differentiation in the aging immune system: until the last clone standing. *Current Opinion in Immunology* 23 (4), 549–554. 10.1016/j.coi.2011.05.002.
- Burrows, S.R., Chen, Z., Archbold, J.K., Tynan, F.E., Beddoe, T., Kjer-Nielsen, L., Miles, J.J., Khanna, R., Moss, D.J., Liu, Y.C., Gras, S., Kostenko, L., Brennan, R.M., Clements, C.S., Brooks, A.G., Purcell, A.W., McCluskey, J., Rossjohn, J., 2010. Hard wiring of T cell receptor specificity for the major histocompatibility complex is underpinned by TCR adaptability. *Proceedings of the National Academy of Sciences of the United States of America* 107 (23), 10608–10613. 10.1073/pnas.1004926107.
- Busch, D.H., Pamer, E.G., 1999. T cell affinity maturation by selective expansion during infection. *The Journal of experimental medicine* 189 (4), 701–710.
- Callahan, M.K., Postow, M.A., Wolchok, J.D., 2014. CTLA-4 and PD-1 Pathway Blockade: Combinations in the Clinic. *Frontiers in oncology* 4, 385. 10.3389/fonc.2014.00385.
- Cameron, B.J., Gerry, A.B., Dukes, J., Harper, J.V., Kannan, V., Bianchi, F.C., Grand, F., Brewer, J.E., Gupta, M., Plesa, G., Bossi, G., Vuidepot, A., Powlesland, A.S., Legg, A., Adams, K.J., Bennett, A.D., Pumphrey, N.J., Williams, D.D., Binder-Scholl, G., Kulikovskaya, I., Levine, B.L., Riley, J.L., Varela-Rohena, A., Stadtmauer, E.A., Rapoport, A.P., Linette, G.P., June, C.H., Hassan, N.J., Kalos, M., Jakobsen, B.K., 2013. Identification of a Titin-Derived HLA-A1-Presented Peptide as a Cross-Reactive Target for Engineered MAGE A3-Directed T Cells. *Science Translational Medicine* 5 (197), 197ra103. 10.1126/scitranslmed.3006034.
- Chervin, A.S., Stone, J.D., Holler, P.D., Bai, A., Chen, J., Eisen, H.N., Kranz, D.M., 2009. The Impact of TCR-Binding Properties and Antigen Presentation Format on T Cell Responsiveness. *The Journal of Immunology* 183 (2), 1166–1178. 10.4049/jimmunol.0900054.
- Cicin-Sain, L., Brien, J.D., Uhrlaub, J.L., Drabig, A., Marandu, T.F., Nikolich-Zugich, J., Mossman, K.L., 2012. Cytomegalovirus Infection Impairs Immune Responses and Accentuates T-cell Pool Changes Observed in Mice with Aging. *PLoS Pathogens* 8 (8), e1002849. 10.1371/journal.ppat.1002849.
- Cobbold, M., Khan, N., Pourgheysari, B., Tauro, S., McDonald, D., Osman, H., Assenmacher, M., Billingham, L., Steward, C., Crawley, C., Olavarria, E., Goldman, J., Chakraverty, R., Mahendra, P., Craddock, C., Moss, Paul A H, 2005. Adoptive transfer of cytomegalovirus-specific CTL to stem cell transplant patients after selection by HLA-peptide tetramers. *The Journal of experimental medicine* 202 (3), 379–386. 10.1084/jem.20040613.
- Colf, L.A., Bankovich, A.J., Hanick, N.A., Bowerman, N.A., Jones, L.L., Kranz, D.M., Garcia, K.C., 2007. How a Single T Cell Receptor Recognizes Both Self and Foreign MHC. *Cell* 129 (1), 135–146. 10.1016/j.cell.2007.01.048.
- Corse, E., Gottschalk, R.A., Allison, J.P., 2011. Strength of TCR-peptide/MHC interactions and in vivo T cell responses. *Journal of immunology (Baltimore, Md. : 1950)* 186 (9), 5039–5045. 10.4049/jimmunol.1003650.
- Crough, T., Khanna, R., 2009. Immunobiology of Human Cytomegalovirus: from Bench to Bedside. *Clinical Microbiology Reviews* 22 (1), 76–98. 10.1128/CMR.00034-08.
- Davis, M.M., Bjorkman, P.J., 1988. T-cell antigen receptor genes and T-cell recognition. *Nature* 334 (6181), 395–402. 10.1038/334395a0.
- Davis, M.M., Krogsgaard, M., Huppa, J.B., Sumen, C., Purbhoo, M.A., Irvine, D.J., Wu, L.C., Ehrlich, L., 2003. Dynamics of cell surface molecules during T cell recognition. *Annual review of biochemistry* 72, 717–742. 10.1146/annurev.biochem.72.121801.161625.
- Day, E.K., Carmichael, A.J., ten Berge, Ineke J M, Waller, Edward C P, Sissons, J G Patrick, Wills, M.R., 2007. Rapid CD8+ T cell repertoire focusing and selection of high-affinity

References

- clones into memory following primary infection with a persistent human virus: human cytomegalovirus. *Journal of immunology* (Baltimore, Md. : 1950) 179 (5), 3203–3213.
- Degano, M., Garcia, K.C., Apostolopoulos, V., Rudolph, M.G., Teyton, L., Wilson, I.A., 2000. A functional hot spot for antigen recognition in a superagonist TCR/MHC complex. *Immunity* 12 (3), 251–261.
- Dekhtiarenko, I., Jarvis, M.A., Ruzsics, Z., Cicin-Sain, L., 2013. The Context of Gene Expression Defines the Immunodominance Hierarchy of Cytomegalovirus Antigens. *The Journal of Immunology* 190 (7), 3399–3409. 10.4049/jimmunol.1203173.
- den Braber, I., Mugwagwa, T., Vrisekoop, N., Westera, L., Mögling, R., de Boer, Anne Bregje, Willems, N., Schrijver, Elise H R, Spierenburg, G., Gaiser, K., Mul, E., Otto, S.A., Ruiters, An F C, Ackermans, M.T., Miedema, F., Borghans, José A M, de Boer, Rob J, Tesselaar, K., 2012. Maintenance of peripheral naive T cells is sustained by thymus output in mice but not humans. *Immunity* 36 (2), 288–297. 10.1016/j.immuni.2012.02.006.
- Derby, M.A., Alexander-Miller, M.A., Tse, R., Berzofsky, J.A., 2001. High-Avidity CTL Exploit Two Complementary Mechanisms to Provide Better Protection Against Viral Infection Than Low-Avidity CTL.
- Ding, Y.H., Smith, K.J., Garboczi, D.N., Utz, U., Biddison, W.E., Wiley, D.C., 1998. Two human T cell receptors bind in a similar diagonal mode to the HLA-A2/Tax peptide complex using different TCR amino acids. *Immunity* 8 (4), 403–411.
- Dirks, J., Egli, A., Sester, U., Sester, M., Hirsch, H.H., 2013. Blockade of programmed death receptor-1 signaling restores expression of mostly proinflammatory cytokines in anergic cytomegalovirus-specific T cells. *Transplant infectious disease : an official journal of the Transplantation Society* 15 (1), 79–89. 10.1111/tid.12025.
- Dössinger, G., Bunse, M., Bet, J., Albrecht, J., Paszkiewicz, P.J., Weißbrich, B., Schiedewitz, I., Henkel, L., Schiemann, M., Neuenhahn, M., Uckert, W., Busch, D.H., 2013. MHC multimer-guided and cell culture-independent isolation of functional T cell receptors from single cells facilitates TCR identification for immunotherapy. *PloS one* 8 (4), e61384. 10.1371/journal.pone.0061384.
- Dunne, P.J., Faint, J.M., Gudgeon, N.H., Fletcher, J.M., Plunkett, F.J., Soares, Maria Vieira D, Hislop, A.D., Annels, N.E., Rickinson, A.B., Salmon, M., Akbar, A.N., 2002. Epstein-Barr virus-specific CD8(+) T cells that re-express CD45RA are apoptosis-resistant memory cells that retain replicative potential. *Blood* 100 (3), 933–940. 10.1182/blood-2002-01-0160.
- Ebert, S., Podlech, J., Gillert-Marien, D., Gergely, K.M., Büttner, J.K., Fink, A., Freitag, K., Thomas, D., Reddehase, M.J., Holtappels, R., 2012. Parameters determining the efficacy of adoptive CD8 T-cell therapy of cytomegalovirus infection. *Medical Microbiology and Immunology* 201 (4), 527–539. 10.1007/s00430-012-0258-x.
- Einsele, H., Kapp, M., Grigoleit, G.U., 2008. CMV-specific T cell therapy. *Blood cells, molecules & diseases* 40 (1), 71–75. 10.1016/j.bcmed.2007.07.002.
- Elkington, R., Walker, S., Tania Crough, Moira Menzies, Judy Tellam, Mandvi Bharadwaj, and Rajiv Khanna, 2003. Ex vivo profiling of CD8 responses to HCMV reveals broad and multispecific reactivities in healthy virus carriers. *Journal of Virology* 77 (4).
- Ellefsen, K., Harari, A., Champagne, P., Bart, P.-A., Sekaly, R.-P., Pantaleo, G., 2002. Distribution and functional analysis of memory antiviral CD8 T cell responses in HIV-1 and cytomegalovirus infections. *European journal of immunology* 32 (12), 3756–3764. 10.1002/1521-4141(200212)32:12<3756:AID-IMMU3756>3.0.CO;2-E.
- Farrington, L.A., Smith, T.A., Grey, F., Hill, A.B., Snyder, C.M., 2013. Competition for Antigen at the Level of the APC Is a Major Determinant of Immunodominance during Memory Inflation in Murine Cytomegalovirus Infection. *The Journal of Immunology* 190 (7), 3410–3416. 10.4049/jimmunol.1203151.

References

- Feuchtinger, T., Opherk, K., Bethge, W.A., Topp, M.S., Schuster, F.R., Weissinger, E.M., Mohty, M., Or, R., Maschan, M., Schumm, M., Hamprecht, K., Handgretinger, R., Lang, P., Einsele, H., 2010. Adoptive transfer of pp65-specific T cells for the treatment of chemorefractory cytomegalovirus disease or reactivation after haploidentical and matched unrelated stem cell transplantation. *Blood* 116 (20), 4360–4367. 10.1182/blood-2010-01-262089.
- Gamadia, L.E., Remmerswaal, Ester B M, Weel, J.F., Bemelman, F., van Lier, Rene A W, ten Berge, Ineke J M, 2003. Primary immune responses to human CMV: a critical role for IFN-gamma-producing CD4+ T cells in protection against CMV disease. *Blood* 101 (7), 2686–2692. 10.1182/blood-2002-08-2502.
- Gao, G.F., Tormo, J., Gerth, U.C., Wyer, J.R., McMichael, A.J., Stuart, D.I., Bell, J.I., Jones, E.Y., Jakobsen, B.K., 1997. Crystal structure of the complex between human CD8alpha(alpha) and HLA-A2. *Nature* 387 (6633), 630–634. 10.1038/42523.
- Garboczi, D.N., Ghosh, P., Utz, U., Fan, Q.R., Biddison, W.E., Wiley, D.C., 1996. Structure of the complex between human T-cell receptor, viral peptide and HLA-A2. *Nature* 384 (6605), 134–141. 10.1038/384134a0.
- Garcia, K.C., Scott, C.A., Brunmark, A., Carbone, F.R., Peterson, P.A., Wilson, I.A., Teyton, L., 1996. CD8 enhances formation of stable T-cell receptor/MHC class I molecule complexes. *Nature* 384 (6609), 577–581. 10.1038/384577a0.
- Garcia, K.C., Tallquist, M.D., Pease, L.R., Brunmark, A., Scott, C.A., Degano, M., Stura, E.A., Peterson, P.A., Wilson, I.A., Teyton, L., 1997. Alphabeta T cell receptor interactions with syngeneic and allogeneic ligands: affinity measurements and crystallization. *Proceedings of the National Academy of Sciences of the United States of America* 94 (25), 13838–13843.
- Gerlach, C., Rohr, J.C., Perie, L., van Rooij, N., van Heijst, J. W. J., Velds, A., Urbanus, J., Naik, S.H., Jacobs, H., Beltman, J.B., de Boer, R. J., Schumacher, T. N. M., 2013. Heterogeneous Differentiation Patterns of Individual CD8+ T Cells. *Science* 340 (6132), 635–639. 10.1126/science.1235487.
- Goronzy, J.J., Fulbright, J.W., Crowson, C.S., Poland, G.A., O'Fallon, W.M., Weyand, C.M., 2001. Value of immunological markers in predicting responsiveness to influenza vaccination in elderly individuals. *Journal of Virology* 75 (24), 12182–12187. 10.1128/JVI.75.24.12182-12187.2001.
- Govern, C.C., Paczosa, M.K., Chakraborty, A.K., Huseby, E.S., 2010. Fast on-rates allow short dwell time ligands to activate T cells. *Proceedings of the National Academy of Sciences* 107 (19), 8724–8729. 10.1073/pnas.1000966107.
- Graef, P., Buchholz, V.R., Stemberger, C., Flossdorf, M., Henkel, L., Schiemann, M., Drexler, I., Hofer, T., Riddell, S.R., Busch, D.H., 2014. Serial transfer of single-cell-derived immunocompetence reveals stemness of CD8(+) central memory T cells. *Immunity* 41 (1), 116–126. 10.1016/j.immuni.2014.05.018.
- Gras, S., Saulquin, X., Reiser, J.-B., Debeaupuis, E., Echasserieau, K., Kissenpfennig, A., Legoux, F., Chouquet, A., Le Gorrec, M., Machillot, P., Neveu, B., Thielen, N., Malissen, B., Bonneville, M., Housset, D., 2009. Structural Bases for the Affinity-Driven Selection of a Public TCR against a Dominant Human Cytomegalovirus Epitope. *The Journal of Immunology* 183 (1), 430–437. 10.4049/jimmunol.0900556.
- Griffiths, S.J., Riddell, N.E., Masters, J., Libri, V., Henson, S.M., Wertheimer, A., Wallace, D., Sims, S., Rivino, L., Larbi, A., Kemeny, D.M., Nikolich-Zugich, J., Kern, F., Klenerman, P., Emery, V.C., Akbar, A.N., 2013. Age-Associated Increase of Low-Avidity Cytomegalovirus-Specific CD8+ T Cells That Re-Express CD45RA. *The Journal of Immunology* 190 (11), 5363–5372. 10.4049/jimmunol.1203267.
- Hadrup, S.R., Strindhall, J., Kollgaard, T., Seremet, T., Johansson, B., Pawelec, G., thors Straten, P., Wikby, A., 2006. Longitudinal studies of clonally expanded CD8 T cells

References

- reveal a repertoire shrinkage predicting mortality and an increased number of dysfunctional cytomegalovirus-specific T cells in the very elderly. *Journal of immunology* (Baltimore, Md. : 1950) 176 (4), 2645–2653.
- Harari, A., Cellerai, C., Bellutti Enders, F., Kostler, J., Codarri, L., Tapia, G., Boyman, O., Castro, E., Gaudieri, S., James, I., John, M., Wagner, R., Mallal, S., Pantaleo, G., 2007. Skewed association of polyfunctional antigen-specific CD8 T cell populations with HLA-B genotype. *Proceedings of the National Academy of Sciences of the United States of America* 104 (41), 16233–16238. 10.1073/pnas.0707570104.
- Harari, A., Zimmerli, S.C., Pantaleo, G., 2004. Cytomegalovirus (CMV)-Specific cellular immune responses. *Human Immunology* 65 (5), 500–506. 10.1016/j.humimm.2004.02.012.
- Hebeisen, M., Baitsch, L., Presotto, D., Baumgaertner, P., Romero, P., Michielin, O., Speiser, D.E., Rufer, N., 2013a. SHP-1 phosphatase activity counteracts increased T cell receptor affinity. *The Journal of clinical investigation* 123 (3), 1044–1056. 10.1172/JCI65325.
- Hebeisen, M., Oberle, S.G., Presotto, D., Speiser, D.E., Zehn, D., Rufer, N., 2013b. Molecular Insights for Optimizing T Cell Receptor Specificity Against Cancer. *Frontiers in Immunology* 4. 10.3389/fimmu.2013.00154.
- Hennecke, J., Carfi, A., Wiley, D.C., 2000. Structure of a covalently stabilized complex of a human alphabeta T-cell receptor, influenza HA peptide and MHC class II molecule, HLA-DR1. *The EMBO journal* 19 (21), 5611–5624. 10.1093/emboj/19.21.5611.
- Hertoghs, Kirsten M L, Moerland, P.D., van Stijn, A., Remmerswaal, Ester B M, Yong, S.L., van de Berg, Pablo J E J, van Ham, S Marieke, Baas, F., ten Berge, Ineke J M, van Lier, Rene A W, 2010. Molecular profiling of cytomegalovirus-induced human CD8+ T cell differentiation. *The Journal of clinical investigation* 120 (11), 4077–4090. 10.1172/JCI42758.
- Holtappels, R., Böhm, V., Podlech, J., Reddehase, M.J., 2008. CD8 T-cell-based immunotherapy of cytomegalovirus infection: "proof of concept" provided by the murine model. *Medical microbiology and immunology* 197 (2), 125–134. 10.1007/s00430-008-0093-2.
- Hombrink, P., Hadrup, S.R., Bakker, A., Kester, Michel G. D., Falkenburg, J. H. Frederik, von dem Borne, Peter A., Schumacher, Ton N. M., Heemskerk, Mirjam H. M., Kanellopoulos, J., 2011. High-Throughput Identification of Potential Minor Histocompatibility Antigens by MHC Tetramer-Based Screening: Feasibility and Limitations. *PLoS ONE* 6 (8), e22523. 10.1371/journal.pone.0022523.
- Hombrink, P., Raz, Y., Kester, Michel G D, Boer, R. de, Weißbrich, B., von dem Borne, Peter A, Busch, D.H., Schumacher, Ton N M, Falkenburg, J H Frederik, Heemskerk, Mirjam H M, 2013. Mixed functional characteristics correlating with TCR-ligand koff -rate of MHC-tetramer reactive T cells within the naive T-cell repertoire. *European Journal of Immunology* 43 (11), 3038–3050. 10.1002/eji.201343397.
- Huang, J., Zarnitsyna, V.I., Liu, B., Edwards, L.J., Jiang, N., Evavold, B.D., Zhu, C., 2010. The kinetics of two-dimensional TCR and pMHC interactions determine T-cell responsiveness. *Nature* 464 (7290), 932–936. 10.1038/nature08944.
- Huppa, J.B., Axmann, M., Mörtelmaier, M.A., Lillemeier, B.F., Newell, E.W., Brameshuber, M., Klein, L.O., Schütz, G.J., Davis, M.M., 2010. TCR–peptide–MHC interactions in situ show accelerated kinetics and increased affinity. *Nature* 463 (7283), 963–967. 10.1038/nature08746.
- Hurwitz, A.A., Cuss, S.M., Stagliano, K.E., Zhu, Z., 2014. T cell avidity and tumor immunity: problems and solutions. *Cancer microenvironment : official journal of the International Cancer Microenvironment Society* 7 (1-2), 1–9. 10.1007/s12307-013-0143-1.
- Huseby, E.S., Crawford, F., White, J., Marrack, P., Kappler, J.W., 2006. Interface-disrupting amino acids establish specificity between T cell receptors and complexes of major

References

- histocompatibility complex and peptide. *Nature Immunology* 7 (11), 1191–1199. 10.1038/ni1401.
- Iancu, E.M., Corthesy, P., Baumgaertner, P., Devevre, E., Voelter, V., Romero, P., Speiser, D.E., Rufer, N., 2009. Clonotype Selection and Composition of Human CD8 T Cells Specific for Persistent Herpes Viruses Varies with Differentiation but Is Stable Over Time. *The Journal of Immunology* 183 (1), 319–331. 10.4049/jimmunol.0803647.
- Jameson, S.C., Hogquist, K.A., Bevan, M.J., 1995. Positive selection of thymocytes. *Annual review of immunology* 13, 93–126. 10.1146/annurev.iy.13.040195.000521.
- Janicki, C.N., Jenkinson, S.R., Williams, N.A., Morgan, D.J., 2008. Loss of CTL function among high-avidity tumor-specific CD8+ T cells following tumor infiltration. *Cancer research* 68 (8), 2993–3000. 10.1158/0008-5472.CAN-07-5008.
- Jiang, N., Huang, J., Edwards, L.J., Liu, B., Zhang, Y., Beal, C.D., Evavold, B.D., Zhu, C., 2011. Two-Stage Cooperative T Cell Receptor-Peptide Major Histocompatibility Complex-CD8 Trimolecular Interactions Amplify Antigen Discrimination. *Immunity* 34 (1), 13–23. 10.1016/j.immuni.2010.12.017.
- Jorgensen, J.L., Esser, U., Fazekas de St Groth, B, Reay, P.A., Davis, M.M., 1992a. Mapping T-cell receptor-peptide contacts by variant peptide immunization of single-chain transgenics. *Nature* 355 (6357), 224–230. 10.1038/355224a0.
- Jorgensen, J.L., Reay, P.A., Ehrlich, E.W., Davis, M.M., 1992b. Molecular components of T-cell recognition. *Annual review of immunology* 10, 835–873. 10.1146/annurev.iy.10.040192.004155.
- Karrer, U., Sierro, S., Wagner, M., Oxenius, A., Hengel, H., Koszinowski, U.H., Phillips, R.E., Klenerman, P., 2003. Memory inflation: continuous accumulation of antiviral CD8+ T cells over time. *Journal of immunology (Baltimore, Md. : 1950)* 170 (4), 2022–2029.
- Kern, P.S., Teng, M.K., Smolyar, A., Liu, J.H., Liu, J., Hussey, R.E., Spoerl, R., Chang, H.C., Reinherz, E.L., Wang, J.H., 1998. Structural basis of CD8 coreceptor function revealed by crystallographic analysis of a murine CD8 α ectodomain fragment in complex with H-2Kb. *Immunity* 9 (4), 519–530.
- Khan, N., 2002. CMV drives the CD8 repertoire towards greater clonality in healthy elderly. *Journal of Immunology*.
- Khan, N., Best, D., Bruton, R., Nayak, L., Rickinson, A.B., Moss, Paul A H, 2007. T cell recognition patterns of immunodominant cytomegalovirus antigens in primary and persistent infection. *Journal of immunology (Baltimore, Md. : 1950)* 178 (7), 4455–4465.
- Khan, N., Cobbold, M., Cummerson, J., Moss, Paul A. H., 2010. Persistent viral infection in humans can drive high frequency low-affinity T-cell expansions. *Immunology* 131 (4), 537–548. 10.1111/j.1365-2567.2010.03326.x.
- Khan, N., Cobbold, M., Keenan, R., Moss, Paul A H, 2002a. Comparative analysis of CD8+ T cell responses against human cytomegalovirus proteins pp65 and immediate early 1 shows similarities in precursor frequency, oligoclonality, and phenotype. *The Journal of infectious diseases* 185 (8), 1025–1034. 10.1086/339963.
- Khan, N., Hislop, A., Gudgeon, N., Cobbold, M., Khanna, R., Nayak, L., Rickinson, A.B., Moss, P. A. H., 2004. Herpesvirus-Specific CD8 T Cell Immunity in Old Age: Cytomegalovirus Impairs the Response to a Coresident EBV Infection. *The Journal of Immunology* 173 (12), 7481–7489. 10.4049/jimmunol.173.12.7481.
- Khan, N., Shariff, N., Cobbold, M., Bruton, R., Ainsworth, J.A., Sinclair, A.J., Nayak, L., Moss, Paul A H, 2002b. Cytomegalovirus seropositivity drives the CD8 T cell repertoire toward greater clonality in healthy elderly individuals. *Journal of immunology (Baltimore, Md. : 1950)* 169 (4), 1984–1992.
- Klarenbeek, P.L., Remmerswaal, E B M, ten Berge, I J M, Doorenspleet, M.E., van Schaik, B D C, Esveldt, R E E, Koch, S.D., Brinke, A. ten, van Kampen, A H C, Bemelman, F.J., Tak, P.P., Baas, F., Vries, N. de, van Lier, R A W, 2012. Deep sequencing of antiviral T-

References

- cell responses to HCMV and EBV in humans reveals a stable repertoire that is maintained for many years. *PLoS Pathogens* 8 (9), e1002889. 10.1371/journal.ppat.1002889.
- Knabel, M., Franz, T.J., Schiemann, M., Wulf, A., Villmow, B., Schmidt, B., Bernhard, H., Wagner, H., Busch, D.H., 2002. Reversible MHC multimer staining for functional isolation of T-cell populations and effective adoptive transfer. *Nature medicine* 8 (6), 631–637. 10.1038/nm0602-631.
- Knall, R.A., 2007. Direct ex vivo identification of individual antigen-specific T cells with optimal avidity for protection.
- Koch, S., Larbi, A., Ozcelik, D., Solana, R., Gouttefangeas, C., Attig, S., Wikby, A., Strindhall, J., Franceschi, C., Pawelec, G., 2007. Cytomegalovirus infection: a driving force in human T cell immunosenescence. *Annals of the New York Academy of Sciences* 1114, 23–35. 10.1196/annals.1396.043.
- Koch, S., Solana, R., Dela Rosa, O., Pawelec, G., 2006. Human cytomegalovirus infection and T cell immunosenescence: a mini review. *Mechanisms of ageing and development* 127 (6), 538–543. 10.1016/j.mad.2006.01.011.
- Krogsgaard, M., Davis, M.M., 2005. How T cells 'see' antigen. *Nature Immunology* 6 (3), 239–245. 10.1038/ni1173.
- La Rosa, C., Diamond, D.J., 2012. The immune response to human CMV. *Future virology* 7 (3), 279–293. 10.2217/fvl.12.8.
- Lachmann, R., Bajwa, M., Vita, S., Smith, H., Cheek, E., Akbar, A., Kern, F., 2011. Polyfunctional T Cells Accumulate in Large Human Cytomegalovirus-Specific T Cell Responses. *Journal of Virology* 86 (2), 1001–1009. 10.1128/JVI.00873-11.
- Ladell, K., Hashimoto, M., Iglesias, M.C., Wilmann, P.G., McLaren, J.E., Gras, S., Chikata, T., Kuse, N., Fastenackels, S., Gostick, E., Bridgeman, J.S., Venturi, V., Arkoub, Z.A., Agut, H., van Bockel, David J, Almeida, J.R., Douek, D.C., Meyer, L., Venet, A., Takiguchi, M., Rossjohn, J., Price, D.A., Appay, V., 2013. A molecular basis for the control of preimmune escape variants by HIV-specific CD8+ T cells. *Immunity* 38 (3), 425–436. 10.1016/j.immuni.2012.11.021.
- Landais, I., Nelson, J.A., 2013. Functional genomics approaches to understand cytomegalovirus replication, latency and pathogenesis. *Current opinion in virology* 3 (4), 408–415. 10.1016/j.coviro.2013.06.002.
- Landolfo, S., Gariglio, M., Gribaudo, G., Lembo, D., 2003. The human cytomegalovirus. *Pharmacology & therapeutics* 98 (3), 269–297.
- Lanzavecchia, A., 2002. Lack of fair play in the T cell response. *Nature immunology* 3 (1), 9–10. 10.1038/ni0102-9.
- Lawson, T.M., Man, S., Wang, E.C., Williams, S., Amos, N., Gillespie, G.M., Moss, P.A., Borysiewicz, L.K., 2001. Functional differences between influenza A-specific cytotoxic T lymphocyte clones expressing dominant and subdominant TCR. *International immunology* 13 (11), 1383–1390.
- Lelic, A., Verschoor, C.P., Ventresca, M., Parsons, R., Eveleigh, C., Bowdish, D., Betts, M.R., Loeb, M.B., Bramson, J.L., 2012. The polyfunctionality of human memory CD8+ T cells elicited by acute and chronic virus infections is not influenced by age. *PLoS pathogens* 8 (12), e1003076. 10.1371/journal.ppat.1003076.
- Lemmermann, N., Gergely, K., Bohm, V., Deegen, P., Daubner, T., Reddehase, M.J., 2010. Immune evasion proteins of murine cytomegalovirus preferentially affect cell surface display of recently generated peptide presentation complexes. *Journal of virology* 84 (3), 1221–1236. 10.1128/JVI.02087-09.
- Lever, M., Maini, P.K., van der Merwe, P Anton, Dushek, O., 2014. Phenotypic models of T cell activation. *Nature reviews. Immunology* 14 (9), 619–629. 10.1038/nri3728.

References

- Lieber, M.R., 1991. Site-specific recombination in the immune system. *FASEB journal : official publication of the Federation of American Societies for Experimental Biology* 5 (14), 2934–2944.
- Linette, G.P., Stadtmauer, E.A., Maus, M.V., Rapoport, A.P., Levine, B.L., Emery, L., Litzky, L., Bagg, A., Carreno, B.M., Cimino, P.J., Binder-Scholl, G.K., Smethurst, D.P., Gerry, A.B., Pumphrey, N.J., Bennett, A.D., Brewer, J.E., Dukes, J., Harper, J., Tayton-Martin, H.K., Jakobsen, B.K., Hassan, N.J., Kalos, M., June, C.H., 2013. Cardiovascular toxicity and titin cross-reactivity of affinity-enhanced T cells in myeloma and melanoma. *Blood* 122 (6), 863–871. 10.1182/blood-2013-03-490565.
- Liu, B., Chen, W., Evavold, B.D., Zhu, C., 2014a. Accumulation of dynamic catch bonds between TCR and agonist peptide-MHC triggers T cell signaling. *Cell* 157 (2), 357–368. 10.1016/j.cell.2014.02.053.
- Liu, B., Zhong, S., Malecek, K., Johnson, L.A., Rosenberg, S.A., Zhu, C., Krogsgaard, M., 2014b. 2D TCR-pMHC-CD8 kinetics determines T-cell responses in a self-antigen-specific TCR system. *European journal of immunology* 44 (1), 239–250. 10.1002/eji.201343774.
- Luescher, I.F., Vivier, E., Layer, A., Mahiou, J., Godeau, F., Malissen, B., Romero, P., 1995. CD8 modulation of T-cell antigen receptor-ligand interactions on living cytotoxic T lymphocytes. *Nature* 373 (6512), 353–356. 10.1038/373353a0.
- Lydie Trautmann, 2005. Selection of T Cell Clones Expressing High-Affinity Public TCRs within Human Cytomegalovirus-Specific CD8 T Cell Responses. *The Journal of Immunology*.
- Macaulay, R., Riddell, N.E., Griffiths, S.J., Akbar, A.N., Henson, S.M., 2013. Differing HLA types influence inhibitory receptor signalling in CMV-specific CD8+ T cells. *Human immunology* 74 (3), 302–309. 10.1016/j.humimm.2012.11.014.
- Macdonald, W.A., Chen, Z., Gras, S., Archbold, J.K., Tynan, F.E., Clements, C.S., Bharadwaj, M., Kjer-Nielsen, L., Saunders, P.M., Wilce, Matthew C J, Crawford, F., Stadinsky, B., Jackson, D., Brooks, A.G., Purcell, A.W., Kappler, J.W., Burrows, S.R., Rossjohn, J., McCluskey, J., 2009. T cell allorecognition via molecular mimicry. *Immunity* 31 (6), 897–908. 10.1016/j.immuni.2009.09.025.
- Maeda, Y., Nishikawa, H., Sugiyama, D., Ha, D., Hamaguchi, M., Saito, T., Nishioka, M., Wing, J.B., Adeegbe, D., Katayama, I., Sakaguchi, S., 2014. Detection of self-reactive CD8(+) T cells with an anergic phenotype in healthy individuals. *Science (New York, N.Y.)* 346 (6216), 1536–1540. 10.1126/science.aaa1292.
- Malherbe, L., Hausl, C., Teyton, L., McHeyzer-Williams, M.G., 2004. Clonal selection of helper T cells is determined by an affinity threshold with no further skewing of TCR binding properties. *Immunity* 21 (5), 669–679. 10.1016/j.immuni.2004.09.008.
- Manning, T.C., Kranz, D.M., 1999. Binding energetics of T-cell receptors: correlation with immunological consequences. *Immunology today* 20 (9), 417–422.
- McKeithan, T.W., 1995. Kinetic proofreading in T-cell receptor signal transduction. *Proceedings of the National Academy of Sciences of the United States of America* 92 (11), 5042–5046.
- Messaoudi, I., Lemaoult, J., Guevara-Patino, J.A., Metzner, B.M., Nikolich-Zugich, J., 2004. Age-related CD8 T cell clonal expansions constrict CD8 T cell repertoire and have the potential to impair immune defense. *The Journal of experimental medicine* 200 (10), 1347–1358. 10.1084/jem.20040437.
- Moon, J.J., Chu, H.H., Pepper, M., McSorley, S.J., Jameson, S.C., Kedl, R.M., Jenkins, M.K., 2007. Naive CD4(+) T cell frequency varies for different epitopes and predicts repertoire diversity and response magnitude. *Immunity* 27 (2), 203–213. 10.1016/j.immuni.2007.07.007.

References

- Moore, T.V., Lyons, G.E., Brasic, N., Roszkowski, J.J., Voelkl, S., Mackensen, A., Kast, W.M., Le Poole, I. Caroline, Nishimura, M.I., 2009. Relationship between CD8-dependent antigen recognition, T cell functional avidity, and tumor cell recognition. *Cancer Immunology, Immunotherapy* 58 (5), 719–728. 10.1007/s00262-008-0594-2.
- Morgan, R.A., Chinnsamy, N., Abate-Daga, D., Gros, A., Robbins, P.F., Zheng, Z., Dudley, M.E., Feldman, S.A., Yang, J.C., Sherry, R.M., Phan, G.Q., Hughes, M.S., Kammula, U.S., Miller, A.D., Hessman, C.J., Stewart, A.A., Restifo, N.P., Quezado, M.M., Alimchandani, M., Rosenberg, A.Z., Nath, A., Wang, T., Bielekova, B., Wuest, S.C., Akula, N., McMahon, F.J., Wilde, S., Mosetter, B., Schendel, D.J., Laurencot, C.M., Rosenberg, S.A., 2013. Cancer regression and neurological toxicity following anti-MAGE-A3 TCR gene therapy. *Journal of immunotherapy (Hagerstown, Md. : 1997)* 36 (2), 133–151. 10.1097/CJI.0b013e3182829903.
- Morgan, R.A., Dudley, M.E., Yu, Yik Y L, Zheng, Z., Robbins, P.F., Theoret, M.R., Wunderlich, J.R., Hughes, M.S., Restifo, N.P., Rosenberg, S.A., 2003. High efficiency TCR gene transfer into primary human lymphocytes affords avid recognition of melanoma tumor antigen glycoprotein 100 and does not alter the recognition of autologous melanoma antigens. *Journal of immunology (Baltimore, Md. : 1950)* 171 (6), 3287–3295.
- Munks, M.W., Cho, K.S., Pinto, A.K., Sierro, S., Klenerman, P., Hill, A.B., 2006a. Four distinct patterns of memory CD8 T cell responses to chronic murine cytomegalovirus infection. *Journal of immunology (Baltimore, Md. : 1950)* 177 (1), 450–458.
- Munks, M.W., Gold, M.C., Zajac, A.L., Doom, C.M., Morello, C.S., Spector, D.H., Hill, A.B., 2006b. Genome-wide analysis reveals a highly diverse CD8 T cell response to murine cytomegalovirus. *Journal of immunology (Baltimore, Md. : 1950)* 176 (6), 3760–3766.
- Nauerth, M., 2012. Development of a novel TCR avidity assay for human CD8 T cells.
- Nauerth, M., Weissbrich, B., Busch, D.H., 2013a. The clinical potential for koff-rate measurement in adoptive immunotherapy. *Expert review of clinical immunology* 9 (12), 1151–1153. 10.1586/1744666X.2013.855609.
- Nauerth, M., Weißbrich, B., Knall, R., Franz, T., Dössinger, G., Bet, J., Paszkiewicz, P.J., Pfeifer, L., Bunse, M., Uckert, W., Holtappels, R., Gillert-Marien, D., Neuenhahn, M., Krackhardt, A., Reddehase, M.J., Riddell, S.R., Busch, D.H., 2013b. TCR-ligand koff rate correlates with the protective capacity of antigen-specific CD8+ T cells for adoptive transfer. *Science translational medicine* 5 (192), 192ra87. 10.1126/scitranslmed.3005958.
- Nelson, R.W., Beisang, D., Tubo, N.J., Dileepan, T., Wiesner, D.L., Nielsen, K., Wuthrich, M., Klein, B.S., Kotov, D.I., Spanier, J.A., Fife, B.T., Moon, J.J., Jenkins, M.K., 2015. T cell receptor cross-reactivity between similar foreign and self peptides influences naive cell population size and autoimmunity. *Immunity* 42 (1), 95–107. 10.1016/j.immuni.2014.12.022.
- Nikolich-Zugich, J., Slifka, M.K., Messaoudi, I., 2004. The many important facets of T-cell repertoire diversity. *Nature reviews. Immunology* 4 (2), 123–132. 10.1038/nri1292.
- Obar, J.J., Khanna, K.M., Lefrançois, L., 2008. Endogenous naive CD8+ T cell precursor frequency regulates primary and memory responses to infection. *Immunity* 28 (6), 859–869. 10.1016/j.immuni.2008.04.010.
- Odendahl, M., Grigoleit, G.U., Bönig, H., Neuenhahn, M., Albrecht, J., Anderl, F., Germeroth, L., Schmitz, M., Bornhäuser, M., Einsele, H., Seifried, E., Busch, D.H., Tonn, T., 2014. Clinical-scale isolation of 'minimally manipulated' cytomegalovirus-specific donor lymphocytes for the treatment of refractory cytomegalovirus disease. *Cytotherapy* 16 (9), 1245–1256. 10.1016/j.jcyt.2014.05.023.
- O'Donoghue, G.P., Pielak, R.M., Smoligovets, A.A., Lin, J.J., Groves, J.T., 2013. Direct single molecule measurement of TCR triggering by agonist pMHC in living primary T cells. *eLife* 2 (0), e00778. 10.7554/eLife.00778.

References

- Olsson, J., Wikby, A., Johansson, B., Löfgren, S., Nilsson, B.O., Ferguson, F.G., 2000. Age-related change in peripheral blood T-lymphocyte subpopulations and cytomegalovirus infection in the very old: the Swedish longitudinal OCTO immune study. *Mechanisms of ageing and development* 121 (1-3), 187–201.
- Ouyang, Q., Wagner, W.M., Wikby, A., Walter, S., Aubert, G., Dodi, A.I., Travers, P., Pawelec, G., 2003. Large numbers of dysfunctional CD8+ T lymphocytes bearing receptors for a single dominant CMV epitope in the very old. *Journal of Clinical Immunology* 23 (4), 247–257.
- Ouyang, Q., Wagner, W.M., Zheng, W., Wikby, A., Remarque, E.J., Pawelec, G., 2004. Dysfunctional CMV-specific CD8(+) T cells accumulate in the elderly. *Experimental gerontology* 39 (4), 607–613. 10.1016/j.exger.2003.11.016.
- Pauken, K.E., Wherry, E.J., 2015. Overcoming T cell exhaustion in infection and cancer. *Trends in immunology*. 10.1016/j.it.2015.02.008.
- Peggs, K., Verfuether, S., Pizzey, A., Ainsworth, J., Moss, P., Mackinnon, S., 2002. Characterization of human cytomegalovirus peptide-specific CD8(+) T-cell repertoire diversity following in vitro restimulation by antigen-pulsed dendritic cells. *Blood* 99 (1), 213–223.
- Peter A. Savage, Jay Boniface, Mark M. Davis, 1999. A Kinetic Basis For T Cell Receptor Repertoire Selection during an Immune Response. *Immunity* 10, 485–492.
- Price, D.A., 2005. Avidity for antigen shapes clonal dominance in CD8+ T cell populations specific for persistent DNA viruses. *Journal of Experimental Medicine* 202 (10), 1349–1361. 10.1084/jem.20051357.
- Price, D.A., Brenchley, J.M., Ruff, L.E., Betts, M.R., Hill, B.J., Roederer, M., Koup, R.A., Migueles, S.A., Gostick, E., Wooldridge, L., Sewell, A.K., Connors, M., Douek, D.C., 2005. Avidity for antigen shapes clonal dominance in CD8+ T cell populations specific for persistent DNA viruses. *The Journal of experimental medicine* 202 (10), 1349–1361. 10.1084/jem.20051357.
- Pryshchep, S., Zarnitsyna, V.I., Hong, J., Evavold, B.D., Zhu, C., 2014. Accumulation of serial forces on TCR and CD8 frequently applied by agonist antigenic peptides embedded in MHC molecules triggers calcium in T cells. *Journal of immunology (Baltimore, Md. : 1950)* 193 (1), 68–76. 10.4049/jimmunol.1303436.
- Puech, P.-H., Nevoltris, D., Robert, P., Limozin, L., Boyer, C., Bongrand, P., Muller, D.J., 2011. Force Measurements of TCR/pMHC Recognition at T Cell Surface. *PLoS ONE* 6 (7), e22344. 10.1371/journal.pone.0022344.
- Purbhoo, M.A., Boulter, J.M., Price, D.A., Vuidepot, A.-L., Hourigan, C.S., Dunbar, P.R., Olson, K., Dawson, S.J., Phillips, R.E., Jakobsen, B.K., Bell, J.I., Sewell, A.K., 2001. The Human CD8 Coreceptor Effects Cytotoxic T Cell Activation and Antigen Sensitivity Primarily by Mediating Complete Phosphorylation of the T Cell Receptor Chain. *Journal of Biological Chemistry* 276 (35), 32786–32792. 10.1074/jbc.M102498200.
- Ratzke, C., Nguyen, M.N., Mayer, M.P., Hugel, T., 2012. From a Ratchet Mechanism to Random Fluctuations Evolution of Hsp90's Mechanochemical Cycle. *Journal of Molecular Biology* 423 (3), 462–471. 10.1016/j.jmb.2012.07.026.
- Reinherz, E.L., Tan, K., Tang, L., Kern, P., Liu, J., Xiong, Y., Hussey, R.E., Smolyar, A., Hare, B., Zhang, R., Joachimiak, A., Chang, H.C., Wagner, G., Wang, J., 1999. The crystal structure of a T cell receptor in complex with peptide and MHC class II. *Science (New York, N.Y.)* 286 (5446), 1913–1921.
- Reiser, J.B., Legoux, F., Machillot, P., Debeauvais, E., Le Moullac-Vaydie, B., Chouquet, A., Saulquin, X., Bonneville, M., Housset, D., 2009. Crystallization and preliminary X-ray crystallographic characterization of a public CMV-specific TCR in complex with its cognate antigen. *Acta crystallographica. Section F, Structural biology and crystallization communications* 65 (Pt 11), 1157–1161. 10.1107/S1744309109037890.

References

- Remmerswaal, Ester B M, Havenith, Simone H C, Idu, M.M., van Leeuwen, Ester M M, van Donselaar, Karlijn A M I, Brinke, A. ten, van der Bom-Baylon, Nelly, Bemelman, F.J., van Lier, Rene A W, ten Berge, Ineke J M, 2012. Human virus-specific effector-type T cells accumulate in blood but not in lymph nodes. *Blood* 119 (7), 1702–1712. 10.1182/blood-2011-09-381574.
- Restifo, N.P., Dudley, M.E., Rosenberg, S.A., 2012. Adoptive immunotherapy for cancer: harnessing the T cell response. *Nature reviews. Immunology* 12 (4), 269–281. 10.1038/nri3191.
- Riddell, S.R., Greenberg, P.D., 1995. Principles for adoptive T cell therapy of human viral diseases. *Annual Review of Immunology* 13, 545–586. 10.1146/annurev.iy.13.040195.002553.
- Robbins, P.F., Morgan, R.A., Feldman, S.A., Yang, J.C., Sherry, R.M., Dudley, M.E., Wunderlich, J.R., Nahvi, A.V., Helman, L.J., Mackall, C.L., Kammula, U.S., Hughes, M.S., Restifo, N.P., Raffeld, M., Lee, C.-C.R., Levy, C.L., Li, Y.F., El-Gamil, M., Schwarz, S.L., Laurencot, C., Rosenberg, S.A., 2011. Tumor Regression in Patients With Metastatic Synovial Cell Sarcoma and Melanoma Using Genetically Engineered Lymphocytes Reactive With NY-ESO-1. *Journal of Clinical Oncology* 29 (7), 917–924. 10.1200/JCO.2010.32.2537.
- Rodenko, B., Toebes, M., Hadrup, S.R., van Esch, Wim J E, Molenaar, A.M., Schumacher, Ton N M, Ovaa, H., 2006. Generation of peptide–MHC class I complexes through UV-mediated ligand exchange. *Nature Protocols* 1 (3), 1120–1132. 10.1038/nprot.2006.121.
- Rudd, B.D., Venturi, V., Li, G., Samadder, P., Ertelt, J.M., Way, S.S., Davenport, M.P., Nikolich-Zugich, J., 2011. Nonrandom attrition of the naive CD8⁺ T-cell pool with aging governed by T-cell receptor:pMHC interactions. *Proceedings of the National Academy of Sciences of the United States of America* 108 (33), 13694–13699. 10.1073/pnas.1107594108.
- Rudolph, M.G., Stanfield, R.L., Wilson, I.A., 2006. How TCRs bind MHCs, peptides, and coreceptors. *Annual review of immunology* 24, 419–466. 10.1146/annurev.immunol.23.021704.115658.
- Ruppert, J., Sidney, J., Celis, E., Kubo, R.T., Grey, H.M., Sette, A., 1993. Prominent role of secondary anchor residues in peptide binding to HLA-A2.1 molecules. *Cell* 74 (5), 929–937.
- Sacre, K., Nguyen, S., Deback, C., Carcelain, G., Vernant, J.-P., Leblond, V., Autran, B., Dhedin, N., 2008. Expansion of human cytomegalovirus (HCMV) immediate-early 1-specific CD8⁺ T cells and control of HCMV replication after allogeneic stem cell transplantation. *Journal of virology* 82 (20), 10143–10152. 10.1128/JVI.00688-08.
- Sansoni, P., Vescovini, R., Fagnoni, F.F., Akbar, A., Arens, R., Chiu, Y.-L., Cičín-Šain, L., Dechanet-Merville, J., Derhovanessian, E., Ferrando-Martinez, S., Franceschi, C., Frasca, D., Fulöp, T., Furman, D., Gkrania-Klotsas, E., Goodrum, F., Grubeck-Loebenstein, B., Hurme, M., Kern, F., Lilleri, D., López-Botet, M., Maier, A.B., Marandu, T., Marchant, A., Matheï, C., Moss, P., Muntasell, A., Remmerswaal, Ester B M, Riddell, N.E., Rothe, K., Sauce, D., Shin, E.-C., Simanek, A.M., Smithey, M.J., Söderberg-Nauclér, C., Solana, R., Thomas, P.G., van Lier, R., Pawelec, G., Nikolich-Zugich, J., 2014. New advances in CMV and immunosenescence. *Experimental Gerontology* 55, 54–62. 10.1016/j.exger.2014.03.020.
- Sauce, D., Larsen, M., Fastenackels, S., Duperrier, A., Keller, M., Grubeck-Loebenstein, B., Ferrand, C., Debré, P., Sidi, D., Appay, V., 2009. Evidence of premature immune aging in patients thymectomized during early childhood. *The Journal of clinical investigation* 119 (10), 3070–3078. 10.1172/JCI39269.
- Sauce, D., Larsen, M., Fastenackels, S., Roux, A., Gorochov, G., Katlama, C., Sidi, D., Sibony-Prat, J., Appay, V., 2012. Lymphopenia-driven homeostatic regulation of naive T

References

- cells in elderly and thymectomized young adults. *Journal of immunology* (Baltimore, Md. : 1950) 189 (12), 5541–5548. 10.4049/jimmunol.1201235.
- Saurwein-Teissl, M., Lung, T.L., Marx, F., Gschosser, C., Asch, E., Blasko, I., Parson, W., Bock, G., Schonitzer, D., Trannoy, E., Grubeck-Loebenstien, B., 2002. Lack of antibody production following immunization in old age: association with CD8(+)CD28(-) T cell clonal expansions and an imbalance in the production of Th1 and Th2 cytokines. *Journal of immunology* (Baltimore, Md. : 1950) 168 (11), 5893–5899.
- Schmitt, A., Tonn, T., Busch, D.H., Grigoleit, G.U., Einsele, H., Odendahl, M., Germeroth, L., Ringhoffer, M., Ringhoffer, S., Wiesneth, M., Greiner, J., Michel, D., Mertens, T., Rojewski, M., Marx, M., Harsdorf, S. von, Döhner, H., Seifried, E., Bunjes, D., Schmitt, M., 2011. Adoptive transfer and selective reconstitution of streptamer-selected cytomegalovirus-specific CD8+ T cells leads to virus clearance in patients after allogeneic peripheral blood stem cell transplantation. *Transfusion* 51 (3), 591–599. 10.1111/j.1537-2995.2010.02940.x.
- Schwanninger, A., Weinberger, B., Weiskopf, D., Herndler-Brandstetter, D., Reitinger, S., Gassner, C., Schennach, H., Parson, W., Würzner, R., Grubeck-Loebenstien, B., 2008. Age-related appearance of a CMV-specific high-avidity CD8+ T cell clonotype which does not occur in young adults. *Immunity & ageing : I & A* 5, 14. 10.1186/1742-4933-5-14.
- Seckert, C.K., Griessl, M., Büttner, J.K., Scheller, S., Simon, C.O., Kropp, K.A., Renzaho, A., Kühnapfel, B., Grzimek, Natascha K A, Reddehase, M.J., 2012. Viral latency drives 'memory inflation': a unifying hypothesis linking two hallmarks of cytomegalovirus infection. *Medical microbiology and immunology* 201 (4), 551–566. 10.1007/s00430-012-0273-y.
- Sester, U., Presser, D., Dirks, J., Gartner, B.C., Kohler, H., Sester, M., 2008. PD-1 expression and IL-2 loss of cytomegalovirus- specific T cells correlates with viremia and reversible functional anergy. *American journal of transplantation : official journal of the American Society of Transplantation and the American Society of Transplant Surgeons* 8 (7), 1486–1497. 10.1111/j.1600-6143.2008.02279.x.
- Sharma, S.K., Alexander-Miller, M.A., 2011. Increased sensitivity to antigen in high avidity CD8+ T cells results from augmented membrane proximal T-cell receptor signal transduction. *Immunology* 133 (3), 307–317. 10.1111/j.1365-2567.2011.03440.x.
- Sierro, S., Rothkopf, R., Klenerman, P., 2005. Evolution of diverse antiviral CD8+ T cell populations after murine cytomegalovirus infection. *European journal of immunology* 35 (4), 1113–1123. 10.1002/eji.200425534.
- Smith, A.L., Wikstrom, M.E., Fazekas de St Groth, B., 2000. Visualizing T cell competition for peptide/MHC complexes: a specific mechanism to minimize the effect of precursor frequency. *Immunity* 13 (6), 783–794.
- Smith, C., Gras, S., Brennan, R.M., Bird, N.L., Valkenburg, S.A., Twist, K.-A., Burrows, J.M., Miles, J.J., Chambers, D., Bell, S., Campbell, S., Kedzierska, K., Burrows, S.R., Rossjohn, J., Khanna, R., 2014. Molecular imprint of exposure to naturally occurring genetic variants of human cytomegalovirus on the T cell repertoire. *Scientific reports* 4, 3993. 10.1038/srep03993.
- Smithey, M.J., Li, G., Venturi, V., Davenport, M.P., Nikolich-Zugich, J., 2012. Lifelong persistent viral infection alters the naive T cell pool, impairing CD8 T cell immunity in late life. *Journal of immunology* (Baltimore, Md. : 1950) 189 (11), 5356–5366. 10.4049/jimmunol.1201867.
- Snyder, C.M., Cho, K.S., Bonnett, E.L., Allan, J.E., Hill, A.B., Harty, J.T., 2011. Sustained CD8+ T Cell Memory Inflation after Infection with a Single-Cycle Cytomegalovirus. *PLoS Pathogens* 7 (10), e1002295. 10.1371/journal.ppat.1002295.

References

- Snyder, C.M., Cho, K.S., Bonnett, E.L., van Dommelen, S., Shellam, G.R., Hill, A.B., 2008. Memory inflation during chronic viral infection is maintained by continuous production of short-lived, functional T cells. *Immunity* 29 (4), 650–659. 10.1016/j.immuni.2008.07.017.
- Stemberger, C., Graef, P., Odendahl, M., Albrecht, J., Dossinger, G., Anderl, F., Buchholz, V.R., Gasteiger, G., Schiemann, M., Grigoleit, G.U., Schuster, F.R., Borkhardt, A., Versluys, B., Tonn, T., Seifried, E., Einsele, H., Germeroth, L., Busch, D.H., Neuenhahn, M., 2014. Lowest numbers of primary CD8(+) T cells can reconstitute protective immunity upon adoptive immunotherapy. *Blood* 124 (4), 628–637. 10.1182/blood-2013-12-547349.
- Stemberger, C., Huster, K.M., Koffler, M., Anderl, F., Schiemann, M., Wagner, H., Busch, D.H., 2007a. A Single Naive CD8+ T Cell Precursor Can Develop into Diverse Effector and Memory Subsets. *Immunity* 27 (6), 985–997. 10.1016/j.immuni.2007.10.012.
- Stemberger, C., Neuenhahn, M., Buchholz, V.R., Busch, D.H., 2007b. Origin of CD8+ effector and memory T cell subsets. *Cellular & molecular immunology* 4 (6), 399–405.
- Stepanek, O., Prabhakar, A.S., Osswald, C., King, C.G., Bulek, A., Naeher, D., Beaufils-Hugot, M., Abanto, M.L., Galati, V., Hausmann, B., Lang, R., Cole, D.K., Huseby, E.S., Sewell, A.K., Chakraborty, A.K., Palmer, E., 2014. Coreceptor scanning by the T cell receptor provides a mechanism for T cell tolerance. *Cell* 159 (2), 333–345. 10.1016/j.cell.2014.08.042.
- Stone, J.D., Artyomov, M.N., Chervin, A.S., Chakraborty, A.K., Eisen, H.N., Kranz, D.M., 2011. Interaction of Streptavidin-Based Peptide-MHC Oligomers (Tetramers) with Cell-Surface TCRs. *The Journal of Immunology* 187 (12), 6281–6290. 10.4049/jimmunol.1101734.
- Strandberg, T.E., Pitkala, K.H., Tilvis, R.S., 2009. Cytomegalovirus antibody level and mortality among community-dwelling older adults with stable cardiovascular disease. *JAMA* 301 (4), 380–382. 10.1001/jama.2009.4.
- Swain, S.L., McKinstry, K.K., Strutt, T.M., 2012. Expanding roles for CD4+ T cells in immunity to viruses. *Nature reviews. Immunology* 12 (2), 136–148. 10.1038/nri3152.
- Sylwester, A.W., Mitchell, B.L., Edgar, J.B., Taormina, C., Pelte, C., Ruchti, F., Sleath, P.R., Grabstein, K.H., Hosken, N.A., Kern, F., Nelson, J.A., Picker, L.J., 2005. Broadly targeted human cytomegalovirus-specific CD4+ and CD8+ T cells dominate the memory compartments of exposed subjects. *The Journal of experimental medicine* 202 (5), 673–685. 10.1084/jem.20050882.
- Teng, M.K., Smolyar, A., Tse, A.G., Liu, J.H., Liu, J., Hussey, R.E., Nathenson, S.G., Chang, H.C., Reinherz, E.L., Wang, J.H., 1998. Identification of a common docking topology with substantial variation among different TCR-peptide-MHC complexes. *Current biology : CB* 8 (7), 409–412.
- Torti, N., Walton, S.M., Brocker, T., Rüllicke, T., Oxenius, A., Hill, A.B., 2011. Non-Hematopoietic Cells in Lymph Nodes Drive Memory CD8 T Cell Inflation during Murine Cytomegalovirus Infection. *PLoS Pathogens* 7 (10), e1002313. 10.1371/journal.ppat.1002313.
- Trautmann, L., Rimbart, M., Echasserieau, K., Saulquin, X., Neveu, B., Dechanet, J., Cerundolo, V., Bonneville, M., 2005. Selection of T cell clones expressing high-affinity public TCRs within Human cytomegalovirus-specific CD8 T cell responses. *Journal of immunology (Baltimore, Md. : 1950)* 175 (9), 6123–6132.
- Trzonkowski, P., Mysliwska, J., Szmit, E., Wieckiewicz, J., Lukaszuk, K., Brydak, L.B., Machala, M., Mysliwski, A., 2003. Association between cytomegalovirus infection, enhanced proinflammatory response and low level of anti-hemagglutinins during the anti-influenza vaccination--an impact of immunosenescence. *Vaccine* 21 (25-26), 3826–3836.
- Tynan, F.E., Burrows, S.R., Buckle, A.M., Clements, C.S., Borg, N.A., Miles, J.J., Beddoe, T., Whisstock, J.C., Wilce, M.C., Silins, S.L., Burrows, J.M., Kjer-Nielsen, L., Kostenko,

References

- L., Purcell, A.W., McCluskey, J., Rossjohn, J., 2005. T cell receptor recognition of a 'super-bulged' major histocompatibility complex class I-bound peptide. *Nature Immunology* 6 (11), 1114–1122. 10.1038/ni1257.
- Valenzuela, H.F., Effros, R.B., 2002. Divergent telomerase and CD28 expression patterns in human CD4 and CD8 T cells following repeated encounters with the same antigenic stimulus. *Clinical immunology (Orlando, Fla.)* 105 (2), 117–125.
- van der Merwe, P.A., Davis, S.J., 2003. Molecular interactions mediating T cell antigen recognition. *Annual review of immunology* 21, 659–684. 10.1146/annurev.immunol.21.120601.141036.
- van Heijst, Jeroen W J, Gerlach, C., Swart, E., Sie, D., Nunes-Alves, C., Kerkhoven, R.M., Arens, R., Correia-Neves, M., Schepers, K., Schumacher, Ton N M, 2009. Recruitment of antigen-specific CD8+ T cells in response to infection is markedly efficient. *Science (New York, N.Y.)* 325 (5945), 1265–1269. 10.1126/science.1175455.
- Veillette, A., Bookman, M.A., Horak, E.M., Bolen, J.B., 1988. The CD4 and CD8 T cell surface antigens are associated with the internal membrane tyrosine-protein kinase p56lck. *Cell* 55 (2), 301–308.
- Viganò, S., Utzschneider, D.T., Perreau, M., Pantaleo, G., Zehn, D., Harari, A., 2012. Functional Avidity: A Measure to Predict the Efficacy of Effector T Cells? *Clinical and Developmental Immunology* 2012 (7), 1–14. 10.1155/2012/153863.
- Voss, S., Skerra, A., 1997. Mutagenesis of a flexible loop in streptavidin leads to higher affinity for the Strep-tag II peptide and improved performance in recombinant protein purification. *Protein engineering* 10 (8), 975–982.
- Wallace, D.L., Zhang, Y., Ghattas, H., Worth, A., Irvine, A., Bennett, A.R., Griffin, G.E., Beverley, Peter C L, Tough, D.F., Macallan, D.C., 2004. Direct measurement of T cell subset kinetics in vivo in elderly men and women. *Journal of immunology (Baltimore, Md. : 1950)* 173 (3), 1787–1794.
- Waller, E., Day, E., Sissons, J G Patrick, Wills, M.R., 2008. Dynamics of T cell memory in human cytomegalovirus infection. *Medical microbiology and immunology* 197 (2), 83–96. 10.1007/s00430-008-0082-5.
- Wang, X.L., Altman, J.D., 2003. Caveats in the design of MHC class I tetramer/antigen-specific T lymphocytes dissociation assays. *Journal of Immunological Methods* 280 (1-2), 25–35. 10.1016/S0022-1759(03)00079-6.
- Weekes, M.P., Wills, M.R., Mynard, K., Carmichael, A.J., Sissons, J.G., 1999. The memory cytotoxic T-lymphocyte (CTL) response to human cytomegalovirus infection contains individual peptide-specific CTL clones that have undergone extensive expansion in vivo. *Journal of virology* 73 (3), 2099–2108.
- Weissbrich, B., Nauerth, M., Busch, D.H., 2013. Adoptive immunotherapy: New assay for the identification of T cells with optimal avidity. *OncoImmunology* 2 (10), e26199. 10.4161/onci.26199.
- Wikby, A., Johansson, B., Olsson, J., Löfgren, S., Nilsson, B.O., Ferguson, F., 2002. Expansions of peripheral blood CD8 T-lymphocyte subpopulations and an association with cytomegalovirus seropositivity in the elderly: the Swedish NONA immune study. *Experimental gerontology* 37 (2-3), 445–453.
- Wills, M.R., Carmichael, A.J., Mynard, K., Jin, X., Weekes, M.P., Plachter, B., Sissons, J.G., 1996. The human cytotoxic T-lymphocyte (CTL) response to cytomegalovirus is dominated by structural protein pp65: frequency, specificity, and T-cell receptor usage of pp65-specific CTL. *Journal of virology* 70 (11), 7569–7579.
- Wolchok, J.D., Kluger, H., Callahan, M.K., Postow, M.A., Rizvi, N.A., Lesokhin, A.M., Segal, N.H., Ariyan, C.E., Gordon, R.-A., Reed, K., Burke, M.M., Caldwell, A., Kronenberg, S.A., Agunwamba, B.U., Zhang, X., Lowy, I., Inzunza, H.D., Feely, W., Horak, C.E., Hong, Q., Korman, A.J., Wigginton, J.M., Gupta, A., Sznol, M., 2013.

References

- Nivolumab plus ipilimumab in advanced melanoma. *The New England journal of medicine* 369 (2), 122–133. 10.1056/NEJMoa1302369.
- Wooldridge, L., Lissina, A., Cole, D.K., van den Berg, Hugo A., Price, D.A., Sewell, A.K., 2009. Tricks with tetramers: how to get the most from multimeric peptide-MHC. *Immunology* 126 (2), 147–164. 10.1111/j.1365-2567.2008.02848.x.
- Wooldridge, L., van den Berg, H. A., Glick, M., Gostick, E., Laugel, B., Hutchinson, S.L., Milicic, A., Brenchley, J.M., Douek, D.C., Price, D.A., Sewell, A.K., 2005. Interaction between the CD8 Coreceptor and Major Histocompatibility Complex Class I Stabilizes T Cell Receptor-Antigen Complexes at the Cell Surface. *Journal of Biological Chemistry* 280 (30), 27491–27501. 10.1074/jbc.M500555200.
- Yager, E.J., Ahmed, M., Lanzer, K., Randall, T.D., Woodland, D.L., Blackman, M.A., 2008. Age-associated decline in T cell repertoire diversity leads to holes in the repertoire and impaired immunity to influenza virus. *The Journal of experimental medicine* 205 (3), 711–723. 10.1084/jem.20071140.
- Zeh, H.J., Perry-Lalley, D., Dudley, M.E., Rosenberg, S.A., Yang, J.C., 1999. High avidity CTLs for two self-antigens demonstrate superior in vitro and in vivo antitumor efficacy. *Journal of immunology (Baltimore, Md. : 1950)* 162 (2), 989–994.
- Zehn, D., Lee, S.Y., Bevan, M.J., 2009. Complete but curtailed T-cell response to very low-affinity antigen. *Nature* 458 (7235), 211–214. 10.1038/nature07657.
- Zhu, Z., Singh, V., Watkins, S.K., Bronte, V., Shoe, J.L., Feigenbaum, L., Hurwitz, A.A., 2013. High-avidity T cells are preferentially tolerized in the tumor microenvironment. *Cancer research* 73 (2), 595–604. 10.1158/0008-5472.CAN-12-1123.
- Zuniga, E.I., Harker, J.A., 2012. T-cell exhaustion due to persistent antigen: quantity not quality? *European Journal of Immunology* 42 (9), 2285–2289. 10.1002/eji.201242852.

8 Acknowledgments

An dieser Stelle möchte ich mich bei Familie, Freunden und Kollegen, die mich durch meine Doktorarbeit hindurch begleitet haben und daher zum Erfolg beigetragen haben, bedanken! Zuerst bedanke ich mich bei meinem Doktorvater Professor Dirk Busch für die Betreuung meiner Dissertation und die Möglichkeit an einem anwendungsorientierten und sehr abwechslungsreichen Projekt zu arbeiten. Neben den vielen wissenschaftlichen und praktischen Erfahrungen an seinem Institut konnte ich mich durch die Teilnahme an verschiedenen nationalen und internationalen Kongressen, sowie DGFI Schulungen immer weiter entwickeln, meine Forschungsarbeit vor unterschiedlichem Publikum präsentieren und viele Kontakte aufbauen.

Desweiteren möchte ich meinem Graduierten-Komitee danken, vor allem für die wissenschaftliche Betreuung meines Projektes. Ich danke Doktor Michael Neuenhahn für die enge Kooperation zur Immunmonitoring Arbeitsgruppe und dem Austausch über aktuelle klinische Daten, wie auch den Zugang zu humanen CMV seropositiven Zellmaterial. Bei Professor Thorsten Hugel bedanke ich mich für die Diskussionen zu den technischen Details zum Aufbau unseres TZR-Liganden „ k_{off} -rate assays“ und dem Beitrag seiner Erfahrungen aus der Biophysik.

Magdalena Nauerth danke ich für die sorgfältige Einarbeitung in die zahlreichen Methoden, die man zur Durchführung der k_{off} -rate Experimente benötigt, sowie die große Vorarbeit zusammen mit Robert Knall zur Entwicklung des TZR-Liganden „ k_{off} -rate assays“. Für die Generierung der CMV-spezifischen T Zell Klone danke ich Jeannette Bet und Paulina Paszkiewicz, sowie Professor Stan Riddell für die Protokolle zur Kultivierung und Expansion der Zellen über solch lange Zeiträume, sowie für seine hilfreichen Ideen und Diskussionen.

Für die Peptid Varianten aus unterschiedlichen CMV Stämmen und auch für spannende Diskussionen während der SFB Meetings danke ich Andreas Mossmann, sowie Ton Schumacher für die UV-spaltbaren Peptide und den kurzen Aufenthalt in seinem Labor. Vielen Dank an Thomas Marandu, Luka Cicin-Sain und Luka's Arbeitsgruppe für den Austausch über murine CMV Infektionen und die Blutproben von murinen CMV infizierten Mäusen! Auch vielen Dank für die tolle Gelegenheit, antigen-spezifische T Zellen aus dem naiven Repertoire zu analysieren, die von Pleun Hombrink und Mirjam Heemskerk isoliert wurden!

Acknowledgments

Großen Dank an Georg Dössinger, Isabell Schiedewitz und Mario Bunse für die Analyse von TCR Sequenzen und Transduktion bestimmter TCRs. Für die FACS Sortierung von Zellen gilt besonderer Dank an Lynette Henkel und Matthias Schiemann.

Ein großes Dankeschön geht an meine Kollegen am Institut, besonders diejenigen auf der zweiten Etage, auf der man stets Ideen austauschen, Rat finden und auch einfach zusammen sitzen konnte! Besonders danke ich meinen Kollegen in der Arbeitsgruppe Busch für die gesellige und hilfreiche Arbeitsatmosphäre! Vielen Dank an Anna Hochholzer, Inge Hensel und Katrin Molter, die unser Labor in Schuss halten! Für hilfreiche Diskussionen und Ideen danke ich Patricia Gräf, Veit Buchholz, Fabian Mohr, Stefan Dreher und Christian Stemberger, sowie für die Erzählungen über Lebensgeschichten und spannende Projekte an Herbert Stadler! Weiteren Dank auch an Patricia Gräf für Unterstützung und Rat in vielen (Doktoranden-) Lebenslagen, sowie an Shwetha Lakshmiathi, Julia Albrecht, Sonakshi Bhattacharjee und Eva Loffredo-Verde. Florian Voit danke ich für das Vorantreiben der Analyse von murinen CMV-SIINFEKL spezifischen T Zell Populationen und die gute Zusammenarbeit!

Besonderer Dank gilt meiner Familie und meinen Freunden, zu denen mittlerweile einige Personen aus dem Labor zählen, für die tolle Zeit ausserhalb des Labors. Insbesondere an meine Eltern, die immer für mich da sind und bei denen ich nach stressigen Phasen am schnellsten entspannen und wieder Kräfte sammeln konnte! Vielen Dank für die viele Geduld und Unterstützung bei der Verwirklichung meiner Ziele!